



Norwegian University of Life Sciences
Faculty of Biosciences
Department of Plant Sciences

Philosophiae Doctor (PhD)
Thesis 2018:39

Abscission in poinsettia, a methodology and –omics approach

Knopp- og blomsterfall i julestjerne,
et metode og –omics studium

Luz Gabriela Muñoz Sanhueza

Abscission in poinsettia, a methodology and –omics approach

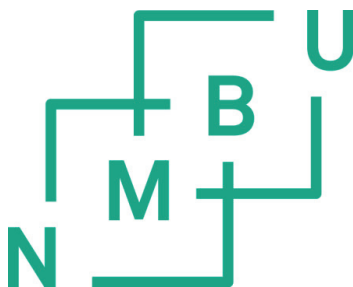
Knopp- og blomsterfall i julestjerne, et metode og –omics studium

Philosophiae Doctor (PhD) Thesis

Luz Gabriela Muñoz Sanhueza

Norwegian University of Life Sciences
Faculty of Biosciences
Department of Plant Sciences

Ås 2018



Thesis number 2018:39
ISSN 1894-6402
ISBN 978-82-575-1511-9

PhD supervisors:

Prof. Trine (A.K.) Hvoslef-Eide

Department of Plant Sciences

Faculty of Biosciences

Norwegian University of Life Sciences

P.O.Box 5003, 1432 Ås, Norway

trine.hvoslef-eide@nmbu.no

Researcher YeonKyeong Lee

Department of Plant Sciences

Faculty of Biosciences

Norwegian University of Life Sciences

P.O.Box 5003, 1432 Ås, Norway

yeonkyeong.lee@nmbu.no

Prof. Jerry D. Cohen

Department of Horticultural Sciences

Microbial and Plant Genomics Institute

University of Minnesota

305 Alderman Hall 1970 Folwell Avenue

Saint Paul, MN 55108, U.S.A.

cohen047@umn.edu

Researcher Mallikarjuna Rao Kovi

Department of Plant Sciences

Faculty of Biosciences

Norwegian University of Life Sciences

P.O.Box 5003, 1432 Ås, Norway

mallikarjuna.rao.kovi@nmbu.no

Evaluation committee

Assoc. Prof. Melinka Alonso Butenko

Department of Biosciences

Section for Genetics and Evolutionary Biology

University of Oslo

Postboks 1066 Blindern

0316 Oslo

m.a.butenko@ibv.uio.no

Prof. Jeremy Roberts

Deputy Vice-Chancellor - Research and Enterprise

Office of Vice-Chancellor

Plymouth University

Room 101, 18 Portland Villas, Drake Circus, Plymouth, Devon, PL4 8AA, U.K.

jerry.roberts@plymouth.ac.uk

Coordinator

Prof. Sissel Torre

Department of Plant Sciences

Faculty of Biosciences

Norwegian University of Life Sciences

P.O.Box 5003, 1432 Ås, Norway

sissel.torre@nmbu.no

TABLE OF CONTENTS

| | |
|---|-----------|
| Acknowledgements | i |
| Summary | iii |
| Sammendrag..... | v |
| Resumen | vii |
| Abbreviations..... | ix |
| List of papers..... | xi |
| 1. Introduction..... | 1 |
| 1.1 Abscission | 1 |
| 1.2 Poinsettia (<i>Euphorbia pulcherrima</i>), as the model for studying abscission | 7 |
| 1.3 Hormonal control of abscission..... | 12 |
| 1.3.1 Auxin control of abscission..... | 12 |
| 1.3.2 Regulation of abscission by the balance of ethylene and auxin | 15 |
| 1.4 Genetic control of abscission..... | 18 |
| 1.4.1 Genes involved in pre-abscission events..... | 18 |
| 1.4.2 Molecular pathways in <i>Arabidopsis</i> | 20 |
| 1.4.3 Cell wall remodeling during abscission..... | 24 |
| 1.5 Omics technologies | 26 |
| 1.5.1 General consideration when working with omics technologies | 26 |
| 1.5.2 Transcriptomic analysis in abscission | 27 |
| 1.5.3 Proteomics analysis in abscission | 28 |
| 2. Aim of this thesis | 31 |
| 3. Experimental approaches used in this thesis..... | 33 |
| 3.1 Induction of the abscission by decapitation of the floral organs | 33 |
| 3.2 Spatial-temporal approach | 34 |
| 3.3 <i>De novo</i> transcriptome | 35 |
| 3.4 Shotgun proteomic | 36 |
| 4. Main results and discussion..... | 39 |

| | | |
|-------|--|----|
| 4.1 | Manuscript 1 Auxin analysis using laser microdissected plant tissues sections ... | 39 |
| 4.2 | Manuscript 2 Proteomics..... | 41 |
| 4.2.1 | Processes occurring on Day 2 according to the temporal comparisons | 43 |
| 4.2.2 | Processes occurring on Day 4 according to the temporal comparisons | 44 |
| 4.2.3 | Processes occurring in the AZ according to the spatial comparisons on D4 and D6 | 45 |
| 4.3 | Manuscript 3 Transcriptomic..... | 46 |
| 4.4 | Comparative results between proteomics and transcriptomic studies in abscission | 48 |
| 4.5 | Abscission signaling cascade elements are present in poinsettia | 53 |
| 4.6 | AZ differentiation in poinsettia might be caused by TFs regulating boundaries and meristem differentiation | 55 |
| 5 | Integrated discussion of the results | 59 |
| 5.1 | Reflections when approaching a combined discussion in transcriptomic and proteomic | 59 |
| 5.2 | Discussion of the results in a broader context | 60 |
| 5.3 | Integrated results from proteomic and transcriptomic on D2 | 61 |
| 5.4 | Integrated results from proteomic and transcriptomic on D4 and D6 | 65 |
| 5.5 | Reflections on the small changes in protein abundance on D2 and D6..... | 69 |
| 6 | Conclusions and future perspectives | 71 |
| 7 | References | 75 |

Acknowledgements

This PhD was funded by the Norwegian University of Life Sciences as a PhD scholarship to the Department of Plant Sciences (IPV). I want to thank to my supervisors Trine Hvoslef-Eide and Jerry Cohen for had selected me for this position. I want to thank all my supervisors for the critical review of the manuscripts and thesis. Your contribution has been invaluable.

I want to thank the staff of the Plant Cell Lab for their support in lab matters and their good disposition to facilitate my work there. I also have to mention the staff from SKP and the excellent facilities they provided for the conduction of my experiments in the greenhouses. Special mention to Tone Melby for her good disposition in the lab, Gry Skjeseth, Ida Hagen and Marit Siira for taking care of my plants and Kari Boger for her patience in teaching me how to propagate poinsettia. I also want to thank to Stein Valsø from SKP for the opportunity he gave me to use the auditorium for the First Latin American Film Festival. Kjell Hellesvik and Dag Wenner thank you for the friendly words you always provided.

I want to thank the administrative staff of NMBU Ingrid Heggelund, Berit Ingebrigtsen and Mara Dagestad for their excellent job and help during my stay in IPV. My sincere gratitude to the Senior Engineer Morten Skaugen from the IKBM Proteomic facility for his patience and his interest in my work.

Special thanks to my globetrotter friend Steven Barnett and my dear friend Jan Svensson, who played a key role in the beginning of this adventure supporting my aim to pursue a PhD.

Some of the best things of my experience as a PhD student it was that I had the chance to interact with so many valuable people around me. Many of them became a strong support in my new life in Norway. Thank you Kjellaug Wik Mikkelsen for let me be part of your life, our long conversations are still one of my treasures, please send my love to our little fluffy friend Mr. Black. I have to say thank you very much to Elin Ørmen and Hilde Raanaas Kolstad from the Imaging Centre, who took my hand during the first year of my studies. I want to thank too to my siblings in science, Beatrice Misaka Langwa, Dereje Haile Buko, Shitaye Desta Gebrewold and Nicolás Mendoza Peña, for sharing so many hours of frustration, joy, group therapy and fantastic African food, and a friendship I know

it will last forever. I cannot forget the rest of the people from the Independent Kingdom of Klimalab, where I self-proclaimed Queen, Amsalu Gobena Roro, Jorunn Olsen, Sissel Torre and Marcos Viejo. Especially good memories of our fantastic karaoke evenings and very looong conversations “a la hora del té de la mañana”. All of you have contributed to make my life nicer and funnier, especially in the difficult times. I want to thank to my Latin American Film Festival brothers, Emilio Alvarenga and Sergio Chávez ¡Hasta la Victoria Siempre!, you gave me one of the most gratifying experiences of my time in Ås, the real colourful taste of Latin America.

I cannot forget my family in Chile, you have been an important part of this journey, mami y papi, los amo y respeto mucho y quiero que sepan que sus enseñanzas y la admiración que siento por ustedes me ha hecho seguir mi camino y ser la persona que ahora soy. Nelson, Viviana, Gaspar y Gabriel, siempre los he tenido en mi corazón a pesar de la distancia, los amo. Jag vil tacka min familj i Sverige, Gunnel, Jann och Mary Ericsson för ditt stöd och kärlek. The last acknowledgement goes for Andreas, my partner in crime and the one without whom I would not had been able to achieve this. Jag elsker dig Tigro.

Summary

Plants detach organs in a highly controlled process called abscission. Leaves, flowers, seeds, fruits, berries and even roots abscise from the plant in response to pathogens or environmental and developmental stimuli. The deciduous plants shed their leaves each autumn and many flowers discard their petals after pollination. Abscission is highly connected to loss of potential yield in productive crops due to affect seed shattering in cereals, harvesting time in fruits, and fruit setting in fruit trees by abscission of the excess of flowers. Therefore, control of abscission has been a part of agricultural practice from the beginning of plant domestication. Additionally, premature abscission might affect the decorative value in ornamental plants, an example being poinsettia (*Euphorbia pulcherrima*), which is a plant originally from Central America and highly appreciated during the Christmas season. Early flower abscission in poinsettia results in quality reduction and has economic implications for producers, making it a crucial horticultural issue to address.

Organ separation occurs in cell layers normally located at the bottom of the organs, and these cell layers are called the abscission zone (AZ). After receiving physiological cues, the AZ starts a developmental program in which the pectin from the middle lamella is dissolved and the cell wall is degraded to achieve total organ detachment while a protective layer is generated to seal the newly exposed surface.

Although hormonal factors are involved in abscission control, such as auxin-ethylene balance, how these events are coordinated is still largely unknown. The decrease of auxin within the AZ has been postulated as being a prerequisite for abscission to occur, but the full details of the developmental program for abscission remains an area of active research.

This thesis sheds light on the processes behind poinsettia flower bud abscission from three different perspectives. 1) The first approach was development of a methodology to harvest plant materials using the laser microdissection microscope (LMD) coupled to cryosectioning and freeze-drying. The tissue harvested this way is suitable to quantify the auxin levels by GC-MS/MS within the AZ cells of poinsettia flower buds. 2) The second was the use proteomics to explore the changes in abundance of proteins during abscission, taking advantage of spatial and temporal changes during the process of

abscission. 3) Finally, the third approach was the use of transcriptomic to assess the changes in gene expression using a compatible protocol to that employed for the proteomic analyses. The study revealed characteristic patterns of spatiotemporal changes in cell wall transformation-related genes and for auxin related genes, as well as the presence of important abscission genes such as *IDA*. The results obtained and reported in this thesis support the idea that abscission is a highly complex process and the results unravel some of the processes underpinning abscission regulation.

Sammendrag

Planter kvitter seg med organer de ikke lenger har bruk for gjennom en svært kontrollert prosess som kalles absisjon. Dette innebærer oftest knopp-, blomster- eller bladfall, men omfatter også frødryss, tap av frukt, bær og til og med røtter. Dette er oftest en respons på patogener, ytre miljø eller stimuli gjennom normal utvikling hos planten. Løvfellende planter slipper sine blad om høsten og mange blomster mister sine kronblad etter pollinering. Absisjon er nært knyttet til tap av mulig avling hos kulturplanter, slik som frødryss før høsting hos kornartene-. Hos frukt og bær er absisjon ofte en selvregulerende prosess der blomster-, kart- og fruktfall bidrar til å redusere fruktsettingen. Å kunne ha kontroll på absisjon har derfor vært viktig siden starten på domestiseringen av planter. I tillegg vil tidlig knopp- og blomsterfall påvirke verdien av prydplanter, for eksempel julestjerne (*Euphorbia pulcherrima*), en plante som kommer fra Sentral Amerika og er en høyt skattet til jul. Tidlig blomsterfall regnes som en kvalitetsfeil, noe som påvirker prisen til produsent. Alle disse tingene betyr at absisjon er en viktig prosess å ha kontroll på innen jord- og hagebruk.

Tap av plantedeler skjer normalt i cellelag under den delen som planten skal kaste, og dette laget kalles absisjonssonen (AZ). Etter å ha mottatt fysiologiske signaler, begynner absisjonssonen på en utvikling som begynner med at pektiner i midtlamellen brytes ned og celleveggen brytes gradvis ned for å forberede kasting, samtidig som et beskyttende lag dannes der organet faller av. Til tross for at man er klar over at plantehormoner påvirker knop- og blomsterfall (absisjon), vet man ennå ikke hvordan dette reguleres i detalj. Nedgangen i auxin i AZ har blitt postulert som en forutsetning for at absisjon skal kunne skje, men dette er fortsatt et område av stor interesse for forskningen.

Denne oppgaven kaster lys over mange av de prosessene som fører til knopp- og blomsterfall hos julestjerne, fra tre ulike vinkler: 1) Den første artikkelen beskriver utviklingen av en metode for å høste svært små områder i blomsterknoppen ved hjelp av laser mikrodisekeringsmikroskop (LMD), sammen med frysesnitting og frysetørking av materialet. Vev høstet på denne måten kan bevare auxiner (og andre nedbrytbare stoff) for kvantitativ analyse ved hjelp av GC-MS/MS av cellene i absisjonssonen hos julestjerne. 2) Bruk av proteomikk for å utforske endringer i proteinmengde og –sammensetning under absisjonsprosessen, ved å se på endringer i både tid og rom. 3) Den siste artikkelen bruker

transkriptomikk for å beskrive de samme prosessene i tid og rom, men ser på genuttrykk og endringer av disse hos julestjerne. Dette doktorgradsarbeidet avslører karakteristiske mønstre i genuttrykk for tid og rom ved nedbryting av celleveggen og for auxinrelaterte gener. Vi fant for første gang tilstedeværelsen av *IDA*, som er vist å være viktig for absisjon også i mange andre arter. Resultatene støtter oppfatningen av at absisjon er en svært kompleks prosess, og gir en utvidet forståelse av noen av prosessene som understøtter reguleringen av absisjon hos planter.

Resumen

Las plantas desechan órganos de manera altamente controlada en un proceso denominado abscisión. La abscisión de hojas, flores, semillas, frutos, bayas e incluso raíces es la respuesta fisiológica a estímulos internos y/o ambientales. Las plantas de hoja caduca botan las hojas cada otoño y muchas flores desechan los pétalos después de la polinización. La abscisión está fuertemente conectada al rendimiento en cultivos productivos ya que afecta la dispersión de las semillas en cereales, el tiempo de cosecha de los frutos y el cuaje en árboles frutales debido a la abscisión del exceso de flores. Por lo tanto, controlar la abscisión ha sido una parte importante de las prácticas agrícolas desde el comienzo de la domesticación de las plantas. Asimismo, la abscisión también afecta a plantas ornamentales, disminuyendo su valor decorativo. Un ejemplo es la abscisión precoz de las flores en la Flor del Inca (*Euphorbia pulcherrima*), planta originaria de Centro América muy cotizada durante la época navideña. La pérdida prematura de las flores en la Flor del Inca causa pérdidas económicas a los productores, por lo cual es un tema a considerar.

La separación del órgano tiene lugar en la llamada zona de abscisión (ZA) que está ubicada normalmente en la base de los órganos y que está conformada por unas pocas capas celulares que retienen un estado de poca diferenciación. Después de recibir las señales fisiológicas, la ZA comienza un programa de desarrollo en el que la pectina en la lámina media celular se disuelve, las paredes celulares se degradan hasta conseguir la separación completa del órgano mientras una capa protectora se genera para sellar la superficie expuesta.

Aunque factores hormonales como el balance de auxina-etileno, podrían controlar la abscisión, no hay acuerdo en cómo los eventos son coordinados. Se postula que la disminución de hormona auxina dentro de la ZA podría ser una de las causas fundamentales por la que la abscisión ocurre, sin embargo, los detalles del programa de desarrollo continúan siendo un área de activa investigación.

La presente tesis estudia la abscisión floral de la especie Flor del Inca desde tres perspectivas diferentes: 1) La primera es el montaje de una metodología experimental para colectar tejido vegetal por medio del microscopio de disección láser acoplado a crio seccionamiento y liofilización. El tejido colectado con esta metodología es apropiado para

su posterior uso en cuantificación de auxina dentro de la ZA usando GC-MS/MS. 2) La segunda es la aplicación de proteómica para explorar las fluctuaciones en el número de proteínas desde un punto de vista espacio-temporal durante la abscisión. 3) Finalmente, la tercera es el uso de transcriptómica para evaluar los cambios de expresión durante la abscisión en el mismo diseño experimental que la proteómica. Los resultados de este estudio revelaron patrones característicos de cambios espaciotemporales en genes relacionados a la transformación de la pared celular y genes relacionados a auxina, así como también la presencia de importantes genes de abscisión, tales como *IDA*. Los resultados obtenidos en esta tesis confirman que la abscisión es un proceso altamente complejo y desvela algunos de los procesos subyacentes a la regulación de la abscisión.

Abbreviations

| | |
|----------|---|
| AFLP- DD | Amplified fragment length polymorphisms- differential display |
| Aux | Auxin |
| AZ | Abscission zone |
| cDNA | Complementary DNA |
| CS | Cryosectioning |
| D | Day |
| DEGs | Differentially expressed genes |
| EC n° | Enzyme commission number |
| FD | Freeze-drying |
| FDR | False discovery rate |
| FT-IR | Fourier transform infra-red |
| GC-MS/MS | Gas chromatograph coupled to tandem mass spectrometer |
| GO | Gene ontology |
| GUS | β -glucuronidase |
| IAA | 2-(1H-indol-3-yl) acetic acid or Indole-3-acetic-acid |
| iTRAQ | Isobaric tag for relative and absolute quantification |
| LMD | Laser microdissection microscope |
| MAPK | Mitogen-activated protein kinase |
| MKK | Mitogen-activated kinase kinase |
| MAPKKK | MAP kinase kinase kinase |
| PG | Polygalacturonase |
| PR | Pathogenesis related proteins |
| qRT-PCR | Real-time quantitative reverse transcription PCR |
| RNA Seq | RNA sequencing |
| SRM | Selected reaction monitoring |
| TF | Transcription factor |
| XTH | Xyloglucan endotransglucosylases/hydrolases |

List of papers

This thesis includes the following manuscripts:

I. **Auxin analysis using laser microdissected plant tissues sections.**

Luz G. Muñoz-Sanhueza, YeonKyeong Lee, Molly Tillmann, Jerry D. Cohen and Anne Kathrine Hvoslef-Eide.

BMC Plant Biol. 2018 Jun 25;18(1):133. doi: 10.1186/s12870-018-1352-z.

II. **Untargeted Proteomics Reveals Global Changes in Pattern of Proteins during Abscission of the flower bud of *Euphorbia pulcherrima*.**

Luz Muñoz-Sanhueza, YeonKyeong Lee and Anne Kathrine Hvoslef-Eide.
Manuscript.

III. ***De novo* transcriptomic analysis in poinsettia flower during abscission.**

Luz Muñoz-Sanhueza, Mallikarjuna Rao Kovi, YeonKyeong Lee and Anne Kathrine Hvoslef-Eide.

Manuscript

1. Introduction

1.1 Abscission

Abscission is the plant process for organ detachment. Leaves, fruits, seeds, flowers and even roots abscise in response to internal or external stimuli (Taylor and Whitelaw, 2001). For example, leaves may abscise because of drought or flooding (Kramer, 1951; Parker and Pallardy, 1985); some flowers abscise their petals as a normal part of their developmental life cycle; and fruit trees abscise mature fruits when they are ready for consumption and seed dispersal.

Organ abscission is an integral part of plant life. All plants have, at some point in their life cycle, at least one event where abscission occurs. In deciduous trees, for example, the circannual loss of the leaves has a seasonal character, favoring the recycling of mineral nutrients at the end of autumn prior to the onset of winter dormancy. Pea seeds are abscised from the funicle as part of their programmed reproductive cycle (Ayeh et al., 2009). Citrus trees regulate fruit production in two rounds of abscission, first the excess of flowers and ovaries are abscised and afterwards the fruitlets themselves are abscised in response to competition for nutrients (Iglesias et al., 2007). The last example is a case of a reproductive optimization strategy that evolved, where the tree is producing high numbers of flowers, even though only surviving few flowers will set fruit. There is a great diversity in behavior in nature regarding abscission of flowers or floral parts: while some flowers abscise in just a few hours after anthesis, others persist longer or do not abscise at all.

Abscission affects both yield and quality in many productive crop plants. Cereal accessions that retained their seeds were selected of domestication because they enhanced the seed harvest yield (Li et al., 2006; Fuller and Allaby, 2009). On the other hand, fruit abscission occurring before harvest time results in economic losses for the producers. In ornamental plants, petals, flower buds or sepal abscission is typically a negative trait because it is associated with early senescence and senescence decreases the floral decorative value (Ferrante et al., 2015) thus resulting in negative economic consequences for commercial nurseries. In contrast, the capacity for plants to shed wilted flowers is often regarded as an asset for bedding plants, thereby reducing the necessity to remove these flowers manually to maintain the decorative value. Thus, not only what will abscise, but also when it happens becomes crucial in agricultural practice. Consequently,

controlling the timing of abscission is a common practice in the production of both fruit trees and ornamental plants.

The situation can become even more complicated when the abscission of several organs must be controlled within the crop simultaneously. An example is during the mechanical harvesting of citrus fruits, where the abscission of three organs must be minimized: unwanted abscission of flowers, fruits and leaves. Pozo and Burns (2009) investigated the effect on abscission by several chemicals that they applied to branches from the start of full bloom to the end of full bloom. They noted different responses depending on the treatment time, which suggested a strong interaction between the abscission of the fruitlets and the loss of leaves. Examples of such abscission accelerators are Ethephon ((2-chloroethyl) phosphonic acid) and CMNP (5-chloro-3-methyl-4-nitro-1H-pyrazole), while 1-MCP (1-methylcyclopropene) is an inhibitor of abscission.

Application of chemical accelerators and/or inhibitors with inappropriate timing can also cause problems. In non-edible plants, such as cotton, the use of diverse defoliant agents on open young bolls, at a wrong time, increased yield losses and altered desirable traits in the fiber (Snipes and Baskin, 1994).

A different approach to controlling abscission in agricultural practice is the use of compounds that mimic or inhibit the effect of certain hormones. Bessis *et al.* (2000) studied the effects on grapevine fruit set by the use of ethylene and anti-ethylene compounds, such as silver thiosulphate (STS), as a hormonal based management system for enhancement of vineyard yield. The synthetic auxin naphthalene acetic acid and STS can be used with a number of plants to reduce flower drop. NAA delayed abscission, in 50% of the flowers, by 2 to 3 weeks in bougainvillea (Hackett et al., 1972) and STS prevented petal abscission in geranium (*Pelargonium hortorum* Bailey), flower abscission in *Calceolaria herbeohybrida* Voss, and bract abscission in bougainvillea (*Bougainvillea glabra* Chois.) (Cameron and Reid, 1983). Abscission occurs in response to several different signals, both internal and external, that have been studied in several plants. Examples of organ abscission and their induction are given in Table 1.

Table 1 Examples of the causes of abscission in different organs and species.

| Cause | Organ abscised | Species or genus | Reference |
|--|----------------|--------------------------------|------------------------------|
| Infection by the fungus <i>Omphalia flavida</i> | Leaves | <i>Coffea</i> (Coffee) | (Sequeira and Steeves, 1954) |
| Polyamines released during the response to stress | Roots | <i>Azolla pinnata</i> | (Gurung et al., 2012) |
| Shortening of the photoperiod | Leaves | <i>Acer saccharum</i> | (Olmsted, 1951) |
| Long-term ozone exposure | Fruit | <i>Solanum lycopersicum</i> L. | (Manning and Feder, 1976) |
| Infection by the fungus <i>Verticillium albo-atrum</i> (Reinke and Berth.) | Leaves | <i>Gossypium hirsutum</i> L. | (Wiese and Devay, 1970) |
| Endogenous ethylene production | Flowers | <i>Plectranthus</i> | (Ascough et al., 2006) |
| Pollination | Petals | <i>Petunia</i> spp. | (Rogers, 2013) |

Abscission takes place in a discrete group of cells, located in the base of the organ to be detached, and this specific area is what forms the abscission zone (AZ). The AZ is a morphologically distinctive structure, defined by a swollen or strangled area in between the part that is detached and the one that remains on the plant. The AZ is made up of small round cells, in a arrested state which, after receiving the right environmental or developmental signal, will become larger and start the separation process (Addicott, 1982; Sexton and Roberts, 1982). The AZ is a highly localized region where the molecular and biochemical changes leading to detachment will occur.

The AZ is pre-defined during development, in most cases, but another type of AZ is the one that only becomes visible during the abscission process. This type occurs with adventitious abscission, which Addicott (1982) defined as “abscission that occurs in tissues away from a recognizable abscission zone in positions that are variable”. This type of abscission might be seasonal, as seen with the distal phyllomorph portion of *Streptocarpus molweniensis* (Noel and Van Staden, 1975) which abscise after the growing season.

Another example of seasonal adventitious abscission occurs in the *Hyacinthus* bulbs which abscise its modified leaves (scale leaves) after every growing season (Kamerbeek and De Munk, 1976). Additionally, injury also induces adventitious abscission. The formation of an AZ in the stems of *Impatiens sultani* after wounding was described by Lloyd (1914) and afterwards was redefined as secondary abscission by Pierik (1971), who observed an AZ development in the base of isolated apple flowers after application of auxin. Pierik (1977, 1980) further extended his results with studies of the process in excised apple and pear pedicels.

The role of auxin in the position of the secondary AZ has been hypothesized to be determined by the lowest concentration of auxin based on studies of the formation position of the secondary AZ in intermodal explants of *Impatiens sultani*. The position of the AZ in primary abscission occur well in advance of the actual abscission activation, but in secondary abscission, the positioning and the differentiation occur almost simultaneously (Warren Wilson et al., 1986; Warren Wilson et al., 1988).

Adventitious and secondary abscission are both referred to in the literature (Roberts et al., 2000; Taylor and Whitelaw, 2001) as terms to distinguish abscission occurring without a pre-defined AZ from the process of abscission with a predetermined AZ (primary abscission). Throughout this thesis, we will use only the term secondary abscission to define this process to avoid confusion in terminology.

Abscission is an active and programmed developmental process, involving several controlled events resulting in affect a plethora of plant responses. Therefore, the elucidation of the mechanisms by which abscission occurs is of enormous significance. Bleecker and Patterson (1997) described a model that remains the currently accepted one for the sequence of events of primary abscission, where there are three distinguishable developmental phases: 1) AZ ontogeny, 2) abscission activation, and 3) trans-differentiation of the protective layer (Figure 1) .

Hvoslef-Eide *et al.* (2016) proposed, based on a series of spatial-temporal studies of the AZ, a more detailed description for the division of phases for secondary abscission in poinsettia flower buds. Studies of the alterations in the cell wall composition in the AZ cells by immunolabeling and Fourier transform infrared microspectroscopy (FT-IR) (Lee et al., 2008), and the differential expression of genes in the AZ from Day 0 (D0) until Day 7 (D7), using Amplified Fragment Length Polymorphisms- Differential Display (AFLP-DD) and Real-

Time Quantitative Reverse Transcription PCR (qRT-PCR) (Figure 2) (Munster, 2006), provided finer resolution to the changes defining the phases than what was previously described.

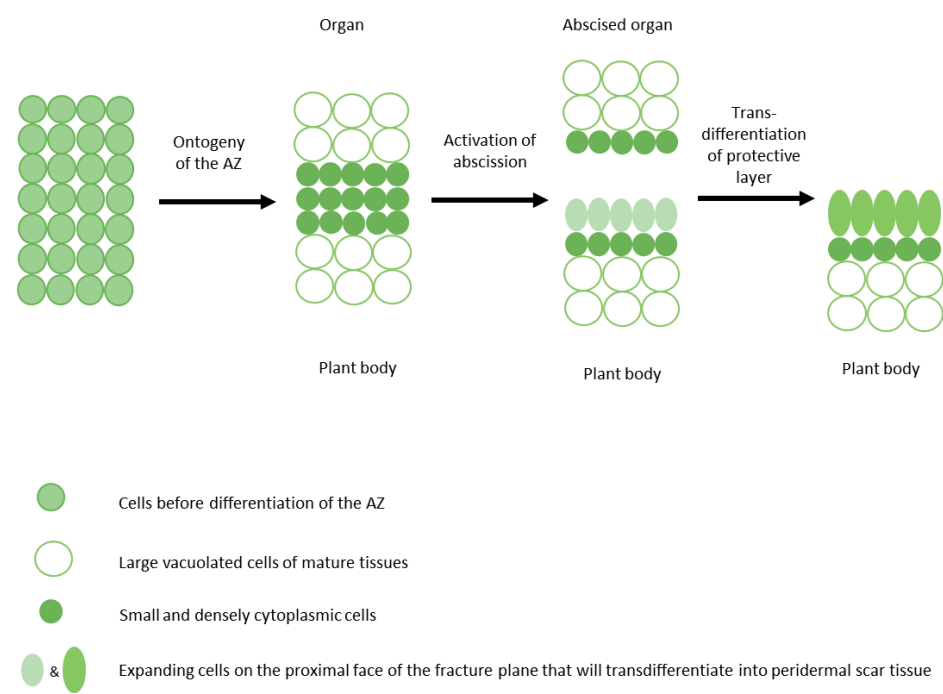


Fig. 1 Changes associated with the flower abscission in Arabidopsis, figure modified from Bleecker and Patterson (1997).

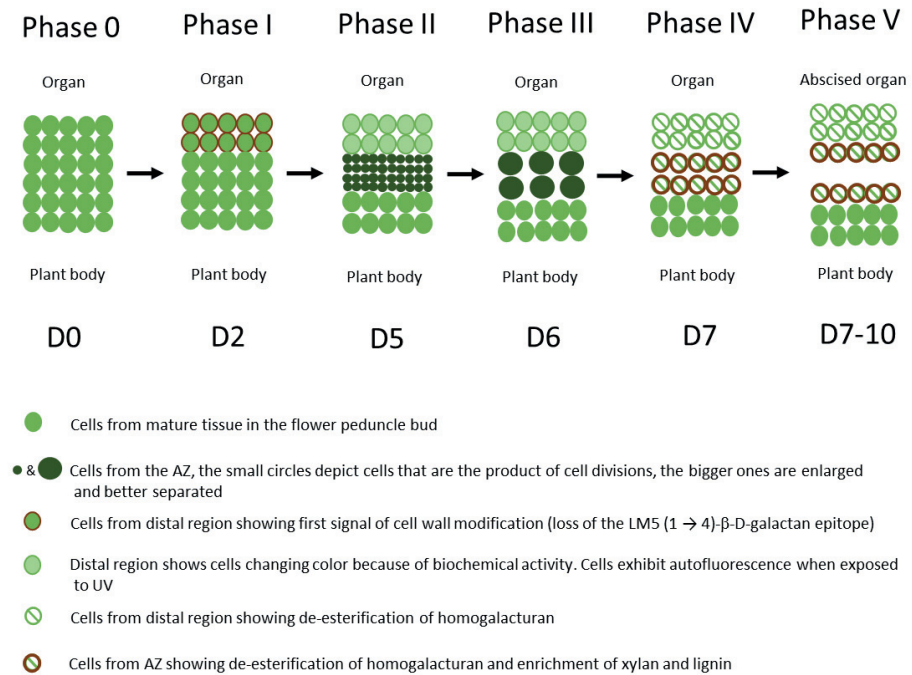


Fig. 2 A pictorial showing the finer division of the phases of poinsettia flower bud abscission. The figure is based on information in Lee *et al.* (2008) and Hvoslef-Eide *et al.* (2016).

Hvoslef-Eide's (2016) model incorporated cell division activity in the AZ prior to the activation of the process and this is a feature shared with other species, such as *Phaseolus vulgaris* explants (Webster, 1968) and *Coleus* leaves (Sexton *et al.*, 1977). However *Arabidopsis*, Begonia flowers (Hänisch Ten Cate *et al.*, 1973), tobacco pedicels, *Phaseolus vulgaris* (van Doorn and Stead, 1997) and tomato (Roberts *et al.*, 1984) show a lack of cell division in the AZ. In contrast, the Bleecker and Patterson (1997) model depicted the elongation of the cells in the AZ, this feature is absent in poinsettia, instead the cells round up, enlarge and separate from each other for as long as the abscission process progresses (Lee *et al.*, 2008).

1.2 Poinsettia (*Euphorbia pulcherrima*), as the model for studying abscission

The *Euphorbiaceae* family is one of the most diverse in the plant kingdom with approximately 7500 species comprising succulents, bushes, herbs and trees (Webster, 2014). Members of this family with important economic value are Cassava (*Manihot esculenta*), Physic nut (*Jatropha curcas*) and Castor bean (*Ricinus communis*). *Euphorbia pulcherrima*, poinsettia or Christmas flower, as it is known in many countries, originated from the Central American region, Mexico and Guatemala, where it grows as a robust shrub that can reach up to 4 m in height in the wild. After its introduction to North America in 1825 (Taylor et al., 2011) by Colonel Poinsett (hence the common name Poinsettia), this plant has become an important horticultural plant and a symbol for Christmas in many parts of the world because of its unique decorative value for the festive season of Christmas.

Poinsettia, or julestjerne in Norwegian, was introduced to Norway by Thormod Hegg in 1946 (Strømme, 1994). Very soon afterward, its production became a commercial success, especially after the development of the variety Anette Hegg in 1967 (Strømme, 1994). Its compact shape and free branching behavior boosted production and stimulated the development of new compact varieties all over the world. After this beginning, poinsettia has become an increasingly important potted plant in Norway and abroad. It is still one of the most important ornamental potted plant in Norway with an estimate of almost six million plants sold every Christmas season.

The characteristic colorful organs in poinsettia are not the flowers, but modified leaves called bracts, which change color from green to red when growing under short day conditions (10 h light, 20°C day and night, 74% RH) (Figure 3A). The flowering in poinsettia is induced by short days, but might be induced also in longer days, if the temperature is low enough, depending on the variety. Poinsettia flowers arise in the apical portion of the plant (Figure 3B); they lack petals (Figure 5A) and are either female or male. They are organized in a particular arrangement: composed by a central first order flower, surrounded by three second order flowers, which in turn are surrounded by six third order flowers (Figure 4).



Fig. 3 A) *Euphorbia pulcherrima* plant. The white arrow indicates a modified leaf called bract, which changes from green to red under short day conditions (10 h). **B)** Poinsettia inflorescence.



Fig. 4 A) Depiction of the arrangement of flowers in the poinsettia inflorescence. **B)** Apical view looking downward on the same flower arrangement.

Two to three weeks after the flower has reached anthesis under short day conditions (Figure 5A), the flower pedicels each develop an abscission zone that becomes visible as the upper portion of the bud starts to senesce and becomes yellowish, while the part that will remain attached to the plant stays green (Figure 5B). From an ornamental perspective, flower bud abscission is not desirable, since the flowers contribute to the ornamental value. Poinsettia plants grown under low light irradiances increase in the amount of floral abscission (Bailey and Miller, 1991). Moe *et al.* (1992), who investigated the effect of light and temperature during night and day on floral abscission in poinsettia, also showed a stimulation of floral abscission in low light. They discovered, however, that

plants grown at lower day temperatures than the night temperature presented a delayed abscission. Apart from that, the increase in light intensity had an positive influence in that it decreased floral abscission (Moe et al., 1992).

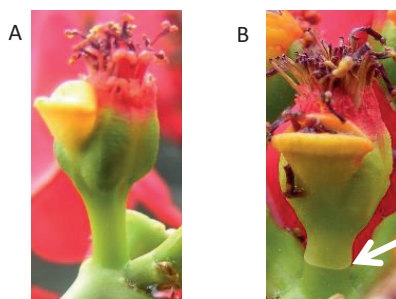


Fig. 5 A) Flower pedicel. **B)** Natural abscission zone after 2 or 3 weeks.

The Norwegian Horticultural Growers Association recommend the study of the early flower abscission observed during poinsettia production to improve ornamental quality. This recommendation lead to a large strategic program between Norwegian University of Life Sciences and the Norwegian Institute of Bioeconomy Research. When studying flower abscission in poinsettia it is difficult to predict when the abscission happens. Because flowers abscise at different times, collecting homogenous material for experiments was previously problematic. Thus, when Hvoslef-Eide's group developed a method to synchronize flower abscission, the problem with homogeneous harvesting was largely solved. Synchronization was achieved by floral organ decapitation, which induced the formation of an AZ on D4 and the flower abscission after 7 to 8 days (Figure 6) (Munster, 2006). This inducible system allowed synchronization of abscission of the six third order flowers of the inflorescence such that it is possible to harvest them at the same time for the various studies. This has proven to be an attractive and critical feature of this model system.

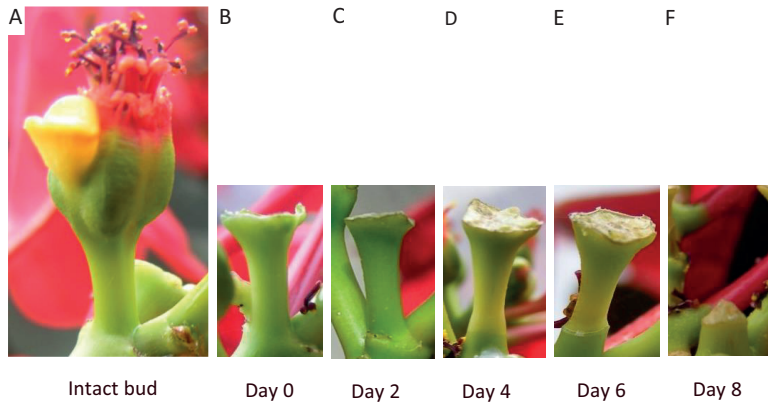


Fig. 6 Progression of the formation of the abscission zone after the decapitation of the flower. **A)** Intact flower bud before decapitation. **B)** Day 0 decapitated bud. **C)** Day 2, two days after decapitation the bud does not present any visible sign that differs from the Day 0. **D)** At Day 4 the bud has developed a visible abscission zone. **E)** Flower bud six days after induction and the signs of cell wall degradation and senescence are visible in the outer side of the pedicel. **F)** Proximal region at Day 8 still attached after the detachment of the decapitated flower bud. Note the cone-shaped AZ.

Morphologically, the induced and natural abscission show the same development in Figure 7. The control (Figure 7A) corresponds to an intact flower bud where no abscission is ongoing and it has not been induced by decapitation. Figure 7B shows how an induced bud looks like 1-2 days prior to abscission. Morphologically, the abscission process starts from the outside and continues from there into the core of the pedicel. As the pedicel, and the bud, continues to grow and develop, the pedicel elongates and each circumference of cells will be lifted a little higher for every step. This is totally comparable to the natural abscission (Figure 7C), where the same morphology and pattern of cell separation starting from the outer layer of the poinsettia bud, as that of the induced abscission in Figure XB.

Auxin prevents abscission to occur as long as the auxin gradient across the AZ is maintained (Addicott et al., 1955). The auxin activity produced by the floral organs vary with the developmental stage of the plant decreasing along the flower development (Jeffcoat and Cockshull, 1972). When the auxin gradient across the AZ is disrupted, the

abscission program is initiated (Addicott et al., 1955). Distal applications of auxin retard abscission in several experimental systems (Addicott, 1982), consequently when the floral organs are removed by the decapitation, the source of auxin is eliminated causing a depletion of auxin in the AZ that will lead to the onset of the organ detachment. Therefore, the abscission induced by decapitation used in this thesis recapitulates the natural abscission that occurs in the flower bud 2 to 3 weeks after anthesis.

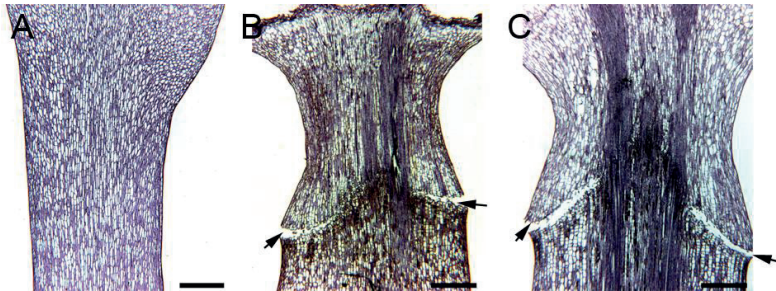


Fig. 7 Longitudinal sections of the poinsettia flower buds, **A)** Bud without abscission. **B)** Abscission after the decapitation stimuli and **C)** Bud showing natural abscission. The arrows show the points of cell separation. Scale bars are 400 μm . Image reprinted with the permission of the authors Hvoslef-Eide *et al* (2016).

Poinsettia flower abscission follows the same directionality pattern described by Gilliland *et al.* (1976) for *Hibiscus* pedicel separation, starting from the epidermis towards inside. This pattern explains the typical inverted cone observed in the proximal region after organ detachment (Figure 6F and Figure 8).

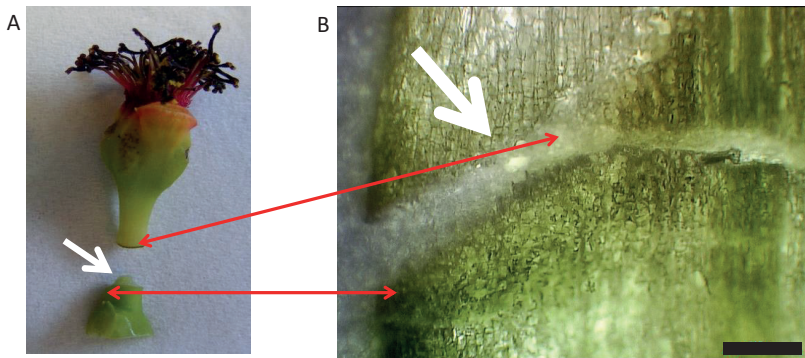


Fig. 8 A) Typical inverted cone shape of the abscission zone of the poinsettia flower bud. **B)** Longitudinal section of an abscission zone in the laser microdissection microscope. White arrow shows the inverted cone shape. Red arrows mark the equivalent points in both pictures. Bar = 310 μm .

This abscission-induced system has been used to compare the primary abscission in pea and secondary abscission in poinsettia. AFLP-DD showed 18 differentially expressed genes (DEGs) with putative roles in abscission in poinsettia among the different time points. Six out of the 18 genes were also found differentially expressed in pea (wild type versus two abscission-less mutants) by RNA *in situ* hybridization, suggesting that even with the genetic distance between these two species, abscission follows a conserved mechanism (Hvoslef-Eide et al., 2016). Likewise, the Hvoslef-Eide group has unraveled the sequential order of cell wall transformation during abscission in poinsettia by detecting epitope disappearance using monoclonal antibodies and FT-IR (Lee et al., 2008).

This thesis contributes to the understanding of abscission with three accomplishments; the first one is development of a methodology to harvest minute amounts of tissue to quantify auxin from the AZ only. The methodology involves cryosectioning, freeze-drying and LMD harvesting. We were able to harvest the AZ cells and quantify their auxin content (manuscript 1) (Muñoz-Sanhueza et al., 2018). Additionally, we carried out two experiments using –omics technologies; transcriptomic and proteomic (manuscripts in preparation). The first –omic approach was a *de novo* transcriptomic analysis in order to find more candidate genes involved in controlling abscission in the poinsettia flower (manuscript 2). In addition, the second –omic approach was the untargeted proteomic experiment conducted using the same transcriptomic experimental layout, which investigated variations in protein abundances during abscission (manuscript 3).

1.3 Hormonal control of abscission

1.3.1 Auxin control of abscission

Auxin or 2-(1H-indol-3-yl) acetic acid (IAA) is a phytohormone that regulates cell division, cell elongation and cell differentiation and by doing so influences plant development and adaptation (Vanneste and Friml, 2009).

Auxin also regulates the abscission process. The regulatory role of auxin in abscission had been established by early experiments. For example, in the early 1930s authors including F. Laibach, G. Mai, C.D. La Rue and F.E. Gardner, among others, described a series of experiments where the application of pollen-auxin or a variety of other auxin related compounds to the distal region, delayed the abscission of debladed petioles and fruits (Addicott, 1982). Additionally, Addicott and Lynch (1951) also described studies where auxin applied to the proximal portion of an explant accelerated abscission. Shoji *et al.* (1951) measured by bioassay the extractable auxin activity in beans leaflets and leaf petioles, and found that the amount of auxin activity in the leaflets was three fold higher than in the petioles and dropped after the leaflet abscised, while in the petiole the auxin activity remained the same .

Changes in auxin activity lead to the auxin gradient theory for abscission initiation, which was proposed in the middle of the fifties by Addicott, Lynch and Carns (1955). This theory postulates that abscission is regulated endogenously by a gradient of auxin across the AZ and that abscission only takes place when the “normal gradient” (higher activity of auxin in the distal region and lower in the proximal), is disrupted or when the gradient is reversed (Figure 8).

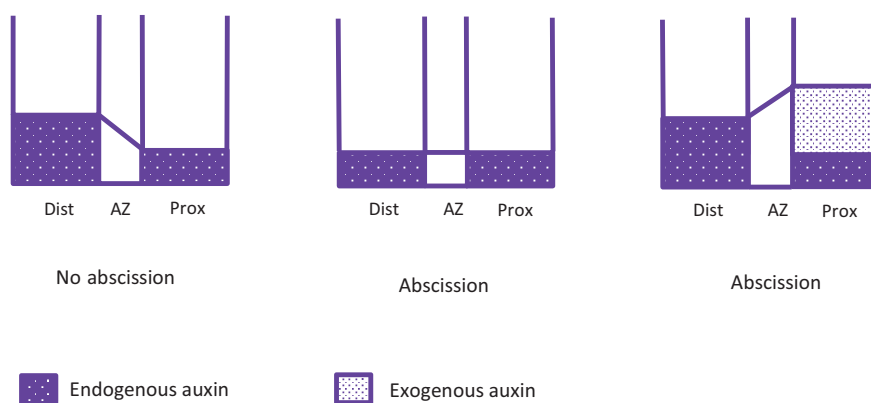


Fig. 8 Theory of auxin gradient requirement for abscission initiation; figure re-drawn from Addicott *et al.* (1955).

Basu *et al.* (2013) were able to manipulate the auxin levels within the AZ cells by using an AZ-specific promotor (polygalacturonase At2g41850) fused to 2 different bacterial

genes. The first gene, *iaaM*, encodes an indole-3-acetamide biosynthesis gene, tryptophan 2-monooxygenase, whose expression increased the auxin level in the AZ, and the second bacterial gene, *iaaL*; indoleacetate-lysine synthetase, decreased auxin levels by conjugation to a form poorly hydrolyzed by most plants. The authors showed that in those transformants with less auxin in the AZ, abscission occurred well before than those with elevated auxin. Genetic evidence extending our understanding of the importance of auxin in regulating abscission was reported by Ellis *et al.* (2005), who demonstrated that *Arabidopsis* mutants in the auxin response factor 1 and 2 (*arf1* and *arf2*) genes exhibited delayed senescence and abscission.

The role of auxin in controlling the degradation of pectin by regulated intracellular transport of the enzyme polygalacturonase (PG) to the middle lamella of the cell wall during abscission was shown by Degan *et al.* (2001). Meir *et al.* (2010) investigated how the transcriptome of the tomato flower AZ changed after auxin related genes were down-regulated following removal of the flower. This action caused flower AZ acquired sensitivity to ethylene, and consequently auxin and ethylene-related transcription factors as well as many other genes with regulatory functions were affected. They showed that application of auxin inhibited these changes in the transcriptome induced by the excision of the flower, suggesting that the acquisition of the sensitivity to ethylene was connected with the changes in expression of auxin-regulated genes.

Many lines of evidence have shown the importance of auxin in abscission; however, an auxin gradient disruption within the AZ zone has not been reported by analytical measurements so far. A great deal of the current comprehension of the response to auxin within the plant has been obtained using molecular constructs containing a reporter system. One of the first of these reporter systems was DR5 (Ulmasov *et al.*, 1997) which is a synthetic auxin responsive element linked to a reporter such as green fluorescent protein (GFP), producing fluorescence in response to auxin. Another example of this type of auxin reporter construct is DII-VENUS (Brunoud *et al.*, 2012), which uses a 35S promoter linked to an auxin co-receptor fused to the fluorescent molecule VENUS, promoting its degradation in the presence of the hormone. These reporter systems (reviewed in Tivendale and Cohen, 2015) have helped to increase our knowledge about auxin responsive tissues, however they do not actually measure the endogenous content of auxin (Liao *et al.*, 2015).

The response to auxin is dependent on both the local concentration as well as the responsiveness of the tissue to that auxin concentration (Li et al., 2013; Shi et al., 2015). Because of this inter-relationship, it is critically important to determine the actual concentration of the hormone in target cells. The necessity to quantify the levels of auxin within specific groups of cells is given by the fact that it is widely recognized that the morphogenetic effects of auxin are tightly linked to their distribution (Uggla et al., 1996).

The amount of plant material needed in order to perform a quantification of auxin, although decreasing dramatically over time, remains high relative to the resolution required for visualization of endogenous auxin gradients. The new technologies in mass spectrometry has permitted the lowering in the amount of initial material required and, at the same time, increasing the sensitivity (Tivendale and Cohen, 2015). The advent of SRM techniques, which is a targeted variant of MS/MS, increased even greater the selectivity and, by reduction of background interference, afforded higher sensitivity, thus taking auxin quantification to levels never before imagined (Liu et al., 2012). A main challenge when quantifying auxin is its low concentration in plant tissues, on the range of 5-50 ng/g of fresh weight (FW) (Porfírio et al., 2016) and furthermore its tendency to degradation during purification.

This thesis includes the development of methodology that tackles the low-level detection issues required for auxin quantification in small sections of plants, dissected by laser microdissection. The methodology is a harvesting procedure that combines the use of cryosectioning and freeze-drying in order to preserve the plant tissue, avoid disruption of spatial relationships and limit and account for auxin degradation. It employs LMD for small sample collection to add the tissue specificity required to collect precisely the abscission zone cell layers.

1.3.2 Regulation of abscission by the balance of ethylene and auxin

In the previous section the controlling role of auxin in abscission was discussed, however, auxin is not the only important hormone in regulating abscission, other growth regulators also play important roles, among them ethylene. Ethylene is small aliphatic unsaturated gaseous hydrocarbon that regulates fruit, leaf and petal abscission (Addicott, 1982). Ethylene applied externally induces abscission in many plant systems, moreover it has been reported that endogenous ethylene increases just before abscission occurs.

Girardin was the first to report of street trees becoming defoliated due to stress in places where the street light has gas leaks in 1864 (ref from Sexton *et al*, 1985). After that, correlation involving ethylene and abscission have been confirmed innumerable times in different species and organs (Sexton et al., 1985). More evidence of the involvement of ethylene in abscission came from studies using chemicals that interfere with the action of ethylene such as STS (silver thiosulphate) or the ethylene biosynthesis such as AVG (aminoethoxyvinylglycine). These compounds delay or inhibit abscission in different experimental systems (Abeles et al., 1992). A different line of evidence comes from the discovery of mutants like the tomato *Never-ripe (Nr)* that show delayed abscission (Tucker et al., 1984). The *NR* gene encodes the response regulator domain of the ethylene receptor ETR-1, so these mutants fail in the perception of the hormone (Wilkinson et al., 1995). More recently, evidence that ethylene induces the expression of genes related with cell wall transformation such as beta-xylosidase (Ruperti et al., 2002a), pectate lyase (Cheng et al., 2015) and cellulase (Tucker et al., 1988) show that ethylene also participates in the cell separation phase of abscission.

In spite of all the data in favor of the involvement of ethylene in abscission control, strong evidence that ethylene is not indispensable for abscission to occur is available with the use of mutants that are insensitive to ethylene. Arabidopsis mutant *etr1* and *ein2*, showed a delay in the flower abscission, however they eventually experienced all the stages in the abscission of a wild type plant (Ecker, 1995; Bleecker and Patterson, 1997) implying that the role of ethylene in abscission might be expendable. Likewise, reports of some fruits such as oil palm fruit, exhibiting a delay in abscission when ethephon, an ethylene releasing chemical was applied (Chan et al., 1972), or some flowers that abscise their organs without apparent intervention of ethylene (Sexton et al., 2000), challenge the strict view of ethylene as an accelerator of abscission.

According to Van Doorn (2002), poinsettias flower are highly sensitive to external applications of ethylene, which induces abscission. These results are not in agreement with previous findings in Hvostlef-Eide's group, where intact poinsettia plants did not induce abscised flowers (Munster, 2006). Munster found that ethylene only affected poinsettia flowers when they have been induced to abscise through decapitation. In such cases when the decapitation occurs below the floral bottom, the application of ethylene induced a displaced AZ, similar to the explant bean case of Webster and Leopold (1972).

The current accepted model regarding the interplay between auxin and ethylene states that the auxin status in the AZ influences the sensitivity to ethylene, additionally ethylene inhibit the auxin activity by restricting its transport and increasing its degradation, rising the sensitivity to itself (Taylor and Whitelaw, 2001). The balance of auxin-ethylene, or hormone-ethylene balance, as they called it, was introduced for the first time by Gawadi and Avery in 1950; they claimed that since ethylene induced aging in young leaves and since the auxin exhibited an inhibitory effect in abscission, the abscission was the result of the unbalance between these two substances. This theory was tested by Hall in 1952 who showed that exogenous ethylene induced abscission even in immature young leaves that were supposed to be high in auxin content, ethylene also induced abscission in petioles, however when the petioles were treated simultaneously with auxin, the abscission was reduced. Rubinstein and Leopold (1963) stated that abscission could be divided in two stages regarding to the effect of auxin, in the first stage auxin retard abscission, while in the second stage auxin promotes it. The authors applied high concentration of auxin to bean petioles explants and intact petioles at different times after the leaf de-blading, either in the distal or in the proximal side to the AZ. They discovered that auxin provoked opposite responses just depending on the time of the application. Auxin applied just after the leaf removal retarded the abscission and auxin applied after 6 hours provoked acceleration of the abscission.

The observations made by Rubinstein and Leopold (1963) together with another hormone physiologists lead to the claim that the stage 1 was the period in which application of auxin retard the abscission, when application of auxin are delayed, auxin is unable to retard abscission and the explant entered to the stage 2. From an ethylene point of view, the stage 1 represent the time when the explants are insensitive to this hormone and the stage 2 refers to the time in the process when the explants become sensitive to ethylene. Taylor and Whitelaw (2001) summarized these findings where auxin regulate the sensitivity to ethylene in the first stage and consequently ethylene regulates the sensitivity itself by inhibiting the transport of auxin or induce its degradation or conjugation (Burg, 1968; Beyer and Morgan, 1971). After the stage 1 and stage 2, together denominated lag phase, a separation phase is initiated, where the break strength decline because of the action of ethylene (Dela Fuente and Leopold, 1969).

The role of auxin and ethylene in abscission has been addressed recently in a transcriptomic study in tomato flower pedicel. Meir *et al.* (2010) investigated the effect of auxin depletion by flower removal in the acquisition of ethylene sensitivity. External applications of auxin and pre-treatment with 1-MCP were also evaluated. Another transcriptomic study that explored the cross talk between auxin and ethylene was performed by Kim *et al.* (2016). They assessed the changes in gene expression on the AZ in soybean leaves after remove the leaf blade, the authors used ethylene to induce the abscission. They found a great deal of TFs related with maintenance of cell fate, organ polarity and lateral growth.

The study of the crosstalk between ethylene and auxin is not new, however, only recently the molecular mechanism that explain the manner by which these two hormones regulate each other is starting show up. A study revealed that AVG, an inhibitor of the ACC synthase, also inhibit the auxin biosynthesis by inhibiting the enzyme tryptophan aminotransferase that catalyze the pass of tryptophan to indole-3-pyruvic (IPyA), which is a substrate for YUCCA (Soeno *et al.*, 2010). Another study explored the connection between ethylene and auxin biosynthesis (Zheng *et al.*, 2013), described that mutations in the pyridoxal-phosphate-dependent aminotransferase *VAS1* alters the pools of auxin and the ethylene precursor 1-aminocyclopropane-1-carboxylate. *vas1* plants present simultaneously decreased levels of auxin and ethylene since *VAS1* uses one intermediate from the ethylene biosynthesis and another from the auxin biosynthetic pathway to produce L-tryptophan and 2-oxo-4-methylthiobutyric acid.

1.4 Genetic control of abscission

1.4.1 Genes involved in pre-abscission events

Organ abscission is the result of a highly coordinated series of events, thus it is somewhat predictable that many genes would be involved during the whole of events that are part of the process. From the initial phase of AZ differentiation, passing through the acquisition of competence to respond to abscission signals to the activation of abscission, and continuing until the last step involving the protective layer formation (Bleecker and Patterson, 1997; Estornell *et al.*, 2013), an abundant array of diverse genes have been described as taking part. Much of our current understanding of how abscission is

controlled comes from the use of reference plant systems and the available mutants that fail or partially fail in abscise their organs.

The first gene described as having a role in the formation of the abscission zone in tomato pedicel was JOINTLESS (J), a mutation in J affects a MADS-Box transcriptional factor (Mao et al., 2000). Another MADS-box transcriptional factor, MACROCALIX (MC) is also needed to develop the AZ in tomato and it was demonstrated that both J and MC interact in order to develop a functional abscission zone in the tomato pedicel (Nakano et al., 2012). With *Arabidopsis* the use of mutants from T-DNA insertion lines has led to the proposal that there are two pathways leading to abscission. The pathway dependent on ethylene was described in the ethylene receptor mutant *etr1-1*, which showed insensitivity to ethylene, as well as delayed abscission, but where abscission was not completely blocked (Bleecker and Patterson, 1997). Another *Arabidopsis* mutant with delayed but not fully blocked abscission, is Ethylene-insensitive (*ein2*), which is involved in ethylene signaling (Ecker, 1995). Additionally, an ethylene-independent pathway has been proposed by the study of mutants *dab* with delayed abscission, but yet sensitive to ethylene (Patterson and Bleecker, 2004).

The clarification on how the activation of abscission takes place has enormous implications, since it opens up the possibility to control the process, not only with external agents such as hormones or a mixture of compounds, but also from the inside of the plant using genetic tools.

Work aimed toward unravelling genes that regulate abscission compared differences between primary abscission in pea and the secondary abscission in poinsettia (Hvoslef-Eide et al., 2016). Using a combination AFLP-DD and qRT-PCR, they discovered 18 putative genes involved in secondary abscission, out of which 6 were also localized using RNA *in situ* hybridization in the AZ of wild type pea (*Pisum sativum*) and its mutant Developmental funiculus (*def*), which has an abscission-less zone. The riboprobe targets were only present in the *def* mutant, and included an unknown region of chromosome 5, the transcript of the Opie3 pol protein, a transcription factor, photosystem II subunit X or UVB-repressible protein and an unknown mitochondrial genome region (Hvoslef-Eide et al., 2016). Only one riboprobe target was found in wild type pea, with two Blast results, organ-specific protein and atypical receptor-like kinase. These results suggest that primary

and secondary abscission are likely governed by common mechanisms (Hvoslef-Eide et al., 2016).

1.4.2 Molecular pathways in *Arabidopsis*

Arabidopsis thaliana has been of great importance in order to establish some of the molecular mechanisms underlying abscission. Much of the research that has established what we currently know about the molecular mechanism underlying flower abscission is coming from research done in *Arabidopsis* (Tranbarger et al., 2017).

The cascade that triggers the activation of the abscission zone program has been better elucidated in recent years. It starts with the activation of the leucine rich repeats receptor-like kinase (LRR-RLK) HAE/HSL1 (Jinn et al., 2000) by the IDA peptide (Butenko et al., 2003). Plants that overexpress IDA exhibit premature organ abscission, secretion of a polysaccharide type arabinogalactan and augmented number of rounded cells in the AZ Stenvik et al. 2006. The IDA peptide activates downstream an, as yet, unknown MAPKKK, which in turn activates the MAP kinase cascade MKK4/5 and MPK3/6 (Cho et al., 2008). This activation leads to suppress the KNOTTED-Like Homeobox protein KNAT1, allowing KNAT2 and KNAT6 to induce the genes leading to cell separation within the abscission zone cells (Shi et al., 2011; Butenko et al., 2012). Even though the study of the signaling cascade has been mainly done in *Arabidopsis*, orthologous of some of these genes, such as the IDA peptide and its receptor kinase HAESA, have being found across species, suggesting that the function of this signaling cascade regarding organ shed has been conserved (Butenko et al., 2003; Stø et al., 2015).

A TF involved in the activation of the abscission is AGAMOUS-like 15 (AGL15), a MADS- BOX TF. When it is constitutively expressed under the control of a strong promotor, it showed a delayed abscission in petals and sepals, but abscised the floral organs when external applications of ethylene were carried out, implying that did not affect the ethylene perception (Fernandez et al., 2000). The authors hypothesize that since AGL15 is normally accumulated in juvenile tissues, its function is to maintain that state repressing aging and senescence. Another AGL TF that accumulates preferentially in immature tissue is the AGL18, plants with overexpression of this TF exhibit delayed abscission and senescence (Adamczyk et al., 2007).

The activation of the abscission encompasses the coordination of several processes; components of the abscission-signaling cascade need to be transported in vesicles from the trans-Golgi network to the cell membrane, likewise there is endocytosis of the cell wall components coming from the disassembly of the cell wall. In addition to this, the activation of the abscission involves the transcription of the cell separation genes, such as polygalacturonases and pectinases among others. Thus, it is not surprising that the activation of the abscission involves different types of genes. A gene that have been studied in relation to the trafficking of molecules during the activations is NEVERSHED (NEV). The NEV is an ADP-ribosylation factor GTPase-activating protein (ARF-GAP) and ARF-GAPs are trafficking regulators. Mutations in NEV block the trafficking of molecules for the cell separation. As the result of the mutation, the AZ cells in *nev* mutants do not undergo expansion and separation and they stay cytoplasmatic and small and the abscission does not occur (Liljegren et al., 2009). By performing a screening of genotypes that rescue the lack of the abscission in the *nev* flowers, three protein kinases have been described as inhibitors of abscission: SOMATIC EMBRYOGENESIS RECEPTOR-LIKE KINASE 1 (SERK1) (Lewis et al., 2010), EVERSHED (EVR) (Leslie et al., 2010) and CAST AWAY (CST) (Burr et al., 2011). Besides the rescue of abscission in the *nev* flowers by these mutants (*nev serk1*, *nev evr* and *nev cst*), the AZ cells present an enlargement and disorganization in the majority of the double mutants (Liljegren, 2012). It has been proposed that these protein kinases act repressing in some way the HAE and HSL2 signaling by inducing the internalization of these receptors (Burr et al., 2011).

In primary abscission, the ontogeny of the AZs occurs early in the plant development and is located normally at the base of the organs to abscise. The AZ cells are characterized by the small size and lack of vacuoles compared to the adjacent tissues (Addicott, 1982). The activation of the abscission process occurs under certain stimuli, either environmental or developmental (Taylor and Whitelaw, 2001). Under these cues, the AZ cells start a program that leads them to increase in size and undergo a series of biochemical changes that ends up with the dissolution of the middle lamella between the cells and the organ detachment (Bleecker and Patterson, 1997). The third stage in the abscission process correspond to the trans-differentiation of the protective layer, which includes suberization of the scar tissue (Addicott, 1982).

During the formation of the AZ in *Arabidopsis* the genes BLADE ON PETIOLE 1 (*BOP1*) and *BOP2* have a preponderant role, double mutants plants of these genes (*bop1/bop2*) which affect a TF that induces asymmetry, fail to develop a functional AZ (McKim et al., 2008). Another TF described as participating this time in the placement of the AZ in sepals and petals in *Arabidopsis thaliana*, is the ASYMMETRIC LEAVES 1 (*AS1*), a member of the MYB transcription factor family. The *as1* plants exhibit an altered pattern of positioning of the AZs towards the distal region and a subsequent delay in abscission of the medial sepals (Gubert et al., 2014).

A diagrammatic depiction of the genes involved in the different steps in the abscission of *Arabidopsis* is given in Figure 9. The progression of abscission has been divided in 3 major processes: 1) Ontogeny of the AZ, 2) Activation of the abscission and 3) Trans differentiation of protective layer (Bleecker and Patterson, 1997). Afterwards, Patterson added the step of competence to respond to abscission signals before the activation of the abscission (Patterson, 2001).

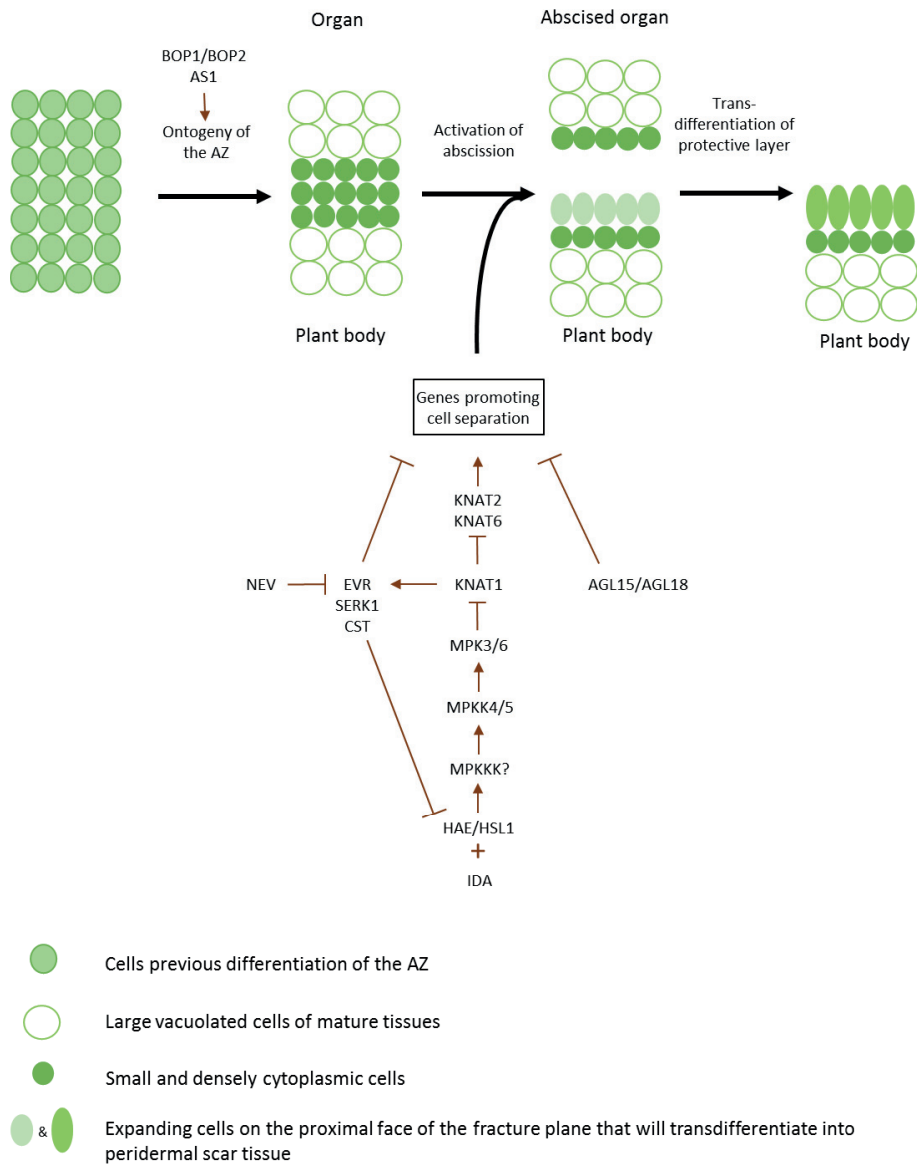


Fig.9 Schematic representation modified from Estornell *et al.* 2013 of some of the genes reported as participating in the abscission in the model plant *Arabidopsis thaliana*. Blunt ends lines express inhibitory effect and arrows activation.

1.4.3 Cell wall remodeling during abscission

Undoubtedly, the most remarkable feature of any process involving abscission is the plasticity of the cell wall of the cells involved in the separation. The primary cell wall is composed of hemicellulose, cellulose and pectin arrangement, with some glycoproteins (Lashbrook and Cai, 2008; Daher and Braybrook, 2015). Likewise, pectin is not a simple polysaccharide, but composed by three main galacturonic acid polymers: HG (homogalacturonan), RG-I (rhamnogalacturonan-I) and RG-II (rhamnogalacturonan II) (Atmodjo et al., 2013). The AZ cells undergo weakening because of middle lamella dissolution, this weakening eventually leads to the complete separation in the fracture plane located in the AZ separation layer (Sexton et al., 1977). The middle lamella is composed of pectic polysaccharides that help to maintain cell adhesion (Ridley et al., 2001). Middle lamella dissolution was one of the first features described by the early botanists (Lee, 1911) because in most cases it is the first place to undergo modifications that can be visually assessed (Bornman, 1967). Morre (1968), for instance, detected dissolution of pectic substances in the abscission zone of explants and leaves of bean. After changes in the middle lamella, the task of not only degrading but also remodeling the primary cell wall is a process involving several proteins. The primary cell wall complexity requires the intervention of a suite of enzymes that degrade the pectin, cellulose and hemicellulose polymers with the aim to facilitate complete organ detachment.

The elucidation of the participation of cell wall transformation proteins has been a matter of intense research over decades. Much evidence has been accumulated regarding the participation of a number of proteins such as PGs (EC 3.2.1.15) (Riov, 1974; Atkinson et al., 2002; Gonzalez-Carranza et al., 2007; Jiang et al., 2008), cellulases or endo- β -1,4-glucanases (EC 3.2.1.4) (Abeles, 1969; del Campillo and Bennett, 1996; Tucker et al., 2007), expansins (Merkouroupoulos and Shirsat, 2003; Cai and Lashbrook, 2008), expansins (Cho and Cosgrove, 2000), beta -galactosidases (Wu and Burns, 2004; Corbacho et al., 2013), beta-glucosidases (Agusti et al., 2009; Corbacho et al., 2013), xylosidases (Ruperti et al., 2002b; Li et al., 2015), XTH (Agusti et al., 2009; Wang et al., 2013; Li et al., 2015; Tsuchiya et al., 2015) and pectin esterases (Ratner et al., 1969; Wang et al., 2005).

PGs cleave the α -1,4-glycosidic bonds of α -galacturonic acids, one of the components of pectin; Riov (1974) detected increased PG activity in citrus leaf explants

during abscission. Virus-induced gene silencing (VIGS) of the gene family of PGs in the tomato petiole inhibited abscission (Jiang et al., 2008) and a T-DNA insertion to silence a PG gene in *Arabidopsis* delayed abscission, but did not stop it completely, most likely because of the high redundancy within the gene family members (Gonzalez-Carranza et al., 2007). Additionally, the overexpression of PGs in apple produced various phenotypes, included one with changes in the abscission of its leaves (Atkinson et al., 2002).

Cellulase, or endo- β -1,4-glucanases, are enzymes that catalyse the endohydrolysis of (1 \rightarrow 4)- β -D-glucosidic linkages in cellulose. Abeles (1969) reported increased cellulase activity in the abscission zones of bean, cotton and coleus explants. Six cellulase genes were later isolated from tomato and after investigating the expression of three of them, it was shown that they had different patterns of expression during the abscission process (del Campillo and Bennett, 1996).

Extensins are another type of protein participating in the transformation of the cell wall during abscission; Cai and Lashbrook (2008) showed that extensins were up-regulated in the stamen AZ of *Arabidopsis*. Merkourpoulos and Shirsat (2003) reported extensin gene expression by using a GUS reporter gene construct targeted to the floral AZ in *Arabidopsis*.

Three cDNA fragments of the beta-galactosidase gene were found in a cDNA subtraction library constructed from AZs of mature orange (Wu and Burns, 2004), this gene was also up-regulated in the AZ of melon during the early stages of abscission induction (Corbacho et al., 2013). XTH catalyses the lysis of the xyloglucan polymers belonging to cell wall hemicellulose. Using northern blotting, the differential expression of two XTHs was shown to be related to abscission progress in the petal of rose (Singh et al., 2011).

Several studies have detected an increment in the expression of genes involved with cell wall metabolism in the AZs of the tomato flower pedicel (Wang et al., 2013), litchi fruit AZ (Li et al., 2015) and citrus leaves AZs (Agusti et al., 2009). β -xylosidases catalyse the cleavage of xylose residues from xylan polysaccharides, one of the component of hemicellulose. A transcript for a β -xylosidase was isolated from a cDNA library constructed from AZs of *Prunus persica* L. Batsch as ethylene responsive probably induced by wounding (Ruperti et al., 2002b). Additionally, in a genome-wide transcript analysis performed in litchi tree, a β -xylosidase gene transcript was up-regulated in the fruit AZ (Li et al., 2015).

Recently a comparative transcriptomic analysis at cell type resolution was reported where they examined abscising and non-abscising tissue during ethylene-promoted abscission. This work established highly conserved roles during abscission for gene family members related to cell wall degradation. (Merelo et al., 2017).

1.5 Omics technologies

1.5.1 General consideration when working with omics technologies

Omics technologies including transcriptomic and proteomic, along with allied methods, are emerging technologies for understanding the behavior of cells, tissues, organs, and the whole organism at the molecular level and provide a holistic approach to the study of physiological issues by detecting a large family of the mRNAs and proteins in a living system. Built on a foundation of computational biology and bioinformatics, they form a critical part of all systems biology approaches and these technologies have the potential to facilitate the development of predictive models for understanding complex developmental changes. While traditional approaches have focused primarily on hypothesis-driven experimental design and as a consequence are a focused reductionist approach, omics technologies are often described as data-driven and/or hypothesis-generating. Both approaches are inherently complementary and can enrich each other because a complex system can either be dissected in small parts to understand it or, in contrast, be defined as a dynamic system (Kell and Oliver, 2003).

One of the main challenges when handling results coming from omics experiments is to properly analyze the inferences that can be made out of the complex datasets generated, especially where ‘multi-level’ omic analyses are employed (Haas et al., 2017). Omic experiments like transcriptomic and proteomic, aim to show variations in transcript or proteins levels that span over several orders of magnitude. The enormous data generated by omics experiments needs appropriate statistical analysis that enable to see the changes of hundreds or thousands genes or proteins simultaneously. The volcano plots, for instance help to visualize those analytes that are statistically significant (low FDR) and with high fold changes (\log_2FC) (Oveland et al., 2015). Another statistical tool used to visualize the multivariate omic experiments is the heatmap, which shows the expression matrix of all the transcripts at the same time (Gehlenborg et al., 2010).

In contrast to most traditional hypothesis-driven science, an inductive approach, which uses the data to generate new concepts or biological systems models, inverts the discovery process by moving from the effect to the cause (Brent, 1999).

This thesis uses two omics technologies in a non-model organism with the aim to test previous hypotheses in the study of abscission, including the role of cell wall transformation and auxin depletion in the process. Additionally, these experiments opened up new lines of study; for example the importance of secondary metabolism and defensive responses in the initiation of abscission.

1.5.2 Transcriptomic analysis in abscission

Transcriptomic or RNA Seq is a high-throughput technique that allows the comprehensive study of the gene transcripts at a given time point within a cell, a population of cells or an organism. The possibility to follow the fluctuations in expression of a high number of genes during a determined condition, arrived with the development of the microarray (Schena et al., 1995) and was improved upon with further new methodologies, like RNA Seq (Bainbridge et al., 2006). Abscission researchers utilized RNA Seq to study abscission for several reasons: first for its potential to apply to species without a sequenced genome, secondly because RNA Seq results are more comparable than the ones obtained with microarrays and thirdly, because the dynamic range of expression levels obtained in RNA Seq is larger than in microarrays (Weber, 2015).

When examining three transcriptomic studies in soybean, tomato and Arabidopsis, Kim *et al.* (2015) described an early up-regulation of gene transcripts encoding enzymes involved in the synthesis and secretion of molecules belonging to a wax cuticle-like material. These authors highlighted not only the cell wall disassembly process, but also the synthesis of the extracellular matrix. Nakano et al. (2012) performed transcriptome analysis of wild type tomato pedicel and compared two mutants, the (*macrocalix*) *mc*-suppressed transformant and a *j* (*jointless*) mutant, that failed to develop a complete AZ and thus exhibited an insufficient abscission. They found 743 ESTs preferentially expressed (at least a 2-fold change) in the wild type, clustered in four major functional groups: phyto-hormone-associated functions, cell wall modification, metabolism of fatty acids and other lipids and transcription factors. The *mc* and *j* mutant were characterized by down-

regulation of several transcription factors involved in the maintenance of shoot apical meristems and the initiation of axillary meristems .

In *Arabidopsis* stamens, Cai and Lasbrook (2008) noted 551 gene transcripts from the abscission zone that showed differential expression with a high level of significance, with a false discovery rate (FDR) equal to 0.0001. These transcripts were from genes including receptor-like kinases, hormone responses related genes, like auxin responsive genes and *PIN4* auxin efflux carrier, and ethylene responsive factors together with *ETHYLENE-INSENSITIVE PROTEIN 3-BINDING PROTEIN*. They also showed that the transcription factor *ZINC FINGER PROTEIN 2* was up-regulated in the AZ of the petals, sepals and stamens using a GUS reporter assay.

In a study involving the depletion of auxin by flower removal in tomato, Meir *et al.* (2010) were able to study the period where the abscission zone acquires its sensitivity to ethylene. They hypothesized that the ability to acquire sensitiveness to ethylene in the AZ was connected with the changed expression of the auxin-regulated genes. They found that flower removal caused a decrease in expression of Aux/IAA (auxin/indole acetic acid proteins) and that auxin application to the pedicel, with the flower removed, reverted the tissue back to their previous level of expression.

Many transcriptomic studies only consider the AZ, narrowing the process to this region of the organ, however Wang *et al.* (2013) used also the proximal and distal regions in the tomato pedicel, and they showed that the AZ had more DEG than the other pedicel regions. The authors also reported that the AZ preferentially expressed TFs, especially a high number of meristem activity regulators such as *WUSCHEL*, *KNAT6*, *LATERAL ORGAN BOUNDARIES DOMAIN PROTEIN 1*, and *BELL-like homeodomain protein 1*, together with the tomato axillary meristem genes *BLIND* and *LATERAL SUPPRESSOR*. They highlighted the putative role of these TFs in maintaining the meristematic stage of the AZ cells in agreement with their behavior during the abscission process.

1.5.3 Proteomics analysis in abscission

The life of an organism is characterized by dynamic changes in the proteome necessitated by the needs for responding to environmental and developmental events and for general cellular maintenance. The proteome, the sum total of all encoded gene products, is studied by the emerging area of proteomic which aims at the identification

and quantification of all the proteins in an organism (Zhang et al., 2013). There are different approaches in proteomics, thus, choosing the most suitable for each case study should consider the limitations and strengths of each technique, together with the best possible option to solve the biological problem. Additionally, it is important to consider the available technical support, including bioinformatics resources.

Plant proteomics have been used to unravel the complex chloroplast proteome in *Arabidopsis*, showing both that one third of the proteins are with unknown function and also identifying proteins unpredicted to localize in the chloroplast (Kleffmann et al., 2004). Another branch of proteomics, phosphoproteomics, deals with the most studied post-translational modification, the phosphorylation of proteins that lead to regulation of their activity (Reinders and Sickmann, 2005). The regulatory mechanisms for innate responses in *Arabidopsis* was investigated using a quantitative approach with phosphoproteomics leading to the discovery of new phosphorylated proteins with role in defense (Nühse et al., 2007).

Despite the large number of studies approaching the changes in gene expression using high throughput transcriptome during the abscission process, the number of papers engaged in investigating on a large scale the proteins acting as effectors during the abscission, is relatively very low. However, small scale studies of the proteins involved in abscission is not new; Abeles and Holm (1967) were pioneers studying the increase of RNA and protein synthesis during the abscission of bean explants stimulated by ethylene. Since that time, much of the efforts have been done to unravel the proteins involved in abscission focused on cell wall transformation effectors during the process. Del Campillo and Lewis (1992) studied the protein accumulation in the bean AZ and they showed seven (PRs) proteins assembled as abscission progressed.

An important large scale proteomic study was performed on abscission tissue by Zhang et al. (2015) using tomato pedicels treated with ethylene or 1-MCP (1-methylcyclopropene), an inhibitor of ethylene response. The authors used the quantitative labeling method iTRAQ coupled with LC-MS/MS (liquid chromatography-tandem mass spectrometry), in order to study changes in protein and phosphoprotein abundance during abscission. They showed that 166 proteins and 73 phosphoproteins were significantly differentially regulated, and with a fold change higher than 1.5. The majority of these proteins were involved in metabolic processes and exhibited known catalytic activity,

while the phosphoproteins were involved in transport and signaling. The identified phosphoproteins showed that a web of kinases and phosphatases were involved in responding to the ethylene treatment.

2. Aim of this thesis

The main aim of this thesis was to shed light on poinsettia flower abscission using two approaches. The first one was to provide a methodology to sample plant tissue for auxin analysis and the second one was to explore the variations in proteins and mRNA abundances during the poinsettia flower abscission.

Paper 1 The main objective of this paper was to devise a harvesting methodology of plant tissue for auxin content quantification in order to demonstrate that it was feasible to obtain direct measurements of the auxin content of specific cells that make the abscission zone. The methodology combined cryosectioning, freeze-drying the sections and harvesting discrete tissues using a LMD, thus allowing for maintaining the integrity of the content of auxin in plant tissues.

Paper 2 The main objective of this paper was to study the dynamic changes within the proteome of the abscission zone, as well as within its distal and proximal regions in the poinsettia flower bud during abscission.

Specific objectives were:

- To assess the decapitation effect in the flower bud
- To find potential effectors of the changes at the different stages in the progression of abscission

Paper 3 The main objective of this paper was to assess the changes in the transcriptome of the abscission zone and adjacent regions of the poinsettia flower bud during abscission.

Specific objectives were:

- To find candidate genes controlling the abscission process by comparing the transcriptomes in a spatial-temporal fashion
- To evaluate the decapitation effect on expression of auxin-related genes
- To evaluate the spatial-temporal expression of cell wall transformation genes
- To look for the *IDA* gene and a potential change in expression

3. Experimental approaches used in this thesis

3.1 Induction of the abscission by decapitation of the floral organs

The induction of abscission in a synchronized fashion due to the decapitation of the floral organs is a methodology that has been used as the basis for synchronizing the abscission of flower buds in poinsettia, facilitating the study of a controlled system comparable to natural abscission. The advantage of this reproducible and inducible system is that it allows a reliable and accurate following up of the processes leading to the formation of the abscission zone, and permits harvesting of the material at any time during the process. This methodology was developed at NMBU by Munster (2006) and has been the basis for detailed poinsettia abscission analysis since its description (Lee et al., 2008; Hvoslef-Eide et al., 2016). The method relies on the correct removal of the floral organs at a specific point (called cutting point 2; Figure 10A), by removal of all floral organs, but not the floral bottom.

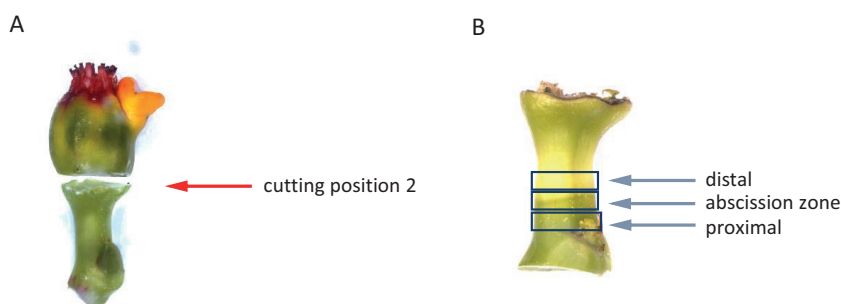


Fig. 10 A) Removal of the floral organs of the poinsettia flower bud, red arrow shows the exact point where the decapitation has to be done to induce the abscission of the remaining pedicel. **B)** Flower bud decapitated and with a visible abscission after five days, the blue arrows show the distinctive tissues harvested in this thesis.

If the decapitation is done in correctly, close to 100% of the decapitated buds form an abscission zone in the flower bud in the predicted location. This zone, once formed, determines also the adjacent areas, the distal portion, corresponding to the part of the bud that will be detached and the proximal part, which will remain attached to the body of the plant (Figure 10B).

The induction of abscission by flower decapitation was used in all manuscripts of this thesis, in order to provide concise and reproducible plant material for the auxin quantification, proteomics and transcriptomic papers.

3.2 Spatial-temporal approach

The three manuscripts forming this thesis each used this system to induce abscission of the flower bud. In the first manuscript, only abscission zone at two time points (Day 0 and Day 6) was used as a ‘proof of concept’ of the method to quantify the auxin levels. However, in the last two manuscripts harvest time points in between these extremes were also included (Day 0, Day 2, Day 4 and Day 6). The adjacent tissues to the abscission zone, distal and proximal regions of the bud, were incorporated in these analyses. The harvest of the same tissues as the process progressed defined the temporal approach (Figure 11A), while the collection of the different portions of the bud, within one time point, characterized the spatial approach (Figure 11B). In the temporal analyses, the goal was to follow the changes in gene and protein expression taking place in the same tissue at different times in the progression of the abscission zone formation by comparing each portion of the bud with its previous stage. In the spatial approach, the abscission zone at every given time point was compared with the two adjacent tissues, to discover genes or proteins that specified each region in contrast to those shared by the abscission zone and the other two parts.

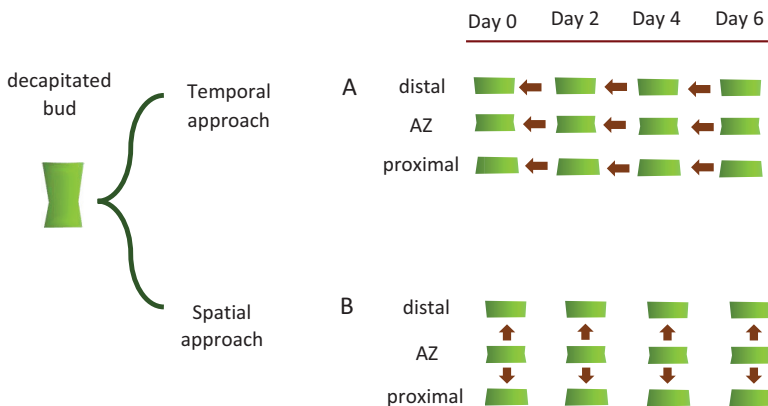


Fig. 11 Schematic representation of the temporal and spatial approaches used in this work. After decapitation of the floral organs in poinsettia, the tissues harvested were analyzed in two ways. **A)** Temporal scope considered the comparison of the same type of tissue over time. **B)** Spatial scope consisted in take the abscission zone as tissue to compare the adjacent ones at each time point. In each case, the arrows show the directionality of the comparisons done. AZ= abscission zone.

3.3 *De novo* transcriptome

Due to the lack of a reference genome for *E.pulcherrima*, a *de novo* transcriptome approach was used in this thesis. The several steps involved are explained in Figure 12 and below.

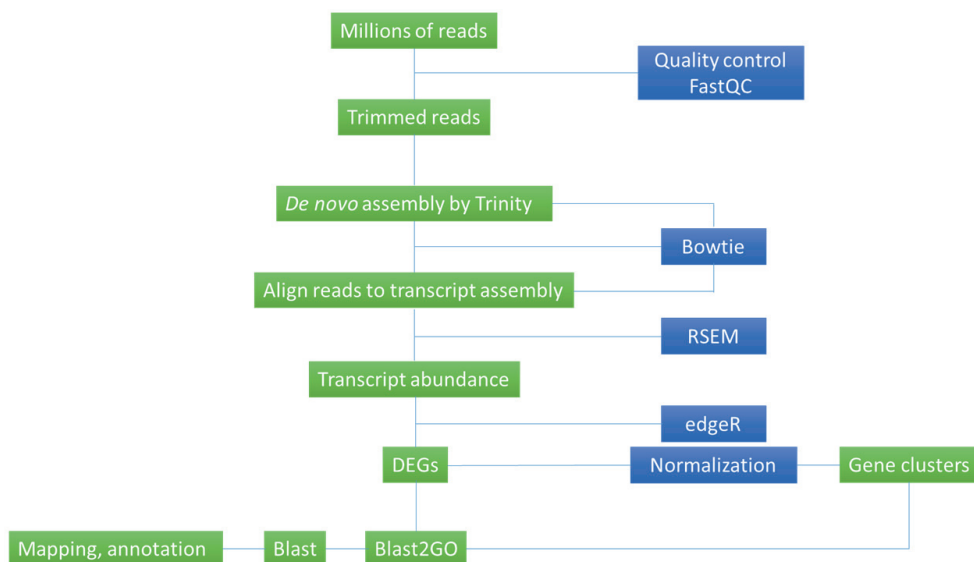


Fig. 12 Workflow of RNA sequence data analysis, DEGs Differentially expressed genes, edgeR, RSEM (RNA-Seq by Expectation Maximization) for transcriptome analysis in poinsettia abscission.

The RNA was sheared after isolation and reversely transcribed in order to construct a library of cDNA, which was sequenced by both ends (paired-end) of the cDNA using one

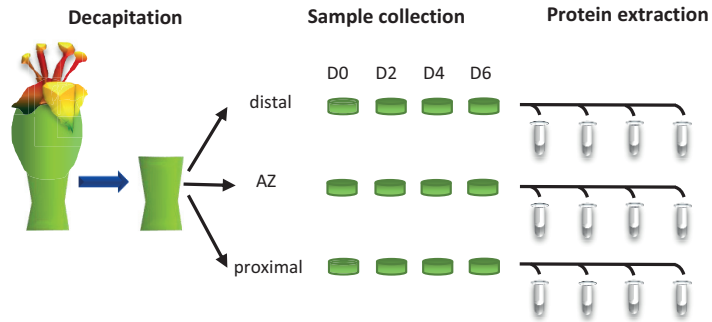
of the available NGS (Next generation sequencing) platforms; Illumina in this experiment. The short reads (90 bp) were checked for quality by using a set of parameters and the adapter was trimmed. Those reads with good quality were mapped to the transcriptome and then assembled into contiguous sequences (contigs). The abundance of each transcript was then quantified and then normalized according the length of the fragment: Fragments Per Kilobase Million (FPKM). After normalization, the levels of DEGs were detected according to the set of statistical parameters desired. Finally, the DEGs were annotated using different software programs and databases, such as Blast2GO (Conesa et al., 2005) (Figure 12).

3.4 Shotgun proteomic

The strategy selected for this work was a form of 'shotgun' proteomics (Figure 13), where a complex mixture of proteins (from each region and time point) from the protein extraction step was digested with trypsin; producing a mixture of tryptic peptides that were separated using liquid chromatography. These peptides were then ionized and mass analyzed by the mass spectrometer according to their m/z (mass to charge ratio), generating thousands of mass spectra. The most abundant ions (highest intensities of the mass spectrum peaks (MS)) go for a second round for fragmentation and separates the fragments by MS/MS yielding sequence specific characteristic fragmentations.

The resulting mass spectra were analyzed by a sophisticated software platform (MaxQuant) that incorporates a search engine (Andromeda) in order to find protein matches for the peptide sequences that have been analyzed during the run. The peptides identification is done by the tandem mass spectra comparison coming from the peptides fragmentation with the theoretical tandem mass spectra of an *in silico* protein digestion in a database. Perseus software was used for the statistical analysis (Tyanova et al., 2016). Shotgun proteomics was not only used for identification, but also for indirect quantification.

A



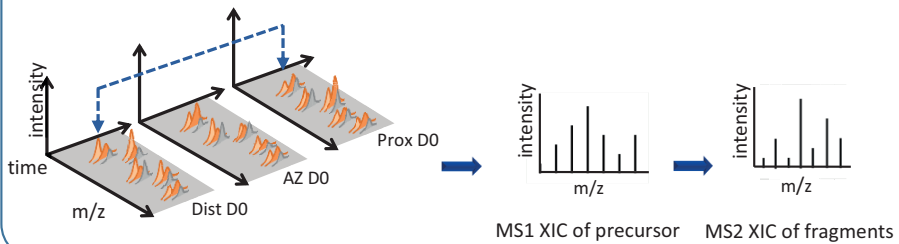
B Digestion and clean-up

Chromatographic separation of the peptides in LC-MS



C Quantification in full scan Max Quant (XIC)

Identification by the MS2 scan Andromeda (XIC)



D Statistical analysis, Perseus software

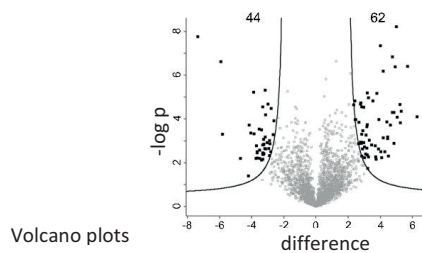
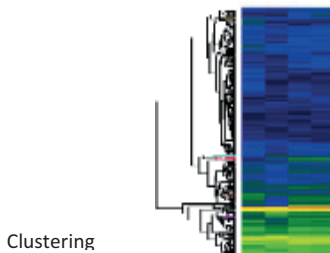


Fig 13. Steps in the shotgun proteomics experiment in a poinsettia flower bud. **A)** The first steps are floral organ decapitation, sample collection at different time points and flower bud regions and then the protein extraction. **B)** The mixture of proteins was lysed with a protease and the sample was cleaned-up to inject the peptides into the LC and detect by MS. **C)** The peptides produced are separated in the LC and analyzed with MS/MS producing thousands of mass spectra. These mass spectra are analyzed by software in order to find protein matches for the peptides that have been identified during the run. **D)** The statistical analysis is conducted using the software Perseus, hierarchical clustering and volcano plots are produced. AZ= abscission zone. D= day. XIC= extracted ion chromatogram.

4. Main results and discussion

4.1 Manuscript 1 Auxin analysis using laser microdissected plant tissues sections

Manuscript 1 describes the setup of a new methodology for the safe harvest of plant tissue for establishing a protocol to quantify auxin levels in small amounts of tissue. The methodology was applied to poinsettia flower buds AZs in two time points, Day 0 and Day 6. To maintain the tissue in a pristine state with as little degradation of auxin as possible, the methodology involves three steps; (1) tissue cryosectioning, (2) freeze-drying of cryosections and (3) specific AZ cells harvest with the LMD, using a pre-cooled aluminum stage to maintain low temperatures.

The protocol used to quantify the auxin levels in the samples collected using the methodology set in paper 1 is based on solid-phase extraction (SPE) and GC triple-quadrupole MS (GC-MS/MS) (Liu et al., 2012). This quantification protocol is currently the one that requires the least amount of tissue (Porfírio et al., 2016), from 2 to 20 mg, but had previously only been tested on fresh or frozen tissue. This manuscript reports the first attempt with plant material harvested using laser microdissection of freeze-dried cryosections.

In manuscript 1 we demonstrated that using this kind of harvesting methodology, the tissue integrity was preserved as needed to localize the AZ cells and minimize auxin degradation and diffusion. Different thickness of the cryosectioned tissues were evaluated according to two parameters: 1) feasibility to be microdissected by the laser and 2) feasibility to identify the target cells (AZ), the thickness that fulfilled with these two requirements was 250 μm and this allowed the possibility to secure the amount of plant tissue needed to run the quantification protocol.

The areas collected using the LMD microscope were for the D0 $61.8 \pm 1.92 \text{ mm}^2$ and for the D6 $54.9 \pm 1.25 \text{ mm}^2$, corresponding to $15.4 \pm 0.48 \text{ mg}$ and $13.7 \pm 0.31 \text{ mg}$, respectively. The results of the auxin quantification with the LMD samples for D0 was $2.68 \pm 0.62 \text{ ng/g FW}$ and for D6 was $3.34 \pm 0.81 \text{ ng/g FW}$. These results were validated using cryosections (cross-sectioned tissues of 250 μm) of the AZ of the same time points, but not freeze-dried and not harvested with LMD. The samples harvested in this way showed an auxin content of $19.92 \pm 8.7 \text{ ng/g FW}$ for the D0 and $3.33 \pm 0.29 \text{ ng/g FW}$ for the D6 and

were in the same order of magnitude as the samples studied with the new harvesting methodology detailed in manuscript 1.

The importance of being able to quantify the levels of auxin within the AZ is crucial because auxins have been designated as the major factor controlling abscission in the hypothesis termed “Theory of auxin gradient in abscission initiation” which states that “Auxin is the principal endogenous regulator of abscission; its gradient across the abscission zone regulates the onset and rate of abscission. Abscission does not occur with auxin gradients characteristic of healthy, mature tissue: with high auxin distal to the abscission zone and low auxin proximal to the abscission zone. Abscission occurs after a fall in the ratio of distal to proximal auxin. Abscission is accelerated when the gradient is reversed” (Addicott et al., 1955).

Addicott *et al.* (1955) postulated this theory based on extensive work both from his laboratory as well as other reports who described the retardant effect of auxin and auxin induced delays in abscission when it was applied to whole branches or the distal part of the organs (La Rue, 1936; Gardner et al., 1940; Gardner and Cooper, 1943; Shoji et al., 1951). While this theory persist regarding the gradient of auxin within the AZ, definitive analyses with analytical methods have not as yet been reported.

Gradients of morphogenic compounds are postulated to be the positional signal for several developmental processes, such as patterning of vascular tissues (Ye, 2002) and the induction of root primordia (Overvoorde et al., 2010). However little analytical evidence has been presented. Uggla et al 1996 showed the existence of a radial auxin gradient in a transversal section of cambium in *Pinus sylvestris*, this gradient might be responsible for secondary growth. Using GC-MS and cryosectioning, they described that in the meristematic cambium zone, the auxin levels reached between 3 to 6 $\mu\text{g/g}$ FW decreasing to 80 ng/g FW in the xylem and phloem. The highest concentration is three orders of magnitude higher than our results, however the authors showed that the decrease from 3 to 6 $\mu\text{g/g}$ FW to 80 ng/g FW occurs in only 250 μm in radial distance, showing the large variation of auxin values within a few cell layers (Uggla et al., 1996).

The methodology set in manuscript 1 opens up the possibility to collect specific groups of cells to quantify the actual auxin levels in discrete tissues in order to characterize the gradients over small distances, like differentiation of meristems. The methodology proved to be suitable to collect AZs tissues from two stages of development in poinsettia

flower buds, however, the direct comparison between both AZs at the two different time points is not relevant to defining auxin gradients, because the adjacent regions above and below the AZ were not used for the quantification. The effect of auxin as a morphogen is not necessarily linked to absolute levels, but it is possible the gradient within the tissues defines a specific morphological characteristic. Another important issue to consider when measuring auxin levels in plant tissues is that the content of auxin in a plant is highly variable, possibly in response to environmental perturbations, (Michalczuk et al., 1992; Rapparini et al., 2002), so plants need to be grown under highly controlled conditions. It is expected that this methodology will help to unravel questions about the content of auxin and spatial relationships, not only in the AZs, but also in the adjacent regions of the AZ.

Even though this methodology was designed to assist in the harvesting of plant material for auxin quantification, we also used it to harvest the AZ and adjacent regions distal and proximal for RNA isolation to perform the transcriptomic analysis of manuscript 3. Thus, this methodology has also proved its suitability to maintain RNA integrity. The methodology has the potential for a plethora of uses where plant tissue from small areas is needed while maintaining the tissue in as pristine condition as possible.

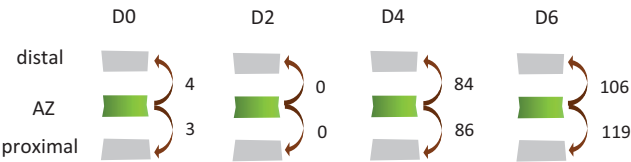
4.2 Manuscript 2 Proteomics

This manuscript details the changes in protein abundances that occur in poinsettia flower buds during the course of the abscission process. Three regions of the flower bud were assessed, the AZ and the adjacent regions distal and proximal. The same regions were compared over a period of six days for the temporal scope (Figure 12B). For the spatial comparisons, the AZ of each time point was compared with the other two regions distal and proximal (Figure 14A).

Changes in the protein abundances in the spatial comparisons were visible on D4 and D6 (Figure 14A) while in the temporal comparisons, the differences were seen only up till D4 (Figure 14B). The parameters for establishing which proteins changed their abundances was a FDR of 0.01 and a fold change ≥ 2 , under these conditions 3086 proteins changed their abundances.

The number of protein sequences from poinsettia in databases is extremely low, reaching only 572 in the National Center for Biotechnology Information (NCBI) (<https://www.ncbi.nlm.nih.gov/protein/?term=euphorbia%20pulcherrima>) to September 2018 therefore, the protein annotation was performed using a database created as an outcome of the transcriptomic study (manuscript 3). A file with the longest coding DNA sequences (cds) was uploaded to the software for the protein statistical analysis to match the protein sequences with the differential abundances.

A



B

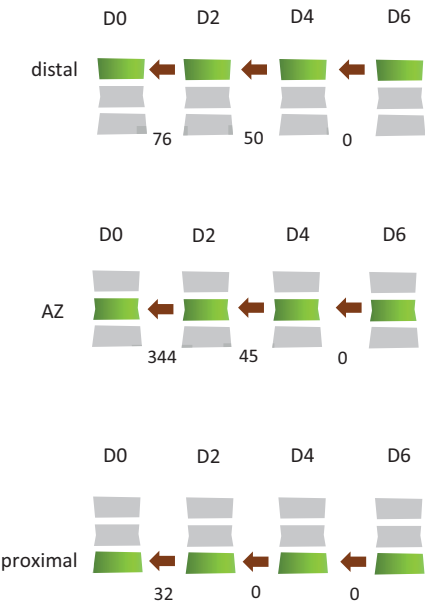


Fig. 14 Depiction of changes in protein abundances during **A)** Spatial comparisons and **B)** Temporal comparisons. The arrows indicate the comparison directionality and the digits show the numbers of proteins varying in abundances. Green color indicates the flower bud region compared.

After identifying which proteins increased or decreased during the six days, and their location, it was possible to hypothesize which processes had taken place during abscission of poinsettia flower buds.

4.2.1 Processes occurring on Day 2 according to the temporal comparisons

It was surprising to see that the distal region responded less abruptly to the decapitation than the AZ. The temporal comparison showed that the AZ on D2 had the highest number of protein changes compared to the AZ on D0 (control), 285 proteins were reduced in abundance. It seems that the AZ had the highest number of proteins decreasing than any other region after the decapitation. This probably resulted from the shutting down of several anabolic processes such as photosynthesis, sugar metabolism and protein biosynthesis (Figure 15A).

Proteins with a putative role in cell wall transformations and stress responses increased the first two days in the AZ as well as in the distal region (Figure 15B). Additionally, we observed that the three regions of the bud on D2 revealed a defensive response of similar proportions (26 to 29%, data in manuscript 2) compared to the D0 (Figure 15C). The increased abundance of enzymes in secondary metabolism picked up on D2 in the three regions of the bud can be interpreted as a part of the defensive response observed on D2 (Figure 15C). Proteins from primary metabolism, including carbohydrate, lipid, nucleotide, amino acid and one carbon metabolism, increased their abundances during the D2 (Figure 15C).

D2

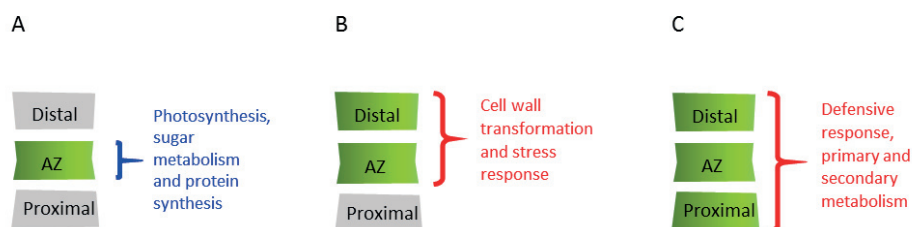


Fig. 15 Schematic representation of the processes occurring in the different regions of the poinsettia flower bud during D2. In green, the regions that were affected by the events described in the legend. Legend in blue, those processes that are catalyzed by proteins that decreased in abundance and the legend in red are the processes that showed an increase in protein abundance. **A)** Processes impaired in the AZ D2. **B)** Processes with increased numbers of proteins in the AZ and the distal region. **C)** Processes with increased number of proteins in the three regions studied.

4.2.2 Processes occurring on Day 4 according to the temporal comparisons

The changes in the amount of proteins leading up to D4 was only noticeable in the distal region and the AZ. Some of the processes already started leading up to D2, continued to increase up to D4, for example, more enzymes from cell wall transformation, secondary metabolism and proteins from primary metabolism and stress response increased their abundances (Figure 16).

D4

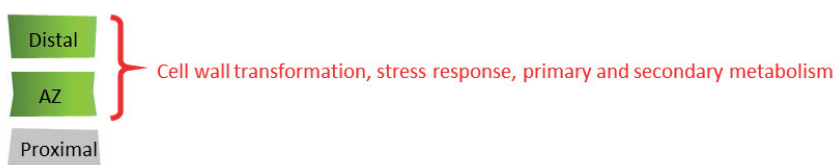


Fig. 16 Schematic representation of the processes occurring on the D4 in the AZ and the distal region of the poinsettia flower bud. Red legend represents the increase of protein abundances in the processes stated.

4.2.3 Processes occurring in the AZ according to the spatial comparisons on D4 and D6

Spatial comparisons between the AZ and its adjacent regions, distal and proximal, indicate that secondary metabolism seems to be the main feature of the AZ on D4 and D6 (Figure 17A and B). More than ten enzymes from the phenylpropanoid biosynthetic pathway increased their abundances within the AZ on D4 and D6 (Supplementary Material number 3, 4 and 5 manuscript 2 proteomic). The phenylpropanoid pathway leads to the synthesis of many polyphenolic compounds, such as flavonoids and anthocyanidins, as well as lignin.

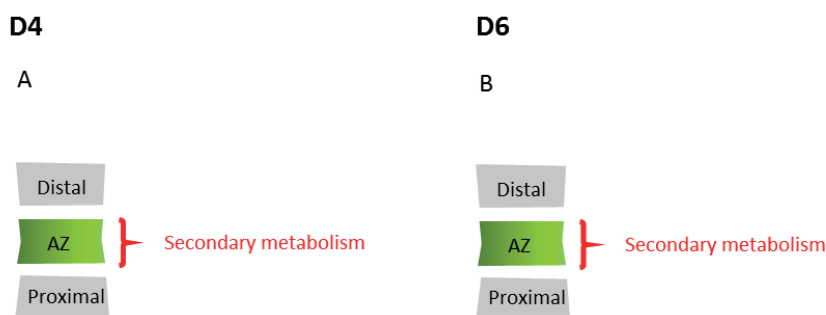


Fig. 17 Schematic representation of the processes occurring in the AZ as shown by the spatial comparisons. Legend in red represents the increase in abundance of proteins from the process stated. **A)** AZ D4 and **B)** AZ D6.

The temporal comparison on D2 as well as the spatial comparisons on D4 and D6 showed the increase in the proteins of secondary metabolism. Previous studies using FT-IR and phloroglucinol-HCl staining in poinsettia flower buds, revealed that the AZ on D7 had lignified tissue (Lee et al., 2008), however these analysis were performed only in D0 and D7, so no information about lignin deposition in between had been reported before. We think that the lignification of the AZ starts leading up to D2, as part of the defensive responses and continues until abscission. Lignin might be a protective layer creating a physical barrier for protection from potential microorganism invasion after organ detachment. Lignin deposition also has been documented in bean leaf abscission after deblading (Poovaiah, 1974). On the other hand, the tomato pedicel transcriptome, using

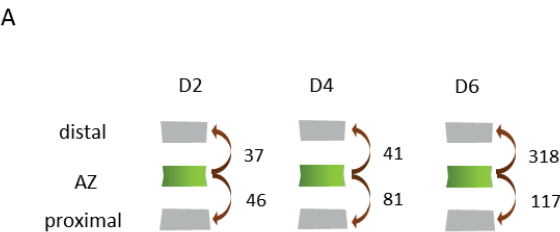
the distal, proximal and AZ regions, showed a decrease in secondary metabolism genes in the AZ (Wang et al., 2013).

4.3 Manuscript 3 Transcriptomic

In the third manuscript, we scrutinized the changes in gene expression occurring during poinsettia flower abscission. The experimental layout was the same as in the proteomic manuscript. Four-day points and three flower pedicel regions were analyzed. Using a level of significance of 0.001 and a fold change of 2, a total of 22101 transcripts changed their expression. There is no reference genome for poinsettia, thus a *de novo* assembly was used to map back the reads obtained after the sequencing.

The AZ on D2 and AZ on D4 showed, based spatial comparisons, a similar number of DEG (Figure 18A), however the AZ on D6 seems very much different from the adjacent regions. It was surprising to see that the spatial comparisons were less informative than the temporal comparisons. If we had performed the temporal comparisons using the D0 as a standard control, it likely would have provided additional DEG, but we decided to use the previous state of each time point as a control in order to follow the processes along the time line during abscission.

The temporal comparisons show the most dramatic change in expression during the transition from the D0 to D2. The three regions of the flower bud expressed more than 5000 DEGs (Figure 18B). When examining whether these DEG were mainly up or down-regulated genes, we observed that the down-regulation contributed by far the most to the number of DEG (Figure 4, manuscript 3).



B

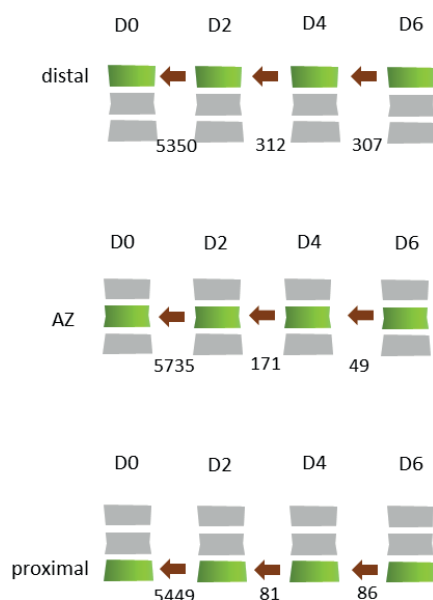


Fig. 18 Depiction summarizing the differentially expressed genes results in the **A)** Spatial comparisons and the **B)** Temporal comparisons of the poinsettia flower bud. The arrows indicate the directionality of the comparison and the digits show the numbers of transcripts changing in expression. Green color indicates the flower bud region compared.

These results suggest that the main changes leading to abscission in the poinsettia flower bud occur early in the process (D2) and this results seems to match with those obtained with proteomic comparisons, where the AZ at D2 was where the most dramatic changes in abundances were found (manuscript 2). It is also in concurrence with previous results in poinsettia (Munster, 2006; Hvoslef-Eide et al., 2016).

The enrichment analysis performed in the AZ on D2, D4 and D6 showed which Gene Ontology (GO) terms were highly represented at each time point. Responses to stress, immune system process and cell wall organization were some of the GO terms overrepresented in the AZ on D2. In AZ on D4, cell wall organization and carbohydrate metabolism were the only two GO terms while in AZ on D6 several GO terms related to macromolecule biosynthesis, such as translation, organic substance biosynthesis and gene expression (Figure 19).

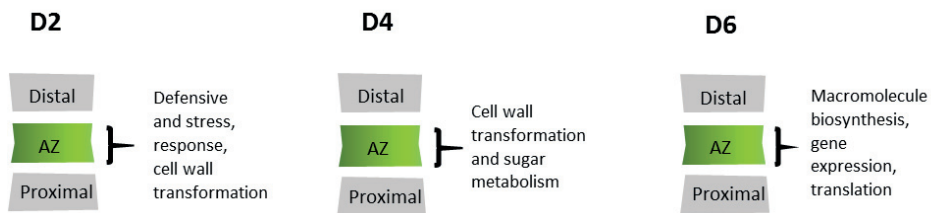


Fig. 19 Scheme showing the GO terms enriched in the AZ at different time points. In green, the AZs.

The manuscript also describes the changes in auxin-related genes in the AZ during the D2, as well as cell wall transformation genes and genes from the abscission-signaling cascade.

4.4 Comparative results between proteomics and transcriptomic studies in abscission

The cell proteome and transcriptome are very dynamic. The fluctuations in the abundances of proteins, as well as expressed genes, reflect how the cell keeps pace with environmental cues. Investigating only one aspect of cellular dynamics gives a fragmented picture of how the cell regulates itself. In this thesis, the proteomic and the transcriptomic experiments share the same experimental layout. Therefore, it is interesting to compare how these two experimental datasets can be compared with each other regarding changes in the number of proteins and expressed genes.

The first feature that catches attention is the low protein number (3086 proteins) detected varying in abundances in the proteomic experiments compared to the transcriptomic experiment (22101 transcripts). Different FDRs were used in both experiments, to reduce the number of hits. $FDR \leq 0.001$ was chosen over 0.01 in the transcriptomic experiment to decrease the transcripts number to a more manageable number, and a $FDR \leq 0.01$ was used in the proteomic experiment, as we still obtained a manageable number. This is an indication of the comprehensive nature of the transcriptomic analysis. As a result of the higher number of transcripts, we also found a

higher diversity in expressed genes compared to proteins; receptors, modulators of activity such as kinases and phosphatases and an impressive number of TFs were discovered differentially expressed (manuscript 3). While proteins with functions in signaling, such as receptors and MAPKs and a TF were discovered in low numbers only in the AZ D2 (manuscript 2).

The results from the spatial comparisons between the proteomic and the transcriptomic experiments showed that the protein and transcript number increased along the time points, reaching the highest number on D6 (Table 2). The temporal comparisons in contrast showed the biggest change on D2 in both experiments, even though the magnitude of the expressed gene transcripts is higher than the proteins (Table 3). Considering that D2 exhibited the biggest change in transcripts and proteins, we hypothesize that the events leading to organ abscission in poinsettia start during the first two days after the induction.

Another difference between the outcomes of both experiments is that the transcriptomic experiment found DEG in all the comparisons and time points (Figure 16A and B), while in proteomic data there are some time points where the experiment did not detect changes.

Table 2 Comparison among transcripts and proteins number in the spatial scope in the transcriptomic and proteomic experiments.

| | | Total spatial | | | |
|-------------|--|---------------|------------|------------|------------|
| | | D2 | | D4 | |
| | | AZ vs Dist | AZ vs Prox | AZ vs Dist | AZ vs Prox |
| transcripts | | 37 | 46 | 41 | 81 |
| proteins | | 0 | 0 | 84 | 86 |

Table 3 Comparison among transcripts and proteins number in the temporal scope in the transcriptomic and proteomic experiments.

| | | Total temporal | | | | | | | | |
|-------------|--|----------------|------|------|------|-----|------|------|----|------|
| | | D2 | | | D4 | | | D6 | | |
| | | Dist | AZ | Prox | Dist | AZ | Prox | Dist | AZ | Prox |
| transcripts | | 5350 | 5735 | 5449 | 312 | 171 | 81 | 307 | 49 | 86 |
| proteins | | 76 | 344 | 32 | 50 | 45 | 0 | 0 | 0 | 0 |

There is no other research combining transcriptome and proteome analysis in abscission, to our knowledge. However, there are surveys comparing gene and protein levels in other processes and species. Many of these studies have discovered surprisingly poor correlations. In a study about the correlation between the protein and gene levels in two *Streptococcus pyogenes* morphotypes (planktonic and biofilm), it was shown that only 46 genes and 41 proteins regularly changed their abundances through the biofilms and the planktonic stage. However, the overlap between them was very low. The authors used the abundance values and normalized them using the z-score, to eventually calculate the Pearson coefficient among them. The coefficient values ranged from 0.279 to 0.539 (Freiberg et al., 2016). Gygi *et al.* (1999) obtained a very high Pearson correlation coefficient (0.93) when studied yeast growing in mid-log phase and compared the abundances of 106 proteins with their correspondent mRNA, however the authors point out that this coefficient is biased by the characteristic of the data set itself, which included few genes with very high levels of protein and messengers. The authors explained that by using a more representative subset of the data set, the Pearson correlation coefficient dropped to 0.356, in addition they found up to a 30 fold change difference in some proteins.

In order to compare these two experiments, we selected the proteins and transcripts that increased in abundance during the transition from D0 to D2, and as the region of highest interest, we chose the AZ. The number of up-regulated transcripts on the AZ D2 compared to the AZ D0 was 1382 (manuscript 3) while the number of proteins that increased their abundances was only 59 (manuscript 2). These two datasets overlap in only 24 transcripts/proteins. Using their relative levels of abundance (Log2 (abundance in

D2/abundance D0)), the Pearson correlation coefficient was calculated (Table 4). The Pearson coefficient was 0.4040 and $R^2 = 0.1632$ (Figure 20). This indicates a modest correlation between these two set of values.

Table 4 Relative abundances of protein and transcripts (Log₂ FC) during the transition between Day 0 to Day 2 in the poinsettia flower AZ.

| Gene product | Log ₂ FC protein | Log ₂ FC transcript |
|---|-----------------------------|--------------------------------|
| wound-induced protein win1 | 3.45 | 8.33 |
| thaumatin-like protein 1b | 6.61 | 8.60 |
| peroxisomal -2-hydroxy-acid oxidase glo4-like | 5.59 | 5.37 |
| peroxisomal -2-hydroxy-acid oxidase glo4-like | 5.59 | 4.65 |
| caffeoyl- o-methyltransferase | 3.32 | 4.57 |
| caffeoyl- o-methyltransferase | 3.32 | 4.55 |
| caffeoyl- o-methyltransferase | 3.32 | 4.17 |
| caffeoyl- o-methyltransferase | 3.32 | 4.56 |
| carbonic chloroplastic-like | 3.91 | 11.14 |
| carbonic chloroplastic-like | 3.91 | 11.53 |
| chlorophyllase partial | 6.13 | 4.75 |
| cysteine proteinase rd21a-like | 3.92 | 3.07 |
| cysteine proteinase rd21a-like | 3.92 | 3.12 |
| endochitinase pr4-like | 5.94 | 11.95 |
| endochitinase pr4-like | 5.94 | 10.58 |
| endochitinase pr4-like | 5.94 | 12.04 |
| endochitinase pr4-like | 5.94 | 11.28 |
| flavanone 3-hydroxylase | 5.32 | 3.25 |
| glucan endo- -beta-glucosidase-like | 2.87 | 4.61 |
| glucan endo- -beta-glucosidase-like | 2.87 | 4.81 |
| No ID | 3.16 | 6.60 |
| No ID | 3.16 | 6.02 |

| | | |
|-------|------|------|
| No ID | 3.16 | 6.61 |
| No ID | 3.16 | 7.15 |

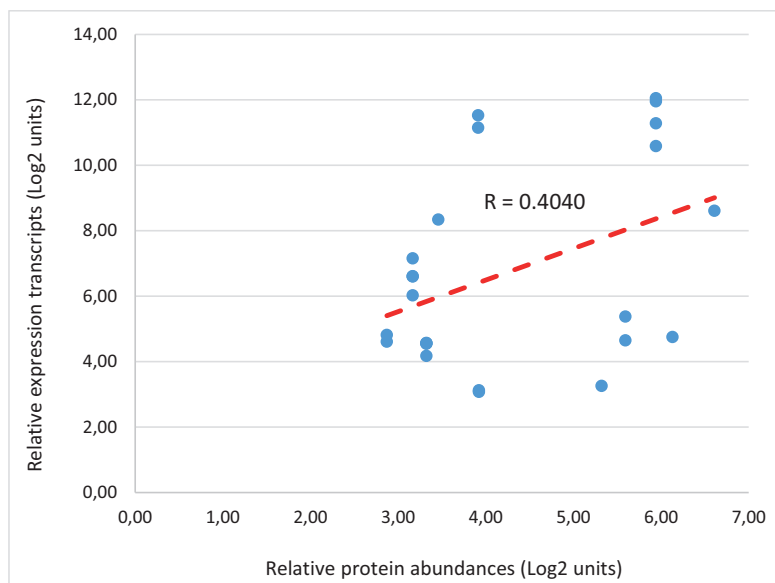


Fig. 20 Plot showing the correlation between the relative protein abundances and the relative expression for 24 transcripts/proteins from the AZ D2 compared to the AZ D0 in poinsettia flower bud. The red dash-line is the trend line and R is the Pearson coefficient.

The correlation between protein and mRNA levels do not match, this might be attributable to the fact that the protein and mRNA levels are regulated in different way. Synthesis and degradation both contribute to the size of the pool of each transcript and each protein within the cell. Protein levels are regulated by the levels of transcripts, but also at translation, post-translational modifications and regulated degradation. Transcription is regulated by factors as efficiency of promoters (Bingham et al., 1986), secondary structures of mRNA that affect the ribosome affinity (Grossman et al., 1985) and modulators of transcription such as the sRNA (Storz et al., 2005). The life span of a transcript is believed to be in some cases shorter than a protein life span, for example *E.coli* RNA showed half-lives between 3-8 minutes in some cases (Bernstein et al., 2002). Not all

the proteins turnover at the same rate (Yang et al., 2010), some proteins, such as TFs have shorter life spans (Belle et al., 2006), while others have very long life span, such as histones (around a hundred days) (Piha et al., 1966).

While the transcriptome experiment gave a more comprehensive overview than the proteomic experiment, it is also true that the transcriptome required more bioinformatics resources, because of the amount of data generated. Additionally, the functional characterization often applied in transcriptomic experiments, such as the Gene Ontology terms is based in protein databases, thus these two sources of information can be compared.

Even though the number of DEG and protein abundances are quite different in both experiments, it is possible to see some elements that are convergent, for example, the transcripts, as well as proteins, from the stress response and some (PRs) proteins increased during the first two days. These results lead us to think that, disregarding the low overlap between transcripts and proteins, the combination of both approaches could be the best way to get a better understanding of the sum of the biochemical reactions (metabolic turn over) that leads to abscission.

4.5 Abscission signaling cascade elements are present in poinsettia

The peptide IDA regulates floral abscission in *Arabidopsis* (Butenko et al., 2003). This discovery was a step forward in the understanding of how abscission is regulated and controlled. The *ida* mutant fails to abscise its floral organs in an ethylene independent manner. Estornell *et al.* (2015) found that the orthologous gene *CitIDA3*, when overexpressed in *Arabidopsis*, results in flowers that exhibited early abscission. Furthermore, orthologous IDA and its receptor HAESA and HAESA-like are widespread within the angiosperms (Stø et al., 2015). These results suggest that the IDA signaling organization is widespread across the plant kingdom.

Our group previously searched for IDA presence in poinsettia in a targeted fashion, however the result was negative (data not published). Additionally, when gene expression in poinsettia during abscission was studied using AFLP-DD, the research did not shed light on the presence of IDA in poinsettia (Hvoslef-Eide et al., 2016). This result lead us previously to think that poinsettia flower abscission might use a different control

mechanism for abscission, since *IDA* is responsible for the floral organs abscission, including filament, sepal and petals abscission and poinsettia does not have petals nor sepal at all. However, the use of a high throughput technology such as RNA-Seq, allowed us to discover the gene *IDA* also in poinsettia and its differential expression across the different flower bud regions, as well as in the timing of its expression (manuscript 3).

We think that the increase of *IDA* expression was not visible in the previously performed AFLP-DD because it is a less sensitive technique than RNA Seq, and also the arbitrary primers used only covered around 80% of the genome. The IDA peptide is the ligand of the leucine-rich repeat-like kinase (LRR-RLK) HAESA (HAE) and HAESA-like 2 (HSL2) receptors, located in the cell membrane. In the transcriptome analysis, we found that IDA was up-regulated on in the distal region on D4 respect to the D2 (manuscript 3). Moreover, we found the receptor HAESA (receptor-like protein kinase 5) down-regulated at D2 in the AZ and in the distal and proximal regions (temporal comparisons), suggesting that different elements from this signaling cascade exhibit different timing (manuscript 3).

Downstream of the HAESA and HAESA-like receptors abscission signaling continues with a phosphorelay of a mitogen activated protein kinase (MAPK) cascade (Cho et al 2008). The activation of a putative MAPKKK activates the MKK4/5, which in turn activates MPK3/6. Our proteomic study revealed that the MKK5 (mitogen-activated protein kinase kinase 5-like) was down-regulated in the AZ on D2 (manuscript 2). The MPK3 (mitogen-activated protein kinase 3) was down-regulated in the AZ on D2 and in the proximal region on D2, during the temporal comparisons (manuscript 3). We speculate that because down-regulation of these members of the MAPK cascade occurred 2 days before the activation of the cascade by the IDA peptide, that their down-regulation might be related to another process ongoing in the cell. Both kinases, MKK5 and MPK3 participate in defensive response (Asai et al 2002) and MPK3 also participates in abiotic stress response (Kovtun et al. 2000), which suggests the postulate that their down-regulation is the consequence of the decapitation more than as part of the activation of the abscission signaling cascade. This explanation is supported by the high redundancy of functions among members of the MAPK cascade (Taj et al 2010).

4.6 AZ differentiation in poinsettia might be caused by TFs regulating boundaries and meristem differentiation

In many species, the AZ is pre-defined long before the abscission takes place (primary abscission), and it is located in a boundary region, such as the base of the organ to be detached (Addicott, 1982). Thus, AZ differentiation happens long before the AZ activation. However, in poinsettia flowers the AZs differentiate just a few days before the actual detachment of the pedicel occurs (secondary abscission) (Munster, 2006). This allowed us to investigate the actual differentiation of the AZ as part of the process of induction of abscission.

The temporal comparison D0 vs D2 highlighted those TFs that were differentially expressed in relation to meristem maintenance, cell fate or boundaries formation (results coming from manuscript 3, but not shown on it, but in Table 5). Our results showed TFs regulators of meristematic function and boundaries not only in the AZ, but also in the adjacent regions, distal and proximal. These results are in contrast to another transcriptomic study using the same three regions, AZ, distal and proximal, in the tomato pedicel. That study found highly expressed shoot apical meristem activity TFs like WUSCHEL, KNAT 6, LOB domain protein 1, BELL like domain among others only in the AZ (Wang et al., 2013). We could interpret this as the difference between primary and secondary abscission, since tomato pedicel AZ is already preformed and there is evidence that the cells in the AZ maintain a meristematic state (Addicott, 1982), so may not be surprising to find TF regulators of meristematic function. In poinsettia, the AZ is not formed until a few days before the actual organ detachment, where the three regions of the flower bud have to undergo a dramatic reprogramming in a short time in order to develop a functional AZ. The fact that the formation of the AZ in poinsettia flower bud takes a few days starting from adult cells, highlights the plant cells' plasticity.

Several TFs control meristem differentiation and boundaries. Previous studies have probed mutations in boundaries TFs affect not only the development of the AZ, but also its functionality in different species. The gene *ARABIDOPSIS THALIANA HOMEBOX GENE1* (*ATH1*) codifies for a BEL1-type homeobox TF regulates the development of the stamen AZ in *Arabidopsis* (Gómez-Mena and Sablowski, 2008). Another example of a BEL1 type homeobox TFs regulating AZ formation is the gene *qSH1* whose single nucleotide mutation

produced the rice mutant that retained their grains (Konishi et al., 2006). Our temporal comparisons identified *BEL1-like* transcripts up-regulated on D2 in the AZ and the distal region, these findings make us believe that the boundaries between the AZ and distal during D2 are still in a developmental process with the assistance of these boundaries genes regulating cell differentiation.

Additionally, we found the TF regulatory protein npr5-like, also called BLADE ON PETIOLE (BOP) up-regulated only in the AZ on D2, suggesting a more specific role in the formation of the AZ in poinsettia. BOP has been shown to regulate the formation of the AZ in species such as *Arabidopsis* and tobacco (McKim et al., 2008; Wu et al., 2012). Boundaries TFs are not only crucial in controlling the formation of the AZ, but also in the activation or the separation stage (Hepworth and Pautot, 2015). The *cuc3* (*CUP-SHAPED COTYLEDON 3*) mutants have fused ovules, strongly suggesting that this TF plays a role in organ separation such as ovule separation in *Arabidopsis* (Goncalves et al., 2015). Furthermore, CUC3 participates in the initiation of axillary meristem and boundary maintenance in *Arabidopsis* embryos (Hibara et al., 2006). We showed that CUC3 was up-regulated in the three regions of the flower bud on D2. The differentiation of a functional AZ in the flower bud of poinsettia starts already on the D2 and requires TFs controlling cell fate and meristems in order to alter the architecture of the few cell layers that will become the functional AZ.

Table 5 List of transcriptional factor regulators of meristem differentiation and boundaries that are up-regulated during the D2 in the three regions of the poinsettia flower bud.

| Transcript | Gene product ID | distal | AZ | proximal |
|--------------------|--------------------------------------|--------|----|----------|
| >TR148562_c5_g1_i2 | bel1-like homeodomain protein 1 | X | | |
| >TR148562_c5_g1_i2 | bel1-like homeodomain protein 1 | | X | |
| >TR125796_c0_g1_i4 | bel1-like homeodomain protein 6 | | X | |
| >TR118410_c1_g1_i1 | bel1-like homeodomain protein 6 | | X | |
| >TR126292_c0_g1_i1 | regulatory protein npr5-like or BOP2 | | X | |
| >TR123391_c0_g1_i1 | regulatory protein npr5-like or BOP2 | | X | |
| >TR140702_c3_g2_i1 | protein cup-shaped cotyledon 3-like | X | | |
| >TR140702_c3_g2_i1 | protein cup-shaped cotyledon 3-like | | X | |

| | | | | |
|--------------------|---------------------------------------|---|---|---|
| >TR140702_c3_g2_i1 | protein cup-shaped cotyledon 3-like | | | X |
| >TR134173_c0_g1_i3 | protein cup-shaped cotyledon 3-like | X | | |
| >TR134173_c0_g1_i3 | protein cup-shaped cotyledon 3-like | | X | |
| >TR134173_c0_g1_i3 | protein cup-shaped cotyledon 3-like | | | X |
| >TR134173_c0_g1_i2 | protein cup-shaped cotyledon 3-like | X | | |
| >TR134173_c0_g1_i2 | protein cup-shaped cotyledon 3-like | | X | |
| >TR180785_c0_g1_i1 | lob domain-containing protein 15 | X | | |
| >TR180785_c0_g1_i1 | lob domain-containing protein 15 | | X | |
| >TR173408_c0_g1_i1 | lob domain-containing protein 15 | X | | |
| >TR173408_c0_g1_i1 | lob domain-containing protein 15 | | X | |
| >TR139584_c2_g1_i1 | lob domain-containing protein 18-like | X | | |
| >TR139584_c2_g1_i1 | lob domain-containing protein 18-like | | X | |
| >TR131135_c0_g2_i1 | lob domain-containing protein 18-like | X | | |
| >TR131135_c0_g2_i1 | lob domain-containing protein 18-like | | X | |

5 Integrated discussion of the results

5.1 Reflections when approaching a combined discussion in transcriptomic and proteomic

As this thesis contains two manuscripts that analyze the results of transcriptomic and proteomic experiments, it seems like an obvious step to correlate the transcripts levels with their proteins abundances to get a better understanding of abscission. However, several studies have probed the issue that these correlations are often quite modest, failing to offer a unifying comprehension of the biological problem under study (Chen et al., 2002; Freiberg et al., 2016). In this thesis, the calculation between mRNA levels and protein abundance was also carried out, primarily as a theoretical exercise. The proteins selected were those that increased in the AZ D2 relative to the AZ D0 and their respective genes. The results showed a Pearson correlation coefficient = 0.4040 (Figure 20). This correlation of around 0.4 is not typically regarded as high, since statisticians prefer above 0.5 to be excited, but does serves as an indication that there is some correlation after all. The relative low correlation also indicates potential differences in how the cell controls the different pools of proteins and transcripts. At least three factors contribute, either together or separately, to affect the relative low correlation between the pool of mRNA and proteins in the cells. The first one is the diverse post-transcriptional mechanisms to transform the mRNA into a protein; the second is the fact that proteins lifespans that can vary substantively and the third one is the intrinsic experimental error and biological noise in both type of experiments (Greenbaum et al., 2003).

An interesting example of post-transcriptional regulation is the case of the proteins that form the light harvesting complex (LHC). The light-harvesting chlorophyll a/b-protein is regulated not only at mRNA level and turnover, but also in the elongation step of the translation, when light is used as an additional control mechanism (Slovin and Tobin, 1982). A similar case is observed in oxygen deprivation in the roots of maize where a set of genes is preferentially translated under anaerobic conditions (Fennoy and Bailey-Serres, 1995).

The half-life of proteins was investigated by Doherty *et al.* (2009) by measuring the half-life of 600 human proteins and they discovered that the half-life values ranged from few minutes to tens of hours. Sharova *et al.* (2009) measured the half-live for mRNA in

mouse cells and discovered that the median was around 7h and also that the half-lives varied with the function of the transcript, TFs and signal transduction-related genes lasted less than structural or metabolic genes. The high turnover of TFs could explain why TFs were not detected at all in the proteomic experiment, but they were discovered abundantly in the transcriptomic study (Table 5, thesis document).

The transcriptomic and proteomic studies share the same biological layout. However, the high-throughput platforms from where the data was obtained were, of course, completely different. Most likely, these data sets will exhibit technical, biological, chemical and physical differences what make them difficult to combine. Therefore, the combination and integrated analysis of multi-omic dataset is still one of the foremost challenges in modern biology and it is in constant evolution (Kaeffer et al., 2014). Systems biology is the branch of biology that deals with the combination and integration of such huge dataset generated by omics experiments at different levels. Systems biology eventually aims to understand not only the structure, but also the dynamics of a living organism taking the entity as a whole and not just the combination of its parts (Kitano, 2002). In the future, strategies implementing a combination of a multi-level approach combined with artificial intelligence would provide an informed comprehension of the biological system (Haas et al., 2017). Undoubtedly, the next step in the race for understanding the biological systems and their dynamics is the use of combined datasets from -omics experiments; however, that task is beyond the defined goals of this thesis.

Using both -omics experimental approaches was beneficial to the study abscission in poinsettia because there is no simple technique that encompasses everything active in a biological process and our results are the best proof of this. We were able to look at different parts of a complex biological system by addressing it from different angles. The next section explores convergent features sharing the same functional context (Haider and Pal, 2013) in both datasets in order to describe the macro processes occurring in the flower bud that lead to organ detachment. Additionally, features captured only by one of both -omics approaches are also put into biological context.

5.2 Discussion of the results in a broader context

The two omics technologies based manuscripts of this thesis assessed the main changes in protein and transcripts levels during the induced abscission of the poinsettia

flower bud. Both experimental approaches shared the same biological layout (manuscript 2 and manuscript 3) and the discussion of the results are separately considered in each manuscript. However, it is possible to make some integrated inferences of the whole system by exploring, not only the correlations between them, but also the noted differences.

5.3 Integrated results from proteomic and transcriptomic on D2

The decapitation treatment triggered processes that led to the abscission of the flower bud in poinsettia, as described by Munster (2006) and in Lee *et al.* (2008). This phenomenon has been observed in several other experimental systems, for instance leaf deblading in soybean (Kuang *et al.*, 1992), flower removal and leaf deblading in *Mirabilis jalapa* (Meir *et al.*, 2006) and flower removal in tomato (Meir *et al.*, 2010).

We can speculate that the removal of the floral organs potentially led to the disruption of the auxin flux within the flower bud. The effects of this action are supported by the decrease of massive numbers of auxin-related genes in the three regions of the bud (Supplementary Material 2B, manuscript 3). Auxin transport seems to be affected as *PIN1* and *PIN8*, genes for auxin efflux transporters are down-regulated in the whole flower bud. *PIN1* has been implicated in transport of auxin during abscission in tomato (Shi *et al.*, 2017). Another down-regulated auxin-related gene was the *PINOID* (*PID*), a kinase that activates *PIN1*. Perturbation in auxin transport would be expected to result in changes in auxin maxima within the tissues, highlighting the importance of abscission as an auxin gradient process in plant development (Addicott *et al.*, 1955; Vanneste and Friml, 2009).

Some of the other auxin-related genes that were down-regulated are several repressors of auxin transcription (*Aux/IAA*), *ARFs*, auxin responsive genes and genes involved in auxin homeostasis (Supplementary Table 2B, manuscript 3). The total implications of the auxin depletion are not easy to address. However, Hvoslef-Eide investigated the effect of the auxin-transport inhibitor N-1-naphthylphthalamic acid (NPA) on intact buds and compared with both, decapitated buds and no decapitation and no NPA as controls. An acceleration in the abscission rate after treatment with increasing levels of NPA was found compared to the non-decapitated buds (Hvoslef-Eide unpublished results). These are clear indications of a role for auxin in poinsettia abscission.

Auxin stimulates almost every feature of plant cell growth and development, from cell division, cell extension and cell expansion to differentiation (Perrot-Rechenmann, 2010). Auxin induces expression of cell wall transformation (CWT) genes, like expansins (*EXP*), xyloglucan endotransglucosylase/hydrolase (*XTH*), pectin methylesterase (*PME*) among others (Majda and Robert, 2018), so it is not surprising that after the auxin transport flux was disrupted, more than 200 CWT genes diminished in their expression in the whole bud (Supplementary Material 3A).

We hypothesize, that decapitation also caused the defensive response observed both in proteomic (Figure 4 A, B and C, manuscript 2) and in transcriptomic (Figure 6A enrichment analysis, manuscript 3) data sets on D2. The defensive response was manifested with the increased levels of three enzymes of the jasmonic acid (JA) biosynthetic pathway, allene oxide synthase, allene oxide cyclase and 12-oxophytodienoate reductase (Turner et al., 2002) (Supplementary Material 2, manuscript 2). Another discovery which may have a link to a defensive response, is the production of pathogenesis related (PR) proteins (Stintzi et al., 1993) and the increase of secondary metabolism enzymes, particularly from the phenylpropanoid biosynthesis pathways (Dixon et al., 2002).

The putative increase in JA in the whole bud on D2 might explain the increase in secondary metabolism biosynthesis (Turner et al., 2002) and explain the PRs increase as well (Xu et al., 1994). However, the synergistic effect of JA and ethylene in defense responses is well documented (Zhu and Lee, 2015) While, it would not be surprising to discover that both hormones act together to orchestrate the responses above described, there is not sufficient evidence in favor of up-regulation ethylene biosynthesis pathways in either of the -omics studies. Only *ACC-oxidase*, one of the three genes involved in the ethylene biosynthetic pathway, was up-regulated in distal and AZ on D2 (data not shown).

JA is a known plant stress response regulator, promoting not only defensive responses, but also senescence (Kim et al., 2015a). A characteristic sign of senescence is chlorophyll degradation (Buchanan-Wollaston et al., 2003). The first enzyme in the chlorophyll degradation pathway is chlorophyllase (CHLASE), another gene induced by JA (Tsuchiya et al., 1999) together with defensive response genes. As with the defensive response proteins, CHLASE is also increased in the three regions of the bud at D2 (Supplementary Material 2, manuscript 2). The *CHLASE* gene was also up-regulated on D2

in the AZ (Table 4, thesis document) and in the other 2 regions (data not shown). Degradation of chlorophyll is also a sign of the preparation of the plant to discard an organ, as it will recycle all the nutrients it can before abscission. Thus, we infer that a preparation to degrade chlorophyll is occurring simultaneously to a defensive response at D2 in the three regions of the bud.

Together with a decrease in chlorophyll, one of the effects described for JA is the repression of photosynthesis-related genes (Reinbothe et al., 1994; Attaran et al., 2014). The same feature was observed in the AZ D2, with a massive fall in the levels of several proteins related to the Photosystem I and II, including proteins that form the antenna complex, such as chlorophyll a-b binding protein (Supplementary Material 1, manuscript 2). The impaired function of the photosynthetic apparatus and potential shutdown of photosynthesis might explain the decrease in proteins from the tricarboxylic acid (TCA) cycle, glycolysis, respiration and glyoxylate cycle which is also observed only in the AZ D2 (Figure 3, manuscript 2). However, the massive decrease in proteins from photosynthesis and carbohydrate metabolism seen in the AZ is not observed in the rest of the flower bud, even though the synthesis of JA seems to be increased also in distal and proximal regions. Therefore, we hypothesize that a different hormonal interplay is influencing the AZ to react differently to the other two regions of the bud.

Not only the proteins related to photosynthesis and carbohydrate metabolism were diminished in the AZ D2, but also proteins from 10 other functional categories (Figure 3, manuscript 2). With a total of 285 proteins changing, it was the most dramatic feature in the proteomic experiment. Another very interesting category was the signaling-related proteins with 19 proteins from different putative signaling pathways (Table 2, manuscript 2), such as ABA, brassinosteroids, ethylene, SA, JA and auxin. Because some signaling components are not exclusive for a single transduction pathway (Leurs et al., 2005) and, in the case of the MAPKs, might participate in different cascades (Asai et al., 2002), it might be impossible to decipher without a doubt, which pathways are actually being activated or inhibited with this experimental approach alone. Thus, further research could explore this topic using, for example, protein and metabolic flux analysis experimental approaches.

A potential increase in reactive oxygen species (ROS), such as peroxide (H_2O_2) and radical superoxide (O_2^-) is taking place in the distal and the AZ at D2. The scavenging enzymes, peroxidase and superoxide dismutase (SOD) are increased in the D2

(Supplementary Material 2, manuscript 2). Conversely, L-ascorbate peroxidase, crucial enzyme from the ascorbate-glutathione cycle, a major peroxide detoxifying system in plants (Caverzan et al., 2012) is decreased in the AZ D2 (Supplementary Material 2, manuscript 2), suggesting that the redox state of the AZ might be in some way vulnerable. ROS signaling has been described in leaf abscission in *Capsicum* (Sakamoto et al., 2008) and more recently in controlling longan fruit pedicel abscission caused by carbohydrate depletion (Yang et al., 2015) and regulating leaf pulvinus abscission in cassava (Liao et al., 2016).

The combination of the proteomic and transcriptomic results, unraveled the molecular changes that results in macro processes leading to abscission of the flower bud. The changes in protein and gene levels displayed by the poinsettia's flower bud before D2, place abscission onset early on. These results confirm what was found in previous work in Hvorslef-Eide's group (Munster, 2006; Lee et al., 2008; Hvorslef-Eide et al., 2016). No other time point for the analysis gave so much information about the diversity of ongoing processes in each bud region (Table 1, manuscript 2 and Figure 4, manuscript 3). Some of the putative processes ongoing by D2 are AZ differentiation by TFs related to boundaries and meristem differentiation (Table 5, thesis document), the beginning of cell wall transformation, the auxin depletion caused by the decapitation and the defensive response in the whole bud, including PRs and augmented secondary metabolism among others. A scheme depicting the putative relationships among processes, genes and proteins changing during the D2 is given below (Figure 21).

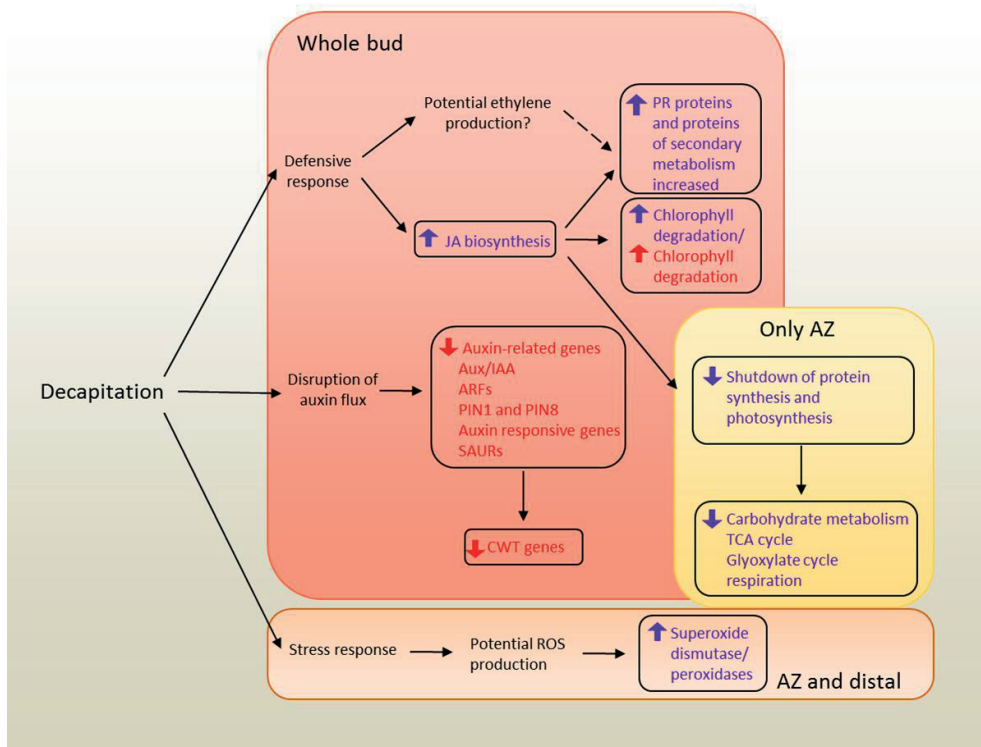


Fig 21 Schematic representation connecting the results from the -omics experiments in poinsettia as analyzed on D2. Color blocks represent one or more regions in the flower bud. Red text is data from the transcriptomic analysis. Purple text is data from proteomic analysis. Dashed arrows are potential effects, but where there is not enough evidence for clarity. Arrows up and down represent increase or decrease in genes or proteins. ARFs= Auxin responsive factors. Aux/IAA= Auxin/indole-3-acetic acid gene. AZ=Abscission zone. CWT=Cell wall transformation. JA=Jasmonic acid. PIN1 and PIN8= Auxin efflux carrier component 1 and Auxin efflux carrier component 8. SAURs=Small auxin up-regulated RNAs. TCA=Tricarboxylic acid.

5.4 Integrated results from proteomic and transcriptomic on D4 and D6

Proteomic and transcriptomic studies revealed that the cells of the AZ undergo transformation of their cell walls. In fact, the GO terms “cell wall organization or biogenesis” together with “carbohydrate metabolism” were the main features of the D4 analysis according to the enrichment analysis of the AZ D4 (Figure 6B, manuscript 3).

Likewise, the pairwise comparisons in proteomic data showed evidence of the changes in abundances of cell wall transformation (CWT proteins in the AZ D4, but also in the distal region (Figure 4D-E, manuscript 2). Additional information was given by the spatial comparison from transcriptomic D6, where several genes were up-regulated in the AZ in comparison with the other two regions (Table 3, manuscript 3). The range of CWT proteins and genes increasing during D4 and D6, fit with a potential degradation of xylan from hemicellulose (β -xylosidases), pectin (polygalacturonases) and cellulose (endo- β -glucanases) and the action of expansins and extensins.

At D4, characteristic macro signs of senescence started to be visible, such as the yellowing of the distal region (Figure 6, thesis document). As part of senescence, proteins are degraded to mobilize the nutrients (Buchanan-Wollaston et al., 2003). In this context, proteases increased from 5% on D2 (Figure 4B, manuscript 2) to 20% on D4 (Figure 4D, manuscript 2) in the distal part. Among the proteases that increased, was the Senescence-specific cysteine protease SAG12 (Supplementary Material 2, manuscript 2). The *SAG12* gene is used as a senescence marker because it is only up-regulated during senescence as part of natural development, and not by stress-induced or hormone treatments as is the case with many other *SAG* genes (Weaver et al., 1998). This result strongly suggests that the distal region D4 has entered into senescence; the same result was found for the distal region on D6 (data not shown).

Ethylene is released during senescence, accordingly its biosynthetic enzymes are increased in senescent organs (Lim et al., 2007). The increase of the enzyme 1-aminocyclopropane-1-carboxylate oxidase homolog 4-like (ACC oxidase) on distal D4, suggests that ethylene is being produced (Supplementary Material 2, manuscript 2). The same ACC oxidase was found to be increased in distal D6 (Supplementary Material 4, manuscript 2).

Augmented proteolysis, the visible yellowing of the distal part, and the increase in ACC oxidase all provide confirmation that the senescence of this part of the bud occurs prior to the complete detachment of the organ. However, senescence is not always associated to abscission, there are plenty of organs that are detached without any signs of senescence (Rogers, 2013).

The enrichment analysis of the AZ on D6 shows several GO terms related to biosynthesis of macromolecules (Figure 6C manuscript 3). Likewise, the hierarchical

clustering on D6 (Figure 7 and Figure 8 manuscript 2) shows preferentially an increase of enzymes from the secondary metabolism, so we infer that the AZ on D6 is characterized by a lot of biosynthetic activity for secondary metabolites, such as lignin, lignan and other polymers like suberin. Putative increase in lignin content is in accordance with previous findings in poinsettia using FT-IR analysis (Lee et al., 2008). The hierarchical clustering revealed an increase in a high number of enzymes from the phenylpropanoid biosynthetic pathway in the AZ on D4, and on D6.

Apart from changes in secondary metabolism, the functional category with the highest increase of proteins in the AZ on D4 and D6 is primary metabolism. This includes nucleotide, lipid and amino acid metabolisms, among others. The enzyme bifunctional 3-dehydroquinate dehydratase shikimate chloroplastic-like increased in the AZ on D4 (Supplementary Material 3, manuscript 2) and the AZ on D6 (Supplementary Material 4, manuscript 2). This enzyme is part of the shikimate pathway, a seven-step pathway leading to the synthesis of chorismate, a precursor for the aromatic amino acids, tyrosine, phenylalanine and tryptophan (Herrmann and Weaver, 1999). The aromatic amino acids give rise to a wide variety of compounds with a role in plant growth, in defense and other environmental responses (Maeda and Dudareva, 2012). One of the aromatic amino acids produced by the shikimate pathway is L-phenylalanine, which is the starting point for the phenylpropanoid biosynthetic pathway (Vogt, 2010), connecting the primary metabolism to the secondary metabolism. These results imply that from before D4 through to D6, primary metabolism is modified to supply precursors for polyphenol compounds, such as flavonoids, anthocyanidins, lignin and many others (Figure 8, manuscript 2).

Increase lignin might act as mechanical barriers for pathogens and water loss after the organ is detached (van Nocker, 2009). It has already been reported that in poinsettia the AZ is enriched in lignin by the D7 (Lee et al., 2008), thus, we can conclude that lignin biosynthesis is regulated well in advance of the macromolecular changes in the AZ cells that can be physicochemically detected.

Another similarity between AZ D4 and AZ D6 is the putative presence of lignan and suberin. The enzymes Secoisolariciresinol dehydrogenase and Omega-hydroxypalmitate O-feruloyl transferase from the biosynthetic pathways of these compounds (Suzuki and Umezawa, 2007; Molina et al., 2009) increased for both time points (Supplementary Material 3, manuscript 2) and (Supplementary Material 4, manuscript 2). To the best of

our knowledge, there are no reports connecting lignan to abscission. Suberin, on the other hand, is a recognized component of the protective layer offering protection against desiccation and pathogens (van Doorn and Stead, 1997; Kim, 2014). Suberin biosynthesis is part of the lipid metabolism, however some of its components are made of phenylpropanoid- derivatives, connecting both primary and secondary metabolism. Additionally, the deposition of suberin as one of the last stages in the abscission of an organ (Kim, 2014; Kim et al., 2015b). In contrast, our data suggest that the formation of the protective layer begins much earlier, perhaps simultaneously to the cell separation itself, when the increase in CWT genes and proteins are brought into the picture.

The Figure 22 shows an illustration of the processes and groups of proteins and genes changing levels in the AZ and distal region of a poinsettia flower bud on D4 and D6.

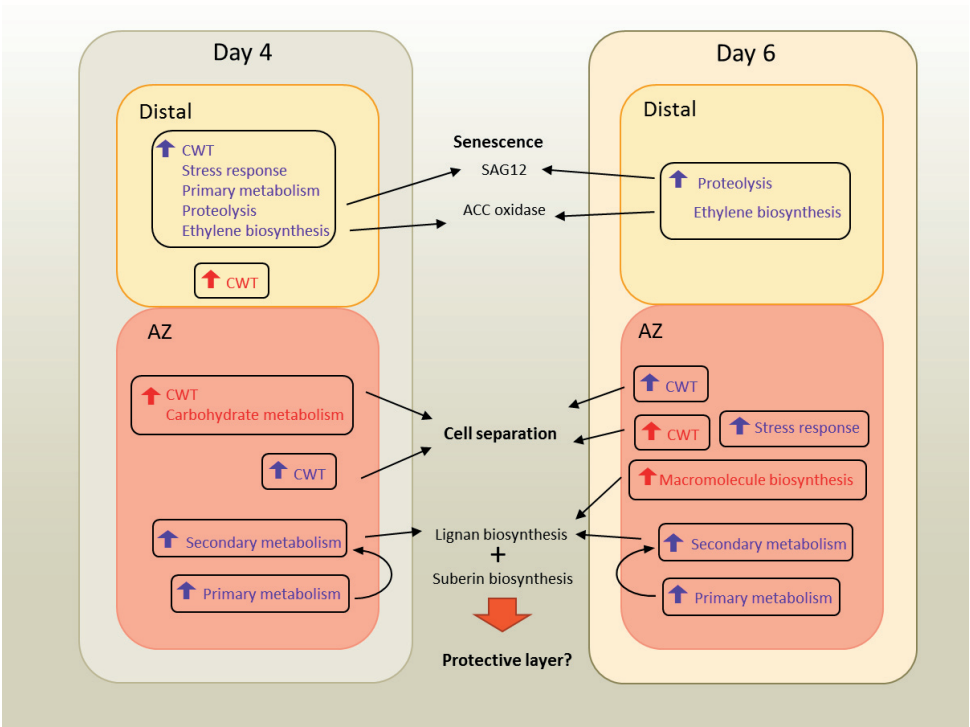


Fig 22 Schematic representation of the proteins and genes that are changing in levels and the potential processes driven by them in the distal and AZ of a poinsettia flower bud on D4 and D6. Color blocks represent the different regions of the flower bud that exhibit changes during D4 and D6. Red text is data from the transcriptomic study. Purple text is

data from the proteomic analysis. Purple and red arrows represent increases in protein and gene levels respectively. ACC= 1-aminocyclopropane-1-carboxylate. AZ= Abscission zone. CWT= Cell wall transformation. SAG= Senescence-specific cysteine protease.

5.5 Reflections on the small changes in protein abundance on D2 and D6

According to Kammers *et al.* (2015), the detection of significant changes in protein abundance is a key assignment in mass spectrometry-based trials. However, some of our results are a little puzzling in that respect. Specifically, a feature that attracted our attention was that there was no significant change in protein abundance between the AZ and the other two regions on D2 (Figure 14A, thesis document). This seems even more intriguing, when considering that in the temporal comparisons, the AZ D2 showed the highest decrease in protein abundance with respect to the AZ D0 (Figure 14B, thesis document). A similar observation was seen on D6, where no temporal changes were detected between any of the three regions compared with their previous region on D4, when the spatial changes were higher on D6 than for any other spatial comparisons.

To clarify these cases where no significant change in protein abundance was found, it is important to highlight that when doing the pairwise comparisons, the volcano plots show the change in abundance of all the proteins that varied in the whole experiment simultaneously, helping to visualize the fold change and their level of significance (Oveland *et al.*, 2015). In our case, this was 3086 proteins. The ones that are significantly changing are calculated with the statistical parameters fixed as FDR=0.01 and fold change=2 and are placed outside the volcano curve (Figures 2A-F, Figure 5A-D, manuscript 2). Thus, even if most of the proteins are in fact varying in their abundances, their changes may be too subtle to be considered by this analysis, and, as a result, they are located inside the volcano curve, and hence not considered significant. Only those that fit with the statistical criteria explained above will be selected as significant. Consequently, it is a procedural misconception, to think that there is no changes whatsoever in protein abundances. There are changes, however their level of significance varies.

6 Conclusions and future perspectives

The results obtained in this thesis confirm that abscission is a highly complex process that involves the participation of many factors. This thesis studied the flower abscission in poinsettia from two different omics levels, as well as one methodology paper. The first one was develop a new method for harvesting tissue suitable for auxin quantification and the second and third one was using high throughput technologies to study the fluctuations in proteins and mRNAs during the abscission.

The first manuscript proposed a harvesting methodology for minute targeted samples. As a result, we successfully harvested poinsettia AZ cells on two stages of development and quantified the actual auxin levels in them. The future work should concentrate on using the harvesting methodology together with the quantification protocol, to establish the auxin concentrations along the poinsettia flower bud. A main goal would be to demonstrate undoubtedly the auxin gradients across the AZ; this would validate the auxin theory of abscission initiation postulated by Addicott *et al.* (1955).

The transcriptomic results showed that the auxin transporter genes *PIN1* and *PIN8* were down-regulated during D2 compared to D0, a future work could be to immunolocalize these transporters in histological sections from an intact flower bud and a decapitated one sampled at different time points. These would provide a dynamic perspective of how the auxin transporters respond to the decapitation.

On D2 the decapitation induced a stress response characterized by the increase in peroxidases and a defensive response, characterized by PRs proteins, secondary metabolism and JA biosynthesis (manuscript 2). Simultaneously, the auxin-responsive genes diminished in their expression (manuscript 3) as well as photosynthesis, sugar metabolism and protein synthesis decrease (manuscript 2). Since during D2 the most dramatic changes in abundances were observed, future work should focus on this period, perhaps exploring sampling at shorter time points and characterizing the AZ according to secondary metabolites content and JA signaling and content.

Future work could continue to use multi-omic technologies, especially to perform a metabolomics experiment using the same layout as the other two experiments would provide the possibility to explore some metabolic pathways that might be over represented in the flower bud during abscission. Particular interest would be the amino

acid metabolism, for example tryptophan metabolism, because it is related to auxin biosynthesis. Sugar metabolism is connected to cell wall transformation, so would constitute another interesting pathway to assess. Polyphenolic metabolites are of special interest because secondary metabolism seems to be predominant in the AZ D4 and AZ D6. Having the abscission poinsettia metabolome could allow us to match the results of the proteomic and transcriptomic experiments and integrate by multi-omics the changes behind poinsettia abscission.

To go deeper into how proteins regulate abscission, it would be useful to perform a phosphoproteomic experiment using iTRAQ to assess the phosphorylation state in the set of proteins that are changing their abundances. After all, protein phosphorylation is the main post translational modification and it is connected with some hormone signaling cascades, also an important target in abscission.

Being a non-model organism propagated clonally, poinsettia lacks in a mutant collection and many molecular tools, however the results obtained in this thesis and previous work from Hvostlef-Eide's group, suggest that poinsettia flower bud abscission shares characteristics with reference species such as, tomato and *Arabidopsis*. Therefore, since we discovered that *IDA* is present in the poinsettia genome and is up-regulated during the D4, the next step would be to evaluate if this gene has a conserved effect in controlling abscission as in *Arabidopsis* and citrus. Again, because the lack of abscission mutants in poinsettia, the experiment could be performed in the *Arabidopsis ida* mutant.

Both proteomic and transcriptomic experiments set a foundation for a better understanding of poinsettia flower bud abscission, to further mine these data sets is an open possibility that would not be restricted to what was performed in this thesis. Another interesting direction for the work to take in the future would be to re-do the temporal comparisons using the D0 as the control for all the time points. As we decided to follow up the processes in a temporal scale, the temporal comparisons were done using each time point as the control of the later stage; however, this could have led to a diminution of information for the D4 and D6. Thus perhaps performing the temporal comparisons using D0 as the control for all the time points, could shed some light into the events taking place on D4 and D6.

In this thesis we have described the potential role of specific proteins and genes in poinsettia flower bud abscission, however some aspects remain a mystery that need to be

investigated further. One of these is the mechanism by which the AZ is formed from adult tissue; a hint was given with the identification of some TFs involved in boundaries and meristem differentiation. Further work could use some of these TFs sequences and design probes to locate them with a finer temporal resolution.

7 References

- Abeles, F.B. (1969). Abscission: Role of Cellulase. *Plant Physiology* 44(3), 447-452.
- Abeles, F.B., Morgan, P.W., and Saltveit, M.E.J. (1992). "Fruit Ripening, Abscission, and Postharvest Disorders," in *Ethylene in Plant Biology*. 2nd ed (New York Academic Press), 182-221.
- Adamczyk, B.J., Lehti-Shiu, M.D., and Fernandez, D.E. (2007). The MADS domain factors AGL15 and AGL18 act redundantly as repressors of the floral transition in Arabidopsis. *Plant J* 50(6), 1007-1019. doi: 10.1111/j.1365-313X.2007.03105.x.
- Addicott, F.T. (1982). *Abscission*. London, England: Univeristy of California Press, LTD. .
- Addicott, F.T., and Lynch, R.S. (1951). Acceleration and Retardation of Abscission by Indoleacetic Acid. *Science* 114 (2974), 688-689. doi: [doi: 10.1126/science.114.2974.688].
- Addicott, F.T., Lynch, R.S., and Carns, H.R. (1955). Auxin Gradient Theory of Abscission Regulation. *Science* 121(3148), 644-645. doi: 10.1126/science.121.3148.644.
- Agusti, J., Merelo, P., Cercos, M., Tadeo, F., and Talon, M. (2009). Comparative transcriptional survey between laser-microdissected cells from laminar abscission zone and petiolar cortical tissue during ethylene-promoted abscission in citrus leaves. *BMC Plant Biology* 9(1), 127.
- Asai, T., Tena, G., Plotnikova, J., Willmann, M.R., Chiu, W.L., Gomez-Gomez, L., et al. (2002). MAP kinase signalling cascade in Arabidopsis innate immunity. *Nature* 415(6875), 977-983. doi: 10.1038/415977a.
- Ascough, G.D., Mtshali, N.P., Nogemane, N., and van Staden, J. (2006). Flower abscission in excised inflorescences of three *Plectranthus* cultivars. *Plant Growth Regulation* 48(3), 229-235.
- Atkinson, R.G., Schröder, R., Hallett, I.C., Cohen, D., and MacRae, E.A. (2002). Overexpression of polygalacturonase in transgenic apple trees leads to a range of novel phenotypes involving changes in cell adhesion. *Plant Physiology* 129(1), 122-133.
- Atmodjo, M.A., Hao, Z., and Mohnen, D. (2013). Evolving views of pectin biosynthesis. *Annual Review of Plant Biology* 64, 747-779. doi: 10.1146/annurev-arplant-042811-105534.
- Attaran, E., Major, I.T., Cruz, J.A., Rosa, B.A., Koo, A.J.K., Chen, J., et al. (2014). Temporal Dynamics of Growth and Photosynthesis Suppression in Response to Jasmonate Signaling. *Plant Physiology* 165(3), 1302.
- Ayeh, K., Lee, Y., Ambrose, M., and Hvostlef-Eide, A. (2009). Characterization and structural analysis of wild type and a non-abscission mutant at the development funiculus (Def) locus in *Pisum sativum* L. *BMC Plant Biology* 9(1), 76.
- Bailey, D.A., and Miller, W.B. (1991). Poinsettia developmental and postproduction responses to growth-retardants and irradiance. *Hortscience* 26(12), 1501-1503.
- Bainbridge, M.N., Warren, R.L., Hirst, M., Romanuik, T., Zeng, T., Go, A., et al. (2006). Analysis of the prostate cancer cell line LNCaP transcriptome using a sequencing-by-synthesis approach. *BMC Genomics* 7(1), 246. doi: 10.1186/1471-2164-7-246.
- Basu, M.M., Gonzalez-Carranza, Z.H., Azam-Ali, S., Tang, S., Shahid, A.A., and Roberts, J.A. (2013). The manipulation of auxin in the abscission zone cells of Arabidopsis flowers reveals that indoleacetic acid signaling is a prerequisite for organ shedding. *Plant Physiology* 162(1), 96-106. doi: 10.1104/pp.113.216234.
- Belle, A., Tanay, A., Bitincka, L., Shamir, R., and O'Shea, E.K. (2006). Quantification of protein half-lives in the budding yeast proteome. *Proceedings of the National Academy of Sciences* 103(35), 13004-13009. doi: 10.1073/pnas.0605420103.
- Bernstein, J.A., Khodursky, A.B., Lin, P.-H., Lin-Chao, S., and Cohen, S.N. (2002). Global analysis of mRNA decay and abundance in *Escherichia coli* at single-gene resolution using two-color fluorescent DNA microarrays. *Proceedings of the National Academy of Sciences* 99(15), 9697.

- Bessis, R., Charpentier, N., Hilt, C., and Fournioux, J.-C. (2000). Grapevine fruit set: Physiology of the abscission zone. *Australian Journal of Grape and Wine Research* 6(2), 125-130. doi: 10.1111/j.1755-0238.2000.tb00170.x.
- Beyer, E.M., Jr., and Morgan, P.W. (1971). Abscission: The Role of Ethylene Modification of Auxin Transport. *Plant Physiology* 48(2), 208-212.
- Bingham, A.H.A., Ponnambalam, S., Chan, B., and Busby, S. (1986). Mutations that reduce expression from the P2 promoter of the *Escherichia coli* galactose operon. *Gene* 41(1), 67-74.
- Bleecker, A.B., and Patterson, S.E. (1997). Last exit: senescence, abscission, and meristem arrest in *Arabidopsis*. *The Plant Cell* 9(7), 1169-1179.
- Bornman, C. (1967). Some ultrastructural aspects of abscission in *Coleus* and *Gossypium*. *South African Journal of Science* 63, 325-331.
- Brent, R. (1999). Functional genomics: Learning to think about gene expression data. *Current Biology* 9(9), R338-R341. doi: 10.1016/S0960-9822(99)80208-5.
- Brunoud, G., Wells, D.M., Oliva, M., Larrieu, A., Mirabet, V., Burrow, A.H., et al. (2012). A novel sensor to map auxin response and distribution at high spatio-temporal resolution. *Nature* 482(7383), 103-106.
- Buchanan-Wollaston, V., Earl, S., Harrison, E., Mathas, E., Navabpour, S., Page, T., et al. (2003). The molecular analysis of leaf senescence - a genomics approach. *Plant Biotechnology Journal* 1(1), 3-22.
- Burg, S.P. (1968). Ethylene, Plant Senescence and Abscission. *Plant Physiology* 43(9 Pt B), 1503-1511.
- Burr, C.A., Leslie, M.E., Orłowski, S.K., Chen, I., Wright, C.E., Daniels, M.J., et al. (2011). CAST AWAY, a membrane-associated receptor-like kinase, inhibits organ abscission in *Arabidopsis*. *Plant Physiol* 156(4), 1837-1850. doi: 10.1104/pp.111.175224.
- Butenko, M.A., Patterson, S.E., Grini, P.E., Stenvik, G.E., Amundsen, S.S., Mandal, A., et al. (2003). Inflorescence deficient in abscission controls floral organ abscission in *Arabidopsis* and identifies a novel family of putative ligands in plants. *The Plant Cell* 15(10), 2296-2307.
- Butenko, M.A., Shi, C.L., and Aalen, R.B. (2012). KNAT1, KNAT2 and KNAT6 act downstream in the IDA-HAE/HSL2 signaling pathway to regulate floral organ abscission. *Plant Signaling & Behavior* 7(1), 135-138. doi: 10.4161/psb.7.1.18379.
- Cai, S., and Lashbrook, C.C. (2008). Stamen abscission zone transcriptome profiling reveals new candidates for abscission control: enhanced retention of floral organs in transgenic plants overexpressing *Arabidopsis* ZINC FINGER PROTEIN2. *Plant Physiology* 146(3), 1305-1321. doi: 10.1104/pp.107.110908.
- Cameron, A.C., and Reid, M.S. (1983). Use of silver thiosulfate to prevent flower abscission from potted plants. *Scientia Horticulturae* 19(3), 373-378.
- Caverzan, A., Passaia, G., Rosa, S.B., Ribeiro, C.W., Lazzarotto, F., and Margis-Pinheiro, M. (2012). Plant responses to stresses: Role of ascorbate peroxidase in the antioxidant protection. *Genetics and Molecular Biology* 35(4 Suppl), 1011-1019.
- Chan, K.W., Corley, R.H.V., and Seth, A.K. (1972). Effects of growth regulators on fruit abscission in oil palm, *Elaeis guineensis*. *Annals of Applied Biology* 71(3), 243-249. doi: 10.1111/j.1744-7348.1972.tb05088.x.
- Chen, G., Gharib, T.G., Huang, C.-C., Taylor, J.M.G., Misek, D.E., Kardia, S.L.R., et al. (2002). Discordant Protein and mRNA Expression in Lung Adenocarcinomas. *Molecular and Cellular Proteomics* 1(4), 304.
- Cheng, C., Zhang, L., Yang, X., and Zhong, G. (2015). Profiling gene expression in citrus fruit calyx abscission zone (AZ-C) treated with ethylene. *Molecular Genetics and Genomics* 290(5), 1991-2006. doi: 10.1007/s00438-015-1054-2.
- Cho, H.T., and Cosgrove, D.J. (2000). Altered expression of expansin modulates leaf growth and pedicel abscission in *Arabidopsis thaliana*. *Proceedings of the National Academy of Sciences* 97(17), 9783-9788. doi: 10.1073/pnas.160276997.

- Cho, S.K., Larue, C.T., Chevalier, D., Wang, H., Jinn, T.-L., Zhang, S., et al. (2008). Regulation of floral organ abscission in *Arabidopsis thaliana*. *Proceedings of the National Academy of Sciences* 105(40), 15629-15634. doi: 10.1073/pnas.0805539105.
- Conesa, A., Gotz, S., Garcia-Gomez, J.M., Terol, J., Talon, M., and Robles, M. (2005). Blast2GO: a universal tool for annotation, visualization and analysis in functional genomics research. *Bioinformatics* 21(18), 3674-3676. doi: 10.1093/bioinformatics/bti610.
- Corbacho, J., Romojaro, F., Pech, J.-C., Latché, A., and Gomez-Jimenez, M.C. (2013). Transcriptomic Events Involved in Melon Mature-Fruit Abscission Comprise the Sequential Induction of Cell-Wall Degrading Genes Coupled to a Stimulation of Endo and Exocytosis. *PLoS ONE* 8(3), e58363. doi: 10.1371/journal.pone.0058363.
- Daher, F.B., and Braybrook, S.A. (2015). How to let go: pectin and plant cell adhesion. *Frontiers in Plant Science* 6(523). doi: 10.3389/fpls.2015.00523.
- Degan, F.D., Child, R., Svendsen, I., and Ulvskov, P. (2001). The Cleavable N-terminal Domain of Plant Endopolygalacturonases from Clade B May Be Involved in a Regulated Secretion Mechanism. *Journal of Biological Chemistry* 276(38), 35297-35304. doi: 10.1074/jbc.M102136200.
- del Campillo, E., and Bennett, A.B. (1996). Pedicel breakstrength and cellulase gene expression during tomato flower abscission. *Plant Physiology* 111(3), 813-820.
- del Campillo, E., and Lewis, L.N. (1992). Identification and kinetics of accumulation of proteins induced by ethylene in bean abscission zones. *Plant Physiology* 98(3), 955-961.
- Dela Fuente, R., and Leopold, A. (1969). Kinetics of abscission in the bean petiole explant. *Plant physiology* 44(2), 251-254.
- Dixon, R.A., Achnine, L., Kota, P., Liu, C.J., Reddy, M.S., and Wang, L. (2002). The phenylpropanoid pathway and plant defence-a genomics perspective. *Mol Plant Pathol* 3(5), 371-390. doi: 10.1046/j.1364-3703.2002.00131.x.
- Doherty, M.K., Hammond, D.E., Clague, M.J., Gaskell, S.J., and Beynon, R.J. (2009). Turnover of the Human Proteome: Determination of Protein Intracellular Stability by Dynamic SILAC. *Journal of Proteome Research* 8(1), 104-112. doi: 10.1021/pr800641v.
- Ecker, J.R. (1995). The Ethylene Signal-Transduction Pathway in Plants. *Science* 268(5211), 667-675.
- Ellis, C.M., Nagpal, P., Young, J.C., Hagen, G., Guilfoyle, T.J., and Reed, J.W. (2005). AUXIN RESPONSE FACTOR1 and AUXIN RESPONSE FACTOR2 regulate senescence and floral organ abscission in *Arabidopsis thaliana*. *Development* 132(20), 4563-4574.
- Estornell, L.H., Agusti, J., Merelo, P., Talon, M., and Tadeo, F.R. (2013). Elucidating mechanisms underlying organ abscission. *Plant Sci* 199-200, 48-60. doi: 10.1016/j.plantsci.2012.10.008.
- Estornell, L.H., Wildhagen, M., Pérez-Amador, M.A., Talón, M., Tadeo, F.R., and Butenko, M.A. (2015). The IDA peptide controls abscission in *Arabidopsis* and *Citrus*. *Frontiers in Plant Science* 6. doi: 10.3389/fpls.2015.01003.
- Fennoy, S.L., and Bailey-Serres, J. (1995). Post-transcriptional regulation of gene expression in oxygen-deprived roots of maize. *The Plant Journal* 7(2), 287-295. doi: doi:10.1046/j.1365-313X.1995.7020287.x.
- Fernandez, D.E., Heck, G.R., Perry, S.E., Patterson, S.E., Bleecker, A.B., and Fang, S.-C. (2000). The Embryo MADS Domain Factor AGL15 Acts Postembryonically: Inhibition of Perianth Senescence and Abscission via Constitutive Expression. *Plant Cell* 12(2), 183-198.
- Ferrante, A., Trivellini, A., Scuderi, D., Romano, D., and Vernieri, P. (2015). Post-production physiology and handling of ornamental potted plants. *Postharvest Biology and Technology* 100(0), 99-108.
- Freiberg, J.A., Le Breton, Y., Tran, B.Q., Scott, A.J., Harro, J.M., Ernst, R.K., et al. (2016). Global Analysis and Comparison of the Transcriptomes and Proteomes of Group A *Streptococcus* Biofilms. *mSystems* 1(6).

- Fuller, D.Q., and Allaby, R. (2009). "Seed Dispersal and Crop Domestication: Shattering, Germination and Seasonality in Evolution under Cultivation," in *Annual Plant Reviews Volume 38: Fruit Development and Seed Dispersal*. Wiley-Blackwell), 238-295.
- Gardner, F., Marth, P.C., and Batjer, L. (1940). Spraying with plant growth substances for control of the pre-harvest drop of apples. *Proceedings. American Society for Horticultural Science*, 1939 37, 415-428.
- Gardner, F.E., and Cooper, W.C. (1943). Effectiveness of Growth Substances in Delaying Abscission of Coleus Petioles. *Botanical Gazette* 105(1), 80-89.
- Gawadi, A.G., and Avery, G.S. (1950). Leaf abscission and the so-called abscission layer. *Am J Bot* 37(2), 172-180.
- Gehlenborg, N., O'Donoghue, S.I., Baliga, N.S., Goesmann, A., Hibbs, M.A., Kitano, H., et al. (2010). Visualization of omics data for systems biology. *Nat Methods* 7(3 Suppl), S56-68. doi: 10.1038/nmeth.1436.
- Gilliland, M.G., Bornman, C.H., and Addicott, F.T. (1976). Ultrastructure and Acid Phosphatase in Pedicel Abscission of Hibiscus. *American Journal of Botany* 63(7), 925-935.
- Gómez-Mena, C., and Sablowski, R. (2008). ARABIDOPSIS THALIANA HOMEBOX GENE1 Establishes the Basal Boundaries of Shoot Organs and Controls Stem Growth. *The Plant Cell* 20(8), 2059-2072. doi: 10.1105/tpc.108.059188.
- Goncalves, B., Hasson, A., Belcram, K., Cortizo, M., Morin, H., Nikovics, K., et al. (2015). A conserved role for CUP-SHAPED COTYLEDON genes during ovule development. *The Plant Journal* 83(4), 732-742. doi: 10.1111/tpj.12923.
- Gonzalez-Carranza, Z.H., Elliott, K.A., and Roberts, J.A. (2007). Expression of polygalacturonases and evidence to support their role during cell separation processes in Arabidopsis thaliana. *Journal of Experimental Botany*, erm222. doi: 10.1093/jxb/erm222.
- Greenbaum, D., Colangelo, C., Williams, K., and Gerstein, M. (2003). Comparing protein abundance and mRNA expression levels on a genomic scale. *Genome Biology* 4(9), 117-117.
- Grossman, A., N Zhou, Y., Gross, C., Heilig, J., Christie, G., and Calendar, R. (1985). Mutations in the rpoH (htrp) gene of Escherichia coli K-12 phenotypically suppress a temperature-sensitive mutant defective in the sigma 70 subunit of RNA polymerase. *Journal of Bacteriology* 161, 939-943.
- Gubert, C.M., Christy, M.E., Ward, D.L., Groner, W.D., and Liljegren, S.J. (2014). ASYMMETRIC LEAVES1 regulates abscission zone placement in Arabidopsis flowers. *BMC Plant Biol* 14, 195. doi: 10.1186/s12870-014-0195-5.
- Gurung, S., Cohen, M.F., Fukuto, J., and Yamasaki, H. (2012). Polyamine-Induced Rapid Root Abscission in Azolla pinnata. *Journal of Amino Acids* 2012, 9. doi: 10.1155/2012/493209.
- Gygi, S.P., Rochon, Y., Franza, B.R., and Aebersold, R. (1999). Correlation between Protein and mRNA Abundance in Yeast. *Molecular and Cellular Biology* 19(3), 1720-1730.
- Haas, R., Zelezniak, A., Iacovacci, J., Kamrad, S., Townsend, S., and Ralser, M. (2017). Designing and interpreting 'multi-omic' experiments that may change our understanding of biology. *Current Opinion in Systems Biology* 6, 37-45. doi: doi.org/10.1016/j.coisb.2017.08.009.
- Hackett, W., Sachs, R., and DeBie, J. (1972). Growing bougainvillea as a flowering pot plant. *California Agriculture* 26(8), 12-13.
- Haider, S., and Pal, R. (2013). Integrated analysis of transcriptomic and proteomic data. *Current Genomics* 14(2), 91-110. doi: 10.2174/1389202911314020003.
- Hall, W.C. (1952). Evidence on the Auxin-Ethylene Balance Hypothesis of Foliar Abscission. *Botanical Gazette* 113(3), 310-322. doi: 10.1086/335723.
- Hepworth, S.R., and Pautot, V.A. (2015). Beyond the Divide: Boundaries for Patterning and Stem Cell Regulation in Plants. *Frontiers in Plant Science* 6(1052). doi: 10.3389/fpls.2015.01052.

- Herrmann, K.M., and Weaver, L.M. (1999). The Shikimate Pathway. *Annual Review of Plant Physiology and Plant Molecular Biology* 50(1), 473-503. doi: 10.1146/annurev.arplant.50.1.473.
- Hibara, K., Karim, M.R., Takada, S., Taoka, K., Furutani, M., Aida, M., et al. (2006). Arabidopsis CUP-SHAPED COTYLEDON3 regulates postembryonic shoot meristem and organ boundary formation. *The Plant Cell* 18(11), 2946-2957. doi: 10.1105/tpc.106.045716.
- Holm, R.E., and Abeles, F.B. (1967). Abscission: The Role of RNA Synthesis. *Plant Physiology* 42(8), 1094-1102.
- Hvoslef-Eide, A.K., Munster, C.M., Mathiesen, C.A., Ayeh, K.O., Melby, T.I., Rasolomanana, P., et al. (2016). Primary and Secondary Abscission in *Pisum sativum* and *Euphorbia pulcherrima*—How Do They Compare and How Do They Differ? *Frontiers in Plant Science* 6(1204). doi: 10.3389/fpls.2015.01204.
- Hänisch Ten Cate, C.H., Vanderpl, J.J., and Bruinsma, J. (1973). Abscission of flower bud pedicels in *Begonia* .III. anatomical pattern of abscission. *Acta Botanica Neerlandica* 22(6), 681-685.
- Iglesias, D.J., Cercós, M., Colmenero-Flores, J.M., Naranjo, M.A., Ríos, G., Carrera, E., et al. (2007). Physiology of citrus fruiting. *Brazilian Journal of Plant Physiology* 19, 333-362.
- Jeffcoat, B., and Cockshull, K.E. (1972). Changes in the Levels of Endogenous Growth Regulators during Development of the Flowers of *Chrysanthemum morifolium*. *Journal of Experimental Botany* 23(76), 722-732.
- Jiang, C., Lu, F., Imsabai, W., Meir, S., and Reid, M.S. (2008). Silencing polygalacturonase expression inhibits tomato petiole abscission. *Journal of Experimental Botany* 59(4), 973-979. doi: 10.1093/jxb/ern023.
- Jinn, T.L., Stone, J.M., and Walker, J.C. (2000). HAESA, an *Arabidopsis* leucine-rich repeat receptor kinase, controls floral organ abscission. *Genes & Development* 14(1), 108-117.
- Kaefer, A., Landesfeind, M., Feussner, K., Morgenstern, B., Feussner, I., and Meinicke, P. (2014). Meta-analysis of pathway enrichment: combining independent and dependent omics data sets. *PLoS One* 9(2), e89297. doi: 10.1371/journal.pone.0089297.
- Kamerbeek, G.A., and De Munk, W.J. (1976). A review of ethylene effects in bulbous plants. *Scientia Horticulturae* 4(2), 101-115.
- Kammers, K., Cole, R.N., Tiengwe, C., and Ruczinski, I. (2015). Detecting significant changes in protein abundance. *EuPA Open Proteomics* 7, 11-19. doi: doi.org/10.1016/j.euprot.2015.02.002.
- Kell, D.B., and Oliver, S.G. (2003). Here is the evidence, now what is the hypothesis? The complementary roles of inductive and hypothesis-driven science in the post-genomic era. *BioEssays* 26(1), 99-105. doi: 10.1002/bies.10385.
- Kim, J. (2014). Four shades of detachment: Regulation of floral organ abscission. *Plant Signaling & Behavior* 9(11), e976154. doi: 10.4161/15592324.2014.976154.
- Kim, J., Chang, C., and Tucker, M.L. (2015a). To grow old: regulatory role of ethylene and jasmonic acid in senescence. *Frontiers in Plant Science* 6, 20. doi: 10.3389/fpls.2015.00020.
- Kim, J., Sundaresan, S., Philosoph-Hadas, S., Yang, R., Meir, S., and Tucker, M.L. (2015b). Examination of the abscission-associated transcriptomes for soybean, tomato and Arabidopsis highlights the conserved biosynthesis of an extensible extracellular matrix and boundary layer. *Frontiers in Plant Science* 6. doi: 10.3389/fpls.2015.01109.
- Kim, J., Yang, J., Yang, R., Sicher, R.C., Chang, C., and Tucker, M.L. (2016). Transcriptome analysis of soybean leaf abscission identifies transcriptional regulators of organ polarity and cell fate. *Frontiers in Plant Science* 7. doi: 10.3389/fpls.2016.00125.
- Kitano, H. (2002). Systems biology: a brief overview. *Science* 295(5560), 1662-1664. doi: 10.1126/science.1069492.

- Kleffmann, T., Russenberger, D., von Zychlinski, A., Christopher, W., Sjölander, K., Gruissem, W., et al. (2004). The Arabidopsis thaliana Chloroplast Proteome Reveals Pathway Abundance and Novel Protein Functions. *Current Biology* 14(5), 354-362.
- Konishi, S., Izawa, T., Lin, S.Y., Ebana, K., Fukuta, Y., Sasaki, T., et al. (2006). An SNP Caused Loss of Seed Shattering During Rice Domestication. *Science* 312(5778), 1392-1396. doi: 10.1126/science.1126410.
- Kramer, P.J. (1951). Causes of injury to plants resulting from flooding of the soil. *Plant Physiology* 26(4), 722-736.
- Kuang, A., Peterson, C.M., and Dute, R.R. (1992). Leaf abscission in soybean - cytochemical and ultrastructural-changes following benzylaminopurine treatment. *Journal Of Experimental Botany* 43(257), 1611-1619.
- La Rue, C.D. (1936). The effect of auxin on the abscission of petioles. *Proceedings of the National Academy of Sciences* 22(5), 254-259.
- Lashbrook, C.C., and Cai, S. (2008). Cell wall remodeling in Arabidopsis stamen abscission zones: Temporal aspects of control inferred from transcriptional profiling. *Plant Signaling & Behavior* 3(9), 733-736.
- Lee, E. (1911). The Morphology of Leaf-fall. *Annals of Botany* 25(97), 51-106.
- Lee, Y., Derbyshire, P., Knox, J.P., and Hvoslef-Eide, A.K. (2008). Sequential cell wall transformations in response to the induction of a pedicel abscission event in Euphorbia pulcherrima (poinsettia). *The Plant Journal* 54(6), 993-1003. doi: 10.1111/j.1365-313X.2008.03456.x.
- Leslie, M.E., Lewis, M.W., Youn, J.-Y., Daniels, M.J., and Liljegren, S.J. (2010). The EVERSLED receptor-like kinase modulates floral organ shedding in Arabidopsis. *Development* 137(3), 467-476. doi: 10.1242/dev.041335.
- Leurs, R., Bakker, R.A., Timmerman, H., and de Esch, I.J. (2005). The histamine H3 receptor: from gene cloning to H3 receptor drugs. *Nature Reviews Drug Discovery* 4(2), 107-120. doi: 10.1038/nrd1631.
- Lewis, M.W., Leslie, M.E., Fulcher, E.H., Darnielle, L., Healy, P.N., Youn, J.Y., et al. (2010). The SERK1 receptor-like kinase regulates organ separation in Arabidopsis flowers. *Plant J* 62(5), 817-828. doi: 10.1111/j.1365-313X.2010.04194.x.
- Li, C., Wang, Y., Ying, P., Ma, W., and Li, J. (2015). Genome-wide digital transcript analysis of putative fruitlet abscission related genes regulated by ethephon in litchi. *Frontiers in Plant Science* 6, 502. doi: 10.3389/fpls.2015.00502.
- Li, C., Zhou, A., and Sang, T. (2006). Rice Domestication by Reducing Shattering. *Science* 311(5769), 1936-1939. doi: 10.1126/science.1123604.
- Li, W., Zhou, Y., Liu, X., Yu, P., Cohen, J.D., and Meyerowitz, E.M. (2013). LEAFY Controls Auxin Response Pathways in Floral Primordium Formation. *Science Signaling* 6(270), ra23.
- Liao, C.-Y., Smet, W., Brunoud, G., Yoshida, S., Vernoux, T., and Weijers, D. (2015). Reporters for sensitive and quantitative measurement of auxin response. *Nature Methods* 12(3), 207-210. doi: 10.1038/nmeth.3279.
- Liao, W., Wang, G., Li, Y., Wang, B., Zhang, P., and Peng, M. (2016). Reactive oxygen species regulate leaf pulvinus abscission zone cell separation in response to water-deficit stress in cassava. *Scientific Reports* 6, 21542. doi: 10.1038/srep21542.
- Liljegren, S.J. (2012). Organ abscission: exit strategies require signals and moving traffic. *Curr Opin Plant Biol* 15(6), 670-676. doi: 10.1016/j.pbi.2012.09.012.
- Liljegren, S.J., Leslie, M.E., Darnielle, L., Lewis, M.W., Taylor, S.M., Luo, R., et al. (2009). Regulation of membrane trafficking and organ separation by the NEVERSHED ARF-GAP protein. *Development* 136(11), 1909-1918. doi: 10.1242/dev.033605.
- Lim, P.O., Kim, H.J., and Nam, H.G. (2007). Leaf senescence. *Annual Review of Plant Biology* 58, 115-136. doi: 10.1146/annurev.arplant.57.032905.105316.

- Liu, X., Hegeman, A., Gardner, G., and Cohen, J. (2012). Protocol: High-throughput and quantitative assays of auxin and auxin precursors from minute tissue samples. *Plant Methods* 8:31(1), 1-17. doi: 10.1186/1746-4811-8-31
- Lloyd, F.E. (1914). Injury and abscission in *Impatiens sultani*. *Sixth Annual Report of the Quebec Society for the Protection of Plants from Insects and Fungous Diseases*, 72-79.
- Maeda, H., and Dudareva, N. (2012). The Shikimate Pathway and Aromatic Amino Acid Biosynthesis in Plants. *Annual Review of Plant Biology* 63(1), 73-105. doi: doi:10.1146/annurev-arplant-042811-105439.
- Majda, M., and Robert, S. (2018). The Role of Auxin in Cell Wall Expansion. *International Journal of Molecular Sciences* 19(4), 951. doi: 10.3390/ijms19040951.
- Manning, W., and Feder, W. (1976). "Effects of ozone on economic plants," in *Effects of air pollutants on plants (Society for Experimental Biology, Seminar Series:1)*. Cambridge University Press), 47-60.
- Mao, L., Begum, D., Chuang, H., Budiman, M., Szymkowiak, E., Irish, E., et al. (2000). JOINTLESS is a MADS-box gene controlling tomato flower abscission zone development. *Nature* 406(6798), 910 - 913.
- McKim, S.M., Stenvik, G.-E., Butenko, M.A., Kristiansen, W., Cho, S.K., Hepworth, S.R., et al. (2008). The BLADE-ON-PETIOLE genes are essential for abscission zone formation in *Arabidopsis*. *Development* 135(8), 1537-1546. doi: 10.1242/dev.012807.
- Meir, S., Hunter, D.A., Chen, J.-C., Halaly, V., and Reid, M.S. (2006). Molecular Changes Occurring during Acquisition of Abscission Competence following Auxin Depletion in *Mirabilis jalapa*. *Plant Physiology* 141(4), 1604-1616. doi: 10.1104/pp.106.079277.
- Meir, S., Philosoph-Hadas, S., Sundaresan, S., Selvaraj, K.S., Burd, S., Ophir, R., et al. (2010). Microarray analysis of the abscission-related transcriptome in the tomato flower abscission zone in response to auxin depletion. *Plant Physiology* 154(4), 1929-1956. doi: 10.1104/pp.110.160697.
- Merelo, P., Agustí, J., Arbona, V., Costa, M.L., Estornell, L.H., Gómez-Cadenas, A., et al. (2017). Cell Wall Remodeling in Abscission Zone Cells during Ethylene-Promoted Fruit Abscission in Citrus. *Frontiers in Plant Science* 8(126). doi: 10.3389/fpls.2017.00126.
- Merkouroupoulos, G., and Shirsat, A. (2003). The unusual *Arabidopsis* extensin gene atExt1 is expressed throughout plant development and is induced by a variety of biotic and abiotic stresses. *Planta* 217(3), 356-366.
- Michalczuk, L., Cooke, T.J., and Cohen, J.D. (1992). Auxin levels at different stages of carrot somatic embryogenesis. *Phytochemistry* 31(4), 1097-1103.
- Moe, R., Fjeld, T., and Mortensen, L.M. (1992). Stem elongation and keeping quality in poinsettia (*Euphorbia pulcherrima* Willd) as affected by temperature and supplementary lighting. *Scientia Horticulturae* 50(1-2), 127-136.
- Molina, I., Li-Beisson, Y., Beisson, F., Ohlrogge, J.B., and Pollard, M. (2009). Identification of an *Arabidopsis* Feruloyl-Coenzyme A Transferase Required for Suberin Synthesis. *Plant Physiology* 151(3), 1317-1328. doi: 10.1104/pp.109.144907.
- Morre, D.J. (1968). Cell Wall Dissolution and Enzyme Secretion During Leaf Abscission. *Plant Physiology* 43(9 Pt B), 1545-1559.
- Muñoz-Sanhueza, L.G., Lee, Y., Tillmann, M., Cohen, J.D., and Hvoslef-Eide, A.K. (2018). Auxin analysis using laser microdissected plant tissues sections. *BMC Plant Biology* 18(1), 133. doi: 10.1186/s12870-018-1352-z.
- Munster, C. (2006). *On the flower abscission of poinsettia (Euphorbia pulcherrima Willd. Ex Klotzsch) - A molecular and plant hormonal study*. Norwegian University of Life Sciences.
- Nakano, T., Kimbara, J., Fujisawa, M., Kitagawa, M., Ihashi, N., Maeda, H., et al. (2012). MACROCALYX and JOINTLESS interact in the transcriptional regulation of tomato fruit abscission zone development. *Plant Physiology* 158(1), 439-450. doi: 10.1104/pp.111.183731.

- Noel, A.R.A., and Van Staden, J. (1975). Phyllomorph Senescence in *Streptocarpus molweniensis*. *Annals of Botany* 39(163), 921-929.
- Nühse, T.S., Bottrill, A.R., Jones, A.M.E., and Peck, S.C. (2007). Quantitative phosphoproteomic analysis of plasma membrane proteins reveals regulatory mechanisms of plant innate immune responses. *The Plant Journal* 51(5), 931-940. doi: 10.1111/j.1365-3113.2007.03192.x.
- Olmsted, C.E. (1951). Experiments on Photoperiodism, Dormancy, and Leaf Age and Abscission in Sugar Maple. *Botanical Gazette* 112(4), 365-393. doi: 10.1086/335673.
- Oveland, E., Muth, T., Rapp, E., Martens, L., Berven, F.S., and Barsnes, H. (2015). Viewing the proteome: how to visualize proteomics data? *Proteomics* 15(8), 1341-1355. doi: 10.1002/pmic.201400412.
- Overvoorde, P., Fukaki, H., and Beeckman, T. (2010). Auxin Control of Root Development. *Cold Spring Harbor Perspectives in Biology* 2(6), a001537. doi: 10.1101/cshperspect.a001537.
- Parker, W.C., and Pallardy, S.G. (1985). Drought-induced leaf abscission and whole-plant drought tolerance of seedlings of seven black walnut families. *Canadian Journal of Forest Research* 15(5), 818-821. doi: 10.1139/x85-132.
- Patterson, S.E. (2001). Cutting Loose. Abscission and Dehiscence in Arabidopsis. *Plant Physiology* 126(2), 494-500. doi: 10.1104/pp.126.2.494.
- Patterson, S.E., and Bleeker, A.B. (2004). Ethylene-Dependent and -Independent Processes Associated with Floral Organ Abscission in Arabidopsis. *Plant Physiology* 134(1), 194-203. doi: 10.1104/pp.103.028027.
- Perrot-Rechenmann, C. (2010). Cellular responses to auxin: division versus expansion. *Cold Spring Harbor Perspectives in Biology* 2(5), a001446. doi: 10.1101/cshperspect.a001446.
- Pierik, R.L.M. (1971). Auxin-induced secondary abscission in isolated apple flowers. *Naturwissenschaften* 58(11), 568-569. doi: 10.1007/bf00598726.
- Pierik, R.L.M. (1977). Induction of Secondary Abscission in Apple Pedicels in vitro. *Physiologia Plantarum* 39(4), 271-274. doi: 10.1111/j.1399-3054.1977.tb01882.x.
- Pierik, R.L.M. (1980). Hormonal regulation of secondary abscission in pear pedicels in vitro. *Physiologia Plantarum* 48(1), 5-8. doi: 10.1111/j.1399-3054.1980.tb03210.x.
- Piha, R.S., Cuénod, M., and Waelsch, H. (1966). Metabolism of Histones of Brain and Liver. *Journal of Biological Chemistry* 241(10), 2397-2404.
- Poovaiah, B.W. (1974). Formation of callose and lignin during leaf abscission. *American Journal of Botany* 61, 829-834.
- Porfírio, S., Gomes da Silva, M.D.R., Peixe, A., Cabrita, M.J., and Azadi, P. (2016). Current analytical methods for plant auxin quantification – A review. *Analytica Chimica Acta* 902, 8-21.
- Pozo, L., and Burns, J.K. (2009). Organ Loss and Yield Impacts of 'Valencia' Sweet Orange in Response to Fruit Abscission Agents. *HortScience* 44(1), 83-88.
- Rapparini, F., Tam, Y.Y., Cohen, J.D., and Slovin, J.P. (2002). Indole-3-Acetic Acid Metabolism in *Lemna gibba* Undergoes Dynamic Changes in Response to Growth Temperature. *Plant Physiology* 128(4), 1410-1416. doi: 10.1104/pp.011005.
- Ratner, A., Goren, R., and Monselise, S.P. (1969). Activity of pectin esterase and cellulase in the abscission zone of citrus leaf explants. *Plant Physiology* 44(12), 1717-1723.
- Reinbothe, S., Mollenhauer, B., and Reinbothe, C. (1994). JIPs and RIPs: the regulation of plant gene expression by jasmonates in response to environmental cues and pathogens. *The Plant Cell* 6(9), 1197-1209. doi: 10.1105/tpc.6.9.1197.
- Reinders, J., and Sickmann, A. (2005). State-of-the-art in phosphoproteomics. *Proteomics* 5(16), 4052-4061. doi: 10.1002/pmic.200401289.
- Ridley, B.L., O'Neill, M.A., and Mohnen, D. (2001). Pectins: structure, biosynthesis, and oligogalacturonide-related signaling. *Phytochemistry* 57(6), 929-967.
- Riov, J. (1974). A polygalacturonase from citrus leaf explants: role in abscission. *Plant Physiology* 53(2), 312-316.

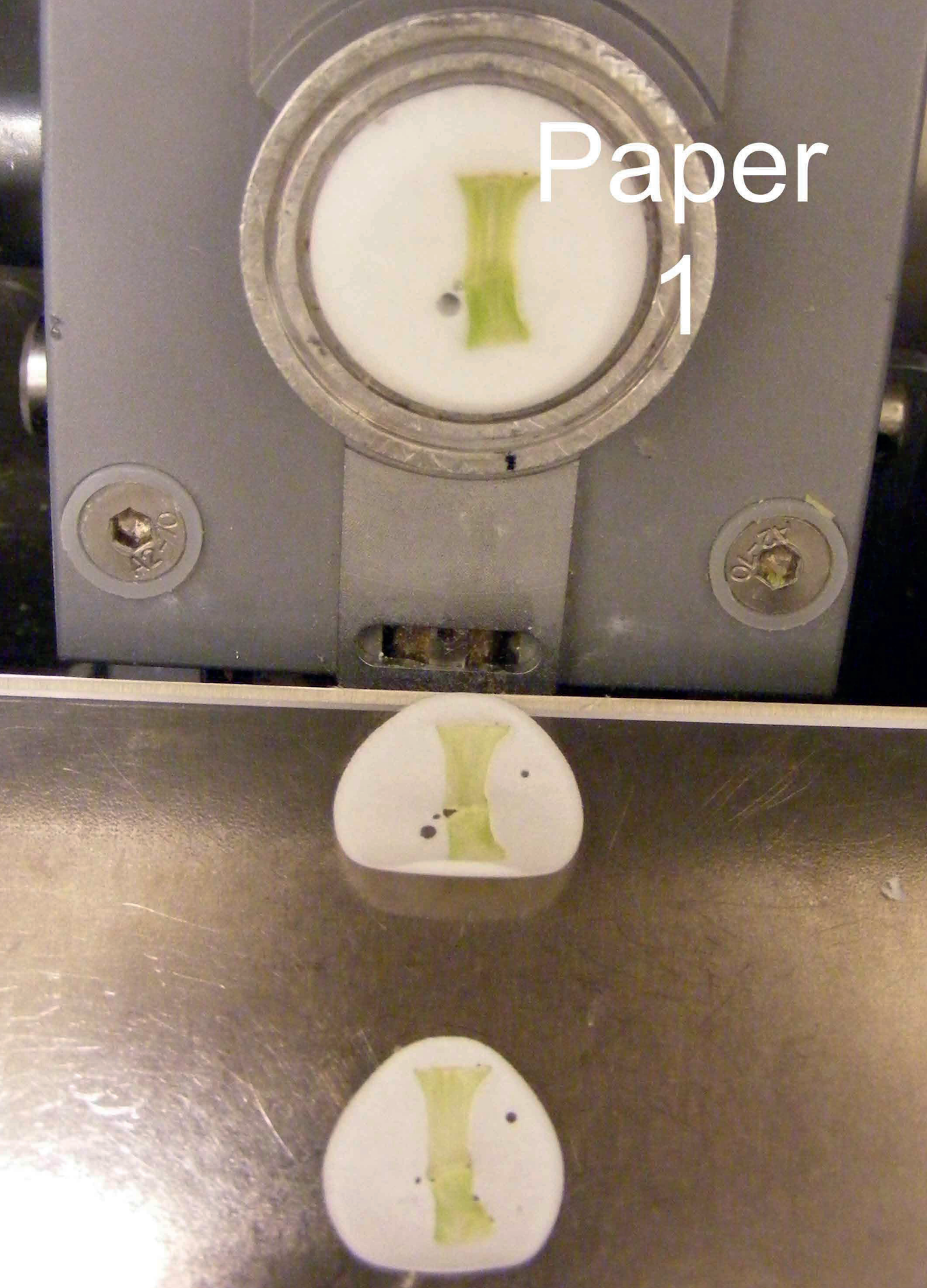
- Roberts, J.A., Schindler, C.B., and Tucker, G.A. (1984). Ethylene-promoted tomato flower abscission and the possible involvement of an inhibitor. *Planta* 160(2), 159-163. doi: 10.1007/bf00392864.
- Roberts, J.A., Whitelaw, C.A., Gonzalez-Carranza, Z.H., and McManus, M.T. (2000). Cell Separation Processes in Plants—Models, Mechanisms and Manipulation. *Annals of Botany* 86(2), 223-235. doi: 10.1006/anbo.2000.1203.
- Rogers, H.J. (2013). From models to ornamentals: how is flower senescence regulated? *Plant Molecular Biology* 82(6), 563-574. doi: 10.1007/s11103-012-9968-0.
- Rubinstein, B., and Leopold, A.C. (1963). Analysis of the Auxin Control of Bean Leaf Abscission. *Plant Physiology* 38(3), 262.
- Ruperti, B., Cattivelli, L., Pagni, S., and Ramina, A. (2002a). Ethylene-responsive genes are differentially regulated during abscission, organ senescence and wounding in peach (*Prunus persica*) *Journal of Experimental Botany* 53 (368), 429-437.
- Ruperti, B., Cattivelli, L., Pagni, S., and Ramina, A. (2002b). Ethylene-responsive genes are differentially regulated during abscission, organ senescence and wounding in peach (*Prunus persica*). *Journal of Experimental Botany* 53(368), 429-437.
- Sakamoto, M., Munemura, I., Tomita, R., and Kobayashi, K. (2008). Involvement of hydrogen peroxide in leaf abscission signaling, revealed by analysis with an in vitro abscission system in *Capsicum* plants. *Plant J* 56(1), 13-27. doi: 10.1111/j.1365-313X.2008.03577.x.
- Schena, M., Shalon, D., Davis, R.W., and Brown, P.O. (1995). Quantitative Monitoring of Gene Expression Patterns with a Complementary DNA Microarray. *Science* 270(5235), 467-470. doi: 10.1126/science.270.5235.467.
- Sequeira, L., and Steeves, T.A. (1954). Auxin Inactivation and Its Relation to Leaf Drop Caused by the Fungus *Omphalia Flavida*. *Plant Physiology* 29(1), 11-16.
- Sexton, R., Jamieson, G.G.C., and Allan, M.H.I.L. (1977). An ultrastructural study of abscission zone cells with special reference to the mechanism of enzyme secretion. *Protoplasma* 91(4), 369-387. doi: 10.1007/BF01291927.
- Sexton, R., Laird, G., and van Doorn, W.G. (2000). Lack of ethylene involvement in tulip tepal abscission. *Physiologia Plantarum* 108(3), 321-329. doi: doi:10.1034/j.1399-3054.2000.108003321.x.
- Sexton, R., Lewis, L.N., Trewavas, A.J., and Kelly, P. (1985). "16 - ETHYLENE AND ABSCISSION," in *Ethylene and Plant Development*, eds. J.A. Roberts & G.A. Tucker. Butterworth-Heinemann), 173-196.
- Sexton, R., and Roberts, J.A. (1982). Cell biology of abscission. *Annual Review of Plant Physiology and Plant Molecular Biology* 33, 133-162.
- Sharova, L.V., Sharov, A.A., Nedorezov, T., Piao, Y., Shaik, N., and Ko, M.S.H. (2009). Database for mRNA Half-Life of 19 977 Genes Obtained by DNA Microarray Analysis of Pluripotent and Differentiating Mouse Embryonic Stem Cells. *DNA Research* 16(1), 45-58. doi: 10.1093/dnares/dsn030.
- Shi, C.-L., Stenvik, G.-E., Vie, A.K., Bones, A.M., Pautot, V., Proveniers, M., et al. (2011). Arabidopsis Class I KNOTTED-Like Homeobox Proteins Act Downstream in the IDA-HAE/HSL2 Floral Abscission Signaling Pathway. *The Plant Cell* 23(7), 2553-2567. doi: 10.1105/tpc.111.084608.
- Shi, Y.-F., Wang, D.-L., Wang, C., Culler, Angela H., Kreiser, Molly A., Suresh, J., et al. (2015). Loss of GSNOR1 Function Leads to Compromised Auxin Signaling and Polar Auxin Transport. *Molecular Plant* 8(9), 1350-1365.
- Shi, Z., Jiang, Y., Han, X., Liu, X., Cao, R., Qi, M., et al. (2017). SIPIN1 regulates auxin efflux to affect flower abscission process. *Scientific Reports* 7(1), 14919. doi: 10.1038/s41598-017-15072-7.
- Shoji, K., Addicott, F.T., and Swets, W.A. (1951). AUXIN IN RELATION TO LEAF BLADE ABSCISSION. *Plant Physiology* 26(1), 189-191.

- Singh, A.P., Tripathi, S.K., Nath, P., and Sane, A.P. (2011). Petal abscission in rose is associated with the differential expression of two ethylene-responsive xyloglucan endotransglucosylase/hydrolase genes, RbXTH1 and RbXTH2. *Journal of Experimental Botany* 62(14), 5091-5103. doi: 10.1093/jxb/err209.
- Slovin, J.P., and Tobin, E.M. (1982). Synthesis and turnover of the light-harvesting chlorophylla/b-protein in *Lemna gibba* grown with intermittent red light: possible translational control. *Planta* 154(5), 465-472. doi: 10.1007/bf01267815.
- Snipes, C.E., and Baskin, C.C. (1994). Influence of early defoliation on cotton yield, seed quality, and fiber properties. *Field Crops Research* 37(2), 137-143.
- Soeno, K., Goda, H., Ishii, T., Ogura, T., Tachikawa, T., Sasaki, E., et al. (2010). Auxin biosynthesis inhibitors, identified by a genomics-based approach, provide insights into auxin biosynthesis. *Plant Cell Physiol* 51(4), 524-536. doi: 10.1093/pcp/pcq032.
- Stintzi, A., Heitz, T., Prasad, V., Wiedemann-Merdinoglu, S., Kauffmann, S., Geoffroy, P., et al. (1993). Plant 'pathogenesis-related' proteins and their role in defense against pathogens. *Biochimie* 75(8), 687-706. doi: doi.org/10.1016/0300-9084(93)90100-7.
- Storz, G., Altuvia, S., and Wassarman, K.M. (2005). AN ABUNDANCE OF RNA REGULATORS. *Annual Review of Biochemistry* 74(1), 199-217. doi: 10.1146/annurev.biochem.74.082803.133136.
- Strømme, E. (1994). "Thormod Hegg - the man and his work," in *The Scientific basis of poinsettia production*, ed. E.E. Strømme. (Aas-NLH, Norway: The Agricultural University of Norway Advisory Service), 9-14.
- Stø, I.M., Orr, R.J., Fooyontphanich, K., Jin, X., Knutsen, J.M., Fischer, U., et al. (2015). Conservation of the abscission signaling peptide IDA during Angiosperm evolution: withstanding genome duplications and gain and loss of the receptors HAE/HSL2. *Frontiers in Plant Science* 6, 931. doi: 10.3389/fpls.2015.00931.
- Suzuki, S., and Umezawa, T. (2007). Biosynthesis of lignans and norlignans. *Journal of Wood Science* 53(4), 273-284. doi: 10.1007/s10086-007-0892-x.
- Taylor, J.E., and Whitelaw, C.A. (2001). Signals in abscission. *New Phytologist* 151(2), 323-340.
- Taylor, J.M., Lopez, R.G., Currey, C.J., and Janick, J. (2011). The poinsettia: History and transformation. *Chronica Horticulturae* 51(3), 23-28.
- Tivendale, N.D., and Cohen, J.D. (2015). Analytical History of Auxin. *Journal of Plant Growth Regulation* 34(4), 1-15. doi: 10.1007/s00344-015-9519-4.
- Tranbarger, T.J., Tucker, M.L., Roberts, J.A., and Meir, S. (2017). Editorial: Plant Organ Abscission: From Models to Crops. *Frontiers in Plant Science* 8(196). doi: 10.3389/fpls.2017.00196.
- Tsuchiya, M., Satoh, S., and Iwai, H. (2015). Distribution of XTH, Expansin, and Secondary-wall-related CesA in Floral and Fruit Abscission Zones during Fruit Development in Tomato (*Solanum lycopersicum*). *Frontiers in Plant Science* 6. doi: 10.3389/fpls.2015.00323.
- Tsuchiya, T., Ohta, H., Okawa, K., Iwamatsu, A., Shimada, H., Masuda, T., et al. (1999). Cloning of chlorophyllase, the key enzyme in chlorophyll degradation: Finding of a lipase motif and the induction by methyl jasmonate. *Proceedings of the National Academy of Sciences* 96(26), 15362-15367.
- Tucker, G.A., Schindler, C.B., and Roberts, J.A. (1984). Flower abscission in mutant tomato plants. *Planta* 160(2), 164-167.
- Tucker, M.L., Burke, A., Murphy, C.A., Thai, V.K., and Ehrenfried, M.L. (2007). Gene expression profiles for cell wall-modifying proteins associated with soybean cyst nematode infection, petiole abscission, root tips, flowers, apical buds, and leaves. *Journal of Experimental Botany* 58(12), 3395-3406. doi: 10.1093/jxb/erm188.
- Tucker, M.L., Sexton, R., del Campillo, E., and Lewis, L.N. (1988). Bean Abscission Cellulase : Characterization of a cDNA Clone and Regulation of Gene Expression by Ethylene and Auxin. *Plant Physiology* 88(4), 1257-1262.
- Turner, J.G., Ellis, C., and Devoto, A. (2002). The Jasmonate Signal Pathway. *The Plant Cell* 14(suppl 1), S153-S164. doi: 10.1105/tpc.000679.

- Tyanova, S., Temu, T., Sinitcyn, P., Carlson, A., Hein, M.Y., Geiger, T., et al. (2016). The Perseus computational platform for comprehensive analysis of (prote)omics data. *Nature Methods* 13(9), 731-740. doi: 10.1038/nmeth.3901.
- Uggla, C., Moritz, T., Sandberg, G., and Sundberg, B. (1996). Auxin as a positional signal in pattern formation in plants. *Proceedings of the National Academy of Sciences* 93(17), 9282-9286.
- Ulmasov, T., Murfett, J., Hagen, G., and Guilfoyle, T.J. (1997). Aux/IAA proteins repress expression of reporter genes containing natural and highly active synthetic auxin response elements. *The Plant Cell* 9(11), 1963-1971. doi: 10.1105/tpc.9.11.1963.
- van Doorn, W.G. (2002). Effect of ethylene on flower abscission: a survey. *Annals of Botany* 89(6), 689-693.
- van Doorn, W.G., and Stead, A.D. (1997). Abscission of flowers and floral parts. *Journal of Experimental Botany* 48(4), 821-837. doi: 10.1093/jxb/48.4.821.
- van Nocker, S. (2009). Development of the abscission zone. *Stewart Postharvest Review* 5(1).
- Vanneste, S., and Friml, J. (2009). Auxin: A Trigger for Change in Plant Development. *Cell* 136(6), 1005-1016.
- Vogt, T. (2010). Phenylpropanoid Biosynthesis. *Molecular Plant* 3(1), 2-20. doi: doi.org/10.1093/mp/ssp106.
- Wang, X., Liu, D., Li, A., Sun, X., Zhang, R., Wu, L., et al. (2013). Transcriptome Analysis of Tomato Flower Pedicel Tissues Reveals Abscission Zone-Specific Modulation of Key Meristem Activity Genes. *PLoS ONE* 8(2), e55238. doi: 10.1371/journal.pone.0055238.
- Wang, Y.C., Li, T.L., Meng, H.Y., and Sun, X.Y. (2005). Optimal and spatial analysis of hormones, degrading enzymes and isozyme profiles in tomato pedicel explants during ethylene-induced abscission. *Plant Growth Regulation* 46, 97-107.
- Warren Wilson, J., Warren Wilson, P.M., and Walker, E.S. (1988). Effects of applied IAA on the position of abscission sites induced in wounded explants from *Impatiens sultani* internodes. *Annals of Botany* 62(3), 235-243.
- Warren Wilson, P.M., Warren Wilson, J., and Addicott, F.T. (1986). Induced abscission sites in internodal explants of *Impatiens sultani* - a new system for studying positional control. *Annals of Botany* 57(4), 511-530.
- Weaver, L.M., Gan, S., Quirino, B., and Amasino, R.M. (1998). A comparison of the expression patterns of several senescence-associated genes in response to stress and hormone treatment. *Plant Molecular Biology* 37(3), 455-469.
- Weber, A.P.M. (2015). Discovering New Biology through Sequencing of RNA. *Plant Physiology* 169(3), 1524.
- Webster, B.D. (1968). Anatomical Aspects of Abscission. *Plant Physiology* 43(9), 1512-1544.
- Webster, B.D., and Leopold, A.C. (1972). Stem Abscission in Phaseolus vulgaris Explants. *Botanical Gazette* 133(3), 292-298. doi: 10.2307/2473918.
- Webster, G.L. (2014). "Euphorbiaceae," in *Flowering Plants. Eudicots*, ed. K. Kubitzki. Springer Berlin Heidelberg), 51-216.
- Wiese, M.V., and Devay, J.E. (1970). Growth Regulator Changes in Cotton Associated with Defoliation Caused by Verticillium albo-atrum. *Plant Physiology* 45(3), 304-309.
- Wilkinson, J.Q., Lanahan, M.B., Yen, H.C., Giovannoni, J.J., and Klee, H.J. (1995). An ethylene-inducible component of signal transduction encoded by never-ripe. *Science* 270(5243), 1807-1809.
- Wu, X.M., Yu, Y., Han, L.B., Li, C.L., Wang, H.Y., Zhong, N.Q., et al. (2012). The tobacco BLADE-ON-PETIOLE2 gene mediates differentiation of the corolla abscission zone by controlling longitudinal cell expansion. *Plant Physiology* 159(2), 835-850. doi: 10.1104/pp.112.193482.
- Wu, Z.C., and Burns, J.K. (2004). A β -galactosidase gene is expressed during mature fruit abscission of 'Valencia' orange (*Citrus sinensis*). *Journal of Experimental Botany* 55(402), 1483-1490.

- Xu, Y., Chang, P., Liu, D., Narasimhan, M.L., Raghothama, K.G., Hasegawa, P.M., et al. (1994). Plant Defense Genes Are Synergistically Induced by Ethylene and Methyl Jasmonate. *The Plant Cell* 6(8), 1077-1085. doi: 10.1105/tpc.6.8.1077.
- Yang, X.Y., Chen, W.P., Rendahl, A.K., Hegeman, A.D., Gray, W.M., and Cohen, J.D. (2010). Measuring the turnover rates of Arabidopsis proteins using deuterium oxide: an auxin signaling case study. *The Plant Journal* 63(4), 680-695. doi: 10.1111/j.1365-313X.2010.04266.x.
- Yang, Z., Zhong, X., Fan, Y., Wang, H., Li, J., and Huang, X. (2015). Burst of reactive oxygen species (ROS) in pedicel mediated fruit abscission after carbohydrate supply was cut off in longan (*Dimocarpus longan*). *Frontiers in Plant Science* 6. doi: 10.3389/fpls.2015.00360.
- Ye, Z.-H. (2002). VASCULAR TISSUE DIFFERENTIATION AND PATTERN FORMATION IN PLANTS. *Annual Review of Plant Biology* 53(1), 183-202. doi: 10.1146/annurev.arplant.53.100301.135245.
- Zhang, X.-l., Qi, M.-f., Xu, T., Lu, X.-j., and Li, T.-l. (2015). Proteomics profiling of ethylene-induced tomato flower pedicel abscission. *Journal of Proteomics* (0).
- Zhang, Y., Fonslow, B.R., Shan, B., Baek, M.-C., and Yates, J.R. (2013). Protein Analysis by Shotgun/Bottom-up Proteomics. *Chemical Reviews* 113(4), 2343-2394. doi: 10.1021/cr3003533.
- Zheng, Z., Guo, Y., Novák, O., Dai, X., Zhao, Y., Ljung, K., et al. (2013). Coordination of auxin and ethylene biosynthesis by the aminotransferase VAS1. *Nature Chemical Biology* 9, 244. doi: 10.1038/nchembio.1178.
- Zhu, Z., and Lee, B. (2015). Friends or Foes: New Insights in Jasmonate and Ethylene Co-Actions. *Plant and Cell Physiology* 56(3), 414-420. doi: 10.1093/pcp/pcu171.

Paper
1




METHODOLOGY ARTICLE

Open Access



Auxin analysis using laser microdissected plant tissues sections

Luz G. Muñoz-Sanhueza¹, YeonKyeong Lee¹, Molly Tillmann², Jerry D. Cohen² and Anne Kathrine Hvoslef-Eide^{1*} 

Abstract

Background: Quantitative measurement of actual auxin levels in plant tissue is complimentary to molecular methods measuring the expression of auxin related genes. Current analytical methods to quantify auxin have pushed the limit of detection to where auxin can be routinely quantified at the pictogram (pg) level, reducing the amount of tissue needed to perform these kinds of studies to amounts never imagined a few years ago. In parallel, the development of technologies like laser microdissection microscopy (LMD) has allowed specific cells to be harvested from discrete tissues without including adjacent cells. This method has gained popularity in recent years, especially for enabling a higher degree of spatial resolution in transcriptome profiling. As with other quantitative measurements, including hormone quantifications, sampling using traditional LMD is still challenging because sample preparation clearly compromises the preservation of analytes. Thus, we have developed and validated a sample preparation protocol combining cryosectioning, freeze-drying, and capturing with a laser microdissection microscope to provide high-quality and well-preserved plant materials suitable for ultrasensitive, spatially-resolved auxin quantification.

Results: We developed a new method to provide discrete plant tissues for indole-3-acetic acid (IAA) quantification while preserving the plant tissue in the best possible condition to prevent auxin degradation. The method combines the use of cryosectioning, freeze-drying and LMD. The protocol may also be used for other applications that require small molecule analysis with high tissue-specificity where degradation of biological compounds may be an issue. It was possible to collect the equivalent to 15 mg of very specific tissue in approximately 4 h using LMD.

Conclusions: We have shown, by proof of concept, that freeze dried cryosections of plant tissue were suitable for LMD harvest and quantification of the phytohormone auxin using GC-MS/MS. We expect that the ability to resolve auxin levels with both spatial- and temporal resolution with high accuracy will enable experiments on complex processes, which will increase our knowledge of the many roles of auxins (and, in time, other phytohormones) in plant development.

Keywords: Auxin quantification, Isotope dilution analysis, Laser microdissection microscope, GC-MS/MS quantification, Plant sample preparation, Minute samples, Freeze drying, Lyophilisation, Cryosectioning

Background

With the ability to analyse very low hormone levels comes the desire to be able to sample very specific plant tissues in order to uncover the precise hormonal changes regulating development. Phytohormones are often active in very specific tissues or cell layers within a tissue, and the ability to distinguish one cell type from another can be revolutionary in the understanding of these responses.

Auxins can serve as an example of the more delicate phytohormones, and are involved in a plethora of different plant growth and developmental responses, including lateral and adventitious root formation, cell expansion, apical dominance, gravitropism, and abscission, among others. The effect of a mobile auxin signal was first described in the latter half of the nineteenth century by Ciesielski [1] on root responses to gravity, but the chemical identity of the signalling compound was not discovered until the first half of the twentieth century that identified indole-3-acetic acid [2].

The physiological response to auxin is highly dependent on local concentrations. Thus, biosynthesis, degradation,

* Correspondence: trine.hvoslef-eide@nmbu.no

¹Department of Plant Sciences (IPV), Faculty of Biosciences, Norwegian University of Life Sciences, Norway Campus Ås, Universitetsunet 3, 1430 Ås, Norway

Full list of author information is available at the end of the article



© The Author(s). 2018 **Open Access** This article is distributed under the terms of the Creative Commons Attribution 4.0 International License (<http://creativecommons.org/licenses/by/4.0/>), which permits unrestricted use, distribution, and reproduction in any medium, provided you give appropriate credit to the original author(s) and the source, provide a link to the Creative Commons license, and indicate if changes were made. The Creative Commons Public Domain Dedication waiver (<http://creativecommons.org/publicdomain/zero/1.0/>) applies to the data made available in this article, unless otherwise stated.

and transport of auxin play central roles in maintaining what appears to be a delicate homeostatic equilibrium among auxin precursors, free hormone, and conjugates.

As we discussed previously [3], spatial-temporal resolution of auxin activity has been visualized using various reporter systems. These methods are based on constructs using synthetic promoters such as DR5 [4] or co-receptors such as the fusion protein DII-VENUS [5]. They have been developed, and are particularly useful for reference plant species with standardized transformation protocols. Although these techniques have important utility for understanding sites of auxin activity they do not quantitatively measure auxin levels and, as Liao et al. [6] emphasized in their report, “It is important to note that neither reporter shows a linear response to auxin concentrations or treatment duration, and hence these cannot be used to infer actual auxin levels.” Nevertheless, these methods complement the absolute quantification procedure described here for measurements in specific tissues.

The capacity to detect and quantify auxin metabolites in plant tissues has been a major driving force in plant biology since the first bioassays were developed in the 1920s and 1930s [3]. Auxins are present in very low concentrations in plant tissues, typically in the range of 5–50 ng/g fresh weight [7]. We have found that poinsettia flower buds have, in agreement with these general ranges, IAA concentrations in the range of 1.2 to 55 ng/g FW (Hvoslef-Eide, et al., manuscript in prep). Early studies required kilogram amounts of plant materials, as well as days to months of effort, for a single measurement [3]. To overcome these limitations, improved auxin purification methods and the utilization of increasingly more sensitive instruments have been developed. Since its initial application for quantification of auxins, isotope dilution [3] has played an important role in auxin quantification by mass spectrometry. It has allowed the application of modern sample manipulation and the utilization of constantly improving instrumentation, to such an extent that the procedures have reached impressive limits, especially regarding to the amount of plant material needed for an analysis [8]. These highly sensitive physical methods for analysis have the potential to provide insight into the role of auxin in the plant's physiology because they open up the possibility to measure auxin distribution with high spatial resolution [9].

Laser microdissection microscopy (LMD) allows specific cells to be harvested from complex tissues, even to the level of the single cell, providing a starting point for downstream analyses including quantitative real-time polymerase chain reaction (PCR), microarray, DNA genotyping, RNA transcript profiling, generation of cDNA libraries, etc. This technology has been available since 1996 [10], but the first application in a plant study was not until 2002 [11].

LMD has been primarily used in combination with RNA isolation and gene expression studies [12, 13], which can be accomplished on paraffin-embedded tissue. LMD applications for analysis of small molecule metabolites, especially phytohormones, present additional challenges due to the intrinsic low concentration of these molecules, their solubility in embedding matrix materials and water, and the possibility of compound degradation, especially under ambient temperatures. These characteristics make traditional LMD protocols inappropriate for auxin sample preparation because use of solvents and fixatives during the dehydration and fixation processes would solubilize and/or result in degradation of the hormone *in situ*. In order to maintain the original phytohormone content of the tissues, cryosectioning followed by freeze-drying has been applied, since freeze-drying does not alter the hormone content [14]. Cryosectioning has more typically been applied to animal tissues rather than plant tissues because the presence of vacuoles and cell walls in plants often make it difficult to preserve the integrity of cell structures [15, 16]. However, an increase in thickness of the cryosections improves results with such tissues. Here, we report an efficient sample preparation method that combines three steps: (1) cryosectioning of the plant tissue, (2) freeze-drying of the cryosections, and (3) harvesting the cells using LMD. This protocol describes collection of plant materials for the subsequent auxin extraction and quantification using the GC-MS/MS and isotope dilution [8]. Due to the lack of protocols that combine the use of LMD and auxin quantification, and since an important role for auxin in plant development is its function as a positional signal [9], this work has potential for leading to a significant improvement in the quality of information provided by hormone analysis.

Methods

Plant materials

Cuttings with at least two leaves approximately 5 cm long were harvested from poinsettia (*Euphorbia pulcherrima*, Willd. ex Klotzsch) ‘Millenium.’ Mother plants and cuttings were grown under long day conditions (16 h light, 22 °C day and 20 °C night) and cuttings were kept in 70% relative humidity (RH) for four weeks. After the cuttings were rooted, they were transferred to 12 cm pots and kept under the same conditions for an additional two to three weeks. To induce flowering, the plantlets were transferred to short day conditions (10 h light, 20 °C) and RH 74%. The inflorescence of poinsettia is arranged with a main flower (first order flower), surrounded by three second order flowers, in turn surrounded by six third order flowers [17]. Six third order flower buds of identical development were used in this study.

Abscission induction by flower bud decapitation

When third order flower buds were fully developed, they were decapitated with a razor blade at cutting point 2 according to our previous publications (cp2; Fig. 1a). By doing this, the floral organs are removed but the remaining flower is kept intact [18, 19]. This induces formation of the abscission zone, which was visible after approximately four days (D4), and the bud abscised approximately seven days after induction (D7).

Validation of the method with control samples

To validate the biological sampling method, we collected the area of interest within the abscission zone from the bud immediately after decapitation (D0) and then from the abscission zone six days after decapitation (Fig. 2). The abscission zone typically has a very irregular tri-dimensional cone shape, thus making it difficult to collect manually without inclusion of adjacent cell layers; this characteristic makes it an ideal candidate for the precision of LMD (Fig. 3). The results of this sampling were compared with simple cross sections of flower buds collected at the same stage in the abscission zone area. The difference between the experimental samples and the control samples was a comparison of freeze-dried tissue harvested with precision using the laser microdissection microscope in contrast to frozen cross sections that included unwanted cell types. We thus expected the results to fall within the same order of magnitude, but would not necessarily yield exactly the same values for the tissue IAA concentrations.

Materials

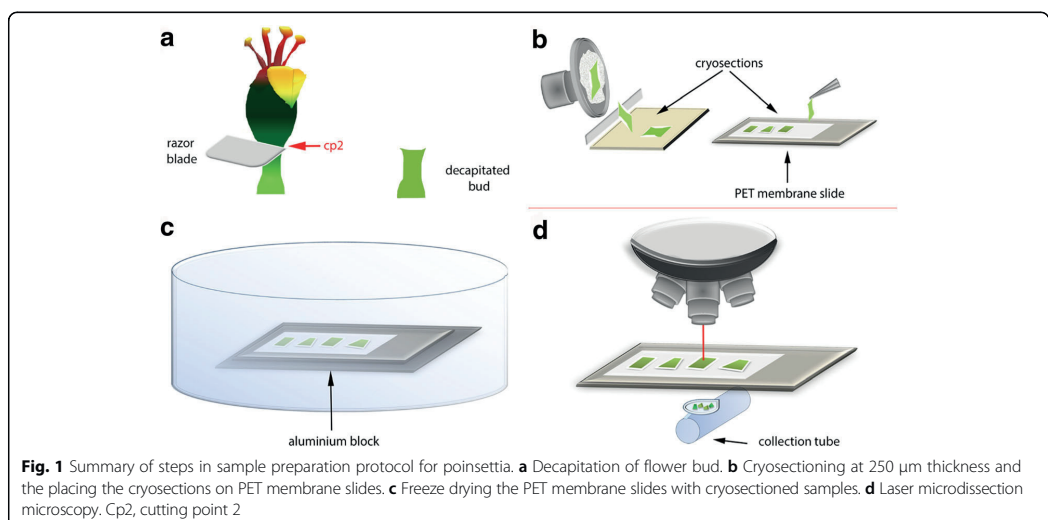
- Tissue-Tek® OCT™ Compound and Cryomolds® (Sakura Finetek, Netherlands)
- Frame slides PET (polyethylene terephthalate)-membrane 1.4 µm, ref. n° 11,505,190 (Leica Microsystems, Germany)
- Tweezers 2A (A. Dumont & Fils, Switzerland)
- Custom-made aluminium blocks 3.0 cm × 8.5 cm × 0.4 cm
- RNase free Microcentrifuge tubes 0.6 ml
- Frame support Leica n°11,532,325 (Leica Microsystems, Germany)
- Accu-Edge® 4689 Low Profile Microtome Blades (Feather Japan)

Equipment

- Cryostat Microtome HM560 (Microm, Germany)
- Freeze drier with top container (Heto Holten A/S, Allerød, Denmark)
- Laser microdissection microscope Leica 6000 (Leica Microsystems, Germany) with software V6.7.2.4295
- Laser Leica CTR 6500 (Leica Microsystems, Germany)

Pre-sampling procedures

The abscission zone tissues from poinsettia flower buds in two different stages of the abscission zone progression were selected for this study, and specific cell layers corresponding to the abscission zones were harvested using LMD. The morphology of the abscission zone is very characteristic, making it easy to identify under a microscope.



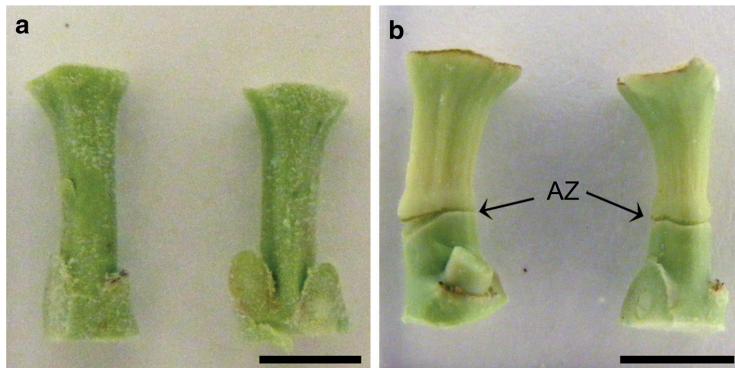


Fig. 2 Decapitated poinsettia flower buds; **a** Day 0. **b** 6 days after decapitation. AZ, abscission zone. Arrows indicate abscission zone. Bars 5 mm

Three biological replicates were used in this study. An average of two flower buds per replicate were used for Day 0 and 2.8 flower buds for Day 6. Every replicate was subjected to: (1) the sample preparation procedure consisting of cryosectioning, freeze-drying, and LMD (Fig. 1), and (2) the final analytical procedure consisting of auxin extraction, derivatization and quantification using the protocol developed by Liu et al. [8]

This protocol includes five parts:

1. Longitudinal cryosectioning of flower buds using a cryostat
2. Freeze-drying cryosections generated from the previous step
3. LMD of freeze-dried cryosections in order to harvest specific tissue in the abscission zone
4. Method validation

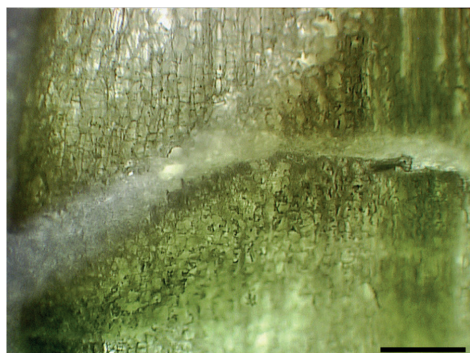


Fig. 3 Longitudinal section of poinsettia flower bud at 6 days after decapitation (D6), abscission zone can be identified from its inverted cone shape. Bar, 310 μ m

5. Auxin extraction from microdissected tissues and quantification by GC-MS/MS

Tissue collection and cryosectioning

D0 buds were decapitated and collected immediately, and D6 buds were harvested six days after decapitation. For both time points, whole decapitated buds were harvested and placed in liquid nitrogen immediately after collection and stored at -80°C until cryosectioning. Cryosectioning was performed using a Cryostat Microtome HM560 (Microm, Germany) with an Accu-Edge[®] 4689 Low Profile Microtome Blade (Feather Japan). The temperature of the blade and specimen (sample holder) were modified in the cryostat to -16°C and -15°C , respectively; optimal temperatures can vary from tissue to tissue depending on their macro structure. To find the optimal combination for every sample type, trial tests were necessary with test plant materials.

The desired cryosection thickness can also differ depending on the goal of the study and the nature of the tissue. In this study, the thickness was typically about 250 μ m, although acceptable results were obtained from sections ranging from 70 μ m to 350 μ m. The flower bud was placed on the sample holder using a drop of Optimal Cutting Temperature (OCT[™] Tissue-Tek[®] Compound and Cryomolds[®], Sakura Finetek, Netherlands) embedding medium to keep it fixed in the desired position (Fig. 4). Some extra OCT was added around the flower bud just before beginning the fast freeze process inside the cryostat chamber. Excess OCT can be removed from the edges of the tissue with a razor blade when needed. In order to prevent degradation of auxins during cryosectioning, straight tweezers with flat tips (Tweezers 2A A. Dumont & Fils, Switzerland) were used to manipulate the flower buds while the flower buds were kept on dry ice. Once the cryosections were transferred to the PET membrane slide

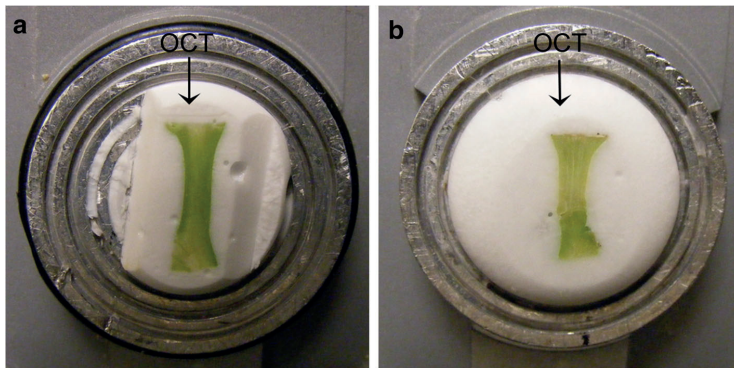


Fig. 4 Sample holder with poinsettia buds in OCT compound ready for cryosection. **a** Bud at D0 (day of decapitation). **b** Bud at D6 (6 days after decapitation). OCT: optimum cutting temperature. Arrows indicate OCT compound

using the cold tweezers, a Leica acrylic frame support (n°11,532,325, Leica Microsystems, Germany) was placed directly under the slice for several seconds to help the cryosections adhere to the slide surface. When placed correctly, the tissue and OCT will both spread evenly onto the membrane. This placement was done quickly to avoid exposing the cryosections to higher temperatures. Three to four cryosections were placed on each slide (Fig. 5). While OCT was useful in helping cryosections adhere to the slide membrane, it must be used with care to avoid contamination of the tissue through liquefying. Cryosections can stick to the membrane without OCT, but tissue edges may fold over during the freeze-drying process resulting in loss of the sample from the PET membrane slide. The PET membrane slides were kept in a controlled temperature chamber at -19°C in the cryostat or on dry ice after each cryosection.

Freeze drying

The PET membrane slides with the cryosections were placed on top of pre-frozen custom-made aluminium blocks of 4 mm thickness in order to maintain them in a

frozen state (Fig. 6). The cryosections were freeze-dried in vacuo until the tissues were totally dried. The freeze-dried slides were stored at -80°C until microdissection. To test the tissue integrity and the feasibility of distinguishing desired structures after freeze-drying, different thicknesses of tissue sections were evaluated (70, 100, 200, 250 and $300\text{ }\mu\text{m}$).

Microdissection

Microdissection was performed using a Leica 6000 laser microdissection microscope (Leica, Microsystems, Germany). The laser (CryLaS FTSS 355–50, Germany) was turned on at least 20 min in advance to allow it to warm up before starting the dissection. Laser parameters were set using Laser Microdissection software (V6.7.2.4295, Leica Microsystems, Germany) as follows: power 60, aperture 45, speed 20, and specimen balance 0. These parameters, optimized for the material we used in this study, can be adjusted in order to obtain the best conditions for every new tissue. The cutting position of the laser was calibrated using a new PET membrane slide or an area of membrane without any tissue. A clean microcentrifuge tube was placed in the collector

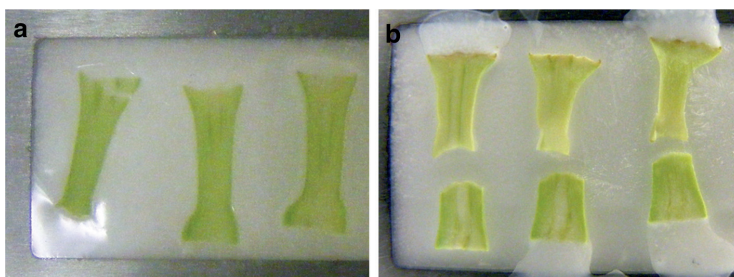


Fig. 5 PET membrane slides with cryosections of poinsettia buds. **a** D0 (day of decapitation). **b** D6 (six days after decapitation)



Fig. 6 4 mm thickness aluminium blocks under the PET membrane slides during the freeze dry process

device under the microscope stage and a slide with the cryosections was placed in the slide holder to start the dissection. The area of interest was selected and dissected, and the microdissected tissues were collected by gravity.

Microdissection was performed on only one slide at a time, and the remaining slides were kept cold in the dark (both important to prevent IAA degradation). All cryosections collected were 250 μm thick, and section volumes were calculated by multiplying the area by the thickness. Because the fragility and small size of the microdissections make them difficult to handle for weighing with a balance, fresh weight information can be more accurately calculated in uniform plant samples using volume to weight conversions determined from larger samples.

Validation samples

To validate the methodology, the flower buds providing the control material were frozen in liquid nitrogen and cross-sectioned with the cryostat around the area of the abscission zone. Three buds were used for each time point. Since the samples were frozen immediately after collection, the weight of each cross section was calculated by measuring the areas with the program ImageJ 1.49n (Rasband, W.S., ImageJ, U. S. National Institutes of Health, Bethesda, Maryland, USA, <https://imagej.nih.gov/ij/>, 1997–2016) and multiplying the result by 0.5 mm according to the thickness of the cross sections (500 μm). Reproducibility was evaluated in the control samples and the LMD samples by considering the average of the three measurements and calculating the standard error. Auxin quantification was performed in the same manner as the experimental material [8].

Auxin quantification

The protocol for auxin extraction [8] is optimally performed in 1.5 ml microcentrifuge tubes; thus, the tissue collected with LMD in a 0.6 ml microcentrifuge tube was transferred. Due to the small size of the cryosections

and the potential presence of the slide membrane underneath them, electrostatic forces require that extra care must be taken. The protocol used in this study can be used to quantify auxin, as well as auxin biosynthetic precursors like tryptophan, indole, indole-3-pyruvic acid (IPyA) and indole-3-butyric acid (IBA). This protocol employs isotope dilution using [$^{13}\text{C}_6$] IAA as the internal standard [20] and requires only 2 to 20 mg of plant material. Approximately 340 pg of internal standard was added to every replicate in this study. The metabolite extract was derivatized with diazomethane [21] and analysed by selecting reaction monitoring (SRM) mode on a GC-MS/MS according to Liu et al. [8]. A small modification to the original protocol was made in the final resuspension step following derivatization, using 10 μL of ethyl acetate instead of 15 μL . Samples were analysed by GC-MS/MS immediately after preparation in this study, although when necessary, samples can be stored at -80°C .

Results

We have described a reliable protocol for sample collection and auxin analysis using small amounts of discrete plant tissues. The protocol combines cryosectioning plant tissues, freeze-drying these cryosections, and laser microdissection for harvesting the specific cells or cell layers. IAA levels are then quantified in the collected plant material by GC-MS/MS with [$^{13}\text{C}_6$] IAA as an internal standard.

Cryosectioning and freeze-drying

1. The integrity of all the cryosections from 70 μm to 200 μm thickness were well preserved after freeze-drying (Fig. 7).
2. The integrity of the cryosection at 250 μm thickness was well preserved after the freeze drying process and was the most suitable thickness for the bud tissue studied
3. For some studies, thicker cryosections (300 to 350 μm) may be desired. These thicknesses were also found to preserve the structure of the frozen tissue (data not shown).

Laser microdissection

4. The laser was able to dissect all thicknesses tested (data not shown). Nevertheless, the thickness of the cryosections at 300 and 350 μm made it more difficult to obtain the correct visualization of the abscission zone because the number of cell layers masked the three-dimensional shape. Thus, for our purpose, it was decided to use 250 μm (Fig. 8).
5. The area harvested using LMD for the average of the D0 samples (three replicates) was $61.8 \pm 3.32 \text{ mm}^2$,

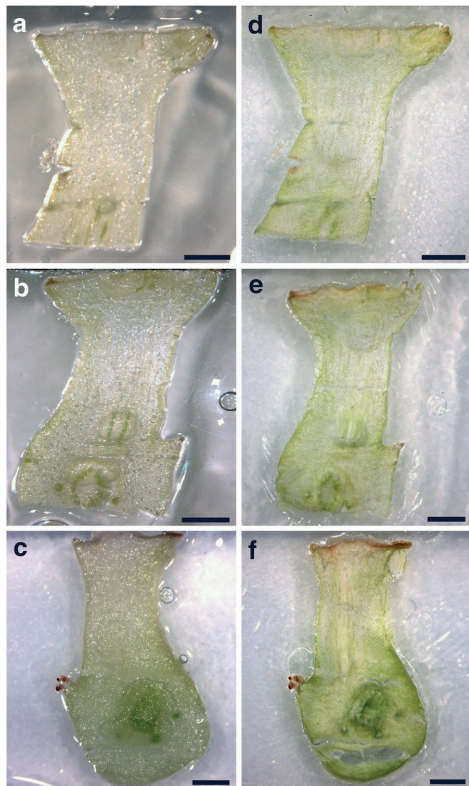


Fig. 7 **a, b, c** Frozen cryosections of poinsettia buds at 70 μ m, 100 μ m and 200 μ m respectively. **d, e, f** The same as in **a, b** and **c** but freeze dried cryosections. Bars, 1 mm. The preservation of the integrity is clear in all the cryosections

corresponding to 15.4 ± 0.83 mg of fresh tissue, while the average area for D6 (three replicates) was 54.9 ± 2.17 mm², equivalent to 13.7 ± 0.53 mg of fresh weight (Table 1).

Auxin quantification

- The chromatogram peaks coincide with the internal standard, indicating the correct auxin identification (Fig. 9).
- Auxin quantification using GC-MS/MS with cryosectioned, freeze-dried and microdissected tissue at different times of abscission zone development showed similar levels of endogenous auxin. For example, D0 and D6 auxin levels were 2.68 ± 0.63 ng/g FW and 3.34 ± 0.82 ng/g FW, respectively (Table 1).
- Auxin quantification with validation samples of frozen cross sections containing abscission zones showed 19.92 ± 8.7 ng/g FW in D0 and 3.33 ± 0.29 ng/g FW in D6. These results confirm that IAA levels from the samples harvested with LMD fall into the same order of magnitude as the cross sections harvested in the control protocol using the cryostat.

Discussion

Auxin quantification protocols for minute plant tissues are under constant development as procedures and equipment improve. The procedure used here was developed by us and first reported in 2012 [8]. It remains as one that needs a relatively small amount of tissue for a single assay, primarily because of the specificity provided by the selecting reaction monitoring (SRM) mode of the GC/MS-MS and precision is provided by the use of isotope dilution with a [¹³C]-labelled internal standard [20]. An important next step for improvement in auxin analysis is the ability to target with specificity the tissue of interest. However, even with the micro methods, the issues of IAA degradation during sample collection, determination of the amounts of

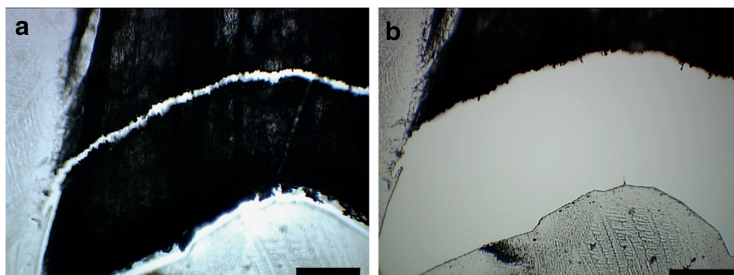


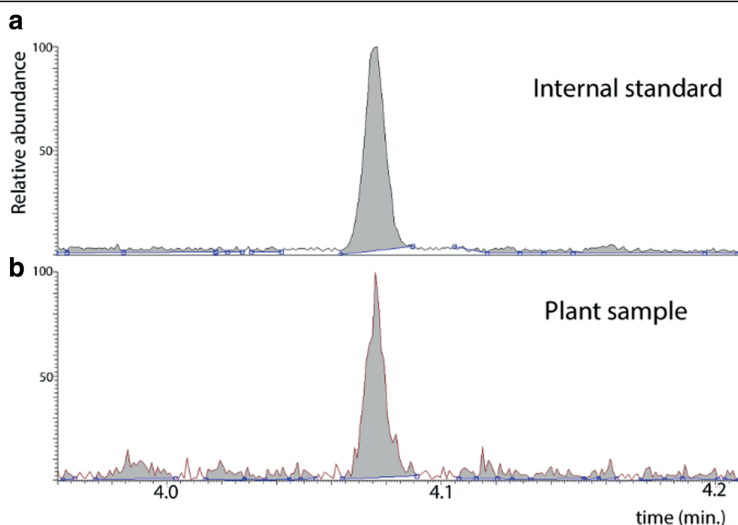
Fig. 8 **a** Abscission zone selected to dissect from flower bud of poinsettia six days after decapitation (D6) on the laser microdissection microscope. **b** The same cryosection after laser microdissection. Bars 310 μ m

Table 1 Summary of collected average areas, fresh weight and auxin concentration in each replicate with standard errors of the mean from day 0 (D0) and six days after decapitation (D6) of abscission zones in poinsettia buds

| | Sample name | Area mm ² | Weight mg | Auxin ng/g FW |
|---------|-------------|----------------------|-------------|---------------|
| | D0-rep1 | 68.1 | 17 | 2.2 |
| | D0-rep2 | 56.8 | 14.2 | 1.9 |
| | D0-rep3 | 60.5 | 15.1 | 3.9 |
| Average | D0 | 61.8 ± 1.92 | 15.4 ± 0.48 | 2.68 ± 0.62 |
| | D6-rep1 | 55.7 | 13.9 | 2.9 |
| | D6-rep2 | 58.2 | 14.6 | 4.9 |
| | D6-rep3 | 50.8 | 12.7 | 2.2 |
| Average | D6 | 54.9 ± 1.25 | 13.7 ± 0.31 | 3.34 ± 0.81 |

tissue for these very small samples, and also how to collect enough of a specific tissue to obtain a good response in the MS remained significant problems. LMD emerged as a feasible way to select and harvest specific areas or cells of known thickness and surface area, but the pre-treatment of the sections, fixation and staining processes most commonly employed lead to the degradation and/or solubilisation of the hormones and other small molecules present in the tissue. This issue was largely overcome by cryosectioning the tissue, thus avoiding any further fixation and staining. An important additional step of freeze-drying with the help of a

frozen aluminium block underneath the slide containing the whole cryosection contributed to the success of this protocol. Two factors were extremely important when deciding which conditions were optimal for treating the plant material: (1) minimizing the preparation time of the tissue to reduce the potential degradation of auxin and (2) obtaining enough material to get reliable quantification by mass spectrometry. Three parameters were evaluated: (1) the thickness of the cryosections, (2) the distinguishability of the abscission zone under the microscope, i.e. the ability to distinguish the macro structures we were targeting, and (3) the feasibility of using a laser to dissect these cryosections. The use of cryosectioning for plant tissues is not a common choice because the presence of vacuoles and cell walls makes it more difficult than for mammalian tissue samples [22]. Also, when they are used, it is very uncommon to find examples of cryosections with a thickness greater than 30 µm due to limitations of microscopy visualization (light penetration). This is especially true for some microscopy applications that require thin sections around 10 to 20 µm. However, as long as the structures remained easy to identify under the microscope, increasing the thickness proved to be beneficial in this case because it allowed us to collect larger amounts of tissue in a shorter time. When the downstream analysis involves low level metabolites or other barely traceable compounds, this can be a great advantage over, for example, protracted pre-treatment protocols or other methods.

**Fig. 9** Chromatograph of auxin quantification in a poinsettia bud from laser microdissection microscope sampling combined with GC-SRM-MS for auxin analysis. **a** The internal standard [¹³C₆]IAA. **b** Poinsettias bud sample corresponding to the abscission zone (AZ) from the day of decapitation (D0), i.e. a Control sample

Conclusions

This is the first report of auxin quantification using microdissected plant materials harvested with LMD. Compared with some other plant hormones, auxin is present in relatively low concentration, is difficult to recover quantitatively, and its positional relocation via polar directed transport makes information on its spatial and temporal levels critical analytical challenges. Therefore, the importance of a reliable method for sample preparation, capable of providing tissue-specificity, is very significant and important. This protocol allows new approaches that will increase our knowledge concerning auxin distribution with spatial specificity within plant tissues. Since the sample preparation used in this study allowed us to exclude the use of solvents, the probability of auxin degradation was minimized. Thus, this protocol offers a clear advantage for exploring auxin concentrations at a more precise level of resolution and in a more straightforward manner. The protocol is suited for other applications such as transcriptomic, proteomics, metabolomics etc., where a high resolution in tissue harvesting is needed and minimal degradation of compounds is crucial for reliable results.

Abbreviations

AZ: Abscission zone; FW: Fresh weight; GC-MS/MS: Gas chromatography coupled to tandem mass spectrometry; IAA: Indole-3-acetic-acid; LMD: Laser microdissection; OCT: Optimal cutting temperature

Acknowledgements

The authors are very grateful to Hilde Raanaas Kolstad from the Imaging Centre at the Norwegian University of Life Sciences (NMBU) for her valuable technical help and the training in the use of the Laser Microdissection Microscope and other instruments.

Funding

Norwegian University of Life Sciences (NMBU) PhD scholarship 2013–2016. Norwegian Centennial Chair (NOCO) Program Travel Fellowship, University of Minnesota. This analytical aspect of the research was funded by the National Science Foundation (IOS-1238812) with supplemental support from the Gordon and Margaret Bailey Endowment for Environmental Horticulture and the Minnesota Agricultural Experiment Station.

Availability of data and materials

Data is available in the Norwegian University of Life Sciences data archive for science and can be obtained by contacting the corresponding author, AKHE.

Authors' contributions

LGMS performed the experiments and wrote the paper, YKL provided supervision and improved figures and the manuscript, MT provided help with the IAA quantification, JDC and AKHE designed the research, provided supervision and contributed to the manuscript. All authors read and approved the final manuscript.

Ethics approval and consent to participate

We declare that we have complied with all local legislation, as well as institutional, national, or international guidelines. We have not conducted field studies nor transported plants in any way not in compliance with Convention on the Trade in Endangered Species of Wild Fauna and Flora.

Consent for publication

Not applicable

Competing interests

The authors declare that they have no competing interests.

Author details

¹Department of Plant Sciences (IPV), Faculty of Biosciences, Norwegian University of Life Sciences, Norway Campus Ås, Universitetstunet 3, 1430 Ås, Norway. ²Department of Horticultural Sciences, Microbial and Plant Genomics Institute, University of Minnesota, 305 Alderman Hall, 1970 Folwell Avenue, Saint Paul, MN 55108, USA.

Received: 11 July 2017 Accepted: 15 June 2018

Published online: 25 June 2018

References

- Ciesielski T. Untersuchungen über die Abwärtskrümmung der Wurtzel. Bei. z. Biol. d. Pflanzen (Conn.). 1872;1(1):1–30.
- Abel S, Theologis A. Odyssey of auxin. Cold Spring Harb Perspect Biol. 2010;2(10):a004572.
- Tivendale N, Cohen J. Analytical history of auxin. J Plant Growth Regul. 2015;34(4):1–15.
- Ulmasov T, et al. Aux/IAA proteins repress expression of reporter genes containing natural and highly active synthetic auxin response elements. Plant Cell. 1997;9(11):1963–71.
- Brunoud G, et al. A novel sensor to map auxin response and distribution at high spatio-temporal resolution. Nature. 2012;482(7383):103–6.
- Liao C-Y, et al. Reporters for sensitive and quantitative measurement of auxin response. Nat Methods. 2015;12(3):207–10.
- Porfiri S, et al. Current analytical methods for plant auxin quantification – a review. Anal Chim Acta. 2016;902:8–21.
- Liu X, et al. Protocol: high-throughput and quantitative assays of auxin and auxin precursors from minute tissue samples. Plant Methods. 2012;8(1):31. p. 1–17
- Uggla C, et al. Auxin as a positional signal in pattern formation in plants. Proc Natl Acad Sci. 1996;93(17):9282–6.
- Emmert-Buck MR, et al. Laser capture microdissection. Science. 1996;274(5289):998–1001.
- Asano T, et al. Construction of a specialized cDNA library from plant cells isolated by laser capture microdissection: toward comprehensive analysis of the genes expressed in the rice phloem. Plant J. 2002;32(3):401–8.
- Olofsson L, Lundgren A, Brodelius PE. Trichome isolation with and without fixation using laser microdissection and pressure catapulting followed by RNA amplification: expression of genes of terpene metabolism in apical and sub-apical trichome cells of *Artemisia annua* L. Plant Sci. 2012;183:9–13.
- Ohtsu K, et al. Cell type-specific gene expression profiling in plants by using a combination of laser microdissection and high-throughput technologies. Plant Cell Physiol. 2007;48(1):3–7.
- George KKL, Eggers V, Moulton JE. Use of frozen vacuum-dried material in auxin and other chemical analyses of plant organs: its extraction with dry ether. Bot Gaz. 1941;102(3):590–601.
- Nelson T, et al. LASER MICRODISSECTION OF PLANT TISSUE: what you see is what you get. Annu Rev Plant Biol. 2006;57(1):181–201.
- Balestrini R, Bonfante P. Laser microdissection (LM): applications to plant materials. Plant Biosystems. 2008;142(2):331–6.
- Hvoslef-Eide AK, et al. Primary and secondary abscission in *Pisum sativum* and *Euphorbia pulcherrima*—how do they compare and how do they differ? Front Plant Sci. 2016;6:1204.
- Lee Y, et al. Sequential cell wall transformations in response to the induction of a pedicel abscission event in *Euphorbia pulcherrima* (poinsettia). Plant J. 2008;54:993–1003.
- Hvoslef-Eide, A.K. et al., Primary and secondary abscission in *Pisum sativum* and *Euphorbia pulcherrima* – how do the compare and how do they differ? In: Tranberger TJ, Tucker M, Roberts JA, Meir, S, editors. Plant Organ Abscission: From Models to Crops. Publisher: Frontiers ISBN: 978-2-88945-328-3; 2016. p. 245–261.
- Cohen JD, Baldi BG, Slovin JP. ¹³C₆ [benzene ring] indole 3 acetic acid: a new internal standard for quantitative mass spectral analysis of indole-3-acetic acid in plants. Plant Physiol. 1986;80(1):14–9.
- Barkawi LS, et al. A high-throughput method for the quantitative analysis of auxins. Nat Protocols. 2010;5(10):1609–18.
- Kerk NM, et al. Laser capture microdissection of cells from plant tissues. Plant Physiol. 2003;132(1):27–35.

Paper 2

R149086 c34 g2
R148638 c10 g2
R148332 c4 g1
R147520 c1 g3
R144932 c12 g1
R140002 c9 g1
R121083 c9 g1
R137325 c9 g1
R142699 c9 g1
R133048 c7 g1
R133048 c7 g1
R139364 c14 g1
R133817 c0 g2
R149486 c3 g1
R147566 c10 g1
R140831 c5 g2
R94174 c0 g2
R139645 c1 g1
R130973 c10 g1
R127367 c4 g1
R134442 c10 g1
R127257 c5 g1
R94598 c0 g1
R95526 c1 g2
R165192 c0 g1
R143446 c18 g1
R146739 c14 g2
R96766 c0 g1
R91965 c0 g1
R77513 c0 g1
R147674 c0 g1
R140747 c21 g3
R140555 c4 g1
R124726 c2 g1
R99228 c1 g1
R117243 c3 g1
R99175 c2 g1
R99429 c1 g1
R165246 c2 g1
R172840 c1 g1
R148332 c4 g1
R144022 c5 g1
R142141 c2 g1
R138438 c0 g1
R136792 c11 g1
R187924 c0 g1
R129113 c1 g1
R128947 c6 g1
R124549 c2 g1
R129191 c1 g1
R97650 c7 g1
R3514 c0 g2
R27580 c8 g1
R102949 c0 g1
R112327 c2 g1
R145678 c4 g3
R132941 c0 g1
R145404 c0 g1
R145404 c0 g1
R143332 c0 g1
R137041 c1 g1
R135800 c5 g1
R137225 c0 g1
R76022 c0 g1
R52324 c0 g1
R172700 c0 g1
R15226 c0 g1
R145829 c0 g1
R92266 c3 g1
R140059 c1 g2
R136312 c0 g1
R121772 c1 g1
R124048 c0 g1
R58349 c0 g1
R59010 c0 g1
R137170 c0 g1
R142577 c4 g1
R106794 c0 g1

Untargeted Proteomics Reveals Global Changes in Pattern of Proteins during Abscission of the Flower Bud of *Euphorbia pulcherrima*

Luz Muñoz-Sanhueza, YeonKyeong Lee and *Anne Kathrine Hvoslef-Eide

Department of Plant Sciences, Faculty of Biosciences, Norwegian University of Life

Sciences, P.O. Box 5003, 1432 Aas, Norway

Corresponding author: Anne Kathrine Hvoslef-Eide

trine.hvoslef-eide@nmbu.no

Telephone: +47-67232760

Abstract

Background: Abscission makes perfect sense from an evolutionary point of view, where the plant rids itself of fruits and seeds, as well as the shedding of organs no longer useful. It is however, a major limiting factor for agricultural crop productivity. We used a model system for investigating the dynamics of the proteome during the abscission process using a unique and reproducible method to induce abscission in the flower buds of *Euphorbia pulcherrima* (poinsettia). The abscission zone (AZ) and the adjacent distal and proximal regions were harvested at different stages of the abscission process, from Day 0 (D0) to Day 6 (D6), after induction of flower bud abscission. The differences in protein abundances from flower bud region extracts were compared statistically using Student's t-tests pairwise comparisons.

Based on these results we were able to reconstruct the series of events in each region of the flower bud using both a temporal and a spatial dimensional analysis.

Results: The temporal changes in the abundance of proteins were identified up to 4 days after decapitation, while spatial changes were detected only on D4 and D6. The distal region and the AZ exhibited the most dramatic fluctuations along the time line, while the proximal portion did not show significant changes. A strong decrease in proteins associated with photosynthetic machinery occurred 2 days after the induction of abscission. In addition, a decreased abundance of proteins involved in energy metabolic pathways was also observed at this time point.

Proteins having a role in defense, cell wall transformation and secondary metabolism were mostly increased temporally. The AZ exhibited increases in proteins associated with secondary metabolism during D4 and D6 relative to the other 2 spatially discrete regions of the bud.

Conclusions: The formation of the AZ in poinsettia flower buds correlates with temporal and spatial changes in proteins abundances in the poinsettia buds.

Background

Abscission is the detachment of an unnecessary organ in a plant. Leaves, seeds, flowers or floral parts can abscise in response to developmental signals or environmental conditions such as drought (Agusti et al., 2012), light intensity and temperature (Moe et al., 1992), wounding (Kostenyuk and Burns, 2004) and ozone concentration (Miller et al., 1999). Additionally, abscission can occur to prevent the spread of pathogens from the site of an early infection in order to eliminate the infected organ (Taylor and Whitelaw, 2001).

Abscission has been studied for several millennia. In 285 BC the Greek philosopher Theophrastus recorded numerous examples of higher plants abscising their leaves (Addicott, 1982). However, abscission remains far from being fully understood (Tucker and Kim, 2015; Tranbarger et al., 2017). The importance of studying and understanding abscission lies, in part, in its direct influence on quality and yield in agricultural and horticultural crops. In cereal crop agriculture, the retention of the seeds after their maturation is a necessary trait (Fuller and Allaby, 2009). In ornamental flowering plants, one of the main problems post-production is the abscission of the buds or the floral parts (Ferrante et al., 2015).

In the northern hemisphere, *Euphorbia pulcherrima* (poinsettia) is one of the most important ornamental potted plants during the Christmas season, but early abscission of their small flowers is a negative factor that diminishes their decorative value. We have studied flower abscission in Poinsettia from different aspects (Munster, 2006; Lee et al., 2008; Ayeh et al., 2009; Hvoslef-Eide et al., 2016) to elucidate the mechanisms underlying this event. As a result of these studies, we have shown that poinsettia flower buds are a useful reference plant system to study abscission because abscission can be induced precisely by decapitating the floral bud at a specific point (Lee et al., 2008; Hvoslef-Eide et al., 2016).

During abscission, not only the abscission zone (AZ), but also the adjacent tissues, undergo complex metabolic reprogramming processes. Nutrient resorption will provide the energy and the precursors for the macro catabolic processes underlying the removal of the organ (Aerts, 1996). Cell wall remodeling together with proteolysis and remobilization of nutrients are a part of the complex actions leading the organ separation. The cell wall dissolution and transformation accompanying the organ detachment has been the focus of intense research (Merelo et al., 2017). The participation of cellulases, pectinases,

polygalacturonases and glucanases have been identified (Abeles, 1969; Abeles et al., 1971; Riov, 1974; Roberts and Gonzalez-Carranza, 2009). Lee *et al.* (2008) addressed dynamic changes in the polysaccharides composition of the cell wall during induced abscission in poinsettia using antibodies against specific cell wall epitopes together with Fourier transform infrared microspectroscopy.

Previous efforts concentrated on the role of ethylene and auxin, two plant hormones that affect abscission. High throughput genetic approaches were established using technologies, such as microarray (Cai and Lashbrook, 2008; Agusti et al., 2009; Meir et al., 2010; Botton et al., 2011; Zhu et al., 2011; Nakano et al., 2012; Wang et al., 2013; Sundaresan et al., 2016) and more recently, with the next generation sequencing using RNA-Seq (Cheng et al., 2013; Corbacho et al., 2013; Gil-Amado and Gomez-Jimenez, 2013; Niederhuth et al., 2013; Parra et al., 2013; Ferrero et al., 2015; Kim et al., 2016). In contrast, high throughput plant proteomics has been limited in the study of abscission, even though this branch of 'omic technologies has emerged as a powerful technique to unravel other complex mechanisms underlying biological processes, such as plant-pathogen interaction, senescence, and plant development (Jorrín-Novo et al., 2015). To the best of our knowledge, only one large-scale proteomic study has been performed in abscission. That study revealed a network of phosphorylation by protein kinases and dephosphorylation by protein phosphatases in response to ethylene within the tomato pedicel AZ (Zhang et al., 2015).

Abscission is the result of a complex series of events that take place over time and within specific regions of the organ. Thus, we decided to describe the changes in the proteome of the flower bud during abscission, over time and using not only the highly localized AZ, but also looking specifically at changes in adjacent tissues as well. We hypothesized that the distal region, where the decapitation took place to induce the

abscission, would exhibit a higher number of proteins related to wounding, defense and stress. Many of these proteins could also be associated with abscission, since wounding can also induce premature senescence and abscission. This is the first report of a *de novo* sequencing proteomic study aimed at elucidating the processes behind abscission that not only includes the abscission zone, but also the adjacent tissues. Thus, the aim of this study was to describe the variations on the proteome in the specific regions of the poinsettia flower bud throughout the time of its abscission and define putative roles for the proteins in relation to the progression of abscission.

Materials and Methods

Plant material

Poinsettia 'Millenium' (Syngenta) cuttings of 5 cm height and with at least two leaves were rooted for 2-3 weeks under long day conditions (16 h light at $150 \mu\text{mol m}^{-2} \text{sec}^{-1}$, 22°C day and 20°C night, 70% relative humidity (RH)). Following the root formation period, the seedlings were planted in pots (12 cm) and grown for another 2-3 weeks prior to transfer to short day conditions (10 h light at $150 \mu\text{mol m}^{-2} \text{sec}^{-1}$, 20°C day and night, 74% RH) to induce flowering. The inflorescence of poinsettia is made up of one central flower at the first order surrounded by three second order flowers, which again are surrounded by six third order flowers, as illustrated in Hvoslef-Eide *et al.* (2016). The six third order flowers are physiologically and developmentally identical and were used as a homogeneous source of flower buds to obtain sufficient numbers with which to perform the experiments.

Induction of abscission by decapitation of the flower organs

As noted above, the flower buds of poinsettia do not exhibit a preformed AZ. To synchronize and obtain enough plant material for the studies, abscission was induced in the six third order flowers by decapitating the floral organs with a razor blade, as described previously (Munster, 2006; Lee et al., 2008; Hvoslef-Eide et al., 2016), at a specific point (cutting point 2 or cp2), keeping the region below the cut intact. By doing this, the abscission of the flower bud takes place over a period of approximately 7 days after decapitation and the AZ itself becomes visible 3-4 days after the decapitation (Munster, 2006; Lee et al., 2008; Hvoslef-Eide et al., 2016). To follow the progression of AZ formation, four points of harvest time were chosen: Day 0 (D0), Day 2 (D2), Day 4 (D4) and Day 6 (D6) after decapitation.

Tissue collection

The buds in the control (D0) group were collected immediately after decapitation. Subsequently, buds were harvested every 2 days through the progression of the AZ. Several plants were harvested at each time point, with six flowers taken from each. The whole flower bud was manually removed with a razor blade sectioned into three parts: the AZ, proximal region and distal region. These sections were approximately 1 mm in thickness, weighed immediately after sectioning, frozen in liquid nitrogen and stored at -80°C. Five biological replicates were performed for each time point and tissue type.

Study design

Protein profiles during floral abscission were followed in time (every 48 hours) and space (the three adjacent regions). Temporal changes in each tissue were assessed by

comparing with the previous time point i.e. D2 relative to D0, D4 relative to D2, and D6 relative to D4 (Fig 1 A). Spatial changes in the floral proteome was performed by comparing the abscission zone to proximal and distal regions at each of the four time points (D0, D2, D4 and D6) (Fig 1 B). In total, 12 developmentally different tissues were used in the study.

Protein extraction and quantification

For each time point/zone, approximately 20 mg of tissue was ground to a powder in liquid nitrogen using a mortar and pestle. Protein was extracted by further grinding in 1.5 mL of protein extraction buffer (50 mM Tris-HCl pH 8, 10 mM EDTA, 0.1% v/v β -mercaptoethanol, 1% w/v Triton X-100) and incubating on a shaker at 4°C for 3h. After centrifugation at 14000 g for 10 mins, proteins were precipitated from the supernatant using five volumes of ice-cold ethanol overnight at 4°C. After a second round of centrifugation at 14.000 g for 10 minutes the resulting pellet was re-suspended in a minimal volume of 50 mM Tris-HCl pH 8 (up to 100 μ L or more, depending on pellet viscosity). Protein yield was measured in microtiter plates using Protein Assay Dye Reagent Concentrate (BioRad Laboratories, catalog number 500-0006, Hercules, California USA) based on the Bradford assay standard procedure (Bradford, 1976). The protein standard used was bovine serum albumin. For each sample, approximately 40 μ g of protein was used for trypsin digestion according to the STRap-procedure (Zougman et al., 2014).

Liquid Chromatography-hybrid mass spectrometry (LC-MS/MS)

Samples were analysed by LC-MS/MS using an Ultimate 3000 RSLC nano UPLC coupled to a hybrid quadrupole Orbitrap Q-Exactive mass spectrometer (Thermo Scientific,

Bremen, Germany). For each sample, 1-2 µg of trypsin digest was injected (per run) on a Acclaim PepMap, 75 µm (i.d.) x 50 cm. C18 reversed phase, 2µm particle size, 100Å pore size column (Thermo Scientific Inc.). A 120 min gradient (5-40 % acetonitrile in water with 0.1 % formic acid) with a flow rate 300 nl/min was used. Each sample was injected twice to yield technical replicates. The Top12 Data-dependent acquisition method was as follows: 1 full-scan high resolution MS scan (Resolution=70000 m/Δm) followed by 12 MS/MS scans (Resolution=35,000); the precursor ions were selected by intensity.

De novo peptide sequencing analysis and protein quantification

The raw files generated with the nano LC-MS/MS-system, were processed by MaxQuant software v. 1.5.3.30 (<http://www.coxdocs.org/doku.php?id=maxquant:start>), using the label free relative quantitation of samples (LFQ module) procedure (Cox et al., 2014). The mass spectrometry proteomics data have been deposited to the ProteomeXchange Consortium via the PRIDE (Vizcaíno et al., 2016) partner repository with the dataset identifier PXD009355. The raw mass spectrometry files were uploaded to the PRoteomics IDentifications (PRIDE) Archive-proteomics data repository The Andromeda peptide search engine is integrated into the MaxQuant computational environment (Cox et al., 2011) and was applied to the data set generated from the sample analyses. The output file “proteingroups.txt” of the MaxQuant software was processed by Perseus software version 1.5.2.6 (Max Planck Institute of Biochemistry, Martinsried, Germany (Tyanova et al., 2016)) in order to perform the statistical analysis and visualize the results. The matrix with the label free quantification intensities was transformed to Log₂ in order to obtain a normal distribution of the data. Missing values were imputed from the normal distribution.

Protein annotation and functional characterization

In the absence of a genomic or protein database for *Euphorbia pulcherrima*, *de novo* peptide sequencing was performed and the transcriptional profiling of the same experimental layout (Muñoz-Sanhueza et al, 2018 manuscript in prep). This transcriptomic analysis provided a *de novo* transcriptomic assembly used to create a database with the partial and complete open reading frames (ORFs) longer than 99 amino acids using the software TransDecoder (<https://github.com/TransDecoder/TransDecoder/wiki>) from Trinity (Haas et al., 2013). The database file contained 228,404 sequences and was the foundation used to obtain the sequences of the proteins varying in abundances, which were eventually annotated using Blast2GO (Conesa et al., 2005) and InterProScan (Jones et al., 2014) software.

Results

Quantification and detection of proteins

Abundances of 3086 proteins changed significantly within the whole of the experimental dataset. Hierarchical clustering and Student's t-tests were carried out to compare proteins of the flower bud regions and at different time points. The false discovery rate (FDR) was set at 0.01 and the fold change was set to at least two for subsequent analyses.

Temporal changes in the pattern of proteins

To investigate which proteins were differentially expressed between every part of the flower bud, and its preceding time point, a Student's t-test was performed using each one of the

three regions and at the four sample times. By doing this, we could follow the changes in each part of the bud during the progression of the process that leads to the abscission of the flower bud. The results of these comparisons could, in each case, be included in a matrix with those proteins that fit the conditions of being increased or decreased by a two-fold change and 0.01 FDR. Proteins belonging to the same time point comparison, in this case D2 vs D0, D4 vs D2 and D6 vs D4, were grouped together in order to reconstruct the state of the bud every 48 hours. Nine Student's t-tests were performed, three per each sampling time, corresponding to each part of the flower bud. Significant differences in the protein levels were found in the first five of these comparisons, (Fig 2). No significant differences were observable at any of the three tissues during the transition from the D4 to D6 (data not shown).

A higher number of proteins changed their abundance when analyzed after 48 hours in the three different tissues (distal, AZ and proximal; Fig 2 A, B and C). Particularly notable was the high number of proteins that decreased only in the abscission zone 48 hours after decapitation (AZ D2) compared with the control at D0. During the transition from D2 to D4, changes were observable only in the distal part and in the abscission zone (Fig 1 D and E). No significant difference was seen in the proximal part (Fig 1 F). To identify the possible effectors involved in the abscission process, the proteins that showed a differential change in abundance in the previous test were sorted according to being an increase or decrease abundance change (Table 1).

| Tissue | D2 vs D0 | | D4 vs D2 | |
|----------|----------|----------|----------|----------|
| | Decrease | Increase | Decrease | Increase |
| distal | 17 | 59 | 9 | 41 |
| AZ | 285 | 59 | 2 | 43 |
| proximal | 9 | 23 | 0 | 0 |

Table 1. Number of proteins whose abundance increased or decreased in the poinsettia flower bud, temporal comparisons between the three tissues: distal, abscission zone (AZ) and proximal during poinsettia bud abscission, with 48 hour intervals, Day 0= control, Day 2= 48 hours after decapitation and Day 4= 96 hours after decapitation.

With the exception of the comparison between the abscission zone 48 hours later and the control D0, all the tissues showed more increase than decrease in proteins. The number of proteins that decreased in the transition from the D2 to the D4 was smaller in all the tissues, with only 9 and 2 in the distal and abscission zone area respectively and zero in the proximal part. While the increased were 41 and 43 in the distal and abscission zone area and zero in the proximal portion of the bud.

The first 48 hours after the decapitation found a higher number of proteins changing in abundance. Among those that decreased, seventeen were located in the distal part, nine in the proximal and the higher number of proteins changing in the entire experiment were those that decreased in the abscission zone (285 proteins). Since the highest number of proteins changing in their level was detected in the abscission zone two days after the

decapitation, we decided to classify them into categories to reveal details of the response of this region to the decapitation stimuli.

Identity and function of the decreased proteins after 48

The decapitation induced a massive number of proteins decreasing during the first 48 hours within the abscission zone (285 proteins), compared to only 17 (distal) and 9 (proximal) in the adjacent regions. We thus decided to focus specifically on the functions of the 285 proteins in the abscission zone because of this significant number of changes. We identified the proteins that decreased early and classified them according to their proposed biological role and the results are shown as falling into twelve general categories (Fig 3).

The category “Others” includes proteins with known identity and functionality, but are a smaller subset where their proposed functions do not fit into the major categories. The category “Unclear” includes groups of proteins without positive identification or incomplete annotation. Primary metabolism was the category with the most number of decreased proteins, reaching 46 proteins involved in amino acid-, lipid-, nucleotide-, one carbon metabolism and biosynthesis of cofactors. Photosynthesis, which was the second category more represented, includes proteins from the photosystems I and II and proteins related with the stabilization of the chloroplast and Calvin cycle. The third category with a significant number of proteins that decreased in abundance were proteins involved in carbohydrate metabolism including those from the TCA (tricarbolixic acid) cycle, pentose phosphate pathway, respiration glycolysis and more. The forth category contained proteins involved in different signaling cascades. To further elucidate the mechanisms active during abscission,

we focused in the identity of these proteins. The table 2 summarizes the information of these 19 proteins.

| Protein | Role | Reference |
|--|---|---|
| Transport inhibitor response 1 | Auxin receptor, involved in auxin-activated signaling pathway | Dharmasiri <i>et al.</i> 2005, Kepinski & Leyser 2005 |
| receptor-like protein kinase feronia | Plant development, cell expansion ethylene, brassinosteroids. | Yu <i>et al.</i> 2012, Haruta <i>et al.</i> 2014, Deslauriers and Larson 2010 |
| phototropin-1 | Blue light receptor, diverse functions, cell elongation, lateral root growth, phototropic response of hypocotyl, stomatal opening, chloroplast relocation. | Moni <i>et al.</i> 2015, Inada <i>et al.</i> 2004 |
| probable lrr receptor-like serine threonine-protein kinase at1g53420 | ATP binding and protein serine/threonine kinase activity. Located in cell membrane. Probable role in defense | Afzal <i>et al.</i> 2008 |
| Calcium sensing receptor, chloroplastic | Cellular response to calcium ion, de-etiolation and regulation of stomatal closure. | Weinl <i>et al.</i> 2008 |
| Elicitor-responsive protein 3 | Probable role in defense | Kang <i>et al.</i> 2011 |
| disease resistance rpp13-like protein 4 | Defense | Lewis <i>et al.</i> 2010 |
| Hypersensitive-induced response protein 1, 2 or 3 | Defense | Marmagne <i>et al.</i> 2007 |
| Hypersensitive-induced response protein 3 | Defense | Marmagne <i>et al.</i> 2007 |
| Probable disease resistance protein At4g27220 | The LRR repeats probably act as specificity determinant of pathogen recognition | Tan <i>et al.</i> 2007 |
| MACPF domain-containing protein At4g24290 | Negatively controls the salicylic acid (SA)-mediated pathway of programmed cell death in plant immunity | Noutoshi <i>et al.</i> 2006 |
| mitogen-activated protein kinase kinase 2-like | Signaling pathway that modulates the expression of genes responding to biotic and abiotic stresses and role in pathogen defense by negatively regulating innate immunity. | Taj <i>et al.</i> 2010, Teige <i>et al.</i> 2004, Gao <i>et al.</i> 2008 |

| | | |
|--|--|---|
| mitogen-activated protein kinase kinase 5-like | Defense response, incompatible interaction, floral organ abscission, inflorescence development, plant-type hypersensitive response and positive regulation of ethylene biosynthetic process. | Asai <i>et al.</i> 2002, Liu <i>et al.</i> 2008, Cho <i>et al.</i> 2008 |
| Phospholipase D delta, gamma 1 or beta 1 | Involved in abscisic acid-activated signaling pathway, stomatal closure, stress signaling, positive role in ABA-promoted senescence | Uraji <i>et al.</i> 2012, Distéfano <i>et al.</i> 2012, Katagiri <i>et al.</i> 2001, Jia <i>et al.</i> 2013 |
| Phospholipase D alpha 1 | Involved in abscisic acid-activated signaling pathway, phyto-hormone action and response to stress, wound-induction of jasmonic acid, abiotic stress. | Uraji <i>et al.</i> 2012, Fan <i>et al.</i> 1997, Wang <i>et al.</i> 2000, Mane <i>et al.</i> 2007 |
| 14-3-3-like protein D | Modulators of phosphorylated proteins | Denison <i>et al.</i> 2011 |
| 20 kDa chaperonin, chloroplastic | Involved in abscisic acid signaling | Zhang <i>et al.</i> 2014 |
| SAL1 phosphatase | Involved in abscisic acid signaling pathway and stress responsive genes | Xiong <i>et al.</i> 2001 |
| Diacylglycerol kinase 5, 6 or 7 | Involved in defense response and abiotic stress via protein kinase C-activating G-protein coupled receptor signaling pathway. | Gómez-Merino <i>et al.</i> 2005 |

Table 2. Proteins involved in signal transduction that decrease in the abscission zone of poinsettia flower buds 48 hours after the induction of abscission.

After the first 48 hours, in the distal and proximal portions of the bud, only a small number of proteins decreased compared to the abscission zone, 17 and 9 respectively, including proteins from photosynthesis (4), primary metabolism (7), stress response (3) and others. During the next 48 hours, in the transition from D2 to D4, the number of proteins that decreased substantially included only 11 proteins between the distal part and the

abscission zone, and the proximal part did not display any proteins that significantly changed in abundance. A complete list with the individual proteins decreasing in abundance sorted by the region of the bud on the D2 and D4 is shown in Supplementary material 1.

Identity and function of proteins that increase after 48 and 96 hours

A total of 141 proteins increased after 48 hours in comparison to the D0 (control), and 84 proteins increased in the transition from the D2 to the next harvesting time 48 hours later (D4). They were identified and sorted according to their possible functions (Fig. 4). A complete list with the individual proteins that increased, sorted by the region of the bud in which the change occurred on D2 and D4, is shown in Supplementary material 2.

Changes after 2 days in the three regions of the flower bud

Based on the percentage of the proteins increasing, it can be proposed that the transformation of the cell wall starts in the AZ and the distal region on the D2, but not in proximal region (Table 3).

Almost half of the proteins that increased in each region of the bud during D2 were defense-related. Increases in enzyme proteins associated with the biosynthesis of jasmonic acid (JA), pathogenesis-related proteins (PRs) and enzymes from secondary metabolism (phenylpropanoid pathway) were found in the AZ, distal and proximal regions. Enzyme proteins from three of the steps of JA biosynthesis were found in a gradient along the bud, with more proteins increasing in the distal part than in the proximal region.

Changes after 4 days

There was an incremental increase of proteins with a role in cell wall transformation during D4. The AZ in the flower buds of poinsettia is only visible on D4, so it was expected that new proteins would be found that brought about this remodeling step. Eight new proteins were identified in the distal part and four in the AZ (Table 3). The proteins of secondary metabolism alone reached a level of 42% of the proteins that increased in the AZ, while in distal region it was only 7%.

| Protein name | Sequence ID | Relative abundance [log2(tissue/control)] | |
|---|--|--|-------|
| | | D2 | D4 |
| Distal region | | | |
| protein notum homolog | TR138857_c1_g1_i1;TR136245_c2_g1_i1 | 28.34 | |
| xyloglucan endo transglucosylase hydrolase protein2-like | TR107318_c0_g1_i2;TR101095_c0_g1_i1;TR107318_c0_g1_i1 | | 34.15 |
| beta-d-xylosidase family protein | TR126856_c2_g1_i1;TR127424_c1_g1_i1 | | 21.39 |
| protein trichome birefringence-like 39 | TR8277_c0_g1_i1;TR150803_c0_g1_i1 | | 10.46 |
| beta-galactosidase-like isoform x2 | TR135914_c0_g1_i1;TR136740_c0_g1_i1 | | 15.33 |
| expansin-like b1 | TR125351_c0_g1_i1;TR127805_c1_g1_i3;TR127805_c1_g1_i1;TR127805_c1_g1_i2 | | 11.53 |
| extensin-2-like | TR96655_c0_g2_i3;TR94490_c0_g1_i1;TR96655_c0_g2_i1 | | 10.87 |
| Probable polygalacturonase | TR131616_c1_g1_i1;TR130499_c1_g1_i1 | | 24.78 |
| bifunctional udp-glucose 4-epimerase and udp-xylose 4-epimerase 1 | TR131555_c1_g2_i9;TR131555_c1_g2_i2;TR131555_c1_g2_i11;TR121532_c0_g1_i8;TR121532_c0_g1_i7;TR131555_c1_g2_i7;TR121532_c0_g1_i9;TR121532_c0_g1_i3;TR121532_c0_g1_i10;TR131555_c1_g2_i6;TR131555_c1_g2_i13;TR131555_c1_g2_i10;TR121532_c0_g1_i6;TR121532_c0_g1_i2;TR121532_c0_g1_i1;TR131555_c1_g2_i12;TR121532_c0_g1_i4 | | 9.98 |
| AZ | | | |
| UDP-arabino pyranose mutase 3 | TR140555_c4_g1_i14 | 5.94 | |
| glucan endo--beta-glucosidase-like | TR117243_c3_g1_i1;TR113211_c2_g1_i1 | 7.31 | |
| alpha--glucan-protein synthase | TR141593_c3_g1_i4;TR140555_c4_g1_i12 | 6.41 | |
| alpha--glucan-protein synthase | TR111814_c0_g1_i2;TR111814_c0_g1_i1 | | 38.24 |
| beta-d-xylosidase family protein | TR126856_c2_g1_i1;TR127424_c1_g1_i1 | | 45.64 |

| | | |
|----------------------------|-------------------------------------|-------|
| Probable polygalacturonase | TR187879_c1_g1_i1;TR172871_c0_g1_i1 | 18.05 |
| endo--beta-glucanase | TR53009_c0_g1_i1;TR39616_c0_g1_i1 | 11.31 |

Table 3. Relative abundance values (tissue-control vs. tissue-experiment) of proteins involved in cell wall transformation in the distal region and abscission zone of poinsettia flower buds two and four days after the decapitation of the flower bud.

Spatial changes in the abundance of proteins

To determine which proteins change in abundance throughout the bud at each sampling time, pairwise comparisons were performed between the distal part and the abscission zone, and the proximal part and the abscission zone. This was done at the four sampling times, comprising eight Student's t-test as illustrated by the four significant pairs in Fig. 5.

As expected, the bud from D0 (start point) has few protein changes (only 7) across the three tissues of the buds (data not shown). After 48 hours, there are still few proteins changes (only 2) (data not shown) whereas in the D4 and the D6 buds, when comparing the three tissues, they display a remarkable number of proteins that changed in levels (Table 4).

| Tissue | D4 | | D6 | |
|----------------|-----------|-----------|-----------|-----------|
| | Decreased | Increased | Decreased | Increased |
| AZ vs distal | 45 | 39 | 44 | 62 |
| AZ vs proximal | 37 | 49 | 19 | 100 |

Table 4. Number of proteins that changed in abundance in poinsettia flower buds; spatial comparisons between abscission zone and distal region, as well as abscission zone and proximal region.

A complete list with the individual proteins increasing and decreasing in levels in the AZ on the D4 and D6 is supplied in the Supplementary material 3 and 4, respectively.

In order to reconstruct the pattern of protein changes in the bud at D4 and D6, the intensity values of the 3086 proteins that changed in the entire experiment were clustered using Euclidean distance. The proteins that increased within the abscission zone were located within the clustering to investigate their changing abundance in the three tissues simultaneously. We focused on profiles where proteins increased in the AZ compared with distal and proximal regions (Fig 6 and 7).

Proteins with functions in secondary and primary metabolism were the most represented within the clusters showing increases in the abscission zone during the fourth day after the induction (D4), with 19 and 11 proteins, respectively. While cell wall transformation, stress response, proteolysis, RNA regulation and others grouped in total nine proteins. Examples of these clusters are found in Fig 8 A. No proteins from defense responses increased in the abscission zone compared to the distal and proximal regions.

During the last day of harvesting (D6), high numbers of proteins of secondary and primary metabolism increased in the AZ, with 26 and 21 proteins respectively. Cell wall transformation and other functions comprised eight proteins of each process, whereas stress responses had six proteins that increased. During D6, the proteins of secondary metabolism increased in not only the number of enzyme proteins but also the diversity

compared to D4. The enzyme proteins that increased in abundance within the AZ D6 are schematically represented in the phenylpropanoid biosynthetic pathway below (Fig. 8).

Discussion

Temporal changes in the flower bud after 2 days

The whole bud showed a major defense response by Day 2

Our results suggest that the decapitation induced an increase in the proteins related with mechanical stress or wounding during the first two days. In the whole bud 38 proteins, including three enzymes from the jasmonic acid biosynthetic pathway and different types of pathogenesis-related proteins, increased during D2. Simultaneously, secondary metabolism appears to be activated because 31 enzyme proteins from the phenylpropanoid biosynthesis pathway, which produces phenolic compounds including flavonoids, anthocyanidin and lignin, were increased in the three regions of the bud that we studied.

Enzymes from the phenylpropanoid biosynthetic pathway such as phenylalanine ammonia lyase (PAL), 4-coumarate:CoA ligase (4-CL) and chalcone synthase (CHS), have been described increasing in carrot after treatment with ethylene (Ecker and Davis, 1987). These enzyme proteins, as well as additional ones from this pathway, increased during the second day in poinsettia, implying there is likely production of ethylene early in the process, even though we do not see enzymes from ethylene biosynthesis increasing. Treatment with ethylene has a positive effect in abscission (Agustí et al., 2008) and additionally ethylene may be produced in response to a mechanical or wounding stress and lead to abscission of the organ. The abscission of the tomato pedicel has been induced by flower removal (Roberts et al., 1984). This may suggest that decapitation of the flower bud in poinsettia also

induces an increase in ethylene production and thus regulates a number of genes related with defense.

In addition to the ethylene effects, JA has also been described as inducing genes of the defense response pathways, including enzyme proteins of the phenylpropanoid biosynthesis pathways and pathogenesis-related proteins (PRs) (Ecker and Davis, 1987; Ruperti et al., 2002; Turner et al., 2002). The synergistic up-regulation of PRs genes by ethylene and JA has been reported in tobacco seedlings (Xu et al., 1994). In our study, the increase in enzyme proteins from secondary metabolism might be related to the need to produce precursors for later stages in the abscission process, where deposition of lignin takes place (Poovaiah, 1974).

Proteins associated with cell wall transformation showed an increase in the abscission zone and the distal region by Day 2

The bud does not exhibit any obvious visual changes during the first 48 hours after the decapitation; still we found four proteins increasing during this period (Table 3), indicating that changes are at an early stage and occurring at a level that still does not make the AZ visually distinguishable. In the AZ on D2 after the induction, three enzymes with catabolic and/or anabolic role in cell wall polysaccharides increased; alpha-glucan-protein synthase, a protein immunolocalized by Epel *et al.* (1996) to the plasmodesmata, glucan endo-beta-glucosidase-like, a protein previously shown to be involved in changes in apple fruit during maturation (Zhu et al., 2012) and UDP-arabino pyranose mutase 3, an enzyme required for, among other possible uses, the formation of the pollen cell wall (Sumiyoshi et al., 2015).

The only protein that increased in the distal part on D2 was the protein NOTUM homolog which shows structural similarity with the pectin acetyl esterase 8 from *Arabidopsis thaliana* (AtPAE8, Philippe et al., 2017) . This protein may be involved in modulating the level of acetylation of the pectin in the cell wall, as was previously shown in *Arabidopsis* (de Souza et al., 2014). These results indicate that cell wall transformation during the abscission process is not restricted to its degradation, but also involves cell wall modification as well as biosynthesis of non-cellulosic polysaccharides.

Our results indicate that both the modulation of pectin acetylation in the distal region of the bud, as well as the increased active biosynthetic metabolism of cell wall constituents in the AZ characterize the early events in the abscission process.

Changes taking place only in the abscission zone by Day 2

The suppression of anabolic processes linked to photosynthesis, protein synthesis and carbohydrate metabolism

Although the distal part of the flower bud might be expected to be more affected in terms of protein changes due to decapitation, the analyses show that the abscission zone was by far the most reactive part of the pedicel after two days. With 285 proteins decreasing, it was clear that many physiological functions in the abscission zone were declining. Examples included 41 proteins involved in photosynthesis and 20 proteins related to protein synthesis that declined in the AZ on D2; these changes were probably a product of the defense response orchestrated by increased jasmonate (Reinbothe et al., 1994). Impaired photosynthesis is a well-documented response to different stresses, including cold acclimation (Stitt and Hurry, 2002) and wounding (Lukaszuk et al., 2016), leading to the redirection of resources to the production of secondary metabolites. Impaired

photosynthesis leads to a decrease in carbohydrate metabolism and that was observable in the AZ where 33 proteins from the TCA cycle, glyoxylate cycle, respiration and other related processes declined in abundance by D2.

This strong selective lowering of protein levels in the abscission zone after 48 hours could indicate that this region of the bud is more responsive than the rest of the pedicel. Additionally, it might indicate that a signal suppressing the expression of the genes involved in abscission control (D0) was disrupted after the decapitation of the floral organs. Such a signal hypothesis would be consistent with the observed flux of auxin that has an established role in preventing or delaying abscission (Addicott, 1982; Meir et al., 2015). The existence of an inhibitor of abscission has also been postulated by several other research groups (Addicott, 1982). Roberts *et al.* (1984), proposed auxin as the anti-abscission signal in their studies of the induction of abscission by ethylene application to excised flower pedicels.

We hypothesize a response pathway in the AZ of the poinsettia flower bud where the decrease in the auxin level was sensed and triggered the induction of the abscission process, thus initiating the starting point for the differentiation of this region of the bud as early as D2. Further, this low auxin induction leads to the transformations that will make it distinguishable by D4 and onwards. The decrease in the auxin level in the abscission zone is also reflected by a possibly lowering of auxin responsiveness that would accompany the lower levels of the Transport Inhibitor Response 1 (TIR1) auxin receptor (Dharmasiri et al., 2005) and the abc transporter b family member 1 that is involved in polar auxin transport (Geisler et al., 2005).

Lowered levels of proteins from signaling cascades in the abscission zone on Day 2

An additional exclusive feature of the AZ on D2 is that 19 proteins decline that likely participate in biochemical events involving signaling cascades related with defense and biotic and abiotic stress, including the abscisic acid signaling cascade. For example, mitogen-activated protein kinases (MAPK) cascades drive one of two major signal transduction mechanisms in plants (Taj et al., 2010) and included are processes leading to defense and abiotic stress responses, cell cycle regulation, and response to some hormone regulators (Ichimura et al., 2000; Mockaitis and Howell, 2000; Nishihama et al., 2001; Asai et al., 2002). Cho *et al.* (2008) elucidated aspects of the signaling cascade leading to floral abscission in *Arabidopsis thaliana* when they showed a distinct role in abscission of the *MKK4-MKK5RNAi* mutants. By silencing the MKK4-MKK5 genes with RNAi they were able to implicate the Inflorescence Deficient in Abscission (IDA) peptide as well as its receptor HAE, in concert with MKK4, MKK5, MPK3 and MPK6 as acting together during flower abscission. Our results showed a decline in two members of the MAPK pathway in the abscission zone on D2: MKK2 and MKK5, both are reported to be involved with innate immunity response signaling (Asai et al., 2002; Gao et al., 2008) and MKK2 also appears to be linked to cold and salt stress signaling (Teige et al., 2004). Cross talk and the interplay among members of the MAPKs in many different events in the plant cell makes it difficult to discern if these two elements belong to the same or two different cascades. Nevertheless, the high number of processes that decline on D2, suggest that there may be some interaction between these two kinases and other signaling cascade proteins that are also declining.

Temporal changes in the flower bud after 4 days

Proteins involved in cell wall transformation increased during Day 4 in the abscission zone and distal region

In the transition from the D2 to the D4, 12 proteins related with cell wall transformation were increased in the AZ and the distal region (Table 3). This suggests enzyme proteins were needed in order to transform the AZ into a visible structure. The proteins with the highest increase were β -D-xylosidase family of protein and α -glucan-protein synthase. Xylosidases are important in the degradation xylans within hemicellulose (Minic et al., 2004) and are highly expressed in areas where the secondary cell wall is thickening (Goujon et al., 2003). Increases in these proteins indicate that the cells from the AZ on D4 are actively degrading xylans or related carbohydrates and possibly, based on the prior studies, also starting to thicken their secondary cell wall with other materials such as lignin, cellulose, suberin and cutin. α -Glucan-protein synthase participates in the synthesis of cell wall polysaccharides (Bocca et al., 1999), reinforcing the idea of alterations focused during abscission on the degradation/biosynthesis of cell wall components.

The presence of an enzyme with polygalacturonase activity in the AZ in *Nicotiana tabacum* was established in the early sixties (Yager, 1960) and many other studies have confirmed this over the years (Berger and Reid, 1979; Gonzalez-Carranza et al., 2007). Our results confirm the presence of polygalacturonase in the distal part as well as in the AZ by D4.

Equally, an endo-beta-glucanase increased in the AZ four days after decapitation, although we cannot know from the peptide data the linkage specificity of this glucanase. Endo-1,4-beta-glucanases are often named cellulases and its activities have been described in numerous abscission studies previously (Abeles, 1969; Bonghi et al., 1992; Ferrarese et

al., 1996). Members of the glycosyl hydrolase family, including endo-1,3-beta-glucanase, are included in the pathogenesis-related proteins group 2 (PR 2). Some of the proteins that have been described as having a role in defense, such as the glycosyl hydrolases, could either be contributing to the loosening of the cell wall during abscission or also or alternatively be part of a defense response following the decapitation of the bud. The protein that increases the most in the distal region on D4 was xyloglucan endo transglucosylase hydrolase protein2-like (XTH2-like). This enzyme cleaves and re-ligates xyloglucan polymers in the primary cell wall and has been studied in connection with cell wall expansion, ripening (Rose and Bennett, 1994), and cell wall loosening (Van Sandt et al., 2007). Furthermore, evidence of xyloglucan hydrolysis in the AZ and distal part of poinsettia flower buds 7 days after the induction have been found, suggesting that the hydrolysis of xyloglucan starts on D4 after decapitation and continues until D7 (Lee et al., 2008). Loss of birefringence in the cell walls of the abscission layer of the fruit of *Prunus cerasus* was described using histological evidence in 1969 by Stösser *et al.* , indicating changes in the physical structure of the cell wall. In our experiments, the birefringence was not measured; however, this observation fits well with the presence of the protein trichome birefringence-like 39 in the distal part of the buds on D4. The *Arabidopsis* mutant defective in this gene (*tbr* mutants) do not display any birefringence and their cellulose content is highly reduced (Bischoff et al., 2010). Based on this result, we hypothesize that the increase in abundance of this protein is an indication of the activation of processes leading to an increase in the cellulose content in the distal region on the D4.

Based on the range of proteins identified on D4 in the distal region of the bud, it is possible to deduce not only enzymatic cell wall remodeling ongoing, but also non-enzymatic loosening of cell wall polymers under the influence of the protein expansin-like b1

(McQueen-Mason et al., 1992; Cosgrove, 2000). Furthermore the increase of another constituent of the cell wall, the hydroxyproline-rich glycoprotein (HRGPs), called extensin, has been associated with defense and can be a response to different types of stress (Memelink et al., 1993), including abscission (Merkouropoulos and Shirsat, 2003).

Abscission zone exhibits an increase in proteins of secondary metabolism by Day 4

The increase in abundance of enzymes from the phenylpropanoid biosynthetic pathway suggests that the AZ is a region rich in polyphenolic compounds, possibly including flavonoids, and also actively producing precursors for the biosynthesis of lignin. The deposition of lignin in the AZ and near this region has been documented since early anatomical descriptions of the AZ (Lee, 1911) and is one of the main characteristics of the abscission process. In poinsettia, the reported ultraviolet-induced auto-fluorescence in the AZ D5 suggests that this observation might be related to the accumulation of polyphenolic compounds, such as lignin. Additionally, the cell walls of the AZ became rich in lignin only after 7 days from induction (Lee et al., 2008).

Temporal changes in proteins on Day 4 and Day 6

Since no significant differences were observed at any of the three tissues during the transition from the D4 to D6, it suggests that the changes in protein abundances that already took place up D4 are the ones directing AZ formation. In the progression of the abscission process, each region of the flower bud does not differ significantly from its predecessor after D4. However, although the temporal changes were completed in each region by D4, the AZ and the other two regions in the flower bud showed clear spatial differences on D4 and D6 in the proteins that were present.

Spatial changes in flower bud proteins

For the first two days after induction by decapitation, no changes in protein relative abundance were detected between the AZ and the adjacent regions studied. This result might be the consequence of the increase in the proteins related to the three processes of jasmonic acid biosynthesis, pathogenesis-related proteins and the phenylpropanoid biosynthetic pathway. These changes occurred in the three portions of the pedicel simultaneously and might have masked the large decrease in the AZ at D2 relative the AZ on D0.

The main feature that characterized the AZ on D4 and D6 was the number of proteins that changed in abundance, relative to distal and proximal regions (Table 4), related to primary and secondary metabolism. These changes include increases in two enzymes, one from lignan pathways, secoisolariciresinol dehydrogenase as well as an enzyme important for biosynthesis of suberin, omega-hydroxypalmitate (Molina et al., 2009). Suberin is present in specialized cell walls of the protective layer. The protective layer might be best characterized by active cell division during abscission in some species (Addicott, 1982). Lee *et al* (2008) described the active cell divisions in the poinsettia flower AZ during the fifth day after induction as the differentiation of a separation layer. This suggests that both the protective and the separation layer are forming simultaneously around D4.

The AZ on D4 compared to the AZ on D6 shows that they share many of the same characteristics because the identity of the proteins changing are similar (Supplementary material 3 and 4). However, during D6, the AZ diversifies its protein changes indicating the potential that new processes are being initiated at this time.

Final remarks

- This is the first comprehensive proteomics study to define abscission in poinsettia flower buds.
- This study included not only the proteome of the abscission zone, but also the adjacent regions on either side; distal and proximal. By doing this, we were able to consider the bud as a whole organ in which the fate of the part to be detached is not only decided by the events within the abscission zone, but also in the rest of the pedicel.
- We were also able to detect the defense mechanisms in the AZ as well as the distal and proximal region, which were set in motion by the decapitation.
- The temporal differentiation is most abundant during the first two days, but continues up to four days after the induction of the abscission. The spatial differentiation in the bud was detectable only during the last two days before abscission, on D4 and D6.
- We revealed that 48 hours after the induction of abscission by decapitation, the bud showed a very different pattern of proteins increasing compared with their predecessor control, but very similar within the regions of the bud. The massive defense response might be responsible for masking other possible changes.
- The different regions of the bud responded to decapitation in very different ways, where the abscission zone exhibited the highest number of proteins that decreased in abundance (285) and a high percentage of the proteins that declined were related to functions of the chloroplast, including photosynthesis, carbohydrate metabolism, and energy.

- During the transition from D0 to D2, 19 proteins with roles in signaling cascades declined in the abscission zone. We interpret this result as the start of the changes in signal response systems that leads to the abscission of the organ.
- No significant differences were discovered among the three regions of the bud at D6 compared with their homologous regions at D4.
- Consequently, the lack of significant differences between D4 and D6 might be misleading if it results in the assumption that the state of the entire bud four days after the induction (D4) is analogous to the bud two days later (D6). Indeed, using the spatial comparisons shows that the main differentiation among the three sections of the bud occurs during the last two days, exactly in the transition from D4 to D6.
- Comparing the results from the transition between D0 until D6, it is evident that the proximal part of the bud is less affected by the induction of abscission, while the distal region and the abscission zone (AZ) seem to be more responsive to decapitation.
- The only time point that exhibited changes in both the temporal and spatial studies was D4. From this result, it becomes clear that at D4 the three tissues are evolving in divergent directions and defining their own metabolic identities.

Funding

The authors acknowledge funding for a PhD scholarship from the Norwegian University of Life Sciences in the period April 2013-March 2016.

Author's contributions

LGMS grew the plants, collected the samples, performed the protein extraction and quantification, performed the statistical analysis, made the figures and wrote the manuscript. YKL provided supervision, revised and corrected the manuscript and AKHE provided supervision and revised and corrected the manuscript.

Acknowledgements

We are indebted to senior engineer PhD Morten Skaugen from the Protein Engineering and Proteomics Group (PEP), Department of Chemistry and Biotechnology, Norwegian University of Life Sciences, for technical support and fruitful discussions in the protein analysis. We also thank PhD Paul Derbyshire from the Sainsbury Laboratory, Norwich and Professor Jerry D. Cohen, University of Minnesota, St Paul, USA the critical reading and useful suggestions on the manuscript.

References

- Abeles, F.B. (1969). Abscission: Role of Cellulase. *Plant Physiology* 44(3), 447-452.
- Abeles, F.B., Leather, G.R., Forrence, L.E., and Craker, L.E. (1971). Abscission: regulation of senescence, protein synthesis, and enzyme secretion by ethylene. 6, 6.
- Addicott, F.T. (1982). *Abscission*. London, England: Univeristy of California Press, LTD. .
- Aerts, R. (1996). Nutrient Resorption from Senescing Leaves of Perennials: Are there General Patterns? *Journal of Ecology* 84(4), 597-608. doi: 10.2307/2261481.
- Afzal, A.J., Wood, A.J., and Lightfoot, D.A. (2008). Plant receptor-like serine threonine kinases: roles in signaling and plant defense. *Molecular Plant Microbe Interactions* 21(5), 507-517. doi: 10.1094/mpmi-21-5-0507.
- Agusti, J., Gimeno, J., Merelo, P., Serrano, R., Cercos, M., Conesa, A., et al. (2012). Early gene expression events in the laminar abscission zone of abscission-promoted citrus leaves after a cycle of water stress/rehydration: involvement of CitbHLH1. *Journal of Experimental Botany* 63(17), 6079-6091. doi: 10.1093/jxb/ers270.

- Agusti, J., Merelo, P., Cercos, M., Tadeo, F., and Talon, M. (2009). Comparative transcriptional survey between laser-microdissected cells from laminar abscission zone and petiolar cortical tissue during ethylene-promoted abscission in citrus leaves. *BMC Plant Biology* 9(1), 127.
- Agustí, J., Merelo, P., Cercós, M., Tadeo, F.R., and Talón, M. (2008). Ethylene-induced differential gene expression during abscission of citrus leaves. *Journal of Experimental Botany* 59(10), 2717-2733. doi: 10.1093/jxb/ern138.
- Asai, T., Tena, G., Plotnikova, J., Willmann, M.R., Chiu, W.L., Gomez-Gomez, L., et al. (2002). MAP kinase signalling cascade in Arabidopsis innate immunity. *Nature* 415(6875), 977-983. doi: 10.1038/415977a.
- Ayeh, K., Lee, Y., Ambrose, M., and Hvostlef-Eide, A. (2009). Characterization and structural analysis of wild type and a non-abscission mutant at the development funiculus (Def) locus in *Pisum sativum* L. *BMC Plant Biology* 9(1), 76.
- Berger, R.K., and Reid, P.D. (1979). Role of Polygalacturonase in Bean Leaf Abscission. *Plant Physiology* 63(6), 1133-1137.
- Bischoff, V., Nita, S., Neumetzler, L., Schindelasch, D., Urbain, A., Eshed, R., et al. (2010). TRICHOME BIREFRINGENCE and its homolog AT5G01360 encode plant-specific DUF231 proteins required for cellulose biosynthesis in Arabidopsis. *Plant Physiology* 153(2), 590-602. doi: 10.1104/pp.110.153320.
- Bocca, S.N., Kissen, R., Rojas-Beltrán, J.A., Noël, F., Gebhardt, C., Moreno, S., et al. (1999). Molecular cloning and characterization of the enzyme UDP-glucose: protein transglucosylase from potato^{††}This paper is specially dedicated to the memory of Dr Juana S. Tandecarz, deceased on December 10, 1996. *Plant Physiology and Biochemistry* 37(11), 809-819.
- Bonghi, C., Rascio, N., Ramina, A., and Casadoro, G. (1992). Cellulase And Polygalacturonase Involvement In The Abscission Of Leaf And Fruit Explants Of Peach. *Plant Molecular Biology* 20(5), 839-848.
- Botton, A., Eccher, G., Forcato, C., Ferrarini, A., Begheldo, M., Zermiani, M., et al. (2011). Signaling pathways mediating the induction of apple fruitlet abscission. *Plant Physiology* 155(1), 185 - 208.
- Bradford, M.M. (1976). A rapid and sensitive method for the quantitation of microgram quantities of protein utilizing the principle of protein-dye binding. *Analytical Biochemistry* 72, 248-254.
- Cai, S., and Lashbrook, C.C. (2008). Stamen abscission zone transcriptome profiling reveals new candidates for abscission control: enhanced retention of floral organs in transgenic plants overexpressing Arabidopsis ZINC FINGER PROTEIN2. *Plant Physiology* 146(3), 1305-1321. doi: 10.1104/pp.107.110908.
- Cheng, Y.-Q., Liu, J.-F., Yang, X., Ma, R., Liu, C., and Liu, Q. (2013). RNA-seq Analysis Reveals Ethylene-Mediated Reproductive Organ Development and Abscission in Soybean (*Glycine max* L. Merr.). *Plant Molecular Biology Reporter* 31(3), 607-619. doi: 10.1007/s11105-012-0533-4.
- Cho, S.K., Larue, C.T., Chevalier, D., Wang, H., Jinn, T.-L., Zhang, S., et al. (2008). Regulation of floral organ abscission in Arabidopsis thaliana. *Proceedings of the National Academy of Sciences* 105(40), 15629-15634. doi: 10.1073/pnas.0805539105.
- Conesa, A., Gotz, S., Garcia-Gomez, J.M., Terol, J., Talon, M., and Robles, M. (2005). Blast2GO: a universal tool for annotation, visualization and analysis in functional genomics research. *Bioinformatics* 21(18), 3674-3676. doi: 10.1093/bioinformatics/bti610.
- Corbacho, J., Romojaro, F., Pech, J.-C., Latché, A., and Gomez-Jimenez, M.C. (2013). Transcriptomic Events Involved in Melon Mature-Fruit Abscission Comprise the Sequential Induction of Cell-Wall Degrading Genes Coupled to a Stimulation of Endo and Exocytosis. *PLoS ONE* 8(3), e58363. doi: 10.1371/journal.pone.0058363.

- Cosgrove, D.J. (2000). Loosening of plant cell walls by expansins. *Nature* 407(6802), 321-326.
- Cox, J., Hein, M.Y., Lubner, C.A., Paron, I., Nagaraj, N., and Mann, M. (2014). Accurate Proteome-wide Label-free Quantification by Delayed Normalization and Maximal Peptide Ratio Extraction, Termed MaxLFQ. *Molecular & Cellular Proteomics* 13(9), 2513-2526. doi: 10.1074/mcp.M113.031591.
- Cox, J., Neuhauser, N., Michalski, A., Scheltema, R.A., Olsen, J.V., and Mann, M. (2011). Andromeda: a peptide search engine integrated into the MaxQuant environment. *Journal of Proteome Research* 10(4), 1794-1805. doi: 10.1021/pr101065j.
- de Souza, A., Hull, P.A., Gille, S., and Pauly, M. (2014). Identification and functional characterization of the distinct plant pectin esterases PAE8 and PAE9 and their deletion mutants. *Planta* 240(5), 1123-1138. doi: 10.1007/s00425-014-2139-6.
- Denison, F.C., Paul, A.-L., Zupanska, A.K., and Ferl, R.J. (2011). 14-3-3 proteins in plant physiology. *Seminars in Cell & Developmental Biology* 22(7), 720-727.
- Deslauriers, S.D., and Larsen, P.B. (2010). FERONIA is a key modulator of brassinosteroid and ethylene responsiveness in Arabidopsis hypocotyls. *Molecular Plant* 3(3), 626-640. doi: 10.1093/mp/ssq015.
- Dharmasiri, N., Dharmasiri, S., and Estelle, M. (2005). The F-box protein TIR1 is an auxin receptor. *Nature* 435(7041), 441-445. doi: 10.1038/nature03543.
- Distéfano, A.M., Scuffi, D., García-Mata, C., Lamattina, L., and Laxalt, A.M. (2012). Phospholipase D6 is involved in nitric oxide-induced stomatal closure. *Planta* 236(6), 1899-1907. doi: 10.1007/s00425-012-1745-4.
- Ecker, J.R., and Davis, R.W. (1987). Plant defense genes are regulated by ethylene. *Proceedings of the National Academy of Sciences* 84(15), 5202-5206.
- Epel, B.L., van Lent, J.W.M., Cohen, L., Kotlizky, G., Katz, A., and Yahalom, A. (1996). A 41 kDa protein isolated from maize mesocotyl cell walls immunolocalizes to plasmodesmata. *Protoplasma* 191(1), 70-78. doi: 10.1007/bf01280826.
- Fan, L., Zheng, S., and Wang, X. (1997). Antisense suppression of phospholipase D alpha retards abscisic acid- and ethylene-promoted senescence of postharvest Arabidopsis leaves. *The Plant Cell* 9(12), 2183-2196. doi: 10.1105/tpc.9.12.2183.
- Ferrante, A., Trivellini, A., Scuderi, D., Romano, D., and Vernieri, P. (2015). Post-production physiology and handling of ornamental potted plants. *Postharvest Biology and Technology* 100(0), 99-108.
- Ferrarese, L., Moretto, P., Trainotti, L., Rascio, N., and Casadoro, G. (1996). Cellulase involvement in the abscission of peach and pepper leaves is affected by salicylic acid. *Journal of Experimental Botany* 47(2), 251-257. doi: 10.1093/jxb/47.2.251.
- Ferrero, S., Carretero-Paulet, L., Mendes, M.A., Botton, A., Eccher, G., Masiero, S., et al. (2015). Transcriptomic Signatures in Seeds of Apple (*Malus domestica* L. Borkh) during Fruitlet Abscission. *PLoS One* 10(3), e0120503. doi: 10.1371/journal.pone.0120503.
- Fuller, D.Q., and Allaby, R. (2009). "Seed Dispersal and Crop Domestication: Shattering, Germination and Seasonality in Evolution under Cultivation," in *Annual Plant Reviews Volume 38: Fruit Development and Seed Dispersal*. Wiley-Blackwell, 238-295.
- Gao, M., Liu, J., Bi, D., Zhang, Z., Cheng, F., Chen, S., et al. (2008). MEKK1, MKK1/MKK2 and MPK4 function together in a mitogen-activated protein kinase cascade to regulate innate immunity in plants. *Cell Research* 18(12), 1190-1198.
- Geisler, M., Blakeslee, J.J., Bouchard, R., Lee, O.R., Vincenzetti, V., Bandyopadhyay, A., et al. (2005). Cellular efflux of auxin catalyzed by the Arabidopsis MDR/PGP transporter AtPGP1. *The Plant Journal* 44(2), 179-194. doi: 10.1111/j.1365-3113X.2005.02519.x.
- Gil-Amado, J.A., and Gomez-Jimenez, M.C. (2013). Transcriptome Analysis of Mature Fruit Abscission Control in Olive. *Plant and Cell Physiology* 54(2), 244-269. doi: 10.1093/pcp/pcs179.

- Gómez-Merino, F.C., Arana-Ceballos, F.A., Trejo-Téllez, L.I., Skirycz, A., Brearley, C.A., Dörmann, P., et al. (2005). Arabidopsis AtDGK7, the Smallest Member of Plant Diacylglycerol Kinases (DGKs), Displays Unique Biochemical Features and Saturates at Low Substrate Concentration: THE DGK INHIBITOR R59022 DIFFERENTIALLY AFFECTS AtDGK2 AND AtDGK7 ACTIVITY IN VITRO AND ALTERS PLANT GROWTH AND DEVELOPMENT. *Journal of Biological Chemistry* 280(41), 34888-34899. doi: 10.1074/jbc.M506859200.
- Gonzalez-Carranza, Z.H., Elliott, K.A., and Roberts, J.A. (2007). Expression of polygalacturonases and evidence to support their role during cell separation processes in *Arabidopsis thaliana*. *Journal of Experimental Botany*, erm222. doi: 10.1093/jxb/erm222.
- Goujon, T., Minic, Z., El Amrani, A., Lerouxel, O., Aletti, E., Lapierre, C., et al. (2003). AtBXL1, a novel higher plant (*Arabidopsis thaliana*) putative beta-xylosidase gene, is involved in secondary cell wall metabolism and plant development. *Plant Journal* 33(4), 677-690.
- Haas, B.J., Papanicolaou, A., Yassour, M., Grabherr, M., Blood, P.D., Bowden, J., et al. (2013). De novo transcript sequence reconstruction from RNA-Seq: reference generation and analysis with Trinity. *Nature protocols* 8(8), 10.1038/nprot.2013.1084. doi: 10.1038/nprot.2013.084.
- Haruta, M., Sabat, G., Stecker, K., Minkoff, B.B., and Sussman, M.R. (2014). A peptide hormone and its receptor protein kinase regulate plant cell expansion. *Science* 343(6169), 408-411. doi: 10.1126/science.1244454.
- Hvoslef-Eide, A.K., Munster, C.M., Mathiesen, C.A., Ayeh, K.O., Melby, T.I., Rasolomanana, P., et al. (2016). Primary and Secondary Abscission in *Pisum sativum* and *Euphorbia pulcherrima*—How Do They Compare and How Do They Differ? *Frontiers in Plant Science* 6(1204). doi: 10.3389/fpls.2015.01204.
- Ichimura, K., Mizoguchi, T., Yoshida, R., Yuasa, T., and Shinozaki, K. (2000). Various abiotic stresses rapidly activate *Arabidopsis* MAP kinases ATMPK4 and ATMPK6. *The Plant Journal* 24(5), 655-665.
- Jia, Y., Tao, F., and Li, W. (2013). Lipid Profiling Demonstrates That Suppressing *Arabidopsis* Phospholipase D6 Retards ABA-Promoted Leaf Senescence by Attenuating Lipid Degradation. *PLOS ONE* 8(6), e65687. doi: 10.1371/journal.pone.0065687.
- Jones, P., Binns, D., Chang, H.Y., Fraser, M., Li, W., McAnulla, C., et al. (2014). InterProScan 5: genome-scale protein function classification. *Bioinformatics* 30(9), 1236-1240. doi: 10.1093/bioinformatics/btu031.
- Jorrín-Novo, J.V., Pascual, J., Sánchez-Lucas, R., Romero-Rodríguez, M.C., Rodríguez-Ortega, M.J., Lenz, C., et al. (2015). Fourteen years of plant proteomics reflected in Proteomics: Moving from model species and 2DE-based approaches to orphan species and gel-free platforms. *Proteomics* 15(5-6), 1089-1112. doi: 10.1002/pmic.201400349.
- Kang, C.H., Moon, B.C., Park, H.C., Koo, S.C., Jeon, J.M., Cheong, Y.H., et al. (2011). Rice OsERG3 encodes an unusual small C2-domain protein containing a Ca²⁺-binding module but lacking phospholipid-binding properties. *Biochimica et Biophysica Acta (BBA) - General Subjects* 1810(12), 1317-1322.
- Katagiri, T., Takahashi, S., and Shinozaki, K. (2001). Involvement of a novel *Arabidopsis* phospholipase D, AtPLDδ, in dehydration-inducible accumulation of phosphatidic acid in stress signalling. *The Plant Journal* 26(6), 595-605. doi: 10.1046/j.1365-3113x.2001.01060.x.
- Kepinski, S., and Leyser, O. (2005). The *Arabidopsis* F-box protein TIR1 is an auxin receptor. *Nature* 435(7041), 446-451. doi: 10.1038/nature03542.
- Kim, J., Yang, J., Yang, R., Sicher, R.C., Chang, C., and Tucker, M.L. (2016). Transcriptome analysis of soybean leaf abscission identifies transcriptional regulators of organ polarity and cell fate. *Frontiers in Plant Science* 7. doi: 10.3389/fpls.2016.00125.
- Kostenyuk, I.A., and Burns, J.K. (2004). Mechanical wounding and abscission in citrus. *Physiologia Plantarum* 122(3), 354-361.
- Lee, E. (1911). The Morphology of Leaf-fall. *Annals of Botany* 25(97), 51-106.

- Lee, Y., Derbyshire, P., Knox, J.P., and Hvorslev-Eide, A.K. (2008). Sequential cell wall transformations in response to the induction of a pedicel abscission event in *Euphorbia pulcherrima* (poinsettia). *The Plant Journal* 54(6), 993-1003. doi: 10.1111/j.1365-3113X.2008.03456.x.
- Lewis, J.D., Wu, R., Guttman, D.S., and Desveaux, D. (2010). Allele-Specific Virulence Attenuation of the *Pseudomonas syringae* HopZ1a Type III Effector via the Arabidopsis ZAR1 Resistance Protein. *PLOS Genetics* 6(4), e1000894. doi: 10.1371/journal.pgen.1000894.
- Liu, H., Wang, Y., Xu, J., Su, T., Liu, G., and Ren, D. (2008). Ethylene signaling is required for the acceleration of cell death induced by the activation of AtMEK5 in Arabidopsis. *Cell Res* 18(3), 422-432.
- Lukaszuk, E., Rys, M., Możdżeń, K., Stawoska, I., Skoczowski, A., and Ciereszko, I. (2016). Photosynthesis and sucrose metabolism in leaves of Arabidopsis thaliana aos, ein4 and rcd1 mutants as affected by wounding. *Acta Physiologiae Plantarum* 39(1), 17. doi: 10.1007/s11738-016-2309-1.
- Mane, S.P., Vasquez-Robinet, C., Sioson, A.A., Heath, L.S., and Grene, R. (2007). Early PLD α -mediated events in response to progressive drought stress in Arabidopsis: a transcriptome analysis. *Journal of Experimental Botany* 58(2), 241-252. doi: 10.1093/jxb/erl262.
- Marmagne, A., Ferro, M., Meinel, T., Bruley, C., Kuhn, L., Garin, J., et al. (2007). A High Content in Lipid-modified Peripheral Proteins and Integral Receptor Kinases Features in the Arabidopsis Plasma Membrane Proteome. *Molecular & Cellular Proteomics* 6(11), 1980-1996. doi: 10.1074/mcp.M700099-MCP200.
- McQueen-Mason, S., Durachko, D.M., and Cosgrove, D.J. (1992). Two endogenous proteins that induce cell wall extension in plants. *Plant Cell* 4, 1425-1433.
- Meir, S., Philosoph-Hadas, S., Sundaresan, S., Selvaraj, K.S., Burd, S., Ophir, R., et al. (2010). Microarray analysis of the abscission-related transcriptome in the tomato flower abscission zone in response to auxin depletion. *Plant Physiology* 154(4), 1929-1956. doi: 10.1104/pp.110.160697.
- Meir, S., Sundaresan, S., Rivov, J., Agarwal, I., and Philosoph-Hadas, S. (2015). Role of auxin depletion in abscission control. *Stewart Postharvest Review* 11(2), 1-15. doi: 10.2212/spr.2015.2.2.
- Memelink, J., Swords, K.M.M., de Kam, R.J., Schilperoort, R.A., Hoge, J.H.C., and Staehelin, L.A. (1993). Structure and regulation of tobacco extensin. *The Plant Journal* 4(6), 1011-1022. doi: 10.1046/j.1365-3113X.1993.04061011.x.
- Merelo, P., Agustí, J., Arbona, V., Costa, M.L., Estornell, L.H., Gómez-Cadenas, A., et al. (2017). Cell Wall Remodeling in Abscission Zone Cells during Ethylene-Promoted Fruit Abscission in Citrus. *Frontiers in Plant Science* 8(126). doi: 10.3389/fpls.2017.00126.
- Merkouropoulos, G., and Shirsat, A. (2003). The unusual Arabidopsis extensin gene atExt1 is expressed throughout plant development and is induced by a variety of biotic and abiotic stresses. *Planta* 217(3), 356-366.
- Miller, J.D., Arteca, R.N., and Pell, E.J. (1999). Senescence-Associated Gene Expression during Ozone-Induced Leaf Senescence in Arabidopsis. *Plant Physiology* 120(4), 1015-1024. doi: 10.1104/pp.120.4.1015.
- Minic, Z., Rihoüey, C., Do, C.T., Lerouge, P., and Jouanin, L. (2004). Purification and Characterization of Enzymes Exhibiting β -d-Xylosidase Activities in Stem Tissues of Arabidopsis. *Plant Physiology* 135(2), 867-878. doi: 10.1104/pp.104.041269.
- Mockaitis, K., and Howell, S.H. (2000). Auxin induces mitogen activated protein kinase (MAPK) activation in roots of Arabidopsis seedlings. *The Plant Journal* 24(6), 785-796.
- Moe, R., Fjeld, T., and Mortensen, L.M. (1992). Stem elongation and keeping quality in poinsettia (*EuphorbiaPulcherrima* Willd) as affected by temperature and supplementary lighting. *Scientia Horticulturae* 50(1-2), 127-136.

- Molina, I., Li-Beisson, Y., Beisson, F., Ohlrogge, J.B., and Pollard, M. (2009). Identification of an Arabidopsis Feruloyl-Coenzyme A Transferase Required for Suberin Synthesis. *Plant Physiology* 151(3), 1317-1328. doi: 10.1104/pp.109.144907.
- Moni, A., Lee, A.Y., Briggs, W.R., and Han, I.S. (2015). The blue light receptor Phototropin 1 suppresses lateral root growth by controlling cell elongation. *Plant Biology* 17(1), 34-40. doi: 10.1111/plb.12187.
- Munster, C. (2006). *On the flower abscission of poinsettia (Euphorbia pulcherrima Willd. Ex Klotzsch) - A molecular and plant hormonal study*. Norwegian University of Life Sciences.
- Nakano, T., Kimbara, J., Fujisawa, M., Kitagawa, M., Ihashi, N., Maeda, H., et al. (2012). MACROCALYX and JOINTLESS interact in the transcriptional regulation of tomato fruit abscission zone development. *Plant Physiology* 158(1), 439-450. doi: 10.1104/pp.111.183731.
- Niederhuth, C.E., Patharkar, O.R., and Walker, J.C. (2013). Transcriptional profiling of the Arabidopsis abscission mutant hae hsl2 by RNA-Seq. *BMC Genomics* 14(37), 37. doi: 10.1186/1471-2164-14-37.
- Nishihama, R., Ishikawa, M., Araki, S., Soyano, T., Asada, T., and Machida, Y. (2001). The NPK1 mitogen-activated protein kinase kinase kinase is a regulator of cell-plate formation in plant cytokinesis. *Genes & Development* 15(3), 352-363. doi: 10.1101/gad.863701.
- Noutoshi, Y., Kuromori, T., Wada, T., Hirayama, T., Kamiya, A., Imura, Y., et al. (2006). Loss of NECROTIC SPOTTED LESIONS 1 associates with cell death and defense responses in Arabidopsis thaliana. *Plant Molecular Biology* 62(1), 29-42. doi: 10.1007/s11103-006-9001-6.
- Parra, R., Paredes, M., Sanchez-Calle, I., and Gomez-Jimenez, M. (2013). Comparative transcriptional profiling analysis of olive ripe-fruit pericarp and abscission zone tissues shows expression differences and distinct patterns of transcriptional regulation. *BMC Genomics* 14(1), 866.
- Philippe, F., Pelloux, J., and Rayon, C. (2017). Plant pectin acetyltransferase structure and function: new insights from bioinformatic analysis. *BMC Genomics* 18(1), 456. doi: 10.1186/s12864-017-3833-0.
- Poovaiah, B.W. (1974). Formation of callose and lignin during leaf abscission. *American Journal of Botany* 61, 829-834.
- Reinbothe, S., Mollenhauer, B., and Reinbothe, C. (1994). JIPs and RIPs: the regulation of plant gene expression by jasmonates in response to environmental cues and pathogens. *The Plant Cell* 6(9), 1197-1209. doi: 10.1105/tpc.6.9.1197.
- Riov, J. (1974). A polygalacturonase from citrus leaf explants: role in abscission. *Plant Physiology* 53(2), 312-316.
- Roberts, J.A., and Gonzalez-Carranza, Z.H. (2009). Pectinase functions in abscission. *Stewart Postharvest Review* 5(1), 1-4. doi: 10.2212/spr.2009.1.2.
- Roberts, J.A., Schindler, C.B., and Tucker, G.A. (1984). Ethylene-promoted tomato flower abscission and the possible involvement of an inhibitor. *Planta* 160(2), 159-163. doi: 10.1007/bf00392864.
- Rose, J.K.C., and Bennett, A.B. (1994). Cooperative disassembly of the cellulose-xyloglucan network on plant cell walls: parallels between cell expansion and fruit ripening. *Trends in Plant Science* 4(5), 176-183.
- Rupert, B., Cattivelli, L., Pagni, S., and Ramina, A. (2002). Ethylene-responsive genes are differentially regulated during abscission, organ senescence and wounding in peach (*Prunus persica*) *Journal of Experimental Botany* 53 (368), 429-437.
- Stitt, M., and Hurry, V. (2002). A plant for all seasons: alterations in photosynthetic carbon metabolism during cold acclimation in Arabidopsis. *Curr Opin Plant Biol* 5(3), 199-206.

- Stösser, R., Rasmussen, H.P., and Bukovac, M.J. (1969). Histochemical changes in the developing abscission layer in fruits of *Prunus cerasus* L. *Planta* 86(2), 151-164. doi: 10.1007/bf00379823.
- Sumiyoshi, M., Inamura, T., Nakamura, A., Aohara, T., Ishii, T., Satoh, S., et al. (2015). UDP-arabinopyranose mutase 3 is required for pollen wall morphogenesis in rice (*Oryza sativa*). *Plant and Cell Physiology* 56(2), 232-241. doi: 10.1093/pcp/pcu132.
- Sundaresan, S., Philosoph-Hadas, S., Riov, J., Mugasimangalam, R., Kuravadi, N.A., Kochanek, B., et al. (2016). De novo transcriptome sequencing and development of abscission zone-specific microarray as a new molecular tool for analysis of tomato organ abscission. *Frontiers in Plant Science* 6. doi: 10.3389/fpls.2015.01258.
- Taj, G., Agarwal, P., Grant, M., and Kumar, A. (2010). MAPK machinery in plants: Recognition and response to different stresses through multiple signal transduction pathways. *Plant Signaling & Behavior* 5(11), 1370-1378. doi: 10.4161/psb.5.11.13020.
- Tan, X., Meyers, B.C., Kozik, A., West, M.A., Morgante, M., St Clair, D.A., et al. (2007). Global expression analysis of nucleotide binding site-leucine rich repeat-encoding and related genes in Arabidopsis. *BMC Plant Biology* 7(1), 56. doi: 10.1186/1471-2229-7-56.
- Taylor, J.E., and Whitelaw, C.A. (2001). Signals in abscission. *New Phytologist* 151(2), 323-340.
- Teige, M., Scheikl, E., Eulgem, T., Dóczi, R., Ichimura, K., Shinozaki, K., et al. (2004). The MKK2 Pathway Mediates Cold and Salt Stress Signaling in Arabidopsis. *Molecular Cell* 15(1), 141-152.
- Tranbarger, T.J., Tucker, M.L., Roberts, J.A., and Meir, S. (2017). Editorial: Plant Organ Abscission: From Models to Crops. *Frontiers in Plant Science* 8(196). doi: 10.3389/fpls.2017.00196.
- Tucker, M.L., and Kim, J. (2015). Abscission research: what we know and what we still need to study. *Stewart Postharvest Review* 11(2), 1-7. doi: 10.2212/spr.2015.2.1.
- Turner, J.G., Ellis, C., and Devoto, A. (2002). The Jasmonate Signal Pathway. *The Plant Cell* 14(suppl 1), S153-S164. doi: 10.1105/tpc.000679.
- Tyanova, S., Temu, T., Sinitcyn, P., Carlson, A., Hein, M.Y., Geiger, T., et al. (2016). The Perseus computational platform for comprehensive analysis of (prote)omics data. *Nature Methods* 13(9), 731-740. doi: 10.1038/nmeth.3901.
- Uraji, M., Katagiri, T., Okuma, E., Ye, W., Hossain, M.A., Masuda, C., et al. (2012). Cooperative Function of PLD δ and PLD α 1 in Absciscic Acid-Induced Stomatal Closure in Arabidopsis. *Plant Physiology* 159(1), 450-460. doi: 10.1104/pp.112.195578.
- Van Sandt, V.S.T., Suslov, D., Verbelen, J.-P., and Vissenberg, K. (2007). Xyloglucan Endotransglucosylase Activity Loosens a Plant Cell Wall. *Annals of Botany*, mcm248. doi: 10.1093/aob/mcm248.
- Vizcaino, J.A., Csordas, A., del-Toro, N., Dianes, J.A., Griss, J., Lavidas, I., et al. (2016). 2016 update of the PRIDE database and its related tools. *Nucleic Acids Research* 44(D1), D447-D456. doi: 10.1093/nar/gkv1145.
- Wang, C., Zien, C.A., Afithile, M., Welti, R., Hildebrand, D.F., and Wang, X. (2000). Involvement of Phospholipase D in Wound-Induced Accumulation of Jasmonic Acid in Arabidopsis. *The Plant Cell* 12(11), 2237-2246. doi: 10.1105/tpc.12.11.2237.
- Wang, X., Liu, D., Li, A., Sun, X., Zhang, R., Wu, L., et al. (2013). Transcriptome Analysis of Tomato Flower Pedicel Tissues Reveals Abscission Zone-Specific Modulation of Key Meristem Activity Genes. *PLoS ONE* 8(2), e55238. doi: 10.1371/journal.pone.0055238.
- Weinl, S., Held, K., Schlücking, K., Steinhorst, L., Kuhlert, S., Hippler, M., et al. (2008). A plastid protein crucial for Ca²⁺-regulated stomatal responses. *New Phytologist* 179(3), 675-686. doi: 10.1111/j.1469-8137.2008.02492.x.
- Xiong, L., Lee, B.-h., Ishitani, M., Lee, H., Zhang, C., and Zhu, J.-K. (2001). FIERY1 encoding an inositol polyphosphate 1-phosphatase is a negative regulator of abscisic acid and stress signaling in Arabidopsis. *Genes & Development* 15(15), 1971-1984. doi: 10.1101/gad.891901.

- Xu, Y., Chang, P., Liu, D., Narasimhan, M.L., Raghothama, K.G., Hasegawa, P.M., et al. (1994). Plant Defense Genes Are Synergistically Induced by Ethylene and Methyl Jasmonate. *The Plant Cell* 6(8), 1077-1085. doi: 10.1105/tpc.6.8.1077.
- Yager, R.E. (1960). Possible Role of Pectic Enzymes in Abscission. *Plant Physiology* 35(2), 157-162.
- Yu, F., Qian, L., Nibau, C., Duan, Q., Kita, D., Levasseur, K., et al. (2012). FERONIA receptor kinase pathway suppresses abscisic acid signaling in Arabidopsis by activating ABI2 phosphatase. *Proceedings of the National Academy of Sciences* 109(36), 14693-14698. doi: 10.1073/pnas.1212547109.
- Zhang, X.-l., Qi, M.-f., Xu, T., Lu, X.-j., and Li, T.-l. (2015). Proteomics profiling of ethylene-induced tomato flower pedicel abscission. *Journal of Proteomics* (0).
- Zhang, X., Jiang, T., Yu, Y., Wu, Z., Jiang, S., Lu, K., et al. (2014). Arabidopsis co-chaperonin CPN20 antagonizes Mg-chelatase H subunit to derepress ABA-responsive WRKY40 transcription repressor. *Science China Life Sciences* 57(1), 11-21. doi: 10.1007/s11427-013-4587-9.
- Zhu, H., Dardick, C., Beers, E., Callanhan, A., Xia, R., and Yuan, R. (2011). Transcriptomics of shading-induced and NAA-induced abscission in apple (*Malus domestica*) reveals a shared pathway involving reduced photosynthesis, alterations in carbohydrate transport and signaling and hormone crosstalk. *BMC Plant Biology* 11(1), 138.
- Zhu, Y., Zheng, P., Varanasi, V., Shin, S., Main, D., Curry, E., et al. (2012). Multiple plant hormones and cell wall metabolism regulate apple fruit maturation patterns and texture attributes. *Tree Genetics & Genomes* 8(6), 1389-1406. doi: 10.1007/s11295-012-0526-3.
- Zougman, A., Selby, P.J., and Banks, R.E. (2014). Suspension trapping (STrap) sample preparation method for bottom-up proteomics analysis. *Proteomics* 14(9), 1006-1000. doi: 10.1002/pmic.201300553.

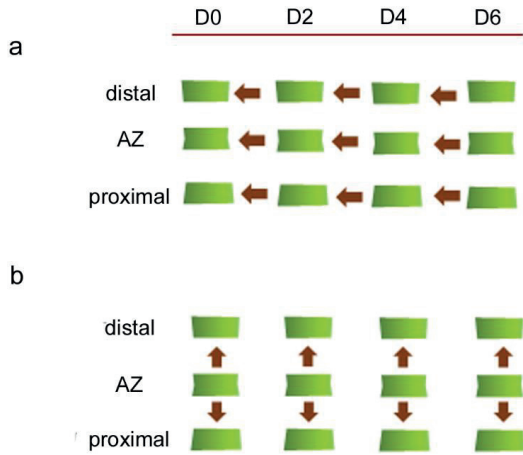


Fig 1. Scheme for the study showing the pairwise comparisons between portions of the poinsettia flower bud at four time points, Day 0 (D0), Day 2 (D2), Day 4 (D4) and Day 6 (D6). Arrows indicate the directionality of the pair wise comparisons made. (A) Temporal comparisons along the time line. (B) Spatial comparisons between parts of the flower. AZ= abscission zone.

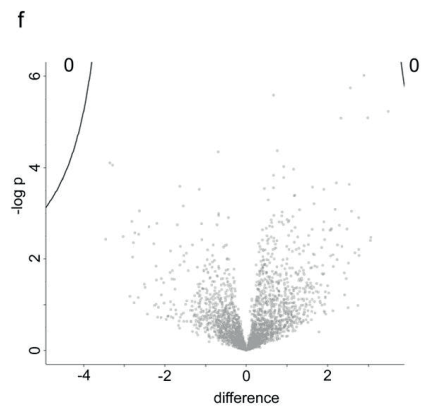
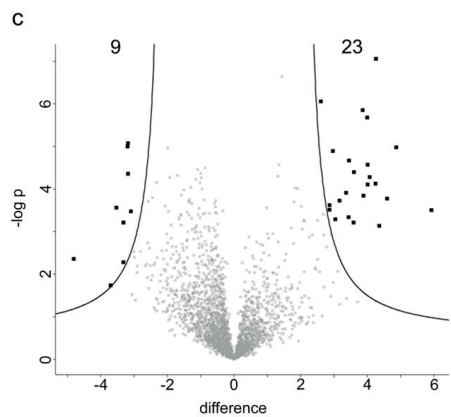
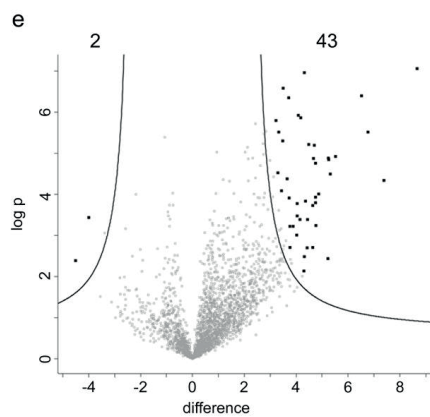
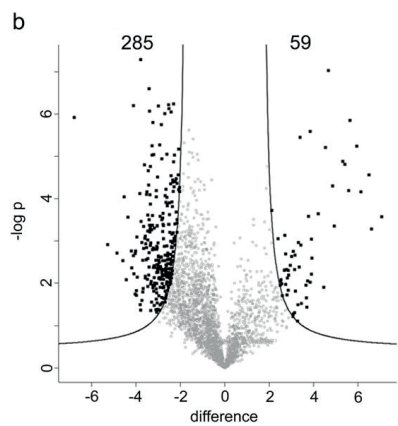
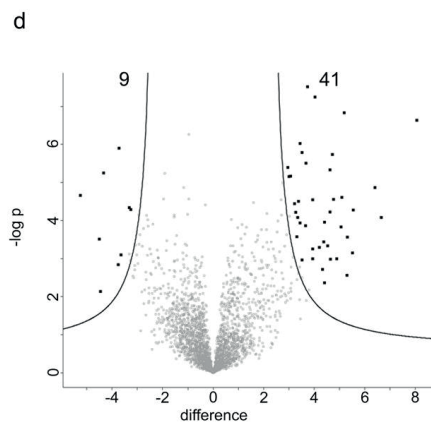
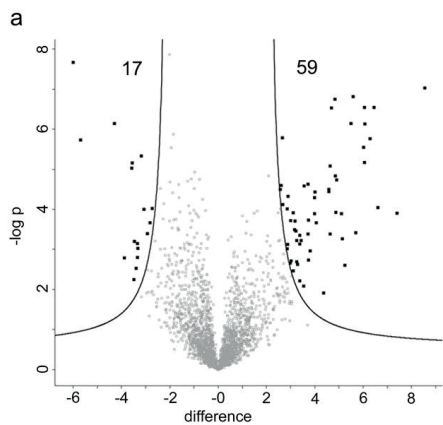


Fig 2. Volcano plots with temporal comparisons between the same tissues at different stages of the abscission progression during poinsettia bud abscission. False discovery rate (FDR) = 0.01, and fold change= two. (A) distal Day 2 vs distal Day 0, (B) abscission zone Day 2 vs abscission zone Day 0, (C) proximal Day 2 vs proximal Day 0, (D) distal Day 4 vs distal Day 2, (E) abscission zone Day 4 vs abscission zone Day 2, (F) proximal Day 4 vs proximal Day 2. In each volcano plot, the differentially expressed proteins are located in the exterior area of the volcano shape and are highlighted in bold. X-axis represents the \log_2 fold change and the y-axis represents the level of significance. The number of decreased and increased proteins is displayed in the upper left and right corners of each volcano plot, respectively.

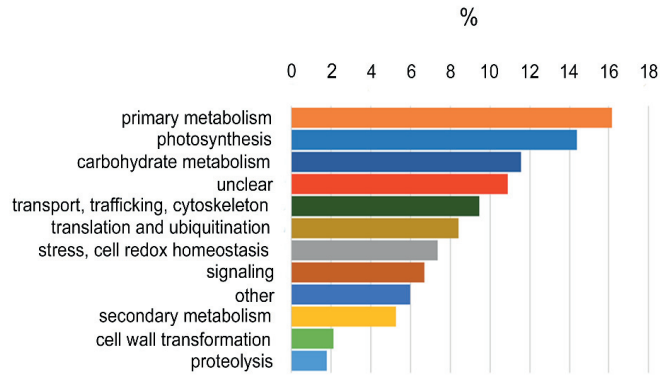


Fig 3. Functional characterization of the 285 proteins decreasing in abundances in the abscission zone of poinsettia flower buds in the first 48 hours after the induction of abscission.

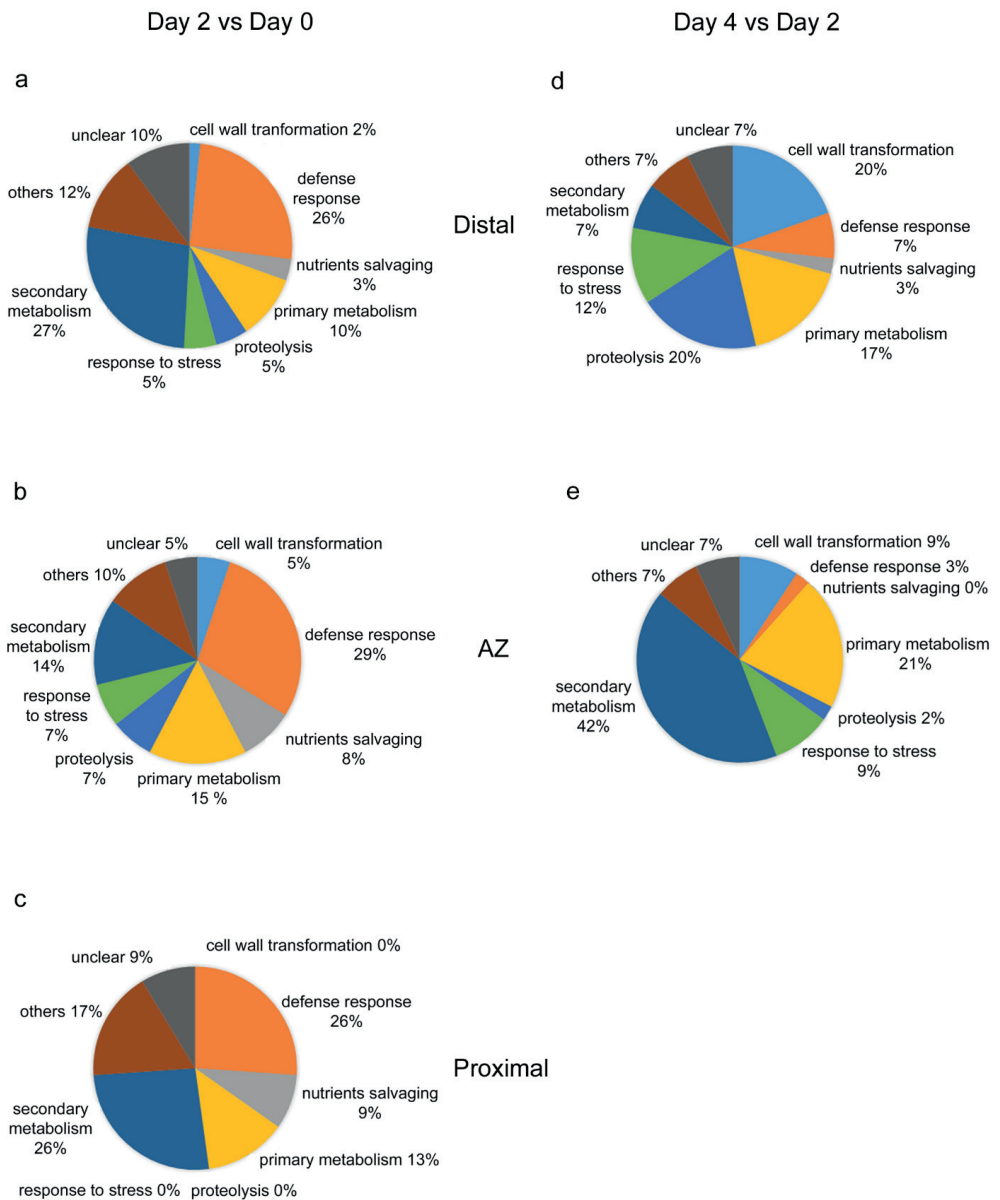


Fig 4. Functional characterization of the 144 and the 84 proteins increased during the transition between Day 0 and Day 2 and (A, B and C) and during the change from Day 2 to Day 4 respectively (D and E). (A) distal Day 2 vs Day 0, (B) abscission zone Day 2 vs Day 0,

(C) proximal Day 2 vs Day 0, (D) distal Day 4 vs Day 2 and (E) abscission zone Day 4 vs Day

2.

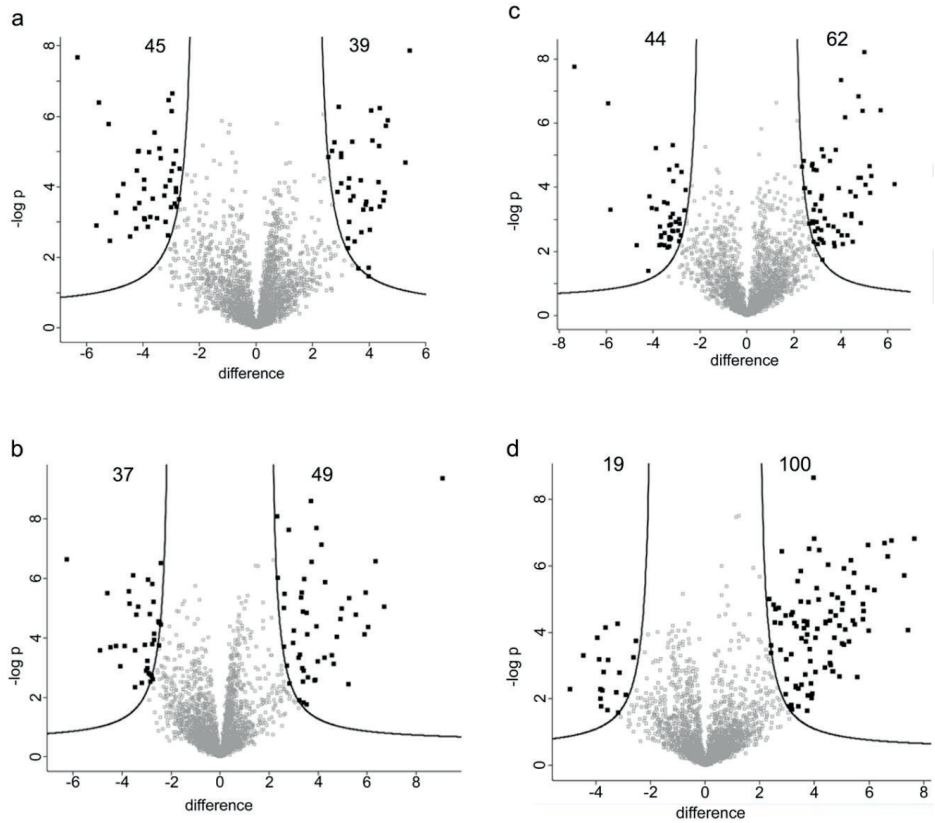


Fig 5. Volcano plot showing the spatial comparisons between tissues belonging to the same time point (FDR= 0.01, fold change=2). (A) abscission zone and distal Day 4, (B) abscission zone and proximal Day 4, (C) abscission zone and distal Day 6 and (D) abscission zone and proximal Day 6. In each volcano plot, the differentially expressed proteins are located in the exterior area of the volcano shape and are highlighted in bold. X-axis represents the \log_2 fold change and y-axis represents the level of significance. The number of decreased and increased proteins is displayed in the upper left and right corners of each volcano plot, respectively.

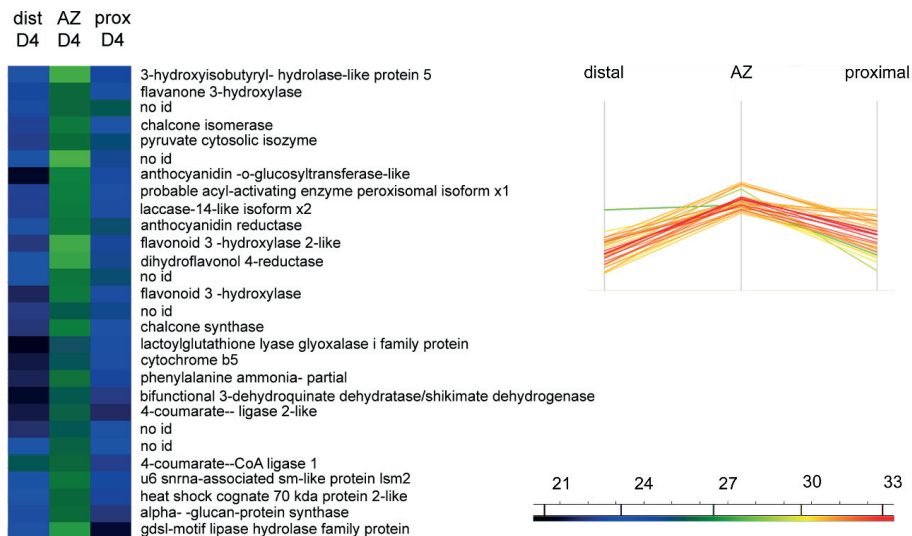


Fig 6. Hierarchical clustering detail, showing 28 proteins and their abundances profiles during Day 4 12 are from secondary metabolism. Example of clusters of proteins sharing the same pattern of protein changes with higher levels in AZ. Color scale corresponds to the log2 of the detection intensities.

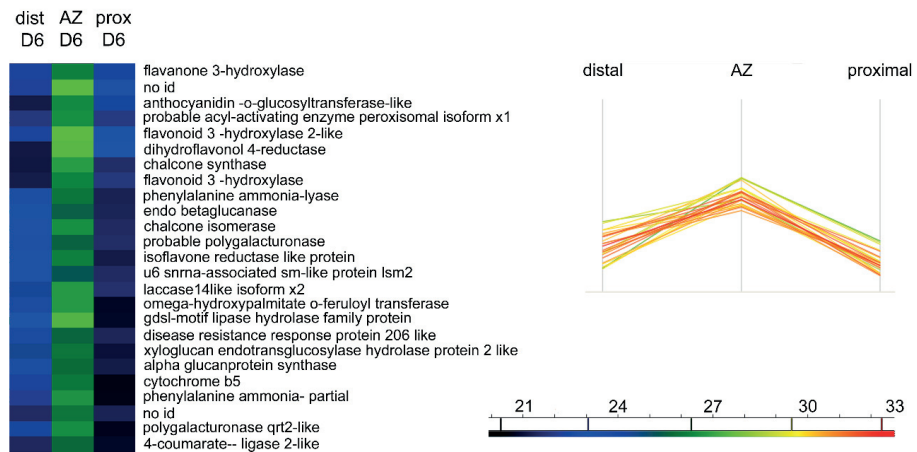


Fig 7. Detail of the hierarchical clustering of the 3086 proteins during Day 6. Example of clusters of proteins sharing the same pattern of protein changes with higher levels in AZ. Color scale corresponds to the log2 of the detection intensities.

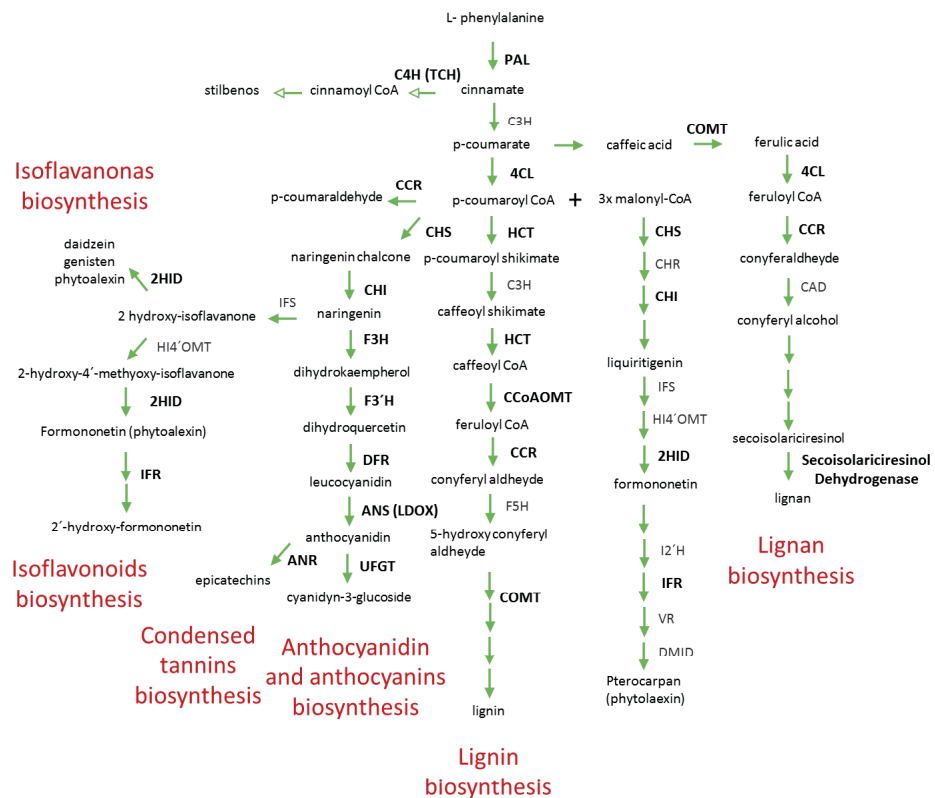


Fig. 8 Proteins from the phenylpropanoid biosynthetic pathway that increased in levels within the AZ D6. In bold the enzymes that increased abundance within the abscission zone on Day 6. In red the families of secondary metabolites that are putatively present within the AZ. Phenylalanine ammonia- lyase (**PAL**), Cinnamate-4-hydroxylase C4H or trans cinnamate hydroxylase (**C4H or TCH**), 4-coumarate CoA ligase (**4CL**), hydroxycinnamoyl-shikimate quinate hydroxycinnamoyl transferase isoform 1 (**HCT**), Coumaroyl ester 3'-hydroxylase (C3H), Caffeoyl-o-methyltransferase (**CCoAOMT**), Cinnamoyl Co reductase (**CCR**), Ferulate-5-hydroxylase (F5H), Caffeic acid-o-methyltransferase (**COMT**), chalcone synthase (**CHS**), chalcone isomerase (**CHI**), Flavanone- 3-hydroxylase (**F3H**), Flavonoid- 3-hydroxylase (**F3'H**), Dihydroflavonol reductase (**DFR**), Anthocyanidin synthase or Leucocyanidin oxygenase (**ANS or LDOX**), Anthocyanidin 3-O-glucosyltransferase 2 (**UGFT**),

Anthocyanidin reductase (**ANR**), 2-hydroxyisoflavanone dehydratase (**2HID**), 2-hydroxyisoflavanone 4'-O-methyltransferase (HI4'OMT), Isoflavone reductase (**IFR**), Isoflavone synthase (IFS), Isoflavone 2'-hydroxylase (I2'H), Vestitone reductase (VR), 7,2'-dihydroxy-4'-methoxy-isoflavanol dehydratase (DMID), **secoisolariciresinol dehydrogenase**.

Supplementary material number 1. Proteins that decrease in level on Day 2 and Day 4 (temporal comparisons)

| Proteins that decrease in the distal region on Day 2 | | | | | | | | | |
|---|---|-------------|--------------------------------|--------------------------------|---|--|--|--|--|
| name sequence | protein name | fold change | log2[mean intensity Distal D0] | log2[mean intensity Distal D2] | relative abundance [log2(cond.1/control)] | function or category | | | |
| TR120538_c6_g1_i2 m.53041;TR119633_c4_g1_i2 m.51665 TR103339_c4_g1_i2 m.34872;TR102503_c1_g1_i1 m.33990;TR102503_c1_g1_i2 m.33991 | Stem-specific protein TSIT1 | 0.14 | 26.07 | 23.25 | -2.82 | AA biosynthesis, nitrogen assimilation Brassinosteroid receptor that regulates negatively BR signalling | | | |
| TR131836_c5_g1_i2 m.81928;TR127427_c8_g1_i1 m.68158;TR95869_c1_g1_i2 m.28481 | Membrane steroid-binding protein 1 | 0.09 | 24.43 | 20.88 | -3.55 | | | | |
| TR159424_c0_g1_i1 m.222672;TR150549_c0_g1_i1 m.221187 | Dehydrin ERD14 | 0.02 | 27.08 | 21.07 | -6.01 | Chaperone, stress related | | | |
| TR120730_c0_g1_i2 m.53442;TR120589_c2_g1_i2 m.53105;TR120730_c0_g1_i1 m.53440;TR120589_c2_g1_i1 m.53103;TR175624_c0_g1_i1 m.225626;TR174513_c0_g1_i1 m.225424 | Tubulin beta-1 chain | 0.09 | 24.07 | 20.60 | -3.47 | cytoskeleton | | | |
| TR87863_c1_g1_i2 m.23585;TR72183_c1_g1_i2 m.18383 | non-specific lipid transfer protein gpi-anchored 1-like | 0.10 | 24.98 | 21.63 | -3.35 | defense | | | |
| TR144523_c5_g1_i2 m.157852;TR141443_c2_g1_i1 m.132651 | Cytochrome b5 | 0.12 | 23.95 | 20.89 | -3.06 | Lipid metabolism, primary metabolism | | | |
| TR70599_c0_g1_i1 m.17576;TR65907_c0_g1_i1 m.15748 | Cytochrome b5 isoform B | 0.05 | 24.66 | 20.37 | -4.29 | Lipid metabolism, primary metabolism | | | |
| TR78931_c0_g1_i1 m.20998;TR65988_c0_g1_i1 m.15772 | fascidin-like arabinogalactan protein 1 | 0.13 | 25.97 | 23.04 | -2.93 | other, adhesion | | | |
| TR75171_c0_g1_i1 m.19501;TR114553_c0_g1_i1 m.45336 | Oxygen-evolving enhancer protein 3-1, chloroplastic | 0.10 | 25.31 | 21.92 | -3.40 | photosynthesis | | | |
| TR147969_c12_g5_i2 m.193489;TR147969_c12_g5_i1 m.193488 | Photosystem II repair protein PS827-H1, chloroplastic | 0.11 | 23.93 | 20.74 | -3.19 | photosynthesis | | | |
| TR124604_c5_g1_i1 m.61555;TR112326_c2_g1_i1 m.42385;TR27791_c1_g1_i1 m.6461;TR124604_c0_g1_i1 m.61554 | chlorophyll a-b-binding protein of lhci type 1-like | 0.07 | 24.63 | 20.74 | -3.89 | photosynthesis | | | |
| TR129361_c1_g2_i1 m.73707;TR112680_c0_g1_i1 m.42840;TR108951_c0_g1_i1 m.39758;TR93018_c0_g1_i1 m.26433 | thiamine thiazole chloroplastic | 0.10 | 26.66 | 23.32 | -3.34 | primary metabolism, coenzyme precursor | | | |
| TR145770_c7_g2_i2 m.169629 | Secoisolaricresinol dehydrogenase (Fragment) | 0.15 | 23.40 | 20.68 | -2.73 | secondary metabolism | | | |
| TR141742_c1_g1_i1 m.134815;TR143052_c0_g1_i4 m.145081;TR143052_c0_g1_i2 m.145079 | 14-3-3-like protein | 0.10 | 24.80 | 21.48 | -3.32 | signalling, modulation of signal | | | |
| TR188258_c3_g1_i1 m.227525;TR180718_c5_g1_i1 m.226218 | 50S ribosomal protein L12, chloroplastic | 0.08 | 24.46 | 20.89 | -3.57 | translation | | | |
| TR71730_c0_g1_i1 m.18172;TR66488_c0_g1_i1 m.15934 | NO ID | 0.02 | 27.04 | 21.35 | -5.70 | unclear | | | |
| | NO ID | 0.09 | 26.00 | 22.52 | -3.49 | unclear | | | |

Proteins that decrease in the abscission zone on Day 2

| name sequence | protein name | fold change | log2(mean intensity AZ D0) | log2(mean intensity AZ D2) | relative abundance [log2(cond./1/control)] | function or category |
|---|--|-------------|----------------------------|----------------------------|--|--|
| TR113024_c0_g1_1 1m.43194;TR124085_c0_g1_2 1m.00224 | 30S ribosomal protein S1 | 0.16 | 25.02 | 22.38 | -2.63 | Ribosome constituent, translation of thylakoid membrane proteins encoded by chloroplast genes. |
| TR121906_c0_g1_1 1m.55994;TR121266_c0_g1_1 1m.54590 | 30S ribosomal protein S5, chloroplastic | 0.08 | 24.92 | 21.30 | -3.62 | Ribosome constituent, plastid translation, chloroplast rRNA processing. |
| TR119598_c3_g1_1 1m.51616;TR111620_c2_g1_1 1m.41317 | 40S ribosomal protein S14 | 0.13 | 24.69 | 21.73 | -2.96 | Ribosome constituent, translation |
| TR90405_c0_g1_1m.24717;TR68021_c0_g1_1 1m.23623 | 50S ribosomal protein L5, chloroplastic | 0.15 | 23.73 | 21.04 | -2.69 | Ribosome constituent, translation, photosynthesis |
| TR116331_c4_g1_1 1m.47556;TR112447_c5_g1_1 1m.42560 | 60S ribosomal protein L18-2 | 0.13 | 24.40 | 21.44 | -2.96 | Ribosome constituent, translation, photosynthesis |
| TR132391_c3_g1_1 2m.84219;TR132391_c3_g1_1 1m.84206;TR100023_c0_g1_1 2m.32269;TR132391_c3_g1_1 2m.84207 | 60s ribosomal protein L27a-3 | 0.16 | 23.89 | 21.25 | -2.64 | Ribosome constituent, translation, photosynthesis |
| TR100377_c1_g2_1 2m.32616;TR72929_c0_g1_1 1m.18625;TR100377_c1_g2_1 1m.32617 | 60S ribosomal protein L30 | 0.13 | 25.67 | 22.76 | -2.91 | Ribosome constituent, translation, rRNA and mRNA regulation |
| TR130023_c3_g1_1 3m.75780;TR1218185_c2_g2_1 2m.55838 | 60S ribosomal protein L32-1 | 0.19 | 24.52 | 22.11 | -2.40 | Ribosome constituent, translation |
| TR136398_c11_g1_1 2m.101458;TR136398_c11_g1_1 3m.101459;TR136518_c2_g1_1 4m.102065;TR172897_c0_g1_1 1m.22575;TR342_c0_g1_1 1m.110;TR22238_c0_g2_1 1m.5265;TR22238_c0_g1_1 1m.5264;TR136398_c0_g2_1 1m.101455;TR136398_c0_g1_1 1m.101454;TR151244_c0_g1_1 1m.221518;TR150658_c0_g1_1 1m.221252 | 60S ribosomal protein L4 | 0.14 | 23.42 | 20.58 | -2.84 | Ribosome constituent, translation |
| TR29209_c1_g1_1 1m.73195;TR128143_c4_g2_1 3m.69998 | 60S ribosomal protein L6 | 0.08 | 25.33 | 21.74 | -3.59 | Ribosome constituent, translation |
| TR9087_c0_g1_1 1m.1844;TR8560_c0_g1_1 1m.1509 | Elongation factor 1-gamma 1 | 0.17 | 23.80 | 21.26 | -2.54 | Translation |
| TR157912_c0_g1_1 1m.222388;TR150092_c0_g1_1 1m.220729;TR114334_c0_g1_1 2m.45029;TR114334_c0_g1_1 1m.45026;TR101653_c0_g1_1 2m.33332;TR101653_c0_g1_1 1m.33329 | Eukaryotic translation initiation factor 3 subunit C | 0.12 | 25.37 | 22.36 | -3.01 | Translation |
| TR146863_c1_g2_1 4m.180809;TR146863_c1_g2_1 2m.180836;TR146863_c1_g2_1 1m.180834;TR145299_c1_g2_1 4m.165247;TR145299_c1_g2_1 1m.165243;TR145299_c1_g2_1 4m.165246;TR146863_c1_g2_1 3m.180838;TR145299_c1_g2_1 2m.165245 | Eukaryotic translation initiation factor 3 subunit D | 0.12 | 25.14 | 22.10 | -3.04 | Translation |
| TR114120_c0_g2_1 1m.44691;TR112070_c0_g2_1 1m.41966;TR112070_c0_g2_1 2m.41967 | Phenylalanine--tRNA ligase beta subunit, cytoplasmic | 0.12 | 25.12 | 22.09 | -3.03 | tRNA aminoacylation, protein biosynthesis. |
| TR132178_c3_g1_1 1m.83202 | Glutamine--tRNA ligase, cytoplasmic subunit, cytoplasmic | 0.16 | 24.94 | 22.25 | -2.68 | AA activation for protein synthesis |
| TR139871_c0_g2_1 4m.121798;TR139871_c0_g2_1 1m.121791;TR133453_c0_g2_1 1m.88024;TR133453_c0_g2_1 3m.88021;TR139871_c0_g2_1 6m.121803 | Proline--tRNA ligase, cytoplasmic | 0.07 | 26.35 | 22.56 | -3.78 | Protein synthesis, translation |
| TR138862_c4_g1_1 2m.115406 | Calreticulin | 0.13 | 23.95 | 21.03 | -2.92 | Protein biosynthesis, folding. |
| TR24215_c0_g1_1 1m.19146;TR149589_c1_g1_1 1m.213489 | ER membrane protein complex subunit 8/9 homolog | 0.17 | 24.02 | 21.46 | -2.56 | Protein biosynthesis, folding. |
| TR144690_c1_g1_1 7m.159354;TR144354_c4_g1_1 3m.156174;TR144690_c1_g1_1 1m.159344;TR144354_c4_g1_7 1m.156180;TR144690_c1_g1_1 4m.159348;TR144354_c4_g1_16 1m.156178;TR144354_c4_g1_4 1m.156179;TR144354_c4_g1_4 1m.156176;TR144354_c4_g1_15 1m.156178 | Probable ubiquitin conjugation factor E4 | 0.06 | 26.06 | 22.08 | -3.98 | pathway protein ubiquitination, Protein modification |
| TR159347;TR144690_c1_g1_18 1m.159356;TR144690_c1_g1_15 1m.159350;TR144690_c1_g1_12 1m.159343;TR144690_c1_g1_15 1m.159351;TR96551_c0_g2_1 1m.12426; | Ubiquitin-activating enzyme E12 | 0.12 | 24.38 | 21.38 | -3.00 | pathway protein ubiquitination, Protein modification |
| TR148591_c3_g1_1 3m.200991 | Ubiquitin-conjugating enzyme E2.1 | 0.21 | 23.68 | 21.47 | -2.22 | pathway protein ubiquitination, Protein modification |
| TR90323_c1_g1_1 1m.24656;TR180422_c2_g1_1 1m.226030;TR66404_c0_g1_1 1m.15915 | Ubiquitin-conjugating enzyme E2.7 | 0.18 | 24.50 | 22.05 | -2.45 | pathway protein ubiquitination, Protein modification |

| | | | | | | |
|---|--|--------------|----------------|----------------|----------------|---|
| TR165711_c0_g1_i1 1m.223886;TR158074_c0_g1_i1 1m.222513 | V-type proton ATPase subunit b1 | 0.09 | 24.65 | 21.13 | -3.52 | Transport |
| TR144590_c0_g1_i3 1m.158422;TR144590_c0_g1_i1 1m.158420;TR142746_c0_g1_i4 1m.142609;TR142746_c0_g1_i3 1m.142608;TR142746_c0_g1_i2 1m.142607;TR142746_c0_g1_i5 1m.142611 | monosaccharide-sensing protein 2 like aquaporin tip2-1 | 0.12 0.01 | 24.70 27.33 | 21.66 20.55 | -3.04 -6.77 | Transport Transport |
| TR99999_c1_g2_i2 1m.32247;TR124242_c4_g1_i1 1m.5948 | | | | | | |
| TR146428_c1_g1_i3 1m.176160;TR146428_c1_g1_i2 1m.176158;TR146428_c1_g1_i1 1m.176156;TR144929_c2_g1_i3 1m.161741;TR146428_c1_g1_i6 1m.176166;TR146428_c1_g1_i5 1m.176164;TR144929_c2_g1_i4 1m.161743;TR144929_c2_g1_i2 1m.161739;TR146428_c1_g1_i4 1m.176163;TR143344_c0_g1_i9 1m.147482;TR143344_c0_g1_i6 1m.147478;TR143344_c0_g1_i4 1m.147475;TR141914_c0_g1_i9 1m.135956;TR141914_c0_g1_i8 1m.135952;TR141914_c0_g1_i6 1m.135949;TR141914_c0_g1_i5 1m.13594 | na ⁺ /h ⁺ -antiporter family protein | 0.08 | 24.93 | 21.37 | -3.56 | Transporter |
| 8;TR141914_c0_g1_i4 1m.135947;TR141914_c0_g1_i2 1m.135945;TR141914_c0_g1_i1 1m.135955;TR144929_c2_g1_i1 1m.161738;TR143344_c0_g1_i3 1m.147474;TR143344_c0_g1_i2 1m.147473;TR141914_c0_g1_i3 1m.135946;TR141914_c0_g1_i1 1m.135957;TR143344_c0_g1_i7 1m.147480;TR143344_c0_g1_i5 1m.147477;TR143344_c0_g1_i8 1m.147481;TR143344_c0_g1_i1 1m.147472;TR141914_c0_g1_i7 1m.135955;TR141914_c0_g1_i1 1m.135944 | probable aquaporin pip-type 7a | 0.16 | 24.82 | 22.19 | -2.63 | Transport, stress |
| TR140985_c5_g4_i5 1m.129405;TR412206_c19_g2_i2 1m.130966;TR140985_c5_g4_i2 1m.129398 | Pyrophosphate-energized vacuolar membrane proton pump | 0.19 | 24.02 | 21.61 | -2.41 | Auxin related |
| TR139683_c4_g1_i1 1m.120646;TR139490_c5_g3_i1 1m.119434 | | | | | | |
| TR149513_c0_g2_i1 1m.212590;TR149487_c0_g2_i1 1m.212228;TR149513_c0_g2_i2 1m.212591;TR149513_c0_g2_i3 1m.212592;TR149487_c0_g2_i5 1m.212232;TR148008_c0_g2_i1 1m.194801;TR148345_c0_g1_i2 1m.197957;TR148345_c0_g1_i1 1m.197955;TR148345_c0_g1_i4 1m.197959;TR148345_c0_g1_i3 1m.197958;TR148345_c0_g1_i5 1m.197960;TR148085_c0_g4_i1 1m.194804;TR148085_c0_g4_i2 1m.194806;TR7085_c0_g1_i1 1m.10233;TR56967_c0_g1_i1 1m.12504;TR97927_c0_g1_i1 1m.30096;TR148085_c0_g4_i2 1m.194807;TR148085_c0_g2_i2 1m.194802;TR148085_c0_g4_i1 1m.19480 | abc transporter b family member 1 mitogen-activated protein kinase kinase 5-like | 0.12 0.19 | 27.60 23.61 | 24.55 21.18 | -3.05 -2.43 | Auxin related Signalling defence or cell fate or abscission |
| TR138185_c4_g1_i1 1m.111276;TR133626_c0_g1_i1 1m.88737 | | | | | | |
| TR149015_c5_g1_i3 1m.206055;TR149015_c5_g1_i2 1m.206052;TR149015_c5_g1_i1 1m.206050;TR148333_c0_g1_i2 1m.197836;TR149015_c5_g1_i4 1m.206057;TR148333_c0_g1_i5 1m.197840;TR148333_c0_g1_i7 1m.197843;TR148333_c0_g1_i6 1m.197842;TR148333_c0_g1_i4 1m.197839 | disease resistance rppl3-like protein 4 Eiditor-responsive protein 3 | 0.20 0.19 | 23.25 23.78 | 20.94 21.39 | -2.31 -2.39 | Defence response, receptor Defence response signalling |
| TR111623_c0_g1_i1 1m.41320;TR111627_c0_g1_i1 1m.41326 | | | | | | |
| TR111556_c0_g1_i3 1m.41248;TR111556_c0_g1_i2 1m.41247;TR102923_c0_g1_i1 1m.34506;TR111556_c0_g1_i1 1m.41246;TR102923_c0_g1_i2 1m.34507;TR158035_c0_g1_i1 1m.224485;TR168886_c0_g1_i1 1m.224404;TR173008_c0_g1_i1m.224970 | Hypersensitive-induced response protein 1 Hypersensitive-induced response protein 3 | 0.11 0.16 | 24.69 24.51 | 21.44 21.85 | -3.25 -2.66 | Defence signalling Defence signalling |
| TR128596_c0_g1_i1 1m.71132;TR124358_c0_g1_i1 1m.60955 | | | | | | |
| TR148907_c4_g3_i4 1m.204693;TR144971_c8_g3_i1 1m.162208;TR144971_c8_g3_i1 1m.162209;TR148907_c4_g3_i8 1m.204698;TR144971_c8_g3_i2 1m.162212;TR148907_c4_g3_i5 1m.204697;TR173550_c0_g1_i1 1m.225171;TR169960_c0_g1_i1 1m.224608 | Probable disease resistance protein At4g27220 MACPF domain-containing protein At4g26290 | 0.15 0.19 | 23.61 23.31 | 20.84 20.90 | -2.78 -2.41 | Defence response, receptor SA mediated cell death in defense |
| TR56096_c0_g1_i1 1m.27899;TR92876_c0_g1_i1 1m.26345 | mitogen-activated protein kinase 2-like | 0.19 | 23.37 | 20.94 | -2.43 | Signalling defence, stress |
| m.88243;TR133518_c9_g1_i6 1m.88248;TR133518_c9_g1_i4 1m.88245 | kinase 2-like | 0.15 | 23.79 | 21.01 | -2.78 | Signalling |
| TR127257_c5_g1_i2 1m.67594 | Phospholipase D alpha 1 | 0.12 | 24.09 | 21.04 | -3.05 | Signalling |
| TR30156_c0_g1_i1 1m.6874;TR13520_c0_g1_i1 1m.2995 | Phospholipase D delta | | | | | |

| | | | | | | |
|--|---|------------------------------|----------------------------------|----------------------------------|----------------------------------|--|
| TR62946_c0_g2_i1 m.14771;TR62946_c0_g1_i1 m.14766;TR78379_c0_g1_i1 m.20752;TR78379_c0_g1_i1 m.20754;TR126660_c0_g1_i3 m.65912;TR125453_c0_g1_i4 m.63322 | phototropin-1 | 0.17 | 24.13 | 21.55 | -2.59 | Light receptor, signalling |
| TR147733_c0_g2_i5 m.190572;TR147631_c1_g2_i1 m.189555;TR147733_c0_g2_i3 m.190568;TR147631_c1_g2_i5 m.189558;TR147733_c0_g2_i4 m.190571;TR147733_c0_g2_i2 m.190567;TR147631_c1_g2_i3 m.189557;TR147631_c1_g2_i2 m.189556;TR147733_c0_g2_i8 m.190576;TR147733_c0_g2_i6 m.190573;TR147733_c0_g2_i4 m.190570;TR147733_c0_g2_i3 m.190569;TR147733_c0_g2_i2 m.190566;TR147631_c1_g2_i5 m.189559;TR147733_c0_g2_i7 m.190574;TR54227_c0_g1_i3 m.11994;TR54227_c0_g1_i1 m.11993;TR48087_c0_g1_i3 m.10032;TR48087_c0_g1_i1 m.10031;TR188909_c0_g1_i1 m.22776;TR159349_c0_g1_i1 m.225948;TR144471_c0_g1_i2 m.157334;TR75948_c0_g1_i2 m.19794 | probable lrr receptor-like serine threonine-protein kinase atlg53420 14-3-3-like protein D 20 kDa chaperonin, chloroplastic SAL1 phosphatase | 0.06 0.14 0.13 0.19 | 26.25 25.63 24.63 24.32 | 22.22 22.80 21.72 21.96 | -4.03 -2.83 -2.91 -2.37 | Receptor, signalling Signalling, intracellular signalling or modulation Signalling ABA phosphatidylinositol signaling pathway, signalling ABA |
| TR184420_c0_g1_i1 m.21778;TR76516_c1_g1_i1 m.20010 | receptor-like protein kinase feronia | 0.17 | 23.67 | 21.10 | -2.57 | Receptor, signalling ABA, auxin and brassinosteroids, cell expansion |
| TR104747_c0_g1_i1 m.35691;TR102112_c0_g1_i3 m.33599 | Calcium sensing receptor, chloroplastic | 0.17 | 23.71 | 21.18 | -2.53 | Receptor, calcium sensor |
| TR140053_c0_g1_i4 m.122806;TR140053_c0_g1_i3 m.122804;TR140053_c0_g1_i2 m.122802;TR140053_c0_g1_i1 m.122800;TR20850_c0_g2_i1 m.4890;TR20850_c0_g2_i1 m.4889;TR93020_c0_g2_i1 m.26438;TR98427_c0_g1_i1 m.30537 | Diallylglycerol kinase 5 | 0.19 | 23.52 | 21.16 | -2.36 | Signalling, DAG to PA |
| TR161370_c0_g1_i1 m.13852;TR61494_c0_g2_i1 m.10662;TR61370_c0_g2_i1 m.13853;TR51494_c0_g1_i1 m.10661 | Protein TRANSPORT INHIBITOR RESPONSE 1 | 0.17 | 23.39 | 20.87 | -2.52 | Auxin receptor |
| TR115886_c0_g1_i2 m.46973;TR115886_c0_g1_i1 m.46972;TR114788_c1_g2_i1 m.45868 | Thylakoid lumenal 29 kDa protein, chloroplastic | 0.10 | 24.71 | 21.36 | -3.35 | Stress related, detoxification |
| TR122733_c0_g1_i1 m.57495;TR122270_c0_g1_i1 m.56594;TR145672_c1_g3_i3 m.168641;TR158869_c0_g1_i1 m.222809;TR166638_c0_g1_i1 m.224163;TR159595_c0_g1_i1 m.222995;TR146769_c0_g2_i9 m.179893;TR146769_c0_g2_i8 m.179892;TR145672_c1_g3_i4 m.168643;TR145672_c1_g3_i10 m.168650;TR145672_c1_g3_i11 m.168638 | kda class i heat shock protein | 0.12 | 24.95 | 21.88 | -3.06 | Stress related |
| TR193426_c0_g1_i1 m.118999;TR140513_c0_g1_i1 m.125945 | L-ascorbate peroxidase T, chloroplastic | 0.12 | 25.72 | 22.70 | -3.02 | Stress related, detoxification |
| TR181260_c0_g1_i1 m.226425;TR165764_c0_g1_i1 m.223909 | L-ascorbate peroxidase, cytosolic | 0.11 | 25.28 | 22.06 | -3.23 | Stress related, detoxification |
| TR131886_c5_g1_i2 m.81928;TR127427_c8_g1_i1 m.68158;TR95969_c1_g1_i2 m.28481 | Dehydrin ERD14 | 0.05 | 26.77 | 22.33 | -4.44 | Chaperone |
| TR127427_c8_g1_i2 m.68161 | Dehydrin ERD14 | 0.08 | 26.75 | 23.18 | -3.58 | Chaperone |
| TR148476_c1_g1_i2 m.199692;TR148476_c1_g1_i1 m.199690;TR147893_c0_g2_i1 m.192629;TR147893_c0_g2_i2 m.192631;TR149469_c2_g1_i1 m.211968;TR112619_c0_g1_i2 m.42785;TR147893_c0_g3_i1 m.192633;TR112619_c0_g1_i1 m.42784;TR7556_c0_g1_i1 m.1099;TR147893_c0_g1_i1 m.192628 | Chaperone protein ClpB1 | 0.10 | 25.12 | 21.77 | -3.35 | Chaperone |
| TR135445_c3_g2_i2 m.96634;TR108720_c0_g1_i1 m.39430;TR121834_c0_g1_i1 m.55834 | heat shock 70kDa protein | 0.18 | 23.70 | 21.24 | -2.46 | Chaperone, stress response |
| TR137084_c4_g2_i3 m.105091;TR134733_c6_g1_i2 m.93993;TR134733_c6_g1_i1 m.93938;TR134733_c6_g1_i4 m.93945;TR137084_c4_g2_i1 m.105087;TR134733_c6_g1_i3 m.93942 | protein suh2 homolog | 0.11 | 23.61 | 20.38 | -3.23 | Chaperone |
| TR67447_c0_g1_i2 m.16361;TR67447_c0_g1_i1 m.16360;TR24493_c0_g1_i1 m.5887 | Desiccation protectant protein Lea14 homolog | 0.10 | 24.90 | 21.52 | -3.38 | Response to desiccation, stress |
| TR128954_c0_g1_i1 m.72276;TR115737_c1_g1_i1 m.46713;TR128954_c0_g1_i3 m.72278;TR115737_c1_g1_i2 m.46714;TR128954_c0_g1_i3 m.72279;TR128954_c0_g1_i2 m.72277;TR115737_c1_g1_i2 m.46715 | protein dii-1 homolog b-like | 0.14 | 24.21 | 21.41 | -2.80 | Oxidative response |
| TR51638_c0_g1_i1 m.10799;TR51689_c0_g1_i1 m.10879;TR51689_c0_g1_i1 m.10878 | Temperature-induced lipocalin-1 | 0.13 | 25.53 | 22.56 | -2.97 | Protection against stress |

| | | | | | | |
|--|---|------|-------|-------|-------|--|
| TR58801_c0_g4_i1 m.12975;TR68801_c0_g3_i1 m.12974;TR58801_c0_g2_i1 m.12973;TR58801_c0_g1_i1 m.12972 | Temperature-induced lipocalin-1 | 0.21 | 23.30 | 21.05 | -2.25 | Protection against stress |
| TR58801_c0_g4_i1 m.12972 | Universal stress protein a-like protein | 0.13 | 24.72 | 21.73 | -2.99 | Resistance to DNA-damaging agents |
| TR94447_c1_g2_i1 m.27378;TR91216_c1_g1_i1 m.25327 | Universal stress protein PHO532 | 0.12 | 24.40 | 21.40 | -3.00 | Resistance to DNA-damaging agents |
| TR98458_c0_g2_i1 m.30550;TR111860_c0_g1_i1 m.41633;TR140832_c0_g1_i1 m.12825;TR121345_c0_g1_i1 m.54809 | Glutaredoxin-C3 | 0.17 | 23.11 | 20.59 | -2.52 | Cell redox homeostasis |
| TR588014_c1_g1_i1 m.27394;TR165226_c0_g1_i1 m.223611 | Protein disulfide isomerase-like 2-1 | 0.10 | 24.61 | 21.30 | -3.31 | Cell redox homeostasis |
| TR137905_c1_g1_i1 m.109538 | Monothiol glutaredoxin-S17 | 0.17 | 24.82 | 22.26 | -2.57 | Maturation of proteins involved in cell redox homeostasis |
| TR92629_c0_g1_i1 m.26236;TR96737_c0_g1_i1 m.29147 | Glutathione S-transferase DHA83, chloroplastic | 0.17 | 24.07 | 21.51 | -2.57 | Detoxification |
| TR145359_c2_g1_i4 m.165808;TR137316_c1_g1_i1 m.106204 | Glutathione S-transferase L1 | 0.17 | 25.80 | 23.26 | -2.53 | Detoxification |
| TR145359_c2_g1_i6 m.165810 | Glutathione S-transferase L3 | 0.12 | 25.54 | 22.52 | -3.02 | Detoxification |
| TR125117_c0_g1_i1 m.62590;TR124089_c0_g1_i1 m.60233 | 2-methyl-6-phytyl-1,4-hydroquinone methyltransferase, chloroplastic | 0.18 | 25.09 | 22.62 | -2.47 | CoA biosynthesis, cofactor biosynthesis, primary metabolism |
| TR92628_c1_g1_i1 m.26234;TR137670_c2_g1_i5 m.108177 | Pantothenate kinase 2 | 0.11 | 24.53 | 21.37 | -3.15 | Cofactor biosynthesis, pyridoxal or thiamine |
| TR139445_c1_g2_i3 m.19110;TR137502_c0_g2_i3 m.107342;TR137502_c0_g2_i1 m.107340 | Pyridoxal kinase | 0.09 | 25.50 | 21.96 | -3.54 | Cofactor biosynthesis, pyridoxal or thiamine |
| TR94801_c0_g2_i3 m.27719;TR90888_c1_g2_i2 m.25095;TR90888_c1_g2_i3 m.25098;TR94801_c0_g2_i4 m.27722;TR90888_c1_g2_i1 m.25093;TR94801_c0_g2_i2 m.27717;TR94801_c0_g2_i1 m.27714;TR94801_c0_g2_i1 m.27715;TR90888_c1_g2_i3 m.25099;TR94801_c0_g4_i1 m.27725;TR90888_c1_g1_i1 m.25092 | molybdopterin biosynthesis protein cnx1 | 0.23 | 23.34 | 21.19 | -2.15 | Molybdenum cofactor biosynthesis |
| TR124604_c5_g1_i1 m.61555;TR112326_c2_g1_i1 m.42385;TR27791_c0_g1_i1 m.6461;TR124604_c0_g1_i1 m.61554 | thiamine thiazole chloroplastic | 0.09 | 27.06 | 23.60 | -3.46 | Vitamin B1 (thiamine) precursor biosynthesis, used to make coenzyme to transfer aldehyde groups. |
| TR143622_c0_g2_i2 m.149748;TR143247_c0_g1_i1 m.146805 | Bifunctional aspartokinase/homoserine dehydrogenase, chloroplastic (Fragment) | 0.18 | 24.56 | 22.12 | -2.44 | L-homoserine, L-methionine and L-threonine biosynthesis, aa biosynthesis, primary metabolism |
| TR159270_c0_g1_i1 m.222928;TR165212_c0_g1_i1 m.223600 | 5-methyltetrahydropteroylglutamate-homocysteine methyltransferase | 0.13 | 24.73 | 21.81 | -2.92 | L-methionine biosynthesis, Amino-acid biosynthesis, primary metabolism. |
| TR15880_c0_g1_i2 m.46983;TR51762_c0_g1_i1 m.10662;TR15890_c0_g1_i1 m.46982;TR45512_c0_g2_i1 m.9625;TR11477_c0_g1_i1 m.2415;TR11477_c0_g2_i1 m.2416 | 2-isopropylmalate synthase 1 | 0.23 | 23.01 | 20.91 | -2.10 | L-leucine biosynthesis, aa biosynthesis, primary metabolism. |
| TR145088_c8_g1_i1 m.163222;TR134901_c0_g1_i1 m.94630 | Probable 3-hydroxyisobutyrate dehydrogenase-like 1, mitochondrial | 0.24 | 23.58 | 21.51 | -2.08 | L-valine degradation, aa metabolism, primary metabolism |
| TR142256_c5_g1_i2 m.138661;TR133853_c3_g1_i1 m.89902 | probable 3-hydroxyisobutyrate mitochondrial isoform x1 | 0.24 | 29.11 | 27.07 | -2.04 | L-valine degradation, primary metabolism |
| TR143823_c0_g1_i1 m.151592;TR143436_c0_g3_i2 m.148309;TR143823_c0_g1_i2 m.151594;TR143436_c0_g3_i1 m.148308;TR143823_c0_g1_i2 m.151593;TR143436_c0_g3_i1 m.148307 | Probable N-acetyl-gamma-glutamyl-phosphate reductase, chloroplastic | 0.11 | 25.07 | 21.91 | -3.15 | L-arginine biosynthesis, aa biosynthesis, primary metabolism |
| TR158204_c0_g1_i1 m.222567;TR157840_c0_g1_i1 m.222326 | Acetylornithine aminotransferase, mitochondrial | 0.18 | 23.86 | 21.41 | -2.45 | L-arginine biosynthesis, aa biosynthesis, primary metabolism |
| TR120538_c6_g1_i2 m.53041;TR119633_c4_g1_i2 m.51665 | Stem-specific protein TS171 | 0.04 | 26.41 | 21.87 | -4.54 | L-asparagine biosynthesis, aa biosynthesis, primary metabolism |
| TR124550_c0_g1_i1 m.61441;TR1122451_c0_g1_i2 m.57036 | d-3-phosphoglycerate dehydrogenase chloroplastic-like | 0.12 | 24.66 | 21.62 | -3.04 | Serine biosynthesis, aa biosynthesis, primary metabolism |
| TR143101_c0_g1_i5 m.145481 | Gamma aminobutyrate transaminase 3, chloroplastic | 0.09 | 25.04 | 21.61 | -3.43 | transamination to degrade GABA, primary metabolism |

| | | | | | | |
|---|---|------|-------|-------|-------|---|
| TR142699_c9_g1_i1 1m.142300 | Adenosylhomocysteinease | 0.18 | 24.49 | 22.01 | -2.48 | AA degradation, primary metabolism, one carbon metabolism |
| TR142039_c6_g1_i1 1m.136978 | Glutamine synthetase cytosolic isozyme | 0.18 | 24.42 | 21.91 | -2.51 | Glutamine biosynthesis, aa synthesis. |
| TR121640_c0_g1_i1 1m.55453 | Glutamine synthetase, chloroplastic | 0.06 | 27.10 | 23.07 | -4.03 | Photorespiration, aa synthesis |
| TR132176_c1_g1_i2 1m.83200 | Alanine-glyoxylate aminotransferase 2 homolog 1, mitochondrial | 0.13 | 24.39 | 21.46 | -2.92 | Photorespiration, pyruvate formation and aa degradation |
| TR132792_c1_g1_i3 1m.85666 | Alanine-glyoxylate aminotransferase 2 homolog 1, mitochondrial | 0.09 | 24.07 | 20.66 | -3.40 | Photorespiration, pyruvate formation and aa degradation |
| TR144202_c0_g1_i3 1m.154540 | Serine hydroxymethyltransferase, mitochondrial | 0.16 | 26.93 | 24.32 | -2.61 | One C metabolism, tetrahydrofolate interconversion |
| TR176749_c0_g1_i1 1m.225776 | Serine hydroxymethyltransferase, mitochondrial | 0.07 | 25.30 | 21.46 | -3.83 | One C metabolism, tetrahydrofolate interconversion |
| TR146716_c2_g1_i9 1m.179287;TR146716_c2_g1_i8 1m.179286 | Serine hydroxymethyltransferase, mitochondrial | 0.14 | 24.31 | 21.47 | -2.84 | One C metabolism, tetrahydrofolate interconversion |
| TR41833_c0_g1_i1 1m.8942;TR89600_c1_g1_i2 1m.24134 | Serine hydroxymethyltransferase, mitochondrial | 0.11 | 26.34 | 23.17 | -3.17 | One C metabolism, tetrahydrofolate interconversion |
| TR96886_c0_g1_i1 1m.29291;TR89676_c0_g1_i1 1m.24256 | Serine hydroxymethyltransferase, mitochondrial | 0.16 | 25.32 | 22.64 | -2.68 | One C metabolism, tetrahydrofolate interconversion |
| TR81212_c0_g1_i1 1m.21706 | Serine hydroxymethyltransferase, mitochondrial | 0.16 | 23.57 | 20.92 | -2.65 | One C metabolism, tetrahydrofolate interconversion |
| TR126637_c0_g1_i4 1m.65876;TR126637_c0_g1_i3 1m.65874;TR122091_c0_g1_i2 1m.56371;TR122091_c0_g1_i1 1m.56369;TR126637_c0_g1_i2 1m.65872;TR126637_c0_g1_i2 1m.65871;TR94794_c0_g1_i1 1m.27709;TR86353_c0_g1_i1 1m.23158 | Phosphoribosylamine-glycine ligase, chloroplastic | 0.14 | 23.80 | 20.94 | -2.86 | Purine Inosine biosynthesis, nucleotide biosynthesis, primary metabolism |
| TR132840_c0_g1_i5 1m.85833;TR132544_c0_g1_i3 1m.95886;TR132840_c0_g1_i1 1m.85829;TR132840_c0_g1_i2 1m.85830;TR135244_c0_g1_i4 1m.95887;TR132840_c0_g1_i4 1m.85832 | UMP-CMP kinase 4 | 0.19 | 23.06 | 20.64 | -2.42 | nucleotide biosynthetic process, primary metabolism |
| TR127421_c3_g1_i3 1m.68134;TR127421_c3_g1_i2 1m.68133;TR103114_c3_g1_i5 1m.34684;TR103114_c3_g1_i3 1m.34682 | Inosine triphosphate pyrophosphatase | 0.09 | 25.18 | 21.78 | -3.40 | nucleotide biosynthetic process, primary metabolism |
| TR100111_c0_g1_i1 1m.32376;TR111665_c0_g1_i1 1m.41401;TR111665_c0_g1_i2 1m.41402;TR100111_c0_g1_i2 1m.32377 | 11-beta-hydroxysteroid dehydrogenase-like 2 | 0.15 | 24.03 | 21.28 | -2.76 | nucleotide catabolic process, primary metabolism |
| TR138727_c2_g1_i1 1m.114619;TR139999_c1_g1_i1 1m.122450;TR138727_c1_g1_i2 1m.114620 | 24-methylenesterol C-methyltransferase 2 | 0.18 | 24.42 | 21.94 | -2.48 | Steroid biosynthesis, Steroid biosynthesis, negative regulation endoreduplication |
| TR87863_c1_g1_i2 1m.23585;TR72183_c1_g1_i2 1m.18383 | Cytochrome b5 or Cytochrome b5, seed isoform | 0.23 | 23.21 | 21.06 | -2.15 | redox of lipids, primary metabolism |
| TR3668_c0_g2_i1 1m.6207;TR16971_c0_g2_i1 1m.4190;TR3668_c0_g1_i1 1m.617;TR16971_c0_g1_i1 1m.4187;TR3668_c0_g1_i1 1m.619;TR16971_c0_g1_i1 1m.4189 | Long chain acyl-CoA synthetase 9, desaturase, chloroplastic peroxisomal | 0.20 | 23.77 | 21.47 | -2.30 | Insertion of double bond in fatty acids. Lipid metabolism, primary metabolism |
| TR145280_c5_g1_i1 1m.165057;TR131312_c0_g1_i1 1m.80196 | ATP-citrate synthase alpha chain protein 1 | 0.19 | 24.07 | 21.71 | -2.36 | Fatty acid metabolism, Lipid metabolism. |
| TR136097_c2_g1_i1 1m.100025 | ATP-citrate synthase alpha chain protein 1 | 0.17 | 24.19 | 21.66 | -2.52 | Fatty acid elongation or isoprenoid biosynthesis |
| TR135601_c1_g1_i3 1m.97456 | ATP-citrate synthase alpha chain protein 1 | 0.23 | 23.03 | 20.89 | -2.15 | Fatty acid elongation or isoprenoid biosynthesis |
| TR146905_c1_g1_i1 1m.181342 | ATP-citrate synthase beta chain protein 1 | 0.15 | 24.22 | 21.49 | -2.73 | Fatty acid elongation or isoprenoid biosynthesis |
| TR137503_c0_g1_i1 1m.107343;TR136301_c1_g1_i1 1m.101003;TR12199_c0_g1_i1 1m.2571;TR175943_c0_g1_i1 1m.225672;TR12199_c0_g2_i1 1m.2572 | pi-plc-x-box domain-containing protein ddb_g0293730-like | 0.08 | 25.18 | 21.53 | -3.65 | Lipid metabolism |

| | | | | | | |
|---|---|------|-------|-------|-------|--|
| TR129711_c1_g1_11[m.74832;TR129058_c0_g2_12][m.7673;TR129058_c0_g2_12][m.7674;TR129711_c1_g1_12][m.74833;TR182132_c0_g1_11][m.226674;TR189617_c0_g1_11][m.227919 | 3-oxoacyl-[acyl-carrier-protein] reductase 3, chloroplastic | 0.16 | 25.06 | 22.42 | -2.64 | Fatty acid biosynthesis. Lipid metabolism |
| TR183846_c0_g1_16[m.112243;TR141656_c9_g1_9][m.134281;TR141656_c9_g1_17][m.134278 | Acetyl-CoA acetyltransferase, cytosolic | 0.14 | 27.17 | 24.37 | -2.80 | fatty acid beta-oxidation |
| TR141656_c9_g1_12[m.134259;TR141656_c9_g1_10][m.134282 | Acetyl-CoA acetyltransferase, cytosolic | 0.11 | 23.83 | 20.62 | -3.20 | fatty acid beta-oxidation |
| TR148475_c2_g2_12[m.199680;TR147808_c0_g1_11][m.191473;TR148475_c2_g2_13][m.195882;TR147808_c0_g1_12][m.191475;TR147808_c0_g1_14][m.191479;TR147808_c0_g1_13][m.191477 | Acetyl-coenzyme A carboxylase carboxyl transferase subunit alpha, chloroplastic | 0.13 | 24.87 | 21.97 | -2.90 | Biosynthesis of Malonyl-CoA from Acetyl Co-a, lipid metabolism, primary metabolism |
| TR131110_c1_g2_11[m.79476;TR1311551_c0_g1_12][m.80970;TR1311551_c0_g1_12][m.80971 | Acy-CoA--sterol O-acyltransferase 1 | 0.10 | 23.70 | 20.35 | -3.36 | Steroid metabolism |
| TR133505_c0_g1_11[m.95050;TR133879_c0_g1_11][m.90041;TR133879_c0_g1_12][m.90043 | bahd acyltransferase dcr-like | 0.09 | 24.38 | 20.94 | -3.45 | Cutin biosynthetic process |
| TR116682_c0_g1_11[m.48023;TR113852_c0_g1_11][m.44308 | gdsI esterase lipase at2g04570-like | 0.24 | 23.31 | 21.25 | -2.06 | Lipid metabolism |
| TR145807_c1_g1_12[m.169982;TR143550_c1_g1_11][m.149123;TR145807_c1_g1_13][m.169983;TR145807_c1_g1_11][m.169981 | Probable aspartyl aminopeptidase | 0.14 | 25.76 | 22.90 | -2.87 | Proteolysis |
| TR139484_c1_g1_11[m.119393;TR140190_c0_g1_11][m.123741;TR139484_c1_g1_12][m.119397;TR118309_c0_g1_11][m.50111;TR120949_c0_g1_12][m.53880;TR140190_c1_g2_12][m.123743;TR140190_c1_g2_11][m.123742 | Probable aspartyl aminopeptidase 2 | 0.11 | 24.24 | 21.06 | -3.18 | Proteolysis |
| TR144183_c2_g1_11[m.154416;TR156719_c6_g1_11][m.102982 | Metacaspase-4 | 0.14 | 26.90 | 24.06 | -2.84 | Proteolysis |
| TR138971_c8_g1_11[m.116078;TR137978_c5_g1_11][m.110030 | leukotriene A-4 hydrolase homolog | 0.12 | 24.78 | 21.72 | -3.06 | Proteolysis |
| TR126546_c0_g1_11[m.65680;TR125150_c0_g1_11][m.62659;TR126546_c0_g1_12][m.65681 | aspartic proteinase-like | 0.09 | 25.19 | 21.68 | -3.50 | Proteolysis |
| TR118520_c0_g1_11[m.50494;TR118520_c0_g1_12][m.50495;TR116147_c0_g1_11][m.47303 | premnaspirodione oxygenase-like | 0.12 | 23.74 | 20.66 | -3.08 | Phytoalexin biosynthesis, secondary metabolism |
| TR144114_c0_g1_13[m.153761;TR144114_c0_g1_12][m.153760;TR143713_c4_g1_11][m.150533;TR143713_c4_g1_12][m.150634;TR144114_c0_g1_14][m.153762;TR144114_c0_g1_11][m.153759 | trans-resveratrol di-o-methyltransferase-like | 0.13 | 24.04 | 21.14 | -2.90 | Secondary metabolism |
| TR144445_c0_g1_12[m.157022;TR144405_c0_g1_17][m.156682;TR144445_c0_g1_13][m.157024;TR144445_c0_g1_11][m.157019;TR144405_c0_g1_12][m.156675;TR144405_c0_g1_13][m.156676;TR144445_c0_g1_14][m.157026;TR144405_c0_g1_15][m.156680_c0_g1_14][m.156678;TR144405_c0_g1_16][m.156681;TR144445_c0_g1_15][m.157027;TR144445_c0_g1_11][m.157020;TR144405_c0_g1_12][m.156674;TR88714_c0_g1_13][m.23857;TR56554_c0_g1_13][m.12428;TR88714_c0_g1_12][m.23856;TR56554_c0_g1_11][m.12427 | 2-C-methyl-D-erythritol 4-phosphate cytidylyltransferase, chloroplastic | 0.18 | 23.15 | 20.63 | -2.51 | |
| TR92139_c0_g1_11[m.25960;TR1441457_c2_g2_11][m.140258;TR137242_c0_g1_11][m.105902 | Phosphomevalonate kinase | 0.09 | 23.95 | 20.49 | -3.46 | precursor |
| TR149459_c0_g2_12[m.211845;TR149459_c0_g2_11][m.211841;TR152511_c0_g1_11][m.221793;TR151709_c0_g1_12][m.221645;TR192524_c0_g1_11][m.228241 | (-)-neomenthol dehydrogenase | 0.11 | 25.92 | 22.72 | -3.19 | Monoterpene biosynthesis. Secondary metabolism |
| TR140557_c3_g1_12[m.126285 | probable terpene synthase 6 | 0.18 | 23.56 | 21.07 | -2.49 | Secondary metabolism |
| TR151565_c0_g1_12[m.14090;TR40145_c0_g2_13][m.8712;TR151565_c0_g2_14][m.140908;TR151565_c0_g1_11][m.140888;TR40145_c0_g2_12][m.8710 | terpene synthase 10-like | 0.16 | 23.85 | 21.21 | -2.64 | Sesquiterpene biosynthesis, secondary metabolism |
| TR129361_c1_g2_11[m.73707;TR112680_c0_g1_11][m.42840;TR108951_c0_g1_11][m.39758;TR93018_c0_g1_11][m.26433 | dinamoyl- reductase 1 | 0.11 | 24.83 | 21.66 | -3.17 | Lignin biosynthesis, secondary metabolism |
| | Secoisolariciresinol dehydrogenase (Fragment) | 0.22 | 23.06 | 20.87 | -2.19 | Lignan biosynthesis, secondary metabolism |

| | | | | | | |
|--|---|------|-------|-------|-------|---|
| TR136142_c0_g1_i1 1m.100202;TR130321_c0_g1_i1 1m.76739 | secoisolaricresinol dehydrogenase-like | 0.10 | 24.27 | 21.01 | -3.26 | Lignan biosynthesis, secondary metabolism |
| TR187882_c0_g1_i1 1m.227296;TR151511_c0_g1_i1 1m.221598 | isoflavone reductase homolog | 0.10 | 24.75 | 21.36 | -3.40 | Secondary metabolism |
| TR133020_c0_g1_i1 1m.86405;TR132504_c0_g1_i3 1m.84718;TR133020_c0_g1_i2 1m.86406 | anthocyanidin 3-O-glucosyltransferase 2-like | 0.15 | 24.46 | 21.68 | -2.77 | Secondary metabolism |
| TR173703_c0_g1_i2 1m.18922;TR146323_c0_g1_i1 1m.175113;TR173703_c0_g1_i1 1m.18921;TR146323_c0_g1_i2 1m.175114 | Protein STRICTOSIDINE SYNTHASE-LIKE 4 | 0.19 | 23.37 | 21.00 | -2.37 | Alkaloid biosynthesis, defense response |
| TR139382_c0_g1_i1 1m.118694;TR139382_c0_g1_i2 1m.118697;TR138997_c0_g1_i1 1m.116254 | nitrile-specifier protein 5 | 0.15 | 24.19 | 21.50 | -2.70 | Other: Breakdown of glucosinolates (secondary metabolites), compounds made of N and S |
| TR194622_c1_g1_i1 1m.27601;TR169665_c0_g1_i1 1m.17092 | 2-methylene-furan-3-one reductase | 0.21 | 25.34 | 23.11 | -2.24 | Secondary metabolism biosynthesis |
| TR143208_c0_g1_i3 1m.146525;TR124391_c5_g1_i1 1m.61024;TR50437_c0_g1_i1 1m.10417;TR130665_c0_g1_i1 1m.6941;TR143208_c0_g1_i2 1m.68529;TR127536_c0_g1_i2 1m.68526;TR130065_c1_g1_i2 1m.75891 | probable xyloglucan endotransglucosylase hydrolase protein 5 | 0.21 | 23.50 | 21.22 | -2.28 | Cell wall transformation |
| TR162854_c0_g1_i1 1m.223308;TR150315_c0_g1_i1 1m.221018 | Pectinesterase/pectinesterase inhibitor U1 | 0.08 | 25.20 | 21.62 | -3.58 | Cell wall transformation |
| TR132745_c0_g1_i1 1m.85548;TR132326_c1_g1_i1 1m.8894 | Endo-1,3,4-beta-D-glucanase | 0.14 | 23.41 | 20.57 | -2.84 | Cell wall transformation |
| TR130065_c0_g1_i1 1m.75890;TR127536_c0_g1_i3 1m.68528;TR127536_c0_g1_i1 1m.68525;TR130065_c0_g1_i3 1m.75893;TR127536_c0_g1_i4 1m.68529;TR127536_c0_g1_i2 1m.68526;TR130065_c1_g1_i2 1m.75891 | Mannose-1-phosphate guanylyltransferase 1 | 0.08 | 25.38 | 21.67 | -3.70 | Synthesis of GDP-mannose used in cell wall biosynthesis. Part of the ascorbate biosynthesis, cofactor transferring electrons. |
| TR132041_c0_g1_i1 1m.82679;TR128629_c1_g1_i1 1m.71269 | Glucan endo-1,3-beta-glucosidase 7 | 0.17 | 24.85 | 22.29 | -2.57 | Carbohydrate metabolic process and cell wall organization |
| TR144191_c3_g1_i4 1m.154476;TR144191_c3_g1_i2 1m.154474 | UTP-glucose-1-phosphate uridylyltransferase | 0.14 | 24.40 | 21.58 | -2.82 | Synthesis of sucrose, starch and cell wall, and callose deposition. |
| TR138943_c0_g1_i2 1m.115866;TR139242_c0_g1_i1 1m.117752;TR138943_c0_g1_i1 1m.115855 | Serine/threonine-protein kinase STY46 | 0.19 | 23.87 | 21.46 | -2.41 | Role in chloroplast biogenesis. Phosphorylates chloroplast precursor proteins in the cytosol |
| TR135355_c0_g1_i1 1m.96269;TR135348_c0_g1_i1 1m.96245 | Protein plastid transcriptionally active 16, chloroplastic | 0.09 | 25.87 | 22.40 | -3.47 | Plastid gene expression |
| TR158266_c0_g1_i1 1m.222597;TR174472_c0_g1_i1 1m.225414 | 28 kDa ribonucleoprotein, chloroplastic | 0.19 | 23.83 | 21.41 | -2.42 | RNA processing in chloroplast |
| TR141098_c0_g1_i2 1m.130198;TR136870_c1_g1_i1 1m.103806;TR141098_c0_g1_i3 1m.130200;TR141098_c0_g1_i4 1m.130202;TR141098_c0_g1_i1 1m.130196;TR136870_c1_g1_i3 1m.103810;TR136870_c1_g1_i2 1m.103808;TR135700_c3_g2_i1 1m.97953 | Cell division protein FtsZ homolog 2-1, chloroplastic | 0.20 | 23.47 | 21.16 | -2.31 | Chloroplast division |
| TR143435_c0_g2_i6 1m.148306;TR143435_c0_g2_i5 1m.148304;TR143435_c0_g2_i4 1m.148302;TR143228_c0_g2_i3 1m.139238;TR143435_c0_g2_i3 1m.148301;TR143435_c0_g2_i2 1m.148298;TR143228_c0_g1_i2 1m.139234;TR143435_c0_g2_i1 1m.148297 | ATP-dependent Clp protease proteolytic subunit 3, chloroplastic | 0.15 | 23.96 | 21.24 | -2.72 | Other: Degradation of misfolded proteins. Chloroplast functioning maintenance |
| TR132148_c0_g1_i1 1m.83098;TR132067_c1_g1_i1 1m.82744 | Plastid-lipid-associated protein, chloroplastic | 0.11 | 26.15 | 22.91 | -3.24 | Thylakoids protection |
| TR115069_c0_g1_i3 1m.45959;TR115069_c1_g1_i2 1m.45958;TR114526_c0_g1_i2 1m.45278 | Probable membrane-associated 30kDa protein, chloroplastic | 0.23 | 22.88 | 20.73 | -2.15 | Thylakoid membrane organization, vesicle organization. |
| TR132148_c0_g1_i1 1m.83098;TR132067_c1_g1_i1 1m.82744 | Protein CURVATURE THYLAKOID 1A, chloroplastic | 0.11 | 24.42 | 21.19 | -3.23 | Thylakoid structure, chloroplast |
| TR63107_c0_g1_i1 1m.14891;TR161663_c1_g1_i1 1m.14141 | | | | | | |
| TR130681_c0_g1_i4 1m.77920;TR130563_c0_g1_i4 1m.77539;TR130563_c0_g1_i3 1m.77537;TR130563_c0_g1_i5 1m.77541;TR130563_c0_g1_i7 1m.77546;TR130563_c0_g1_i1 1m.77535;TR130681_c0_g1_i2 1m.77918;TR130563_c0_g1_i8 1m.77545;TR130563_c0_g1_i2 1m.77536;TR130563_c0_g1_i9 1m.77546;TR130681_c0_g1_i3 1m.77919;TR130681_c0_g1_i1 1m.77917;TR130563_c0_g1_i6 1m.77542 | PGR5-like protein 1A, chloroplastic | 0.17 | 23.85 | 21.30 | -2.56 | Related photosystem I |
| TR146214_c8_g2_i6 1m.174083;TR146214_c8_g2_i7 1m.174092;TR141441_c1_g2_i3 1m.132657;TR146214_c8_g2_i9 1m.174095;TR146214_c8_g2_i10 1m.174089;TR141441_c1_g2_i2 1m.132655;TR146214_c8_g2_i8 1m.174086 | photosystem I p700 apoprotein a2 | 0.10 | 25.38 | 22.05 | -3.32 | photosystem I, photosynthesis |
| TR140881_c1_g1_i1 1m.128588;TR13950_c0_g1_i1 1m.3247;TR13950_c0_g2_i1 1m.3249 | Photosystem I subunit O | 0.10 | 24.84 | 21.47 | -3.37 | photosystem I, photosynthesis |

| | | | | | | |
|--|--|------|-------|-------|-------|---|
| TR188059_c2_g1.i1 1m.227429;TR158193_c5_g1.i1 1m.225563;TR30870_c0_g2.i1 1m.6963;TR30870_c0_g1.i1 1m.6962;TR16577_c0_g2.i1 1m.3948;TR16577_c0_g1.i1 1m.3947 | Photosystem II 10 kDa polypeptide, chloroplastic | 0.04 | 26.88 | 22.29 | -4.59 | Photosystem II, photosynthesis |
| TR148263_c6_g1.i4 1m.196975;TR148263_c6_g1.i1 1m.196971;TR148263_c6_g1_i6 1m.196977;TR148263_c6_g1_i3 1m.196973;TR146683_c3_g1.i1 1m.178876;TR146683_c3_g1_i2 1m.178878;TR146683_c3_g1_i1 1m.178874 | Peroxisredoxin Q, chloroplastic | 0.15 | 24.69 | 22.00 | -2.69 | Detoxification of hydrogen peroxide in photosystem II, Cell redox homeostasis |
| TR124428_c0_g1.i1 1m.61116;TR124649_c0_g1.i1 1m.61630 | ap synthase cf1 alpha subunit | 0.16 | 24.80 | 22.19 | -2.61 | Photosystem |
| TR142076_c1_g1.i1 1m.137211;TR141654_c4_g1.i1 1m.134245 | ATP synthase delta chain, chloroplastic | 0.16 | 24.72 | 22.04 | -2.68 | Photosystem |
| TR138556_c0_g1.i2 1m.13346;TR141335_c0_g2.i1 1m.131983;TR141335_c0_g1.i1 1m.131982 | ATP-dependent zinc metalloprotease FtsH, chloroplastic | 0.17 | 25.56 | 22.98 | -2.58 | Photosystem |
| TR147486_c0_g2.i4 1m.187967;TR147486_c0_g2.i3 1m.187966;TR147486_c0_g2.i2 1m.187964;TR147486_c0_g2.i1 1m.187963;TR135641_c1_g1_i8 1m.97626;TR135641_c1_g1_i5 1m.97625;TR135641_c1_g1_i4 1m.97621;TR135641_c1_g1_i3 1m.97620;TR135641_c1_g1.i1 1m.97618 | Protease Do-like 1, chloroplastic | 0.12 | 24.50 | 21.41 | -3.09 | photosystem II repair |
| TR8885_c0_g1.i1 1m.1716;TR132999_c0_g1.i1 1m.7288;TR8885_c0_g2.i1 1m.1717;TR32999_c0_g2.i1 1m.7289 | upf0603 protein chloroplastic | 0.17 | 24.77 | 22.21 | -2.56 | Photosystem repair |
| TR120095_c0_g1.i1 1m.52139;TR118283_c0_g1.i1 1m.50082;TR120095_c0_g1_i2 1m.52140;TR118283_c0_g1_i2 1m.50083 | Oxygen-evolving enhancer protein 3, chloroplastic | 0.07 | 27.69 | 23.87 | -3.81 | Photosystem assembly |
| TR78931_c0_g1_i1 1m.20998;TR65988_c0_g1_i1 1m.15772 | Protein LOW PSII ACCUMULATION 1, chloroplastic | 0.19 | 24.19 | 21.82 | -2.37 | Photosystem assembly |
| TR75003_c0_g2.i1 1m.19459;TR75003_c0_g2.i1 1m.19458;TR82051_c0_g2.i1 1m.21979;TR82051_c0_g1_i1 1m.21978;REV_TR97820_c2_g1_i3 1m.30023;REV_TR86900_c1_g1_i1 1m.23329;REV_TR97820_c2_g1_i1 1m.30019;REV_TR97820_c2_g1_i2 1m.30021 | Oxygen-evolving enhancer protein 3, chloroplastic | 0.10 | 24.48 | 21.12 | -3.35 | Photosystem assembly |
| TR147969_c12_g1_i9 1m.193481 | oxygen-evolving enhancer protein 3, chloroplastic-like | 0.06 | 25.57 | 21.46 | -4.11 | Regulation of photosystem |
| TR143446_c18_g1_i15 1m.148396;TR147969_c12_g1_i6 1m.193477;TR147969_c12_g1_i2 1m.193472 | chlorophyll a-b-binding protein cab-partial | 0.07 | 24.99 | 21.20 | -3.79 | photosynthesis, light harvesting in photosystem I |
| TR173445_c0_g1.i1 1m.225140 | chlorophyll a-b-binding protein cab-partial | 0.07 | 25.53 | 21.76 | -3.77 | photosynthesis, light harvesting in photosystem I |
| TR173445_c0_g1_i1 1m.225140 | chlorophyll a-b-binding protein | 0.08 | 28.47 | 24.78 | -3.69 | photosynthesis, light harvesting in photosystem I |
| TR173790_c0_g1.i1 1m.225229;TR187938_c0_g1.i1 1m.227342 | chlorophyll a-b-binding protein | 0.19 | 23.92 | 21.55 | -2.37 | photosynthesis, light harvesting in photosystem I |
| TR173790_c0_g1_i1 1m.225229;TR187938_c0_g1.i1 1m.227342 | chlorophyll a-b-binding protein | 0.21 | 23.98 | 21.70 | -2.28 | photosynthesis, light harvesting in photosystem I |
| TR173790_c0_g1_i1 1m.225229;TR187938_c0_g1.i1 1m.227342 | chlorophyll a-b-binding protein | 0.16 | 26.26 | 23.99 | -2.67 | photosynthesis, light harvesting in photosystem I |
| TR173790_c0_g1_i1 1m.225229;TR187938_c0_g1.i1 1m.227342 | chlorophyll a-b-binding protein | 0.12 | 24.85 | 21.79 | -3.06 | photosynthesis, light harvesting in photosystem I |
| TR173790_c0_g1_i1 1m.225229;TR187938_c0_g1.i1 1m.227342 | chlorophyll a-b-binding protein | 0.08 | 28.92 | 25.20 | -3.73 | photosynthesis, light harvesting in photosystem I |
| TR173790_c0_g1_i1 1m.225229;TR187938_c0_g1.i1 1m.227342 | chlorophyll a-b-binding protein | 0.08 | 25.10 | 21.45 | -3.65 | photosynthesis, light harvesting in photosystem I |
| TR173790_c0_g1_i1 1m.225229;TR187938_c0_g1.i1 1m.227342 | chlorophyll a-b-binding protein of lhci type 1-like | 0.09 | 25.08 | 21.68 | -3.40 | photosynthesis, light harvesting in photosystem I |
| TR173790_c0_g1_i1 1m.225229;TR187938_c0_g1.i1 1m.227342 | Protochlorophyllide reductase A, chloroplastic | 0.10 | 24.63 | 21.26 | -3.38 | Chlorophyll biosynthesis, photosynthesis |
| TR173790_c0_g1_i1 1m.225229;TR187938_c0_g1.i1 1m.227342 | Ferredoxin-1, chloroplastic | 0.14 | 23.49 | 20.69 | -2.80 | Electron transport chain, photosynthesis |

| | | | | | | |
|---|--|------|-------|-------|-------|--|
| TR57207_c0_g1_i1 m.12554;TR15520_c0_g1_i1 m.3547;TR22346_c0_g1_i1 m.5307 | Rhodanese-like domain-containing protein 4, chloroplastic | 0.19 | 23.13 | 20.71 | -2.42 | Sustain efficient linear electron flow in thylakoids |
| TR142036_c3_g3_i1 m.136878 | Rhodanese-like domain-containing protein 4, chloroplastic | 0.20 | 23.60 | 21.28 | -2.32 | Sustain efficient linear electron flow in thylakoids |
| TR189365_c0_g1_i1 m.227860;TR174300_c0_g1_i1 m.225375 | Putative quinone-oxidoreductase homolog, chloroplastic | 0.11 | 27.25 | 24.06 | -3.18 | Oxidation-reduction homeostasis |
| TR131085_c1_g1_i1 m.79399;TR130102_c0_g1_i1 m.75998 | Fructose-1,6-bisphosphatase, chloroplastic | 0.16 | 23.69 | 21.05 | -2.65 | Calvin cycle, photosynthesis, carbohydrates biosynthesis |
| TR120756_c0_g1_i1 m.53491;TR133392_c0_g1_i1 m.147324;TR141248_c0_g1_i6 m.131341;TR141248_c0_g1_i5 m.131335;TR141248_c0_g1_i4 m.131336;TR141248_c0_g1_i3 m.131333;TR141248_c0_g1_i2 m.131331;TR141248_c0_g1_i1 m.131328 | Ribulose biphosphate carboxylase oxygenase activase chloroplast | 0.14 | 25.01 | 22.17 | -2.85 | Calvin cycle, photosynthesis, carbohydrates biosynthesis |
| TR112564_c0_g1_i1 m.43118;TR121656_c0_g2_i1 m.55476;TR121656_c0_g1_i1 m.55475;TR146298_c3_g2_i1 m.174844;TR146298_c3_g2_i9 m.174841;TR147270_c2_g1_i2 m.185478;TR147270_c2_g1_i1 m.185476 | Ribulose biphosphate carboxylase small chloroplastic-like | 0.10 | 24.40 | 21.07 | -3.33 | Calvin cycle, photosynthesis, carbohydrates biosynthesis |
| TR95526_c1_g2_i2 m.28217;TR90899_c4_g1_i2 m.25138 | Ribulose biphosphate carboxylase/oxygenase activase, chloroplastic | 0.06 | 24.71 | 20.60 | -4.11 | Calvin cycle, photosynthesis, carbohydrates biosynthesis |
| TR146298_c3_g2_i14 m.174851;TR147270_c2_g3_i5 m.185485 | Gamma carbonic anhydrase 1, mitochondrial | 0.19 | 24.60 | 22.20 | -2.41 | Cellular respiration |
| TR118322_c0_g1_i2 m.50143;TR135824_c2_g1_i3 m.58606;TR130482_c0_g1_i1 m.77279;TR130482_c0_g1_i3 m.77281;TR135824_c3_g1_i4 m.98609;TR130482_c0_g1_i2 m.77280 | | 0.19 | 24.60 | 22.20 | -2.41 | |
| TR172839_c0_g1_i1 m.224860;TR131842_c4_g2_i1 m.81943;TR131842_c4_g1_i1 m.81946;TR147863_c0_g1_i8 m.192325;TR147863_c0_g1_i7 m.192321;TR147863_c0_g1_i6 m.192320;TR147863_c0_g1_i4 m.192316;TR147863_c0_g1_i3 m.192312;TR147863_c0_g1_i2 m.192311;TR147863_c0_g1_i1 m.192309;TR147863_c0_g1_i2 m.190046;TR147863_c0_g1_i1 m.190043;TR6210_c0_g1_i1 m.888;TR26217_c0_g1_i1 m.6112;TR136715_c0_g1_i1 m.102954;TR134257_c0_g1_i1 m.91763 | letm1 and ef-hand domain-containing protein mitochondrial | 0.22 | 23.12 | 20.94 | -2.19 | Respiration, respiratory chain |
| TR147863_c0_g1_i4 m.192315;TR147683_c0_g1_i2 m.190045;TR147863_c0_g1_i8 m.192324;TR147863_c0_g1_i3 m.192313;TR147863_c0_g1_i4 m.190050;TR147863_c0_g1_i1 m.192308;TR147683_c0_g1_i1 m.190042;TR147863_c0_g1_i7 m.192322 | letm1 and ef-hand domain-containing protein mitochondrial | 0.20 | 23.57 | 21.22 | -2.34 | Respiration, respiratory chain |
| TR147683_c0_g1_i7 m.190055;TR147683_c0_g1_i6 m.190053;TR147683_c0_g1_i5 m.190052;TR147683_c0_g1_i3 m.190048 | | 0.20 | 23.57 | 21.22 | -2.34 | |
| TR148430_c3_g1_i6 m.199126;TR148430_c3_g1_i2 m.199112;TR148408_c6_g3_i9 m.198750;TR148430_c3_g1_i9 m.199131;TR148430_c3_g1_i10 m.199135;TR148440_c6_g3_i7 m.198745;TR148408_c6_g3_i6 m.198744;TR148430_c3_g1_i3 m.199111;TR148408_c6_g3_i11 m.198756;TR148408_c6_g3_i11 m.198738;TR148430_c3_g1_i5 m.199123;TR148430_c3_g1_i4 m.199119;TR148408_c6_g3_i11 m.198755;TR148408_c6_g3_i10 m.198753;TR148430_c3_g1_i9 m.199132;TR148430_c3_g1_i10 m.199136;TR148408_c6_g3_i7 m.198746;TR148408_c6_g3_i11 m.198739;TR148430_c3_g1_i11 m.199109;TR148408_c6_g3_i4 m.198742;TR148408_c6_g3_i3 m.198741;TR148430_c3_g1_i11 m.199110;TR148408_c6_g3_i10 m.198754;TR148430_c3_g1_i4 m.199121 | phosphoenolpyruvate carboxykinase | 0.19 | 28.07 | 25.70 | -2.37 | Gluconeogenesis |
| TR131639_c6_g2_i2 m.81263 | phosphoenolpyruvate carboxylase 4 | 0.16 | 25.13 | 22.52 | -2.61 | source for the TCA, respiration |
| TR135788_c2_g1_i3 m.98436;TR135788_c2_g1_i6 m.98442 | phosphoenolpyruvate carboxylase 4 | 0.14 | 26.67 | 23.79 | -2.89 | source for the TCA, respiration |
| TR131639_c6_g2_i3 m.81269 | Phosphoenolpyruvate carboxylase 4 | 0.20 | 22.93 | 20.63 | -2.30 | source for the TCA, respiration |
| TR174380_c0_g1_i1 m.225390;TR180459_c0_g1_i1 m.226060 | Phosphoenolpyruvate carboxylase 1 | 0.18 | 24.24 | 21.79 | -2.44 | source for the TCA, respiration |
| TR131631_c1_g1_i2 m.81219;TR131631_c1_g1_i1 m.81218;TR113345_c0_g1_i2 m.43615;TR113345_c0_g1_i1 m.43614 | xylose kinase | 0.18 | 24.58 | 22.15 | -2.44 | carbohydrate metabolic process |
| TR145287_c0_g1_i1 m.165148;TR145221_c3_g1_i2 m.164575;TR145287_c0_g1_i2 m.165149;TR145287_c0_g1_i3 m.165150 | citrate glyoxysomal | 0.15 | 24.64 | 21.93 | -2.71 | Glyoxylate cycle, carbohydrate metabolism |
| TR141187_c0_g1_i2 m.130725;TR141187_c0_g1_i1 m.130721;TR141187_c0_g1_i3 m.130729;TR142549_c0_g1_i1 m.141032 | fumarate hydratase mitochondrial | 0.08 | 25.37 | 21.78 | -3.59 | TCA cycle, respiration |

[illegible]

| | | | | | | |
|--|--|------|-------|-------|-------|---|
| TR8620_c0_g1_i1 m.1552;TR2250_c0_g1_i1 m.5308 TR22827_c0_g2_i1 m.5562;TR13086_c0_g1_i1 m.2737;TR22827_c0_g1_i1 m.5560; TR13086_c0_g2_i1 m.2739 | Rhodanese-like domain-containing protein 14, chloroplastic short-chain dehydrogenase reductase 2a-like | 0.20 | 22.97 | 20.66 | -2.31 | Other |
| TR70599_c0_g1_i1 m.17576;TR65907_c0_g1_i1 m.15748 | fascilin-like arabinogalactan protein 1 | 0.18 | 23.63 | 21.14 | -2.49 | Other |
| TR128412_c0_g1_i2 m.70579;TR128412_c0_g1_i1 m.70578 TR135483_c1_g1_i5 m.96867;TR135483_c1_g1_i3 m.96864;TR135483_c1_g1_i2 m. 96863;TR135663_c1_g1_i1 m.97748;TR135483_c1_g1_i4 m.96865;TR135483_c1_g1_i1 m.96864;TR135663_c1_g1_i1 m.97750 | fascilin-like arabinogalactan protein 2 | 0.05 | 25.76 | 21.39 | -4.37 | Other, adhesion |
| TR134506_c0_g1_i2 m.92943;TR128377_c0_g1_i4 m.70513;TR134506_c0_g1_i1 m. 92942;TR128377_c0_g1_i3 m.70512;TR128377_c0_g1_i2 m.70510;TR134506_c0_g1_i3 m.92945;TR134506_c0_g1_i5 m.92949;TR128377_c0_g1_i1 m.70509;TR128377_c0_g1_i1 m.70508 | Tobamovirus multiplication protein 2A | 0.20 | 23.93 | 21.60 | -2.33 | Other, adhesion |
| TR126643_c3_g1_i2 m.65870;TR116754_c2_g4_i1 m.48120 TR147321_c15_g3_i3 m.186063;TR147321_c15_g3_i5 m.186066;TR147321_c15_g3_i1 m.186075;TR147321_c15_g3_i8 m.186071;TR147321_c15_g3_i7 m.186069 | scaffold attachment factor b2 | 0.16 | 23.62 | 21.01 | -2.61 | Other |
| TR58428_c0_g1_i1 m.12831;TR31886_c0_g2_i1 m.7126;TR31886_c0_g1_i1 m.7125 TR147270_c2_g4_i4 m.185487;TR147270_c2_g4_i2 m.185483;TR147270_c2_g4_i1 m.185480;TR136050_c2_g1_i2 m.99775;TR147270_c2_g4_i8 m.185493;TR147270_c2_g4_i6 m.185491;TR147270_c2_g4_i5 m.185489;TR136050_c2_g1_i1 m.99773;TR147270_c2_g4_i8 m.185494;TR147270_c2_g4_i6 m.185492 | High mobility group B protein 2 | 0.06 | 25.61 | 21.65 | -3.97 | Other, modulation of chromatin function |
| TR145969_c0_g2_i3 m.171545 TR61569_c0_g3_i1 m.14103;TR61569_c0_g2_i1 m.14102;TR61569_c0_g1_i1 m.14101;TR51635_c0_g3_i1 m.10797;TR51635_c0_g2_i1 m.10796;TR51635_c0_g1_i1 m.10795 | no apical meristem family protein protein argonaute 1 | 0.10 | 26.05 | 22.76 | -3.29 | Other, regulation of RNA regulation |
| TR143503_c5_g1_i3 m.148798;TR143503_c5_g1_i2 m.148797;TR143509_c5_g1_i1 m.148796;TR132511_c0_g1_i3 m.84751;TR132511_c0_g1_i2 m.84754;TR132511_c0_g1_i1 m.84753;TR89932_c0_g1_i1 m.24433;TR87995_c0_g1_i1 m.23513 TR96766_c0_g1_i1 m.29196;TR91965_c0_g2_i2 m.25877 | plasmidogen activator inhibitor 1 mabinding | 0.19 | 24.32 | 21.92 | -2.40 | RNA regulation |
| TR131589_c8_g1_i3 m.81089;TR124297_c2_g4_i3 m.60772 TR131589_c8_g1_i3 m.81093;TR131589_c8_g1_i2 m.81091;TR124297_c2_g1_i2 m.60770;TR124297_c2_g1_i1 m.60768 | L-ascorbate oxidase homolog | 0.12 | 24.01 | 20.98 | -3.03 | Other, Growth process. |
| TR135647_c4_g1_i2 m.97665;TR141052_c4_g1_i2 m.129910;TR141052_c4_g1_i1 m.129908;TR135647_c4_g1_i1 m.97664;TR141052_c4_g1_i3 m.129912;TR141052_c4_g1_i4 m.129914;TR134384_c3_g1_i4 m.92226;TR158409_c0_g1_i1 m.222663;TR96814_c0_g1_i1 m.29241 | Nudix hydrolase 3 | 0.17 | 24.03 | 21.44 | -2.59 | Other, Modulation of substrates, regulation, Regulation of intermediaries |
| TR120376_c1_g1_i1 m.53725;TR112069_c1_g1_i1 m.41963 | Soluble inorganic pyrophosphatase 6, chloroplastic | 0.09 | 25.34 | 21.88 | -3.46 | Other, Rx providing energy for other Rx |
| TR91446_c0_g1_i1 m.25605;TR00811_c0_g1_i1 m.25080 TR129152_c0_g1_i1 m.73048;TR124474_c1_g1_i1 m.61223;TR140446_c4_g5_i1 m.125393 | Subtilisin-like protease SBTL4 | 0.18 | 24.07 | 21.61 | -2.46 | Other, defence, proteolysis |
| TR145548_c0_g1_i7 m.167549;TR144831_c7_g1_i5 m.160803;TR145548_c0_g1_i6 m.167547;TR144831_c7_g1_i1 m.160797;TR145548_c0_g1_i2 m.167541;TR144831_c7_g1_i9 m.160808;TR144831_c7_g1_i6 m.160805;TR144831_c7_g1_i7 m.160807;TR145548_c0_g1_i3 m.167542;TR145548_c0_g1_i8 m.167552;TR144831_c7_g1_i4 m.160800;TR144831_c7_g1_i2 m.160798 | Remorin | 0.16 | 23.80 | 21.20 | -2.60 | Defense signalling |
| | Remorin | 0.10 | 24.32 | 21.04 | -3.28 | Defense signalling |
| | beta- partial | 0.05 | 26.46 | 22.27 | -4.19 | unclear |
| | conserved hypothetical protein | 0.12 | 26.35 | 23.24 | -3.11 | unclear |
| | PREDICTED: uncharacterized protein LOC105637665 | 0.08 | 25.64 | 21.91 | -3.73 | unclear |
| | uncharacterized acetyltransferase at3g50280-like | 0.03 | 27.57 | 22.29 | -5.28 | unclear |
| | uncharacterized oxidoreductase chloroplastic | 0.10 | 24.63 | 21.36 | -3.27 | unclear |

| | | | | | | |
|--|-------|------|-------|-------|-------|---------|
| TR146312_c3_g1_12 m.174991;TR135915_c1_g1_9 m.99012;TR135915_c1_g1_8 m.59010;TR135915_c1_g1_7 m.99007;TR135915_c1_g1_6 m.99004;TR135915_c1_g1_5 m.99000;TR135915_c1_g1_3 m.98998;TR135915_c1_g1_2 m.98993;TR135915_c1_g1_1 m.98990 | NO ID | 0.19 | 23.43 | 21.06 | -2.37 | unclear |
| TR123238_c0_g1_13 m.58224;TR120640_c0_g1_12 m.53235;TR122328_c0_g1_13 m.58228;TR120640_c0_g1_11 m.53233;TR123238_c0_g1_14 m.58230;TR123238_c0_g1_12 m.58226;TR120640_c0_g1_14 m.53239;TR120640_c0_g1_13 m.53237 | NO ID | 0.24 | 23.14 | 21.09 | -2.04 | unclear |
| TR142936_c0_g1_11 m.144173;TR144221_c0_g1_13 m.154739;TR142936_c0_g1_13 m.144178;TR144221_c0_g1_12 m.154737;TR142936_c0_g1_12 m.144176;TR144221_c0_g1_14 m.154741;TR144221_c0_g1_12 m.154736;TR142936_c0_g1_12 m.144175 | NO ID | 0.09 | 24.54 | 21.13 | -3.41 | unclear |
| TR142936_c0_g1_13 m.144179;TR144221_c0_g1_11 m.154735 | NO ID | | | | | |
| TR143872_c0_g2_13 m.151959;TR139801_c0_g1_11 m.118130;TR143872_c0_g2_14 m.151941;TR143872_c0_g2_12 m.151938 | NO ID | 0.09 | 24.96 | 21.50 | -3.46 | unclear |
| TR143805_c0_g2_11 m.151373 | NO ID | 0.13 | 24.65 | 21.65 | -3.00 | unclear |
| TR24686_c0_g1_11 m.59087;TR20607_c0_g1_11 m.4850;TR144064_c5_g1_12 m.162135;TR143575_c12_g1_13 m.149330 | NO ID | 0.19 | 23.98 | 21.60 | -2.38 | unclear |
| TR143234_c2_g1_11 m.146722;TR143464_c2_g1_11 m.148513 | NO ID | 0.06 | 25.85 | 21.83 | -4.02 | unclear |
| TR143816_c0_g1_14 m.151541;TR149384_c0_g2_12 m.210888;TR143816_c0_g1_16 m.151550;TR143816_c0_g1_15 m.151546;TR143816_c0_g1_13 m.151537 | NO ID | 0.17 | 23.77 | 21.22 | -2.55 | unclear |
| TR144202_c0_g1_16 m.154545;TR144202_c0_g1_15 m.154543 | NO ID | 0.13 | 24.78 | 21.82 | -2.96 | unclear |
| TR14161_c1_g1_11 m.3295;TR112932_c0_g2_11 m.43083;TR112932_c0_g1_11 m.43081 | NO ID | 0.09 | 24.72 | 21.30 | -3.42 | unclear |
| TR140569_c7_g1_12 m.126337;TR101372_c0_g1_12 m.33227 | NO ID | 0.16 | 24.46 | 21.82 | -2.64 | unclear |
| TR148466_c8_g1_12 m.199566 | NO ID | 0.11 | 24.91 | 21.74 | -3.17 | unclear |
| TR173220_c0_g1_11 m.225065;TR165853_c0_g1_11 m.223941 | NO ID | 0.17 | 24.45 | 21.87 | -2.58 | unclear |
| TR56869_c1_g1_11 m.28480;TR127427_c2_g1_12 m.68157 | NO ID | 0.06 | 26.46 | 22.48 | -3.98 | unclear |
| TR151427_c0_g1_11 m.221571;TR153065_c0_g1_11 m.221901 | NO ID | 0.13 | 23.96 | 21.04 | -2.92 | unclear |
| TR147811_c0_g1_11 m.191570;TR147046_c0_g1_11 m.182875 | NO ID | 0.15 | 24.43 | 21.70 | -2.73 | unclear |
| TR22472_c0_g4_11 m.5381;TR22472_c0_g3_11 m.5380;TR22472_c0_g2_11 m.5379; | NO ID | | | | | |
| TR22472_c0_g1_11 m.5378;TR127837_c0_g1_11 m.224857 | NO ID | 0.12 | 25.76 | 22.68 | -3.09 | unclear |
| TR8528_c0_g1_11 m.1483;TR120034_c0_g2_11 m.4763;TR8528_c0_g2_11 m.1485;TR20034_c0_g1_11 m.4761 | NO ID | 0.21 | 23.44 | 21.19 | -2.24 | unclear |
| TR109066_c2_g1_11 m.39867;TR105214_c3_g1_11 m.35936;TR129245_c0_g1_11 m.73283;TR126238_c0_g2_11 m.65091;TR129245_c0_g1_13 m.73286;TR126238_c0_g1_11 m.65089;TR129245_c0_g1_12 m.73284 | NO ID | 0.09 | 25.27 | 21.79 | -3.48 | unclear |
| TR139763_c1_g1_12 m.121059;TR142665_c0_g1_12 m.142038;TR142665_c0_g1_14 m.142041 | NO ID | 0.15 | 24.58 | 21.84 | -2.74 | unclear |
| TR131673_c0_g1_12 m.81400;TR131673_c0_g1_13 m.81402;TR131673_c0_g1_15 m.81408;TR131673_c0_g1_14 m.81404;TR131673_c0_g1_11 m.81399 | NO ID | 0.20 | 23.56 | 21.23 | -2.33 | unclear |
| TR187800_c1_g1_11 m.22721;TR1746576_c1_g2_11 m.177680 | NO ID | 0.15 | 24.08 | 21.33 | -2.76 | unclear |
| TR121506_c1_g1_12 m.55069;TR121506_c1_g1_11 m.55068;TR120774_c0_g1_12 m.53510;TR120774_c0_g1_11 m.53509 | NO ID | 0.13 | 24.88 | 21.89 | -2.99 | unclear |
| TR129758_c0_g1_11 m.74927;TR128461_c2_g1_12 m.70739;TR128461_c2_g1_11 m.70738 | NO ID | 0.14 | 24.23 | 21.37 | -2.86 | unclear |
| TR171730_c0_g1_11 m.18172;TR66488_c0_g1_11 m.15984 | NO ID | 0.10 | 26.42 | 23.16 | -3.26 | unclear |
| TR111892_c0_g1_11 m.41668;TR108856_c0_g1_11 m.39613 | NO ID | 0.12 | 24.62 | 21.52 | -3.10 | unclear |

| Proteins that decrease in the proximal region on Day 2 | | | | | | |
|--|---|-------------|----------------------------------|----------------------------------|---|----------------------------------|
| name sequence | protein name | fold change | log2[mean intensity Proximal D0] | log2[mean intensity Proximal D2] | relative abundance [log2(cond.1/control)] | function or category |
| TR69044_c0_g1_i1 m.16923;TR100915_c0_g1_i2 m.32979 | Olee1-like protein | 0.12 | 23.89 | 20.79 | -3.10 | allergens with expansin activity |
| TR7930_c0_g1_i1 m.20640;TR10828_c0_g1_i1 m.2212;TR54264_c0_g1_i1 m.12005;TR97974_c0_g1_i1 m.30172 | Putative pectinesterase/pectinesterase inhibitor 28 | 0.10 | 24.45 | 21.14 | -3.32 | cell wall modification |
| TR131836_c5_g1_i2 m.81928;TR127427_c8_g1_i1 m.68158;TR95869_c1_g1_i2 m.28481 | Dehydrin ERD14 | 0.04 | 26.86 | 22.05 | -4.81 | chaperone, stress response |
| TR180624_c0_g1_i1 m.226169 | Acetyl-CoA acetyltransferase, cytosolic 1 | 0.11 | 23.88 | 20.69 | -3.19 | fatty acid beta oxidation |
| TR126262_c0_g1_i1 m.65164;TR124928_c0_g1_i4 m.62240;TR124928_c0_g1_i1 m.62237;TR126262_c0_g1_i2 m.65165;TR124928_c0_g1_i3 m.62239;TR124928_c0_g1_i2 m.62238;TR884_c0_g1_i1 m.207;TR15080_c0_g1_i1 m.3474;TR85460_c0_g1_i1 m.22897;TR85432_c0_g1_i1 m.22886 | phosphoethanolamine n-methyltransferase 1-like | 0.09 | 24.73 | 21.19 | -3.54 | Lipid biosynthesis |
| TR112028_c0_g1_i3 m.41844;TR112028_c0_g1_i1 m.41842;TR108960_c0_g1_i2 m.39764;TR108960_c0_g1_i1 m.39763 | atp synthase subunit mitochondrial | 0.11 | 23.79 | 20.59 | -3.20 | oxidative phosphorylation |
| TR75003_c0_g3_i1 m.19459;TR75003_c0_g2_i1 m.19458;TR82051_c0_g2_i1 m.21979;TR82051_c0_g1_i1 m.21978;REV__TR97820_c2_g1_i3 m.30023;REV__TR86900_c1_g1_i1 m.23329;REV__TR97820_c2_g1_i1 m.30019;REV__TR97820_c2_g1_i2 m.30021 | oxygen-evolving enhancer protein chloroplastic-like Serine hydroxymethyltransferase, mitochondrial | 0.10 | 25.49 | 22.16 | -3.32 | photosynthesis |
| TR146716_c2_g1_i9 m.179287;TR146716_c2_g1_i8 m.179286 | | 0.11 | 24.26 | 21.07 | -3.19 | primary metabolism |
| TR21599_c0_g2_i1 m.5039;TR794_c0_g1_i1 m.195;TR794_c0_g2_i1 m.196;TR21599_c0_g1_i1 m.5038 | Catalase isozyme 1 | 0.08 | 24.95 | 21.24 | -3.71 | stress response |

| Proteins that decrease in the distal region on Day 4 | | | | | | | | | |
|---|-----------------------------------|-------------|--------------------------------|--------------------------------|---|---------------------------------|--|--|--|
| name sequence | protein name | fold change | log2(mean intensity Distal D2) | log2(mean intensity Distal D4) | relative abundance [log2(cond.1/control)] | function or category | | | |
| TR141685_c0_g1_i1 m.134472;TR140319_c0_g1_i1 m.124511;TR2245_c0_g1_i1 m.458;TR162195_c0_g1_i1 m.223356;TR102187_c0_g1_i1 m.33664;TR90981_c0_g1_i1 m.25199 | heat shock protein 83 | 0.03 | 26.53 | 21.26 | -5.26 | chaperone | | | |
| TR130358_c11_g1_i1 m.76869;TR129030_c5_g1_i1 m.72541 | ATP sulfurylase 1, chloroplastic | 0.11 | 23.93 | 20.68 | -3.25 | other | | | |
| TR146214_c8_g2_i6 m.174083;TR146214_c8_g2_i17 m.174092;TR141441_c1_g2_i3 m.132637;TR146214_c8_g2_i19 m.174095;TR146214_c8_g2_i10 m.174089;TR141441_c1_g2_i2 m.132635;TR146214_c8_g2_i8 m.174086 | photosystem i p700 apoprotein a2 | 0.07 | 24.86 | 21.10 | -3.76 | photosynthesis | | | |
| TR131639_c6_g2_i2 m.81263 | phosphoenolpyruvate carboxylase 4 | 0.08 | 24.38 | 20.65 | -3.73 | primary metabolism, respiration | | | |
| TR140691_c1_g1_i1 m.127264;TR140557_c3_g1_i1 m.126284;TR140557_c3_g1_i3 m.126286 | terpene synthase 10-like | 0.10 | 28.00 | 24.69 | -3.31 | secondary metabolism | | | |
| TR138982_c1_g1_i1 m.116183 | NO ID | 0.08 | 26.16 | 22.51 | -3.65 | unclear | | | |
| TR149513_c0_g2_i1 m.212590;TR149487_c0_g2_i1 m.212228;TR149513_c0_g2_i2 m.212591;TR149513_c0_g2_i3 m.212592;TR149487_c0_g2_i5 m.212232;TR148085_c0_g2_i1 m.194801;TR148345_c0_g1_i2 m.197957;TR148345_c0_g1_i1 m.197955;TR148345_c0_g1_i4 m.197959;TR148345_c0_g1_i3 m.197958;TR148345_c0_g1_i5 m.197960;TR148085_c0_g4_i1 m.194804;TR148085_c0_g4_i2 m.194806;TR7085_c0_g1_i1 m.1033;TR56967_c0_g1_i1 m.12504;TR97827_c0_g1_i1 m.30036;TR148085_c0_g4_i2 m.194807;TR148085_c0_g2_i2 m.194802;TR148085_c0_g4_i1 m.194805 | NO ID | 0.04 | 25.97 | 21.47 | -4.50 | unclear | | | |
| TR145056_c0_g1_i1 m.162990;TR144840_c0_g1_i2 m.160884 | NO ID | 0.04 | 25.97 | 21.47 | -4.50 | unclear | | | |
| TR137662_c0_g1_i2 m.108127;TR137662_c0_g1_i1 m.108126;TR125470_c0_g2_i4 m.63370;TR125470_c0_g2_i3 m.63369 | NO ID | 0.05 | 26.79 | 22.33 | -4.47 | unclear | | | |

| Proteins that decrease in the abscission zone on Day 4 | | | | | |
|--|-------------------------------------|-------------|----------------------------------|----------------------------------|--|
| | | | | | |
| | | | | | |
| name sequence | protein name | fold change | log2(mean intensity AZ D4) | log2(mean intensity AZ D4) | relative abundance [log2(cond.1/control)] |
| TR57118_c0_g2_i1 m.12529;TR57118_c0_g1_i1 m.12528 | Polyneuridine-aldehyde esterase | 0.04 | 26.20 | 21.69 | -4.51 |
| TR131706_c0_g1_i1 m.81531;TR130629_c0_g1_i1 m.77730 | gdsI esterase lipase at5g33370-like | 0.06 | 25.71 | 21.72 | -3.99 |

Supplementary material number 2. Proteins that increased in level on Day 2 and Day 4 (temporal comparisons)

| Proteins that increase in the distal region on Day 2 | | | | | | | | | |
|--|--|-------------|--------------------------------|--------------------------------|---|--------------------------|--|--|--|
| name sequence | protein name | fold change | log2(mean intensity Distal D0) | log2(mean intensity Distal D2) | relative abundance [log2(cond.1/control)] | function or category | | | |
| TR138857_c1_g1_i1 m.115376;TR136245_c2_g1_i1 m.100685 | protein notum homolog | 28.34 | 20.62 | 25.45 | 4.82 | cell wall transformation | | | |
| TR102949_c0_g1_i1 m.34528 | wound-induced protein win1 | 51.74 | 20.76 | 26.45 | 5.69 | defence | | | |
| TR136312_c0_g1_i1 m.101050;TR134199_c0_g1_i1 m.91525 | allene oxide synthase | 67.16 | 20.84 | 26.91 | 6.07 | defence | | | |
| TR144838_c5_g5_i2 m.160868;TR144838_c5_g5_i3 m.160870;TR144838_c5_g5_i1 m.160867;TR133538_c4_g1_i1 m.88294;TR144838_c5_g5_i3 m.160871;TR119196_c0_g2_i2 m.51143;TR126569_c0_g1_i3 m.65714;TR55141_c0_g2_i1 m.12134;TR61315_c0_g2_i1 m.13814 | 12-oxophytodienoate reductase 3 | 5.92 | 24.60 | 27.16 | 2.56 | defence | | | |
| TR145404_c0_g1_i4 m.166220;TR145404_c0_g1_i1 m.166217;TR159871_c0_g1_i1 m.223055;TR178665_c0_g1_i1 m.225939 | subtilisin-like protease | 35.28 | 21.38 | 26.52 | 5.14 | defence | | | |
| TR148572_c4_g1_i3 m.200761;TR124921_c2_g3_i1 m.62236 | 12-oxophytodienoate reductase 11 | 8.00 | 20.99 | 23.99 | 3.00 | defence | | | |
| TR152226_c0_g1_i1 m.3496;TR151159_c0_g1_i1 m.221490 | allene oxide synthase | 66.30 | 21.07 | 27.12 | 6.05 | defence | | | |
| TR90798_c3_g1_i1 m.25016;TR65777_c1_g1_i1 m.15684 | chitinase family protein | 10.34 | 21.32 | 24.69 | 3.37 | defence | | | |
| TR3514_c0_g2_i1 m.603;TR27572_c0_g1_i1 m.6408;TR3514_c0_g1_i1 m.602;TR27572_c0_g2_i1 m.6411;TR3514_c0_g1_i1 m.601;TR27572_c0_g2_i1 m.6410 | endochitinase pr4-like | 377.49 | 21.00 | 29.56 | 8.56 | defence | | | |
| TR51885_c0_g2_i1 m.11075;TR51885_c0_g1_i1 m.11074;TR51469_c0_g2_i1 m.10646;TR51469_c0_g1_i1 m.10645 | allene oxide cyclase chloroplastic-like | 16.72 | 22.05 | 26.11 | 4.06 | defence | | | |
| TR52324_c0_g1_i1 m.11251;TR58137_c0_g1_i1 m.12722;REV_1 | | | | | | | | | |
| TR130988_c0_g1_i2 m.79046;REV_1 | allene oxide synthase | 47.82 | 21.00 | 26.58 | 5.58 | defence | | | |
| TR76022_c0_g1_i1 m.19813;TR70661_c0_g1_i1 m.17634 | allene oxide synthase | 87.97 | 20.54 | 26.99 | 6.46 | defence | | | |
| TR112327_c2_g1_i1 m.42387;TR112867_c4_g2_i1 m.42978 | thaumatin-like protein 1b | 169.05 | 21.50 | 28.90 | 7.40 | defence | | | |
| TR144639_c4_g3_i2 m.158820 | Pathogen-related protein | 5.51 | 25.20 | 27.66 | 2.46 | defence | | | |
| TR116008_c0_g1_i1 m.47148;TR119694_c2_g1_i1 m.51711 | Thaumatococcus-like protein | 6.40 | 26.41 | 29.08 | 2.68 | defence | | | |
| TR145404_c0_g1_i5 m.166221;TR145829_c0_g1_i1 m.170198;TR145404_c0_g1_i3 m.166219;TR145404_c0_g1_i8 m.166224;TR168371_c0_g1_i1 m.224444;TR111120_c0_g1_i1 m.2288 | Subtilisin-like protease SBT1.9 | 29.92 | 21.56 | 26.46 | 4.90 | defence | | | |
| TR124048_c0_g1_i1 m.60067;TR122051_c0_g1_i1 m.56333 | carbonic chloroplastic-like | 64.75 | 21.62 | 27.64 | 6.02 | nutrients salvaging | | | |
| TR111615_c0_g1_i2 m.41310;TR107536_c0_g1_i1 m.37890;TR111615_c0_g1_i1 m.41309;TR107536_c0_g1_i2 m.37891 | chlorophyllase partial | 38.18 | 23.17 | 28.43 | 5.25 | nutrients salvaging | | | |
| TR130422_c0_g1_i1 m.77072;TR94749_c0_g1_i1 m.27678;TR143607_c1_g1_i1 m.149643 | probable mitochondrial chaperone bcs1-b-like | 7.43 | 21.12 | 24.01 | 2.89 | other | | | |

| | | | | | | |
|---|---|----------------|----------------|----------------|--------------|----------------------|
| TR158367_c0_g2_i1 m.222643;TR59080_c0_g1_i1 m.13139;TR158367_c0_g1_i1 m.222639 | abc transporter c family member r14-like cell division control protein 2 homolog c | 25.90 13.19 | 20.71 20.36 | 25.41 24.08 | 4.70 3.72 | other other |
| TR90977_c1_g1_i1 m.25194;TR121194_c0_g1_i1 m.42139 | | | | | | |
| TR92266_c3_g1_i2 m.26039;TR140471_c0_g1_i1 m.125587;TR92266_c3_g1_i1 m.26038;TR140471_c0_g1_i2 m.125588 | eg45-like domain containing protein | 14.03 | 21.50 | 25.31 | 3.81 | other |
| TR95444_c0_g1_i1 m.28168;TR89849_c0_g1_i1 m.24383 | Auxin-binding protein ABP20 | 7.21 | 25.47 | 28.32 | 2.85 | other |
| TR134764_c1_g1_i5 m.94090 | ABC transporter F family member 1 | 7.94 | 22.14 | 25.13 | 2.99 | other |
| TR172700_c0_g1_i1 m.224761;TR151483_c0_g1_i1 m.221591 | Epidermis-specific secreted glycoprotein EP1 | 15.80 | 20.92 | 24.91 | 3.98 | other |
| TR132941_c0_g1_i1 m.86176;TR129779_c0_g1_i2 m.74981;TR132941_c0_g1_i2 m.86177;TR129779_c0_g1_i1 m.74980 | peroxisomal -2-hydroxy-acid oxidase glo4-like | 24.00 | 21.49 | 26.07 | 4.58 | primary metabolism |
| TR137225_c0_g1_i1 m.105818;TR135545_c0_g1_i1 m.97142 | phospho-2-dehydro-3-deoxyheptonate aldolase chloroplastic-like | 28.72 | 21.53 | 26.38 | 4.84 | primary metabolism |
| TR140950_c0_g1_i3 m.129169;TR140950_c0_g1_i1 m.129167;TR140384_c0_g1_i1 m.124969;TR140950_c0_g1_i4 m.129170;TR140950_c0_g1_i2 m.129168;TR140384_c0_g1_i2 m.124970;TR101342_c0_g1_i1 m.33209;TR103652_c0_g1_i1 m.35129 | inosine-5-monophosphate dehydrogenase 2-like pyruvate phosphate pep pyruvate binding domain isoform 1 | 8.99 | 21.29 | 24.46 | 3.17 | primary metabolism |
| TR148524_c4_g1_i1 m.200229 | | 9.81 | 22.87 | 26.17 | 3.29 | primary metabolism |
| TR146872_c7_g1_i13 m.180918;TR145883_c10_g2_i3 m.170696;TR145883_c10_g2_i2 m.170694 | Acetyl-CoA carboxylase 1 | 7.30 | 23.49 | 26.36 | 2.87 | primary metabolism |
| TR140556_c0_g1_i1 m.126283;TR140707_c0_g1_i1 m.127317;TR94_c0_g1_i2 m.5 | Acid beta-fructofuranosidase | 9.53 | 23.50 | 26.75 | 3.25 | primary metabolism |
| TR102628_c0_g1_i1 m.34189;TR102184_c0_g1_i1 m.33662 | basic 7's globulin-like | 10.40 | 22.53 | 25.90 | 3.38 | proteolysis |
| TR145252_c2_g1_i8 m.164769;TR146190_c0_g1_i2 m.173883;TR145252_c2_g1_i2 m.164760;TR145252_c2_g1_i6 m.164766;TR145252_c2_g1_i4 m.164763 | | | | | | |
| TR53471_c0_g1_i1 m.11839;TR139883_c0_g1_i1 m.121836 | prolyl endopeptidase-like | 13.39 | 20.88 | 24.63 | 3.74 | proteolysis |
| TR117084_c1_g1_i1 m.48447;TR108583_c2_g1_i1 m.39201 | cysteine proteinase 15a-like | 8.61 | 21.55 | 24.65 | 3.11 | proteolysis |
| TR121772_c1_g1_i3 m.55703;TR111649_c0_g1_i2 m.41368 | flavonoid 3-hydroxylase | 9.51 | 20.94 | 24.19 | 3.25 | secondary metabolism |
| TR128947_c6_g1_i1 m.72236 | cinnamoyl-reductase | 11.75 | 21.31 | 24.86 | 3.55 | secondary metabolism |
| TR129113_c1_g1_i1 m.72913;TR128964_c2_g1_i1 m.72326;TR128964_c2_g1_i2 m.72327 | flavonoid 3-hydroxylase 2-like | 10.43 | 21.19 | 24.57 | 3.38 | secondary metabolism |
| TR137041_c1_g1_i1 m.104791;TR98968_c1_g1_i1 m.31196;TR137041_c1_g2_i1 m.104792;TR180447_c1_g1_i1 m.226027;TR137041_c1_g2_i1 m.104793 | phenylalanine ammonia-lyase | 24.88 | 20.81 | 25.45 | 4.64 | secondary metabolism |
| TR137449_c3_g1_i1 m.106949;TR139963_c1_g2_i1 m.122248 | caffeoyl-o-methyltransferase | 34.29 | 22.04 | 27.14 | 5.10 | secondary metabolism |
| TR145678_c4_g3_i2 m.168685;TR145678_c4_g3_i1 m.168684;TR145784_c1_g1_i1 m.169772;TR145784_c1_g1_i2 m.169773;TR145678_c4_g3_i3 m.168686 | anthocyanidin reductase | 8.63 | 21.49 | 24.60 | 3.11 | secondary metabolism |
| | reticuline oxidase-like protein | 20.56 | 22.96 | 27.32 | 4.36 | secondary metabolism |

| | | | | | | |
|--|---|-------|-------|-------|------|----------------------|
| TR165246_c2_g1_i1 m.223627;TR157924_c4_g1_i1 m.222400;T R172984_c0_g1_i1 m.224959;TR150363_c0_g1_i1 m.221098 | trans-cinnamate 4-hydroxylase | 78.19 | 20.57 | 26.86 | 6.29 | secondary metabolism |
| TR172840_c1_g1_i1 m.224863;TR150098_c0_g1_i1 m.220735 | hydroxycinnamoyl- shikimate quininate | 11.59 | 21.38 | 24.92 | 3.54 | secondary metabolism |
| TR97650_c7_g1_i1 m.29835;TR10773_c4_g2_i1 m.25784 | hydroxycinnamoyl transferase isoform 1 | 66.80 | 20.54 | 26.61 | 6.06 | secondary metabolism |
| TR98687_c1_g2_i1 m.30826;TR107931_c0_g1_i1 m.38454 | flavanone 3-hydroxylase | 6.08 | 24.66 | 27.26 | 2.60 | secondary metabolism |
| TR98850_c0_g1_i1 m.31055;TR102633_c2_g1_i1 m.34191 | caffeic acid o-methyltransferase | 45.04 | 21.62 | 27.11 | 5.49 | secondary metabolism |
| TR27580_c8_g1_i1 m.6412;TR172918_c12_g1_i1 m.224904;TR1 89856_c0_g1_i1 m.227964;TR158410_c0_g1_i1 m.222664;TR53 365_c0_g2_i1 m.11814;TR16132_c0_g2_i1 m.3718 | cytochrome p450 cyp82d47-like | | | | | |
| TR73121_c2_g1_i1 m.18683;TR80104_c0_g1_i1 m.21413;TR801 04_c0_g2_i1 m.21414 | chalcone synthase | 97.75 | 21.89 | 28.50 | 6.61 | secondary metabolism |
| TR57118_c0_g2_i1 m.12529;TR57118_c0_g1_i1 m.12528 | phenylalanine ammonia-lyase | 6.28 | 21.12 | 23.77 | 2.65 | secondary metabolism |
| TR150273_c0_g1_i1 m.220983;TR158395_c0_g1_i1 m.222657 | Polyneuridine-aldehyde esterase | 29.23 | 20.87 | 25.74 | 4.87 | secondary metabolism |
| TR135433_c1_g3_i1 m.96601;TR148403_c1_g1_i1 m.198612 | 4-coumarate--CoA ligase 1 | 7.20 | 21.38 | 24.23 | 2.85 | secondary metabolism |
| TR165232_c2_g1_i1 m.223616;TR16233_c0_g1_i1 m.3766 | probable glutathione s-transferase | 10.83 | 20.76 | 24.20 | 3.44 | stress response |
| TR187924_c0_g1_i1 m.227328;TR130764_c16_g1_i1 m.78272 | probable glutathione s-transferase | 9.25 | 21.47 | 24.68 | 3.21 | stress response |
| TR129191_c1_g1_i1 m.73168;TR125696_c1_g1_i1 m.63964 | peroxidase p7-like | 13.29 | 21.33 | 25.06 | 3.73 | stress response |
| TR144022_c5_g1_i7 m.153123;TR143552_c3_g1_i3 m.149131 | endo- -beta- NO ID | 13.20 | 21.09 | 24.82 | 3.72 | under |
| TR97106_c1_g1_i1 m.29433;TR95853_c2_g1_i1 m.28470 | lipoxigenase homology domain-containing protein 1-like | 16.17 | 21.26 | 25.27 | 4.02 | under |
| TR143332_c0_g1_i1 m.147353;TR143097_c1_g1_i2 m.145459;T R143097_c1_g1_i3 m.145460;TR143097_c1_g1_i1 m.145458 | NO ID | 8.10 | 23.46 | 26.48 | 3.02 | under |
| TR143984_c0_g1_i3 m.152801;TR144010_c0_g1_i1 m.153052 | NO ID | 24.94 | 21.88 | 26.52 | 4.64 | under |
| TR2751_c0_g2_i1 m.520;TR2751_c0_g1_i1 m.519;TR165671_c0 _g1_i1 m.223869 | NO ID | 24.04 | 20.87 | 25.46 | 4.59 | under |
| | NO ID | 9.11 | 21.02 | 24.21 | 3.19 | under |

| Proteins that increase in the abscission zone on Day 2 | | | | | | |
|---|---|-------------|----------------------------|----------------------------|---|--------------------------|
| name sequence | protein name | fold change | log2(mean intensity AZ D0) | log2(mean intensity AZ D2) | relative abundance [log2(cond.1/control)] | function or category |
| TR117243_c3_g1_i1 m.48628;TR113211_c2_g1_i1 m.43457 | glucan endo- β-glucosidase-like | 7.32 | 28.43 | 31.30 | 2.87 | cell wall transformation |
| TR141593_c3_g1_i4 m.133761;TR140555_c4_g1_i12 m.126276 | alpha -glucan-protein synthase | 6.42 | 24.75 | 27.43 | 2.68 | cell wall transformation |
| TR140555_c4_g1_i14 m.126280 | UDP-arabinopyranose mutase 3 | 5.95 | 22.35 | 24.92 | 2.57 | cell wall transformation |
| TR102949_c0_g1_i1 m.34528 | wound-induced protein win1 | 11.01 | 21.35 | 24.81 | 3.46 | defence |
| TR112327_c2_g1_i1 m.42387;TR112867_c4_g2_i1 m.42978 | thaumatin-like protein 1b | 97.68 | 21.27 | 27.88 | 6.61 | defence |
| TR3514_c0_g2_i1 m.603;TR27572_c0_g1_i1 m.6408;TR3514_c0_g1_i1 m.602;TR27572_c0_g2_i1 m.6411;TR3514_c0_g1_i1 m.601;TR27572_c0_g2_i1 m.6410 | endochitinase pr4-like | 61.52 | 21.70 | 27.65 | 5.94 | defence |
| TR51885_c0_g2_i1 m.11075;TR51885_c0_g1_i1 m.11074;TR51469_c0_g2_i1 m.10646;TR51469_c0_g1_i1 m.10645 | allene oxide cyclase chloroplastic-like | 8.53 | 22.78 | 25.88 | 3.09 | defence |
| TR145404_c0_g1_i4 m.166220;TR145404_c0_g1_i1 m.166217;TR15987_1_c0_g1_i1 m.223055;TR178665_c0_g1_i1 m.225939 | subtilisin-like protease | 91.06 | 20.89 | 27.40 | 6.51 | defence |
| TR145829_c0_g1_i4 m.170201;TR145404_c0_g1_i9 m.166225 | subtilisin-like protease | 30.61 | 20.84 | 25.77 | 4.94 | defence |
| TR52324_c0_g1_i1 m.11251;TR58137_c0_g1_i1 m.12722;REV__TR1309_88_c0_g1_i2 m.79046;REV__TR128743_c0_g1_i1 m.71560 | allene oxide synthase | 25.59 | 20.71 | 25.39 | 4.68 | defence |
| TR76022_c0_g1_i1 m.19813;TR70661_c0_g1_i1 m.17634 | allene oxide synthase | 23.40 | 20.61 | 25.16 | 4.55 | defence |
| TR15226_c0_g1_i1 m.3496;TR151159_c0_g1_i1 m.221490 | allene oxide synthase | 14.54 | 21.44 | 25.30 | 3.86 | defence |
| TR136312_c0_g1_i1 m.101050;TR134199_c0_g1_i1 m.91525 | allene oxide synthase | 13.63 | 21.36 | 25.13 | 3.77 | defence |
| TR139231_c4_g1_i1 m.117676 | subtilisin-like protease | 5.75 | 26.55 | 29.07 | 2.52 | defence |
| TR149218_c2_g1_i2 m.208615;TR149218_c2_g1_i1 m.208614;TR13826_5_c4_g1_i1 m.111704 | Subtilisin-like protease SBT1.7 | 5.33 | 27.41 | 29.82 | 2.41 | defence |
| TR148880_c6_g1_i5 m.204455;TR148880_c6_g1_i2 m.204450 | Subtilisin-like protease SBT1.6 | 9.73 | 20.93 | 24.21 | 3.28 | defence |
| TR77513_c0_g1_i1 m.20483;TR75561_c0_g1_i1 m.19641 | Subtilisin-like protease SBT1.4 | 7.24 | 28.68 | 31.53 | 2.86 | defence |
| TR96766_c0_g1_i2 m.29197;TR91965_c0_g2_i1 m.25876 | subtilisin-like protease | 8.04 | 28.78 | 31.79 | 3.01 | defence |
| TR116008_c0_g1_i1 m.47148;TR119694_c2_g1_i1 m.51711 | Thaumatococcal-like protein | 10.22 | 26.88 | 30.23 | 3.35 | defence |
| TR145404_c0_g1_i5 m.166221;TR145829_c0_g1_i1 m.170198;TR14540_4_c0_g1_i3 m.166219;TR145404_c0_g1_i8 m.166224;TR168371_c0_g1_i1 m.224444;TR11120_c0_g1_i1 m.2288 | Subtilisin-like protease SBT1.9 | 49.93 | 20.87 | 26.51 | 5.64 | defence |
| TR111615_c0_g1_i2 m.41310;TR107536_c0_g1_i1 m.37890;TR111615_c0_g1_i1 m.41309;TR107536_c0_g1_i2 m.37891 | chlorophyllase partial | 70.12 | 23.46 | 29.59 | 6.13 | nutrients salvaging |
| TR124048_c0_g1_i1 m.60067;TR122051_c0_g1_i1 m.56333 | carbonic chloroplastic-like | 15.07 | 21.49 | 25.41 | 3.91 | nutrients salvaging |
| TR151036_c0_g1_i1 m.221394;TR188205_c0_g1_i1 m.227502 | Probable inactive purple acid phosphatase 1, 24 or 27 | 5.69 | 21.37 | 23.88 | 2.51 | nutrients salvaging |

| | | | | | | |
|---|---|-------|-------|-------|------|----------------------|
| TR140059_c1.g2_1 1m.122846;TR139668_c0.g2_1 1m.120514;TR139668_c0.g1_1 1m.120513;TR140059_c1.g2_1 1m.122847 | Probable inactive purple acid phosphatase 1 | 15.00 | 21.56 | 25.47 | 3.91 | nutrients salvaging |
| TR106968_c0.g1_1 1m.37139;TR106889_c0.g1_1 1m.37009;TR106968_c0.g1_1 1m.37129;TR106889_c0.g1_1 1m.37007;TR106968_c0.g1_1 1m.37136;TR106968_c0.g1_1 1m.37005;TR106968_c0.g1_1 1m.37136;TR106968_c0.g1_1 1m.37014;TR106968_c0.g1_1 1m.37131;TR106889_c0.g1_1 1m.37011;TR106968_c0.g1_1 1m.37137;TR106968_c0.g1_1 1m.3713_1 1m.37011;TR106968_c0.g1_1 1m.37015;TR106889_c0.g1_1 1m.37012 | Purple acid phosphatase 23 | 9.09 | 21.06 | 24.25 | 3.18 | nutrients salvaging |
| TR92266_c3.g1_1 1m.26039;TR140471_c0.g1_1 1m.125587;TR92266_c3.g1_1 1m.26038;TR140471_c0.g1_1 1m.125588 | eg45-like domain containing protein | 18.68 | 20.99 | 25.21 | 4.22 | other |
| TR139257_c0.g1_1 1m.117871;TR137117_c0.g1_1 1m.105271;TR137117_c0.g1_1 1m.105270;TR139257_c0.g1_1 1m.117872 | Amidase 1 | 9.80 | 22.88 | 26.17 | 3.29 | other |
| TR172700_c0.g1_1 1m.224761;TR151483_c0.g1_1 1m.221591 | Epidermis-specific secreted glycoprotein | | | | | |
| TR95444_c0.g1_1 1m.28168;TR89849_c0.g1_1 1m.24383 | EP1 | 8.86 | 22.21 | 25.36 | 3.15 | Other |
| TR17815_c0.g1_1 1m.4402;TR173128_c0.g1_1 1m.225038;TR17815_c0.g2_1 1m.4404;TR17815_c0.g2_1 1m.4405 | Auxin-binding protein ABP20 | 6.42 | 26.15 | 28.83 | 2.68 | Other, auxin related |
| TR145147_c1.g1_1 1m.163722;TR145147_c1.g1_1 1m.163721;TR145147_c1.g1_1 1m.163715 | Agmatine deiminase | 6.96 | 21.87 | 24.67 | 2.80 | Other |
| TR4747_c0.g2_1 1m.703;TR4747_c0.g1_1 1m.702;TR14043_c0.g2_1 1m.3277;TR14043_c0.g1_1 1m.3276 | Sulfite oxidase | 8.40 | 20.99 | 24.06 | 3.07 | Other |
| TR132941_c0.g1_1 1m.86176;TR129779_c0.g1_1 1m.74981;TR132941_c0.g1_1 1m.86177;TR129779_c0.g1_1 1m.74980 | 4-hydroxy-4-methyl-2-oxoglutarate aldolase 3 | 12.97 | 21.50 | 25.20 | 3.70 | primary metabolism |
| TR133048_c7.g1_1 1m.86518;TR130901_c8.g1_1 1m.78700;TR133048_c7.g1_1 1m.86521 | peroxisomal -2-hydroxy-acid oxidase g o4-like | 48.25 | 21.09 | 26.69 | 5.59 | primary metabolism |
| TR133048_c7.g1_1 1m.86520 | mta sah | 6.91 | 29.96 | 32.75 | 2.79 | primary metabolism |
| TR140556_c0.g1_1 1m.126283;TR140707_c0.g1_1 1m.127317;TR94_c0.g1_1 1m.5 | mta sah | 7.07 | 29.55 | 32.37 | 2.82 | primary metabolism |
| TR172744_c0.g1_1 1m.224793;TR172741_c1.g1_1 1m.224791 | Acid beta-fructofuranosidase | 8.72 | 23.49 | 26.62 | 3.12 | primary metabolism |
| TR134655_c0.g1_1 1m.93631;TR134814_c0.g1_1 1m.94239;TR134655_c0.g1_1 1m.93632;TR134655_c0.g1_1 1m.93633;TR146149_c5.g3_1 1m.173308;TR146149_c5.g3_1 1m.173309;TR146149_c5.g3_1 1m.173313;TR146149_c5.g3_1 1m.173312;TR146149_c5.g3_1 1m.173311;TR149018_c3.g3_1 1m.206074;TR149018_c3.g3_1 1m.206073;TR149018_c3.g3_1 1m.206077;TR149018_c3.g3_1 1m.206075 | Alpha-glucosidase | 10.74 | 25.02 | 28.44 | 3.43 | primary metabolism |
| TR91321_c0.g1_1 1m.25519;TR117532_c1.g1_1 1m.48991 | Isoamylase 1, chloroplastic | 12.79 | 20.72 | 24.40 | 3.68 | primary metabolism |
| TR128759_c2.g1_1 1m.71604;TR128759_c2.g1_1 1m.71605;TR124389_c0.g1_1 1m.61019;TR128759_c2.g1_1 1m.71600;TR124389_c0.g1_1 1m.61018 | Phosphopantetheine adenylyltransferase | 8.81 | 21.10 | 24.24 | 3.14 | primary metabolism |
| | Adenylylsulfatase HINT1 | 14.38 | 21.22 | 25.07 | 3.85 | primary metabolism |

| | | | | | | |
|--|---|--------|-------|-------|------|----------------------|
| TR137553_c4_g1_i1 m.107585;TR132527_c9_g1_i1 m.84806 | low-temperature-induced cysteine proteinase | 6.75 | 26.35 | 29.10 | 2.75 | proteolysis |
| TR145252_c2_g1_i8 m.164769;TR146190_c0_g1_i2 m.173883;TR145252_c2_g1_i2 m.164760;TR145252_c2_g1_i6 m.164766;TR145252_c2_g1_i4 m.164763 | prolyl endopeptidase-like | 22.01 | 21.76 | 26.22 | 4.46 | proteolysis |
| TR135800_c5_g1_i1 m.98495;TR132526_c2_g1_i2 m.84803;TR132526_c2_g1_i1 m.84800 | cysteine proteinase rd21a-like | 15.16 | 22.54 | 26.46 | 3.92 | proteolysis |
| TR180432_c0_g2_i1 m.226038;TR180914_c0_g1_i1 m.226309;TR180432_c0_g1_i1 m.226037 | Aspartyl protease family protein 1 | 5.82 | 21.11 | 23.65 | 2.54 | proteolysis |
| TR121772_c1_g1_i3 m.55703;TR111649_c0_g1_i2 m.41368 | cinnamoyl-reductase | 10.51 | 21.26 | 24.65 | 3.39 | secondary metabolism |
| TR145678_c4_g3_i2 m.168685;TR145678_c4_g3_i1 m.168684;TR145784_c1_g1_i1 m.169772;TR145784_c1_g1_i2 m.169773;TR145678_c4_g3_i3 m.168686 | reticuline oxidase-like protein | 134.19 | 21.27 | 28.34 | 7.07 | secondary metabolism |
| TR97650_c7_g1_i1 m.29835;TR91773_c4_g2_i1 m.25784 | flavanone 3-hydroxylase | 40.00 | 20.50 | 25.82 | 5.32 | secondary metabolism |
| TR124549_c2_g1_i1 m.61440;TR122350_c3_g1_i1 m.56759 | dihydroflavonol 4-reductase | 6.01 | 20.81 | 23.40 | 2.59 | secondary metabolism |
| TR165246_c2_g1_i1 m.223627;TR157924_c4_g1_i1 m.222400;TR172984_c0_g1_i1 m.224959;TR150363_c0_g1_i1 m.221098 | trans-cinnamate 4-hydroxylase | 7.37 | 21.18 | 24.07 | 2.88 | secondary metabolism |
| TR27580_c8_g1_i1 m.6412;TR172918_c12_g1_i1 m.224904;TR189856_c0_g1_i1 m.227964;TR158410_c0_g1_i1 m.222664;TR53365_c0_g2_i1 m.11814;TR16132_c0_g2_i1 m.3718 | chalcone synthase | 29.21 | 23.20 | 28.07 | 4.87 | secondary metabolism |
| TR137041_c1_g1_i1 m.104791;TR98968_c1_g1_i1 m.311196;TR137041_c1_g2_i1 m.104793 | caffeoyl- o-methyltransferase | 10.02 | 21.91 | 25.23 | 3.32 | secondary metabolism |
| TR57118_c0_g2_i1 m.12529;TR57118_c0_g1_i1 m.12528 | Polynuridine-aldehyde esterase | 42.53 | 20.79 | 26.20 | 5.41 | secondary metabolism |
| TR95819_c3_g1_i1 m.28441;TR91468_c3_g1_i1 m.25612;TR90032_c2_g1_i2 m.24508;TR149468_c2_g1_i3 m.211966;TR90032_c0_g1_i2 m.24506;TR39519_c0_g1_i1 m.8447 | peroxidase 3, peroxidase 5-like | 6.58 | 24.77 | 27.49 | 2.72 | stress response |
| TR147438_c7_g1_i8 m.187431;TR147438_c7_g1_i11 m.187433;TR141974_c3_g1_i2 m.136408;TR147438_c7_g1_i4 m.187427;TR139534_c4_g1_i1 m.119696;TR147438_c7_g1_i5 m.187428;TR147438_c7_g1_i10 m.187432;TR139534_c4_g1_i2 m.119697;TR139534_c4_g1_i15 m.119710;TR139534_c4_g1_i13 m.119708;TR139534_c4_g1_i3 m.119698;TR139534_c4_g1_i6 m.119701;TR139534_c4_g1_i10 m.119705 | partial, Superoxide dismutase [Cu-Zn] | 8.49 | 21.44 | 24.53 | 3.09 | stress response |
| TR141645_c6_g1_i2 m.134170;TR111988_c3_g1_i1 m.41779 | Glycine-rich RNA-binding protein 4 | 7.77 | 24.02 | 26.97 | 2.96 | stress response |
| TR4403_c0_g1_i1 m.672;TR2907_c0_g1_i1 m.543 | Peptide methionine sulfoxide reductase B1 | 13.31 | 20.72 | 24.45 | 3.73 | stress response |
| TR143332_c0_g1_i1 m.147353;TR143097_c1_g1_i2 m.145459;TR143097_c1_g1_i3 m.145460;TR143097_c1_g1_i1 m.145458 | NO ID | 8.97 | 21.80 | 24.97 | 3.17 | unclear |
| TR78848_c0_g1_i1 m.20944;TR74659_c0_g2_i1 m.19348;TR78848_c0_g1_i2 m.20947;TR74659_c0_g2_i2 m.19350;TR122581_c0_g1_i2 m.57255;TR131404_c0_g1_i1 m.80458;TR122581_c0_g1_i1 m.57254 | NO ID | 6.69 | 25.83 | 28.57 | 2.74 | unclear |
| TR107543_c0_g1_i1 m.37897;TR96639_c0_g1_i1 m.29079 | NO ID | 12.64 | 21.67 | 25.33 | 3.66 | unclear |

| Proteins that increase in the proximal region on Day 2 | | | | | | |
|--|--|-------------|----------------------------------|----------------------------------|---|----------------------|
| name sequence | protein name | fold change | log2(mean intensity Proximal D0) | log2(mean intensity Proximal D2) | relative abundance [log2(cond.1/control)] | function or category |
| TR76022_c0_g1_i1 m.19813;TR70661_c0_g1_i1 m.17634 TR52324_c0_g1_i1 m.11251;TR58137_c0_g1_i1 m.12722;REV__TR130988_c0_g1_i2 m.79046;REV__TR128743_c0_g1_i1 m.71560 | allene oxide synthase | 8.94 | 21.19 | 24.35 | 3.16 | defence |
| TR3514_c0_g2_i1 m.603;TR27572_c0_g1_i1 m.6408;TR3514_c0_g1_i1 m.602;TR27572_c0_g2_i1 m.6411;TR3514_c0_g1_i1 m.601;TR27572_c0_g2_i1 m.6410 | allene oxide synthase | 19.13 | 20.29 | 24.55 | 4.26 | defence |
| TR145404_c0_g1_i4 m.166220;TR145404_c0_g1_i1 m.166219;TR145404_c0_g1_i3 m.166219;TR145404_c0_g1_i8 m.166224;TR168371_c0_g1_i1 m.224444;TR11120_c0_g1_i1 m.2288 | endochitinase pr4-like | 14.82 | 21.05 | 24.93 | 3.89 | defence |
| TR145404_c0_g1_i4 m.166220;TR145404_c0_g1_i1 m.166219;TR145404_c0_g1_i3 m.166219;TR145404_c0_g1_i8 m.166224;TR168371_c0_g1_i1 m.224444;TR11120_c0_g1_i1 m.2288 | lipid transfer protein precursor | 7.80 | 20.41 | 23.37 | 2.96 | defence |
| TR145404_c0_g1_i5 m.166221;TR145829_c0_g1_i1 m.170198;TR145404_c0_g1_i3 m.166219;TR145404_c0_g1_i8 m.166224;TR168371_c0_g1_i1 m.224444;TR11120_c0_g1_i1 m.2288 | subtilisin-like protease | 60.64 | 20.81 | 26.73 | 5.92 | defence |
| TR118090_c0_g1_i1 m.49765;TR115594_c0_g1_i1 m.46534;TR115594_c0_g1_i2 m.46536;TR118090_c0_g1_i2 m.49766 | Subtilisin-like protease SBT1.9 | 16.81 | 21.49 | 25.56 | 4.07 | defence |
| TR111615_c0_g1_i2 m.41310;TR107536_c0_g1_i1 m.37890;TR111615_c0_g1_i1 m.41309;TR107536_c0_g1_i2 m.37891 | acid phosphatase 1 | 10.93 | 21.07 | 24.52 | 3.45 | nutrients salvaging |
| TR111712_c0_g1_i2 m.49269;TR117712_c0_g1_i1 m.49268;TR112650_c0_g1_i2 m.42815;TR112650_c0_g1_i1 m.42814 | chlorophyllase partial | 20.55 | 24.39 | 28.75 | 4.36 | nutrients salvaging |
| TR121772_c1_g1_i3 m.55703;TR111649_c0_g1_i2 m.41368 | lachrymatory-factor synthase-like | 6.08 | 21.43 | 24.04 | 2.60 | other |
| TR158367_c0_g2_i1 m.222643;TR59080_c0_g1_i1 m.13139;TR158367_c0_g1_i1 m.222639 | lachrymatory-factor synthase-like | 10.29 | 21.14 | 24.51 | 3.36 | other |
| TR92266_c3_g1_i2 m.26039;TR140471_c0_g1_i1 m.125587;TR92266_c3_g1_i1 m.26038;TR140471_c0_g1_i2 m.125588 | abc transporter c family member 14-like | 14.51 | 21.05 | 24.91 | 3.86 | other |
| TR137225_c0_g1_i1 m.105818;TR135545_c0_g1_i1 m.97142 | eg45-like domain containing protein | 29.23 | 21.05 | 25.92 | 4.87 | other |
| | phospho-2-dehydro-3-deoxyheptonate aldolase chloroplastic-like | 8.20 | 22.43 | 25.47 | 3.04 | primary metabolism |
| TR99429_c1_g1_i1 m.31681;TR99081_c2_g1_i1 m.31313 | 3-hydroxyisobutyryl- hydrolase-like protein | 7.31 | 21.55 | 24.42 | 2.87 | primary metabolism |

| | | | | | | |
|---|--|-------|-------|-------|------|----------------------|
| TR148524_c4_g1_i1 m.200229 | pyruvate phosphate pep pyruvate binding domain isoform 1 | 10.82 | 21.52 | 24.96 | 3.44 | primary metabolism |
| TR137041_c1_g1_i1 m.104791;TR98968_c1_g1_i1 m.3119 | | | | | | |
| 6;TR137041_c1_g2_i1 m.104792;TR180417_c1_g1_i1 m.226027;TR137041_c1_g2_i1 m.104793 | caffeoyl- o-methyltransferase | 12.11 | 21.32 | 24.92 | 3.60 | secondary metabolism |
| TR165246_c2_g1_i1 m.223627;TR157924_c4_g1_i1 m.222400;TR172984_c0_g1_i1 m.224959;TR150363_c0_g1_i1 m.221098 | trans-cinnamate 4-hydroxylase | 16.05 | 21.80 | 25.80 | 4.00 | secondary metabolism |
| TR129113_c1_g1_i1 m.72913;TR128964_c2_g1_i1 m.72326;TR128964_c2_g1_i2 m.72327 | phenylalanine ammonia-lyase | 18.91 | 20.50 | 24.74 | 4.24 | secondary metabolism |
| TR97650_c7_g1_i1 m.29835;TR91773_c4_g2_i1 m.25784 | flavanone 3-hydroxylase | 24.17 | 22.15 | 26.74 | 4.60 | secondary metabolism |
| TR27580_c8_g1_i1 m.6412;TR172918_c12_g1_i1 m.22490 | | | | | | |
| 4;TR189856_c0_g1_i1 m.227964;TR158410_c0_g1_i1 m.222664;TRS3365_c0_g2_i1 m.11814;TR16132_c0_g2_i1 m.3718 | chalcone synthase | 16.08 | 24.12 | 28.13 | 4.01 | secondary metabolism |
| TR57118_c0_g2_i1 m.12529;TR57118_c0_g1_i1 m.12528 | Polyneuridine-aldehyde esterase | 11.98 | 21.21 | 24.79 | 3.58 | secondary metabolism |
| TR144022_c5_g1_i7 m.153123;TR143552_c3_g1_i3 m.149131 | NO ID | 16.10 | 20.79 | 24.80 | 4.01 | undear |
| TR132546_c1_g1_i4 m.84844;TR132546_c1_g1_i3 m.84843;TR132546_c1_g1_i2 m.84842 | NO ID | 7.30 | 21.11 | 23.97 | 2.87 | undear |

| | | | | | | |
|---|--|-------|-------|-------|------|----------------------|
| TR144523_c5_g3_i2 m.157852;TR141443_c2_g1_i1 m.132651 | Cytochrome b5 isoform B | 15.41 | 20.37 | 24.32 | 3.95 | primary metabolism |
| TR124540_c2_g1_i1 m.61424;TR124209_c1_g1_i1 m.60515;TR142169_c0_g1_i3 m.138029;TR142169_c0_g1_i4 m.138030;TR13737390_c0_g1_i3 m.106590;TR142169_c0_g1_i6 m.138032;TR142169_c0_g1_i7 m.138033;TR137390_c0_g1_i4 m.106591;TR137390_c0_g1_i1 m.106588;TR142169_c0_g1_i1 m.138027 | probable aminotransferase tat2 | 11.46 | 20.95 | 24.47 | 3.52 | primary metabolism |
| TR134660_c4_g1_i2 m.93641 | 4-hydroxyphenylpyruvate dioxygenase | 10.94 | 20.84 | 24.30 | 3.45 | primary metabolism |
| TR51875_c0_g1_i1 m.14238;TR51702_c0_g1_i1 m.10888 | alpha amylase family protein | 40.00 | 23.93 | 29.25 | 5.32 | primary metabolism |
| TR53334_c0_g1_i2 m.11804;TR53334_c0_g1_i1 m.11803;TR39690_c0_g1_i1 m.8541 | cytidine deaminase 1-like | 36.52 | 21.13 | 26.32 | 5.19 | primary metabolism |
| TR134660_c4_g1_i1 m.93640;TR130585_c2_g1_i1 m.77591;TR14660_c4_g1_i3 m.93642 | 4-hydroxyphenylpyruvate dioxygenase | 7.76 | 24.25 | 27.20 | 2.96 | primary metabolism |
| TR140093_c4_g1_i4 m.123189;TR137403_c4_g1_i1 m.106693 | Aspartyl protease family protein At5g10770 | 9.71 | 21.56 | 24.84 | 3.28 | proteolysis |
| TR140093_c4_g1_i6 m.123191;TR140093_c4_g1_i5 m.123190 | protein aspartic protease in guard cell 2-like | 8.07 | 21.27 | 24.28 | 3.01 | proteolysis |
| TR134932_c0_g1_i1 m.94738;TR134791_c0_g1_i2 m.94185;TR134791_c0_g1_i1 m.94183;TR134932_c0_g1_i2 m.94740 | senescence-specific cysteine protease sag12-like | 33.45 | 21.45 | 26.51 | 5.06 | proteolysis |
| TR140093_c4_g1_i2 m.123186;TR140093_c4_g1_i1 m.123185;TR130529_c2_g1_i2 m.77464;TR130529_c2_g1_i1 m.77462 | protein aspartic protease in guard cell 2-like | 9.34 | 22.92 | 26.14 | 3.22 | proteolysis |
| TR130652_c2_g1_i2 m.77821;TR130652_c2_g1_i1 m.77820;TR127276_c7_g1_i1 m.67682 | cysteine proteinase | 84.96 | 21.47 | 27.88 | 6.41 | proteolysis |
| TR103610_c0_g1_i1 m.35097;TR102661_c0_g1_i1 m.34224 | casp-like protein 1d1 | 27.30 | 20.66 | 25.43 | 4.77 | proteolysis |
| TR138971_c8_g1_i1 m.116078;TR137978_c5_g1_i1 m.110030 | aspartic proteinase-like | 24.97 | 22.60 | 27.25 | 4.64 | proteolysis |
| TR137544_c1_g1_i1 m.107570;TR137106_c0_g1_i1 m.105235;TR137544_c1_g1_i2 m.107572;TR137106_c0_g1_i2 m.105237 | basic 7s globulin-like | 18.47 | 22.22 | 26.43 | 4.21 | proteolysis |
| TR138438_c0_g1_i1 m.112914;TR138161_c0_g1_i1 m.111124;TR138161_c0_g1_i1 m.111125 | laccase-7-like | 46.07 | 22.73 | 28.26 | 5.53 | secondary metabolism |
| TR69842_c0_g2_i5 m.17194;TR60712_c0_g1_i2 m.13603;TR69842_c0_g2_i4 m.17192;TR69842_c0_g2_i1 m.17189;TR60712_c0_g1_i3 m.13606;TR60712_c0_g1_i1 m.13602 | serine carboxypeptidase-like | 26.36 | 21.39 | 26.11 | 4.72 | secondary metabolism |
| TR132461_c1_g1_i1 m.84509;TR137664_c0_g1_i1 m.108154 | reticuline oxidase-like protein | 29.69 | 20.73 | 25.63 | 4.89 | secondary metabolism |
| TR122998_c1_g1_i1 m.57844;TR115981_c1_g1_i1 m.47096;TR122998_c1_g1_i2 m.57845;TR115981_c1_g1_i2 m.47097 | probable glutathione s-transferase parc | 13.44 | 20.38 | 24.13 | 3.75 | stress response |
| TR52958_c0_g2_i1 m.11481;TR175233_c0_g1_i1 m.225562;TR52958_c0_g1_i1 m.11480 | peroxidase 12 | 24.83 | 21.54 | 26.17 | 4.63 | stress response |
| TR128074_c0_g1_i3 m.69837;TR147117_c0_g2_i7 m.183637;TR147117_c0_g2_i3 m.183629;TR128074_c0_g1_i2 m.69836;TR147117_c0_g1_i1 m.183626;TR128074_c0_g1_i1 m.69834;TR147117_c0_g2_i5 m.183632 | peroxidase 73-like | 39.58 | 20.86 | 26.17 | 5.31 | stress response |

| | | | | | | |
|---|----------------------------|--------|-------|-------|------|-----------------|
| TR187924_c0_g1_i1 m.227328;TR130764_c16_g1_i1 m.78272 | peroxidase p7-like | 10.19 | 25.06 | 28.41 | 3.35 | stress response |
| TR142141_c2_g1_i1 m.137795;TR118663_c1_g1_i1 m.50668;TR12703_c3_g1_i1 m.42853;TR92499_c0_g1_i1 m.26172 | cationic peroxidase 1-like | 269.23 | 21.11 | 29.18 | 8.07 | stress response |
| TR95252_c6_g2_i2 m.28000;TR95252_c6_g2_i1 m.27998;TR92851_c4_g2_i2 m.26331;TR92851_c4_g2_i1 m.26329 | dna binding | 20.95 | 22.05 | 26.44 | 4.39 | unclear |
| TR143332_c0_g1_i1 m.147353;TR143097_c1_g1_i2 m.145459;TR143097_c1_g1_i3 m.145460;TR143097_c1_g1_i1 m.145458 | NO ID | 15.42 | 26.52 | 30.47 | 3.95 | unclear |
| TR129191_c1_g1_i1 m.73168;TR125696_c1_g1_i1 m.63964 | endo- -beta- | 23.33 | 24.82 | 29.36 | 4.54 | unclear |

| | | | | | | |
|--|--|--------|-------|-------|------|----------------------|
| TR73121_c2_g1_i1 m. 18683;TR80104_c0_g1_i1 m.21413;TR80104_c0_g2_i1 m.21414 | phenylalanine ammonia-lyase | 16.42 | 21.63 | 25.67 | 4.04 | secondary metabolism |
| TR63112_c0_g2_i1 m. 14893;TR187887_c0_g1_i1 m.227298;TR63112_c0_g1_i1 m.14892 | chalcone isomerase | 26.82 | 21.45 | 26.20 | 4.75 | secondary metabolism |
| TR99990_c0_g1_i1 m. 32235;TR139304_c5_g1_i2 m.118168;TR68588_c0_g1_i1 m.16820;TR162830_c0_g1_i1 m.223395;TR9794_c0_g1_i1 m.2053 | laccase -14-like isoform x2 | 19.68 | 21.94 | 26.24 | 4.30 | secondary metabolism |
| TR137449_c3_g1_i1 m.106949;TR139963_c1_g2_i1 m.122248 | anthocyanidin reductase | 21.56 | 21.70 | 26.13 | 4.43 | secondary metabolism |
| TR97650_c7_g1_i1 m. 29836;TR91773_c4_g2_i1 m.25785 | flavanone 3-hydroxylase | 29.16 | 20.96 | 25.82 | 4.87 | secondary metabolism |
| TR31732_c0_g1_i1 m. 7106;TR26285_c0_g2_i1 m.6134;TR31732_c0_g2_i1 m.7108;TR26285_c0_g1_i1 m.6132 | zerubione synthase-like isoform x1 | 19.93 | 20.81 | 25.13 | 4.32 | secondary metabolism |
| TR172987_c0_g1_i1 m.224962;TR159528_c0_g1_i1 m.222981 | phenylalanine ammonia- partial | 26.86 | 21.29 | 26.03 | 4.75 | secondary metabolism |
| TR138438_c0_g1_i1 m.112914;TR138161_c0_g1_i1 m.111124;TR138161_c0_g1_i1 m.111125 | laccase -7-like | 92.23 | 20.40 | 26.93 | 6.53 | secondary metabolism |
| TR128175_c2_g1_i1 m.70049;TR127415_c0_g1_i1 m.68120 | 4-coumarate-- ligase 2-like | 26.06 | 20.93 | 25.63 | 4.70 | secondary metabolism |
| TR165246_c2_g1_i1 m.23667;TR157924_c4_g1_i1 m.222400;TR172984_c0_g1_i1 m.224959;TR150363_c0_g1_i1 m.221098 | trans-cinnamate 4-hydroxylase | 16.16 | 24.07 | 28.08 | 4.01 | secondary metabolism |
| TR172840_c1_g1_i1 m.224863;TR150098_c0_g1_i1 m.220735 | hydroxycinnamoyl - shikimate quinase | 37.71 | 22.04 | 27.27 | 5.24 | secondary metabolism |
| TR128947_c6_g1_i1 m.72236 | hydroxycinnamoyl transferase isoform 1 | 39.95 | 21.97 | 27.29 | 5.32 | secondary metabolism |
| TR124549_c2_g1_i1 m.61440;TR122350_c3_g1_i1 m.56759 | flavonoid 3 -hydroxylase 2-like | 13.60 | 23.40 | 27.16 | 3.77 | secondary metabolism |
| TR97650_c7_g1_i1 m. 29835;TR91773_c4_g2_i1 m.25784 | dihydroflavonol 4-reductase | 9.81 | 25.82 | 29.11 | 3.29 | secondary metabolism |
| TR129113_c1_g1_i1 m.72913;TR128964_c2_g1_i1 m.72326;TR128964_c2_g1_i1 m.72327 | flavanone 3-hydroxylase | 37.52 | 23.48 | 28.71 | 5.23 | secondary metabolism |
| TR143362_c2_g1_i1 m.147658;TR130640_c11_g1_i1 m.77780 | phenylalanine ammonia-lyase | 13.49 | 22.63 | 26.38 | 3.75 | secondary metabolism |
| TR150273_c0_g1_i1 m.220983;TR158395_c0_g1_i1 m.222657 | anthocyanidin -o-glucosyltransferase-like | 16.38 | 21.75 | 25.79 | 4.03 | secondary metabolism |
| TR122998_c1_g1_i1 m.57844;TR115981_c1_g1_i1 m.47096;TR122998_c1_g1_i1 m.57845;TR115981_c1_g1_i1 m.47097 | 4-coumarate--CoA ligase 1 | 13.16 | 21.14 | 24.86 | 3.72 | stress response |
| TR142141_c2_g1_i1 m.137795;TR118663_c1_g1_i1 m.50668;TR112703_c3_g1_i1 m.42853;TR92499_c0_g1_i1 m.26172 | probable glutathione s-transferase parac | 406.58 | 21.34 | 30.01 | 8.67 | stress response |
| TR187924_c0_g1_i1 m.227328;TR130764_c16_g1_i1 m.78272 | cationic peroxidase 1-like | 108.62 | 21.99 | 28.75 | 6.76 | stress response |
| TR64432_c0_g1_i3 m.15265;TR64432_c0_g1_i2 m.15264 | peroxidase p7-like | 17.75 | 22.07 | 26.22 | 4.15 | stress response |
| TR129191_c1_g1_i1 m.73168;TR125696_c1_g1_i1 m.63964 | Peroxidase 12 | 19.99 | 22.64 | 26.96 | 4.32 | undear |
| TR144022_c5_g1_i7 m.153123;TR143552_c3_g1_i3 m.149131 | endo- -beta- | 21.54 | 22.97 | 27.40 | 4.43 | undear |
| TR76633_c0_g1_i1 m.20094;TR69832_c0_g1_i1 m.17180;TR76633_c0_g1_i2 m.20095;TR69832_c0_g1_i2 m.17181 | NO ID | 12.57 | 20.86 | 24.51 | 3.65 | undear |
| | Uncharacterized GPI-anchored protein At5g19250 | | | | | |

Supplementary material number 3. Proteins that increase and decrease in level in the AZ on Day 4 (spatial comparisons)

| name sequence | protein name | fold change | log2[mean intensity Distal D4] | log2[mean intensity AZ D4] | relative abundance [log2(cond.1/control)] | function or category |
|---|--|-------------|--------------------------------|----------------------------|---|--------------------------|
| TR53009_c0_g1_i1 m.11552;TR39616_c0_g1_i1 m.8492 | endo- β -glucanase | 9.45 | 21.55 | 24.80 | 3.24 | cell wall transformation |
| TR138895_c0_g1_i2 m.115635;TR138895_c0_g1_i1 m.115632 | Tubulin-folding cofactor A | 8.03 | 20.94 | 23.95 | 3.00 | other |
| TR130358_c11_g1_i1 m.76869;TR129030_c5_g1_i1 m.72541 | ATP sulfurylase 1 | 7.60 | 20.68 | 23.61 | 2.93 | other |
| TR129488_c0_g1_i2 m.74143;TR129488_c0_g1_i1 m.74142;TR113960_c0_g1_i1 m.44458 | 65-kDa microtubule-associated protein 1 | 10.59 | 20.70 | 24.11 | 3.40 | other |
| TR59010_c0_g1_i1 m.13082;TR51682_c0_g1_i2 m.10855 | lactoylglutathione lyase glyoxalase I family protein | 20.60 | 20.87 | 25.23 | 4.36 | other |
| TR136792_c11_g1_i1 m.103397;TR132472_c1_g1_i2 m.84585;TR136792_c11_g1_i3 m.103398;TR132472_c1_g1_i1 m.84584 | gds1-motif lipase hydrolase family protein | 15.78 | 22.96 | 26.94 | 3.98 | primary metabolism |
| TR145939_c0_g2_i5 m.171224;TR145939_c0_g2_i2 m.171221;TR145939_c0_g2_i17 m.171231;TR146052_c2_g1_i2 m.172475 | pyruvate cytosolic isozyme Phospho-2-dehydro-3-deoxyheptonate aldolase 1 | 13.22 | 22.21 | 25.93 | 3.72 | primary metabolism |
| TR124673_c1_g1_i1 m.61669;TR123957_c0_g1_i1 m.59788 | thiamine thiazole chloroplastic | 9.64 | 22.14 | 25.41 | 3.27 | primary metabolism |
| TR124604_c5_g1_i1 m.61555;TR112326_c2_g1_i1 m.42385;TR27791_c0_g1_i1 m.6463;TR124604_c0_g1_i1 m.61554 | probable acyl-activating enzyme peroxisomal isoform x1 | 10.91 | 20.98 | 24.43 | 3.45 | primary metabolism |
| TR143014_c0_g1_i2 m.144805;TR143014_c0_g1_i1 m.144803;TR142866_c0_g1_i2 m.143640;TR142866_c0_g1_i1 m.143638;TR143014_c0_g1_i4 m.144808;TR143014_c0_g1_i3 m.144807 | 3-hydroxyisobutyryl- hydrolase-like protein 5 | 16.37 | 22.29 | 26.33 | 4.03 | primary metabolism |
| TR99429_c1_g1_i1 m.31681;TR99081_c2_g1_i1 m.31313 | Bifunctional 3-dehydroquininate dehydratase/shikimate dehydrogenase | 14.70 | 23.44 | 27.32 | 3.88 | primary metabolism |
| TR145012_c0_g1_i6 m.162617;TR144462_c0_g1_i5 m.157210;TR144462_c0_g1_i2 m.157206;TR145012_c0_g1_i8 m.162618 | | 22.74 | 20.99 | 25.49 | 4.51 | primary metabolism |
| TR94519_c0_g1_i3 m.27480;TR98866_c0_g1_i1 m.31091;TR94519_c0_g1_i2 m.27479;TR98866_c0_g1_i3 m.31095;TR94519_c0_g1_i1 m.27478;TR98866_c0_g1_i3 m.31094;TR98866_c0_g1_i2 m.31093;TR94519_c0_g1_i4 m.27483;TR94519_c0_g1_i1 m.27477;TR146195_c1_g1_i7 m.173920;TR146195_c1_g1_i2 m.173911;TR146195_c1_g1_i8 m.173921;TR146923_c1_g4_i1 m.181492;TR144554_c0_g1_i2 m.158130;TR144554_c0_g1_i1 m.158127 | dihydrofolate reductase-like cytochrome b5 | 17.20 | 20.98 | 25.08 | 4.10 | primary metabolism |
| TR347_c0_g1_i1 m.111;TR16490_c0_g1_i1 m.3897 | d-3-phosphoglycerate dehydrogenase chloroplastic-like | 16.79 | 21.29 | 25.36 | 4.07 | primary metabolism |
| TR145056_c0_g1_i1 m.162990;TR144840_c0_g1_i2 m.160884 | | 24.06 | 21.85 | 26.44 | 4.59 | primary metabolism |
| TR124151_c1_g1_i1 m.60405;TR111678_c0_g1_i1 m.41426;TR124151_c1_g1_i3 m.60407;TR111678_c0_g1_i4 m.41429 | 31 kDa ribonucleoprotein | 6.46 | 20.55 | 23.24 | 2.69 | RNA regulation |
| TR124549_c2_g1_i1 m.61440;TR122350_c3_g1_i1 m.56759 | dihydroflavonol 4-reductase | 16.80 | 23.09 | 27.16 | 4.07 | secondary metabolism |
| TR128175_c2_g1_i1 m.70049;TR127415_c0_g1_i1 m.68120 | 4-coumarate-- ligase 2-like | 20.03 | 21.31 | 25.63 | 4.32 | secondary metabolism |

| | | | | | | |
|--|---|-------|-------|-------|------|----------------------|
| TR117126_c0_g1_i1 m.48486;TR113467_c1_g1_i1 m.43796 | chalcone isomerase | 5.92 | 24.36 | 26.92 | 2.57 | secondary metabolism |
| TR137449_c3_g1_i1 m.106949;TR139963_c1_g2_i1 m.122248 | anthocyanidin reductase | 9.49 | 22.88 | 26.13 | 3.25 | secondary metabolism |
| TR99990_c0_g1_i1 m.32235;TR139304_c5_g1_i2 m.118166;TR68588_c0_g1_i1 m.16820;TR162830_c0_g1_i1 m.223395;TR9794_c0_g1_i1 m.2053 | laccase-14-like isoform x2 | 15.79 | 22.26 | 26.24 | 3.98 | secondary metabolism |
| TR88650_c0_g1_i1 m.23841;TR81613_c0_g1_i1 m.21838 | phenylalanine ammonia-lyase | 6.83 | 21.23 | 24.01 | 2.77 | secondary metabolism |
| TR97650_c7_g1_i1 m.29886;TR91773_c4_g2_i1 m.25785 | flavanone 3-hydroxylase | 9.72 | 22.54 | 25.82 | 3.28 | secondary metabolism |
| TR136343_c0_g3_i1 m.101198;TR35235_c0_g1_i1 m.7648;TR35235_c0_g1_i2 m.7651 | premnaspirodienone oxygenase-like | 8.08 | 21.27 | 24.29 | 3.01 | secondary metabolism |
| TR97650_c7_g1_i1 m.29885;TR91773_c4_g2_i1 m.25784 | flavanone 3-hydroxylase | 10.02 | 25.79 | 29.11 | 3.32 | secondary metabolism |
| TR27580_c8_g1_i1 m.6412;TR172918_c12_g1_i1 m.224904;TR189856_c0_g1_i1 m.227964;TR158410_c0_g1_i1 m.222664;TR53365_c0_g2_i1 m.11814;TR16132_c0_g2_i1 m.3718 | chalcone synthase | 13.82 | 27.02 | 30.80 | 3.79 | secondary metabolism |
| TR63112_c0_g2_i1 m.14893;TR187887_c0_g1_i1 m.227298;TR63112_c0_g1_i1 m.14892 | chalcone isomerase | 14.85 | 22.31 | 26.20 | 3.89 | secondary metabolism |
| TR116020_c0_g1_i1 m.47158;TR108051_c1_g1_i1 m.38609 | chalcone synthase | 20.84 | 21.94 | 26.33 | 4.38 | secondary metabolism |
| TR172987_c0_g1_i1 m.224962;TR159528_c0_g1_i1 m.222981 | phenylalanine ammonia- partial | 23.39 | 21.49 | 26.03 | 4.55 | secondary metabolism |
| TR117084_c1_g1_i1 m.48447;TR108383_c2_g1_i1 m.39201 | flavonoid 3-hydroxylase | 25.31 | 21.54 | 26.20 | 4.66 | secondary metabolism |
| TR128947_c6_g1_i1 m.72236 | flavonoid 3-hydroxylase 2-like | 38.74 | 22.02 | 27.29 | 5.28 | secondary metabolism |
| TR143362_c2_g1_i1 m.147658;TR130640_c11_g1_i1 m.77780 | anthocyanidin -o-glucosyltransferase-like | 43.14 | 20.95 | 26.38 | 5.43 | secondary metabolism |
| TR141645_c6_g1_i1 m.134169;TR111988_c3_g1_i3 m.41782;TR111988_c3_g1_i2 m.41781 | Glycine-rich RNA-binding protein 4 | 11.19 | 21.74 | 25.23 | 3.48 | stress response |
| TR144022_c5_g1_i4 m.153121 | NO ID | 7.39 | 20.94 | 23.83 | 2.89 | unclear |
| TR137662_c0_g1_i2 m.108127;TR137662_c0_g1_i1 m.108126;TR125470_c0_g2_i4 m.63370;TR125470_c0_g2_i3 m.63369 | NO ID | 12.22 | 22.33 | 25.94 | 3.61 | unclear |
| TR145616_c0_g2_i4 m.168118;TR145616_c0_g2_i1 m.168115;TR144727_c0_g1_i2 m.159716 | Uncharacterized protein At1g04910 | 8.09 | 20.97 | 23.99 | 3.02 | unclear |
| TR144022_c5_g1_i3 m.153120;TR144022_c5_g1_i1 m.153119 | NO ID | 9.84 | 21.42 | 24.72 | 3.30 | unclear |
| TR144022_c5_g1_i6 m.153122 | NO ID | 13.00 | 21.75 | 25.45 | 3.70 | unclear |
| TR144022_c5_g1_i7 m.153123;TR143552_c3_g1_i3 m.149131 | NO ID | 20.40 | 23.05 | 27.40 | 4.35 | unclear |

Proteins that de crease in the abscission zone relative to the distal region on Day 4

| name sequence | protein name | fold change | log2(mean intensity Distal D4) | log2(mean intensity AZ D4) | relative abundance [log2(cond.1/control)] | function or cathe gory |
|---|---|-------------|--------------------------------|----------------------------|---|--------------------------|
| TR135914_c0_g1_i1 m.98986;TR136740_c0_g1_i1 m.103077 | beta-galactosidase-like isoform x2 | 0.04 | 27.47 | 22.78 | -4.69 | cell wall transformation |
| TR13970_c0_g2_i1 m.3254;TR107733_c0_g2_i1 m.38138;TR13970_c0_g1_i1 m.3252;TR107733_c0_g1_i1 m.38136;TR13970_c0_g1_i1 m.3253;TR107733_c0_g1_i1 m.38137;TR143597_c1_g4_i1 m.149550;TR839_c0_g1_i1 m.109;TR44235_c0_g1_i1 m.9389;TR188809_c0_g1_i1 m.22772;TR159193_c0_g1_i1 m.222905;TR63425_c0_g1_i1 m.15035;TR54029_c0_g1_i1 m.11947;TR86558_c0_g1_i1 m.23229;TR85888_c0_g1_i1 m.23052 | beta-galactosidase 1-like | 0.06 | 25.47 | 21.29 | -4.17 | cell wall transformation |
| TR126856_c2_g1_i1 m.66536;TR127424_c1_g1_i1 m.68140 | beta-d-xylosidase family protein | 0.06 | 29.79 | 25.83 | -3.97 | cell wall transformation |
| TR131555_c1_g2_i9 m.80987;TR131555_c1_g2_i2 m.80979;TR131555_c1_g2_i11 m.80991;TR121532_c0_g1_i8 m.55138;TR121532_c0_g1_i7 m.55136;TR131555_c1_g2_i7 m.80986;TR121532_c0_g1_i9 m.55140;TR121532_c0_g1_i3 m.55130;TR121532_c0_g1_i10 m.55141;TR131555_c1_g2_i6 m.80984;TR131555_c1_g2_i13 m.80995;TR131555_c1_g2_i10 m.80989;TR121532_c0_g1_i16 m.55134;TR121532_c0_g1_i2 m.55128;TR121532_c0_g1_i1 m.55126;TR131555_c1_g2_i12 m.80994;TR121532_c0_g1_i4 m.55132 | bifunctional udp-glucose 4-epimerase and udp-xylose 4-epimerase 1 | 0.08 | 27.17 | 23.59 | -3.58 | cell wall transformation |
| TR8277_c0_g1_i1 m.1321;TR150803_c0_g1_i1 m.221318 | protein trichome birefringence-like 39 | 0.09 | 24.11 | 20.69 | -3.42 | cell wall transformation |
| TR96655_c0_g2_i3 m.29098;TR94490_c0_g1_i1 m.27421;TR96655_c0_g2_i1 m.29088 | extensin-2-like, extensin-2- partial | 0.06 | 25.59 | 21.63 | -3.96 | cell wall transformation |
| TR143080_c0_g2_i3 m.145310;TR143080_c0_g1_i2 m.145308;TR143080_c0_g1_i1 m.145306;TR17952_c0_g1_i1 m.49563;TR143080_c0_g1_i4 m.145312;TR137895_c0_g1_i3 m.109482;TR137895_c0_g1_i2 m.109480;TR137895_c0_g1_i1 m.109478 | protein trichome birefringence-like 38 | 0.13 | 23.83 | 20.92 | -2.91 | cell wall transformation |
| TR138857_c1_g1_i1 m.115376;TR136245_c2_g1_i1 m.100685 | protein notum homolog | 0.12 | 27.20 | 24.18 | -3.02 | cell wall transformation |
| TR3514_c0_g2_i1 m.603;TR27572_c0_g1_i1 m.6408;TR3514_c0_g1_i1 m.602;TR27572_c0_g2_i1 m.6411;TR3514_c0_g1_i1 m.601;TR27572_c0_g2_i1 m.6410 | endochitinase pr4-like | 0.06 | 32.18 | 28.23 | -3.95 | defence |
| TR144639_c4_g3_i2 m.158820 | Pathogen-related protein | 0.05 | 27.66 | 23.20 | -4.46 | defence |
| TR15226_c0_g1_i1 m.3496;TR151159_c0_g1_i1 m.221490 | allene oxide synthase | 0.12 | 27.44 | 24.35 | -3.09 | defence |
| TR76022_c0_g1_i1 m.19813;TR70661_c0_g1_i1 m.17634 | allene oxide synthase | 0.13 | 27.41 | 24.45 | -2.97 | defence |
| TR148272_c2_g1_i7 m.197047 | subtilisin-like protease | 0.14 | 24.35 | 21.53 | -2.82 | defence |
| TR52324_c0_g1_i1 m.11251;TR58137_c0_g1_i1 m.12722;REV__TR130988_c0_g1_i2 m.79046;REV__TR128743_c0_g1_i1 m.71560 | allene oxide synthase | 0.13 | 27.42 | 24.44 | -2.98 | defence |
| TR180671_c0_g1_i1 m.226195;TR165198_c0_g1_i1 m.223587;TR171185_c0_g1_i1 m.224685;TR29953_c0_g1_i1 m.6850;TR6842_c0_g1_i1 m.992 | polyphenol oxidase | 0.02 | 26.79 | 21.24 | -5.55 | other |
| TR149948_c2_g1_i1 m.218629;TR149013_c3_g1_i5 m.206009;TR149013_c3_g1_i5 m.206017;TR149013_c3_g1_i4 m.206016;TR149013_c3_g1_i3 m.206013;TR149013_c3_g1_i2 m.206012;TR109347_c0_g2_i1 m.39982;TR93893_c0_g1_i2 m.27034 | abc transporter c family member 10-like | 0.10 | 23.45 | 20.07 | -3.37 | other |
| TR131160_c0_g1_i2 m.79649;TR130844_c0_g1_i2 m.78554;TR131160_c0_g1_i1 m.79648 | 1-aminocyclopropane-1-carboxylate oxidase homolog 4-like | 0.11 | 24.79 | 21.54 | -3.25 | other |
| TR134506_c0_g1_i2 m.92943;TR128377_c0_g1_i4 m.70513;TR134506_c0_g1_i1 m.92942;TR128377_c0_g1_i3 m.70512;TR128377_c0_g1_i2 m.70510;TR134506_c0_g1_i3 m.92945;TR134506_c0_g1_i5 m.92949;TR128377_c0_g1_i1 m.70509;TR128377_c0_g1_i1 m.70508 | scaffold attachment factor b2 | 0.14 | 23.92 | 21.08 | -2.84 | other |
| TR128377_c0_g1_i5 m.70515;TR134506_c0_g1_i4 m.92947 | scaffold attachment factor b2 | 0.14 | 24.26 | 21.43 | -2.83 | other |
| TR121665_c1_g1_i2 m.55507;TR115969_c2_g1_i1 m.47087;TR121665_c1_g1_i1 m.55505;TR148812_c13_g1_i2 m.203748;TR121665_c1_g1_i1 m.55506 | branched-chain-amino-acid aminotransferase | 0.11 | 25.20 | 22.07 | -3.12 | other |
| TR124048_c0_g1_i1 m.60067;TR122051_c0_g1_i1 m.56333 | chloroplastic-like | 0.03 | 28.60 | 23.64 | -4.96 | other |
| | carbonic chloroplastic-like | | | | | |

| | | | | | | |
|---|--|------|-------|-------|-------|----------------------|
| TR126787_c4_g1_i2 m.66269;TR128774_c4_g1_i3 m.71662;TR128774_c4_g1_i1 m.71656;TR128774_c4_g1_i4 m.71665;TR128774_c4_i2 m.71659;TR126787_c4_g1_i1 m.66266;TR126787_c4_g1_i1 m.66268;TR128774_c4_g1_i4 m.71666;TR128774_c4_g1_i2 m.71660 | malate glyoxysomal | 0.01 | 27.40 | 21.09 | -6.31 | primary metabolism |
| TR61875_c0_g1_i1 m.14238;TR51702_c0_g1_i1 m.10888 | alpha-aminolase family protein | 0.02 | 29.25 | 23.61 | -5.64 | primary metabolism |
| TR53334_c0_g1_i2 m.11804;TR53334_c0_g1_i1 m.11803;TR39690_c0_g1_i1 m.8541 | cytidine deaminase 1-like | 0.06 | 26.32 | 22.19 | -4.14 | primary metabolism |
| TR8481_c0_g1_i1 m.1442;TR53298_c0_g1_i1 m.11784 | cell wall vacuolar inhibitor of fructosidase 1 | 0.08 | 25.47 | 21.82 | -3.65 | primary metabolism |
| TR146831_c2_g1_i5 m.180543;TR149708_c27_g2_i2 m.215290;TR146831_c2_g1_i4 m.180542;TR146831_c2_g1_i3 m.180539;TR146831_c2_g1_i1 m.180535;TR146831_c2_g1_i2 m.180537;TR149708_c27_g2_i1 m.215289;TR146831_c2_g1_i2 m.180538;TR146831_c2_g1_i1 m.180536 | alpha-aminoadipic semialdehyde synthase | 0.07 | 25.51 | 21.77 | -3.74 | primary metabolism |
| TR140950_c0_g1_i3 m.129169;TR140950_c0_g1_i1 m.129167;TR140384_c0_g1_i1 m.124969;TR140950_c0_g1_i4 m.129170;TR140950_c0_g1_i2 m.129168;TR140384_c0_g1_i2 m.124970;TR101342_c0_g1_i1 m.33209;TR103652_c0_g1_i1 m.35129 | inosine 5'-monophosphate dehydrogenase 2-like | 0.07 | 25.70 | 21.87 | -3.82 | primary metabolism |
| TR131706_c0_g1_i1 m.81531;TR130629_c0_g1_i1 m.77730 | gds1 esterase lipase at5g333370-like | 0.09 | 25.23 | 21.72 | -3.51 | primary metabolism |
| TR124540_c2_g1_i1 m.61424;TR124209_c1_g1_i1 m.60515;TR142169_c0_g1_i3 m.138029;TR142169_c0_g1_i4 m.138030;TR137390_c0_g1_i3 m.106590;TR142169_c0_g1_i6 m.138032;TR142169_c0_g1_i7 m.138033;TR137390_c0_g1_i4 m.106591;TR137390_c0_g1_i1 m.106588;TR142169_c0_g1_i1 m.138027 | probable aminotransferase tat2 | 0.11 | 24.47 | 21.27 | -3.20 | primary metabolism |
| TR61535_c0_g1_i1 m.14066;TR39712_c0_g1_i2 m.8554;TR61535_c0_g1_i2 m.14068;TR39712_c0_g1_i1 m.8552 | delta(-)-dienoyl- mitochondrial | 0.13 | 23.67 | 20.70 | -2.97 | primary metabolism |
| TR124382_c0_g1_i1 m.61016;TR123695_c0_g1_i1 m.59130;TR132427_c0_g1_i6 m.84360;TR139506_c0_g1_i2 m.119511;TR139506_c0_g1_i1 m.119509;TR132427_c0_g1_i4 m.84357;TR132427_c0_g1_i3 m.84354;TR132427_c0_g1_i1 m.84351;TR132427_c0_g1_i5 m.84359 | acetate butyrate-- ligase peroxisomal | 0.14 | 23.40 | 20.57 | -2.84 | primary metabolism |
| TR140093_c4_g1_i6 m.123191;TR140093_c4_g1_i5 m.123190 | protein aspartic protease in guard cell 2-like | 0.07 | 24.28 | 20.49 | -3.80 | proteolysis |
| TR69842_c0_g2_i5 m.17194;TR60712_c0_g1_i2 m.13603;TR69842_c0_g2_i4 m.17192;TR69842_c0_g2_i1 m.17189;TR60712_c0_g1_i3 m.13606;TR60712_c0_g1_i1 m.13602 | serine carboxypeptidase-like | 0.07 | 26.11 | 22.17 | -3.93 | proteolysis |
| TR145664_c6_g1_i1 m.168541;TR138653_c2_g1_i2 m.114143;TR145664_c6_g1_i3 m.168542;TR138653_c2_g1_i1 m.114142;TR138653_c2_g1_i3 m.114144 | probable glutamate carboxypeptidase 2 | 0.12 | 24.17 | 21.13 | -3.04 | proteolysis |
| TR137544_c1_g1_i1 m.107570;TR137106_c0_g1_i1 m.105235;TR137544_c1_g1_i2 m.107572;TR137106_c0_g1_i2 m.105237 | basic % globulin-like | 0.14 | 26.43 | 23.56 | -2.87 | proteolysis |
| TR5938_c0_g1_i1 m.844;TR22617_c0_g1_i1 m.5420 | basic % globulin-like | 0.15 | 29.30 | 26.57 | -2.73 | proteolysis |
| TR134932_c0_g1_i1 m.94738;TR134791_c0_g1_i2 m.94185;TR134791_c0_g1_i1 m.94183;TR134932_c0_g1_i2 m.94740 | senescence-specific cysteine protease sag12-like | 0.03 | 26.51 | 21.62 | -4.88 | proteolysis |
| TR16660_c0_g1_i1 m.4005;TR151367_c0_g1_i1 m.221551 | serine carboxypeptidase-like | 0.15 | 23.44 | 20.72 | -2.71 | proteolysis |
| TR188039_c0_g1_i1 m.22413;TR172929_c0_g1_i1 m.225081 | cannabidiolic acid synthase-like | 0.05 | 25.72 | 21.47 | -4.25 | secondary metabolism |
| TR128074_c0_g1_i3 m.69837;TR147117_c0_g2_i7 m.183637;TR147117_c0_g2_i3 m.183629;TR128074_c0_g1_i2 m.69836;TR147117_c0_g1_i1 m.183626;TR128074_c0_g1_i1 m.69834;TR147117_c0_g2_i5 m.183632 | peroxidase 73-like | 0.03 | 26.17 | 20.99 | -5.18 | stress response |
| TR52958_c0_g2_i1 m.11481;TR175233_c0_g1_i1 m.225562;TR52958_c0_g1_i1 m.11480 | peroxidase 12 | 0.05 | 26.17 | 21.89 | -4.28 | stress response |
| TR143830_c0_g1_i1 m.151655;TR144453_c0_g1_i1 m.157134 | NO ID | 0.03 | 26.10 | 20.89 | -5.21 | unclear |
| TR144453_c0_g1_i1 m.157133;TR143830_c0_g1_i1 m.151654 | NO ID | 0.06 | 25.06 | 20.92 | -4.14 | unclear |
| TR143332_c0_g1_i1 m.147353;TR143097_c1_g1_i2 m.145459;TR143097_c1_g1_i3 m.145460;TR143097_c1_g1_i1 m.145458 | NO ID | 0.05 | 30.47 | 26.25 | -4.22 | unclear |
| TR172690_c0_g3_i1 m.224754;TR172690_c0_g2_i1 m.224752;TR172690_c0_g1_i1 m.224750;TR172690_c0_g1_i1 m.222339 | isoform 1 | 0.11 | 25.40 | 22.20 | -3.21 | unclear |

| Proteins that increase in the abscission zone relative to the proximal region on Day 4 | | | | | | |
|--|--|-------------|----------------------------------|----------------------------|---|--------------------------|
| name sequence | protein name | fold change | log2(mean intensity Proximal D4) | log2(mean intensity AZ D4) | relative abundance [log2(cond.1/control)] | function or category |
| TR126856_c2_g1_i1 m.66536;TR127424_c1_g1_i1 m.68140 | beta-d-xyloridase family protein | 30.26 | 20.91 | 25.83 | 4.92 | cell wall transformation |
| TR187879_c1_g1_i1 m.227292;TR172871_c0_g1_i1 m.224876 | Probable polygalacturonase | 13.20 | 21.34 | 25.06 | 3.72 | cell wall transformation |
| TR53009_c0_g1_i1 m.11522;TR93616_c0_g1_i1 m.8492 | endo-β-glucanase | 10.73 | 21.37 | 24.80 | 3.42 | cell wall transformation |
| TR111814_c0_g1_i2 m.41572;TR111814_c0_g1_i1 m.41570 | alpha-glucan-protein synthase | 14.69 | 21.98 | 25.86 | 3.88 | cell wall transformation |
| TR99175_c2_g1_i1 m.31406 | major allergen pru | 545.15 | 20.92 | 30.01 | 9.09 | defence |
| TR3514_c0_g2_i1 m.603;TR27572_c0_g1_i1 m.6408;TR3514_c0_g1_i1 m.602;TR27572_c0_g2_i1 m.6411;TR3514_c0_g1_i1 m.601;TR27572_c0_g2_i1 m.6410 | endochitinase pr4-like | 65.65 | 22.19 | 28.23 | 6.04 | defence |
| TR112327_c2_g1_i1 m.42387;TR112667_c4_g2_i1 m.42978 | thaumatin-like protein 1b | 25.01 | 25.10 | 29.74 | 4.64 | defence |
| TR102949_c0_g1_i1 m.34528 | wound-induced protein win1 | 38.08 | 23.48 | 28.73 | 5.25 | defence |
| TR76022_c0_g1_i1 m.19813;TR70661_c0_g1_i1 m.17634 | allene oxide synthase | 10.46 | 21.06 | 24.45 | 3.39 | defence |
| TR15226_c0_g1_i1 m.3496;TR151159_c0_g1_i1 m.221490 | allene oxide synthase | 9.83 | 21.05 | 24.35 | 3.30 | defence |
| TR130237_c0_g1_i2 m.76489;TR128267_c0_g1_i1 m.70254;TR130237_c0_g1_i1 m.76488;TR128267_c0_g1_i2 m.70255 | disease resistance response protein | 10.59 | 21.01 | 24.42 | 3.40 | defence |
| TR132941_c0_g1_i1 m.86176;TR129779_c0_g1_i2 m.74981;TR132941_c0_g1_i2 m.86177;TR129779_c0_g1_i1 m.74980 | peroxisomal -2-hydroxy-acid oxidase glø4-like | 15.37 | 22.46 | 26.40 | 3.94 | other |
| TR126156_c0_g1_i1 m.64934;TR125426_c0_g1_i2 m.63270;TR126156_c0_g1_i2 m.64935;TR125426_c0_g1_i1 m.63269 | 206-like | 6.11 | 21.07 | 23.68 | 2.61 | other |
| TR136792_c11_g1_i1 m.103397;TR132472_c1_g1_i2 m.84585;TR136792_c11_g1_i3 m.103398;TR132472_c1_g1_i1 m.84584 | 1-amino cyclopropane-1-carboxylate oxidase 5 | 59.12 | 21.05 | 26.94 | 5.89 | primary metabolism |
| TR94519_c0_g1_i3 m.27480;TR98866_c0_g1_i1 m.31091;TR94519_c0_g1_i2 m.27479;TR98866_c0_g1_i3 m.31095;TR94519_c0_g1_i1 m.27478;TR98866_c0_g1_i3 m.31094;TR98866_c0_g1_i2 m.31093;TR94519_c0_g1_i4 m.27483;TR94519_c0_g1_i1 m.27477;TR146195_c1_g1_i7 m.17392 | gds1-motif lipase hydrolase family protein | 17.61 | 20.94 | 25.08 | 4.14 | primary metabolism |
| 0;TR146195_c1_g1_i2 m.173911;TR146195_c1_g1_i8 m.173921;TR146923_c1_g4_i10 m.181492;TR144554_c0_g1_i2 m.158130;TR144554_c0_g1_i1 m.158127 | dihydrofolate reductase-like | 6.98 | 20.94 | 23.74 | 2.80 | primary metabolism |
| TR132807_c1_g1_i3 m.85722;TR132807_c1_g1_i2 m.85720;TR132807_c1_g1_i1 m.85719;TR121809_c0_g1_i2 m.55779 | S-adenosylmethionine synthase 4 | 10.38 | 22.12 | 25.49 | 3.38 | primary metabolism |
| TR145012_c0_g1_i6 m.162617;TR144462_c0_g1_i5 m.157210;TR144462_c0_g1_i2 m.157206;TR145012_c0_g1_i8 m.162618 | Bifunctional 3-dehydroquininate dehydratase/shikimate dehydrogenase, chloroplastic | 6.09 | 21.06 | 23.67 | 2.61 | primary metabolism |
| TR144462_c0_g1_i4 m.157209;TR145012_c0_g1_i5 m.162614;TR145012_c0_g1_i1 m.162608;TR144462_c0_g1_i3 m.157207;TR145012_c0_g1_i9 m.162621;TR145012_c0_g1_i2 m.162609;TR145012_c0_g1_i8 m.162619;TR145012_c0_g1_i3 m.162610 | bifunctional 3-dehydroquininate dehydratase shikimate chloroplastic-like | 6.65 | 21.39 | 24.13 | 2.73 | primary metabolism |
| TR136285_c0_g1_i3 m.100894;TR132904_c2_g2_i2 m.86040;TR132904_c2_g2_i1 m.86038;TR136285_c0_g1_i4 m.100896;TR136285_c0_g1_i1 m.100893 | UDP-glucuronic acid decarboxylase 2 | 9.40 | 24.24 | 27.48 | 3.23 | primary metabolism |
| TR144872_c7_g1_i1 m.180918;TR145883_c10_g2_i3 m.170696;TR145883_c10_g2_i2 m.170694 | Acetyl-CoA carboxylase 1 | 38.44 | 20.81 | 26.07 | 5.26 | proteolysis |
| TR130652_c2_g1_i2 m.77821;TR130652_c2_g1_i1 m.77820;TR127276_c7_g1_i1 m.67682 | cysteine protease | 9.50 | 21.29 | 24.54 | 3.25 | proteolysis |
| TR180432_c0_g2_i1 m.226038;TR180914_c0_g1_i1 m.226039;TR180432_c0_g1_i1 m.226037 | Asparyl protease family protein 1 | 9.31 | 24.31 | 27.53 | 3.22 | proteolysis |
| TR135800_c5_g1_i1 m.98495;TR132526_c2_g2_i2 m.84803;TR132526_c2_g1_i1 m.84800 | cysteine proteinase rd21a-like | | | | | |

| | | | | | | |
|--|--|-------|-------|-------|------|----------------------|
| TR140093_c4_g1_2 m.123186;TR140093_c4_g1_1 m.123185;TR130529_c2_g1_2 m.77464;TR130529_c2_g1_1 m.77462 | protein aspartic protease in guard cell 2-like | 11.57 | 20.75 | 24.28 | 3.53 | proteolysis |
| TR144716_c0_g1_1 m.159583 | u6 snrna-associated sm-like protein | 11.55 | 22.61 | 26.14 | 3.53 | RNA regulation |
| TR138438_c0_g1_1 m.112914;TR138161_c0_g1_1 m.111125 | lsm2 | 61.41 | 20.99 | 26.93 | 5.94 | secondary metabolism |
| TR137041_c1_g1_1 m.104791;TR98968_c1_g1_1 m.31196;TR137041_c1_g2_1 m.104792;TR180417_c1_g1_1 m.226027;TR137041_c1_g2_2 m.104793 | laccase-7-like | 31.25 | 22.27 | 27.24 | 4.97 | secondary metabolism |
| TR128175_c2_g1_1 m.70049;TR127415_c0_g1_1 m.68120 | caffeoyl- o-methyltransferase | 15.73 | 21.66 | 25.63 | 3.98 | secondary metabolism |
| TR136343_c0_g3_1 m.101198;TR35235_c0_g1_1 m.7648;TR35235_c0_g1_2 m.7651 | 4-coumarate-- ligase 2-like | 10.00 | 20.97 | 24.29 | 3.32 | secondary metabolism |
| TR150273_c0_g1_1 m.220983;TR158395_c0_g1_1 m.22657 | premnaspirodiene oxygenase-like | 11.78 | 22.23 | 25.79 | 3.56 | secondary metabolism |
| TR129113_c0_g1_1 m.72913;TR128964_c2_g1_1 m.72326;TR128964_c2_g1_2 m.72327 | 4-coumarate--CoA ligase 1 | 14.39 | 24.86 | 28.71 | 3.85 | secondary metabolism |
| TR172987_c0_g1_1 m.224962;TR159528_c0_g1_1 m.222981 | phenylalanine ammonia-lyase | 11.98 | 22.45 | 26.03 | 3.58 | secondary metabolism |
| TR130658_c0_g1_2 m.77854;TR130658_c0_g1_1 m.77852;TR138467_c0_g1_12 m.113050;TR138467_c0_g1_11 m.113048;TR138467_c0_g1_16 m.113058;TR138467_c0_g1_15 m.113056;TR138467_c0_g1_14 m.113054;TR130658_c0_g1_17 m.77860;TR130658_c0_g1_14 m.77858;TR130658_c0_g1_18 m.77862;TR130658_c0_g1_13 m.77856 | phenylalanine ammonia- partial | 8.10 | 20.80 | 23.81 | 3.02 | |
| TR136614_c0_g2_1 m.102505;TR135008_c0_g1_1 m.95058 | secoisolaricresinol dehydrogenase-like | 10.31 | 21.56 | 24.93 | 3.37 | secondary metabolism |
| TR128947_c6_g1_1 m.72236 | omega-hydroxykypal mitate o-feruloyl transferase | 7.14 | 24.45 | 27.29 | 2.84 | secondary metabolism |
| TR172840_c1_g1_1 m.224863;TR150098_c0_g1_1 m.220735 | flavonoid 3--hydroxylase 2-like | 80.81 | 20.94 | 27.27 | 6.34 | secondary metabolism |
| TR98850_c0_g1_1 m.31055;TR102633_c2_g1_1 m.34191 | hydroxycinnamoyl- shikimate quinate isoform 1 | 27.01 | 21.90 | 26.66 | 4.76 | secondary metabolism |
| TR98687_c1_g2_1 m.30826;TR107931_c0_g1_1 m.38454 | cytochrome p450 cyp82d47-like | 5.13 | 25.54 | 27.90 | 2.36 | secondary metabolism |
| TR147141_c2_g1_1 m.137795;TR118663_c1_g1_1 m.50668;TR112703_c3_g1_1 m.42853;TR92499_c0_g1_1 m.26172 | caffeic acid o-methyltransferase | 11.31 | 21.30 | 24.80 | 3.50 | stress response |
| TR187924_c0_g1_1 m.227328;TR130764_c16_g1_1 m.78272 | cationic peroxidase 1-like | 19.38 | 24.48 | 28.75 | 4.28 | stress response |
| TR64432_c0_g1_13 m.15265;TR64432_c0_g1_12 m.15264 | peroxidase p7-like | 19.19 | 21.96 | 26.22 | 4.26 | stress response |
| TR118345_c1_g1_1 m.50178;TR118179_c0_g1_1 m.49918;TR47901_c0_g1_1 m.9999;TR82268_c0_g1_1 m.22049 | Peroxidase 12 | 5.05 | 25.78 | 28.11 | 2.34 | stress response |
| TR140002_c9_g1_1 m.122475;TR139701_c10_g2_14 m.120777 | peroxidase 12-like | 10.58 | 22.40 | 25.81 | 3.40 | stress response |
| TR122998_c1_g1_1 m.57844;TR115981_c1_g1_1 m.47096;TR122998_c1_g1_12 m.57845;TR115981_c1_g1_12 m.47097 | heat shock cognate 70 kda protein 2-like | 15.33 | 20.92 | 24.86 | 3.94 | stress response |
| TR129191_c1_g1_1 m.73168;TR125696_c1_g1_1 m.63964 | probable glutathione s-transferase | 46.85 | 21.41 | 26.96 | 5.55 | stress response |
| TR144022_c5_g1_13 m.153120;TR144022_c5_g1_11 m.153119 | endo--beta-parc | 13.05 | 21.02 | 24.72 | 3.71 | unclear |
| TR143332_c0_g1_1 m.147353;TR1433097_c1_g1_2 m.145459;TR1433097_c1_g1_3 m.145460;TR143097_c1_g1_1 m.145458 | NO ID | 23.59 | 21.69 | 26.25 | 4.56 | unclear |
| TR144022_c5_g1_14 m.153121 | NO ID | 7.95 | 20.84 | 23.83 | 2.99 | unclear |
| TR34536_c0_g1_1 m.7544;TR13733_c0_g1_1 m.3062 | hypothetical protein POP TR_0006504880g | 6.19 | 21.27 | 23.90 | 2.63 | unclear |

| | | | | | | |
|--|--|------|-------|-------|-------|----------------------|
| TR145321_c9_g1_i3 m.165455 | Granule-bound starch synthase 1, chloroplastic/amyloplastic | 0.13 | 24.30 | 21.34 | -2.97 | primary metabolism |
| TR145321_c9_g1_i2 m.165454 | Granule-bound starch synthase 1, chloroplastic/amyloplastic | 0.14 | 23.72 | 20.85 | -2.87 | primary metabolism |
| TR78347_c0_g2_i1 m.20740;TR75803_c0_g1_i1 m.19746 | Inositol-3-phosphate synthase | 0.15 | 23.76 | 21.00 | -2.77 | primary metabolism |
| TR142992_c9_g1_i1 m.144628;TR149326_c2_g1_i1 m.210066 | alpha-glucan-branching enzyme chloroplastic amyloplastic-like isoform X2 | 0.06 | 24.78 | 20.71 | -4.07 | primary metabolism |
| TR141833_c0_g1_i1 m.8942;TR89600_c1_g1_i2 m.24184 | Serine hydroxymethyltransferase, mitochondrial | 0.07 | 25.57 | 21.68 | -3.89 | primary metabolism |
| TR147444_c0_g1_i3 m.187498 | Citrate synthase, mitochondrial | 0.05 | 25.85 | 21.60 | -4.25 | primary metabolism |
| TR133147_c0_g1_i2 m.86785;TR145345_c8_g1_i2 m.165650;TR148225_c2_g1_i1 m.208701;TR138520_c0_g1_i1 m.113358;TR138965_c1_g1_i1 m.116010 | aspartic proteinase nepenthesin-1 | 0.03 | 26.48 | 21.59 | -4.89 | proteolysis |
| TR139301_c0_g1_i1 m.118131;TR143872_c0_g2_i3 m.151940;TR114426_c0_g1_i2 m.45150 | scopoletin glucosyltransferase-like Alpha-copaene synthase | 0.15 | 22.93 | 20.48 | -2.46 | secondary metabolism |
| TR149459_c0_g2_i2 m.211845;TR149459_c0_g2_i1 m.211841;TR152511_c0_g1_i1 m.221793;TR151709_c0_g1_i1 m.221645;TR192524_c0_g1_i1 m.228241 | probable terpene synthase 6 | 0.15 | 23.68 | 20.91 | -2.76 | secondary metabolism |
| TR140557_c3_g1_i2 m.126285 | terpene synthase 10-like | 0.09 | 24.86 | 21.31 | -3.55 | secondary metabolism |
| TR115421_c0_g1_i2 m.46344;TR114132_c0_g1_i1 m.44700;TR115421_c0_g1_i1 m.46343;TR114132_c0_g1_i2 m.44701 | probable caffeine synthase 4 | 0.08 | 24.96 | 21.24 | -3.72 | secondary metabolism |
| TR140691_c1_g1_i1 m.127264;TR140557_c3_g1_i1 m.126284;TR140557_c3_g1_i3 m.126286 | terpene synthase 10-like | 0.04 | 29.21 | 24.62 | -4.59 | secondary metabolism |
| TR172734_c1_g1_i1 m.224784;TR165347_c3_g1_i1 m.223704 | peroxidase 42 | 0.09 | 24.58 | 21.16 | -3.41 | stress response |
| TR129152_c0_g1_i1 m.73048;TR124474_c1_g1_i1 m.61223;TR140446_c4_g5_i1 m.125393 | uncharacterized acetyltransferase at3g50280-like | 0.18 | 26.14 | 23.64 | -2.50 | unclear |
| TR143234_c2_g1_i1 m.146722;TR143464_c2_g1_i1 m.148513 | NO ID | 0.14 | 25.63 | 22.77 | -2.86 | unclear |
| TR143872_c0_g2_i3 m.151939;TR139301_c0_g1_i1 m.118130;TR143872_c0_g2_i4 m.151941;TR143872_c0_g2_i2 m.151938 | NO ID | 0.10 | 24.43 | 21.09 | -3.34 | unclear |
| TR123008_c0_g1_i1 m.57852;TR127652_c0_g1_i1 m.68707 | serine-threonine protein plant- | 0.08 | 24.91 | 21.23 | -3.68 | unclear |

| | | | | | | |
|---|---|-------|-------|-------|------|----------------------|
| TR146872_c7_g11_i3 m.180918;TR145883_c10_g2_i3 m.170696;TR145883_c10_g2_i2 m.170694 | Acetyl-CoA carboxylase 1 | 22.83 | 23.22 | 27.73 | 4.51 | primary metabolism |
| TR99429_c1_g1_i1 m.31681;TR99081_c2_g1_i1 m.31313 | 3-hydroxyisobutyryl- hydrolase-like protein 5 | 21.78 | 23.26 | 27.71 | 4.44 | primary metabolism |
| TR124673_c1_g1_i1 m.61669;TR123957_c0_g1_i1 m.59788 | Phospho-2-dehydro-3-deoxyheptonate aldolase 1, chloroplastic | 13.73 | 21.66 | 25.44 | 3.78 | primary metabolism |
| TR143014_c0_g1_i2 m.144805;TR143014_c0_g1_i1 m.144803;TR142866_c0_g1_i2 m.143640;TR142866_c0_g1_i1 m.143638;TR143014_c0_g1_i4 m.144808;TR143014_c0_g1_i3 m.144807 | probable acyl-activating enzyme peroxisomal isoform x1 | 24.77 | 21.89 | 26.52 | 4.63 | primary metabolism |
| TR94519_c0_g1_i3 m.27480;TR98866_c0_g1_i1 m.31091;TR94519_c0_g1_i2 m.2747 | dihydrofolate reductase-like Bifunctional 3-dehydroquininate dehydratase/shikimate dehydrogenase, chloroplastic | 16.24 | 21.07 | 25.09 | 4.02 | primary metabolism |
| 9;TR98866_c0_g1_i3 m.31095;TR94519_c0_g1_i1 m.27478;TR98866_c0_g1_i3 m.310 | | | | | | |
| 94;TR98866_c0_g1_i2 m.31093;TR94519_c0_g1_i4 m.27483;TR94519_c0_g1_i1 m.27 | | | | | | |
| 477;TR146195_c1_g1_i7 m.173920;TR146195_c1_g1_i2 m.173911;TR146195_c1_g1_i | pyruvate cytosolic isozyme d-3-phosphoglycerate dehydrogenase chloroplastic-like | 27.17 | 20.92 | 25.68 | 4.76 | primary metabolism |
| 8 m.173921;TR146923_c1_g4_i10 m.181492;TR144554_c0_g1_i2 m.158130;TR14455 | | | | | | |
| 4_c0_g1_i1 m.158127 | | | | | | |
| TR145012_c0_g1_i6 m.162617;TR144462_c0_g1_i5 m.157210;TR144462_c0_g1_i2 m | plasmalogen activator inhibitor 1 rna-binding | 7.15 | 20.97 | 23.81 | 2.84 | RNA regulation |
| .157206;TR145012_c0_g1_i8 m.162618 | | | | | | |
| TR145939_c0_g2_i5 m.171224;TR145939_c0_g2_i2 m.171221;TR145939_c0_g2_i1 7 | | | | | | |
| m.171231;TR146052_c2_g1_i2 m.172475 | Protein decapping 5 | 5.36 | 20.60 | 23.02 | 2.42 | RNA regulation |
| TR145056_c0_g1_i1 m.162990;TR144840_c0_g1_i2 m.160884 | | | | | | |
| TR147270_c2_g4_i4 m.185487;TR147270_c2_g4_i2 m.185483;TR147270_c2_g4_i1 m | | | | | | |
| .185480;TR136050_c2_g1_i2 m.99775;TR147270_c2_g4_i8 m.185493;TR147270_c2_g | La protein 1 | 9.14 | 21.06 | 24.26 | 3.19 | RNA regulation |
| 0_c2_g4_i8 m.185494;TR147270_c2_g4_i6 m.185492 | | | | | | |
| TR147877_c1_g1_i4 m.192423;TR148339_c1_g1_i3 m.197876;TR147877_c1_g1_i6 m | | | | | | |
| .192428;TR148339_c1_g1_i1 m.197872;TR147877_c1_g1_i3 m.192420;TR147877_c1 | chalcone synthase | 28.70 | 26.31 | 31.15 | 4.84 | secondary metabolism |
| g1_i7 m.192431;TR147877_c1_g1_i2 m.192418;TR148339_c1_g1_i5 m.197879;TR148 | | | | | | |
| 339_c1_g1_i2 m.197874;TR147877_c1_g1_i8 m.192434;TR147877_c1_g1_i5 m.19242 | | | | | | |
| 5;TR147877_c1_g1_i1 m.192416 | secoisolaricresinol dehydrogenase-like | 9.36 | 21.71 | 24.93 | 3.23 | secondary metabolism |
| TR137170_c0_g1_i4 m.105535;TR137170_c0_g1_i5 m.105536;TR136894_c0_g1_i4 m | | | | | | |
| .103927;TR136894_c0_g1_i3 m.103926;TR137170_c0_g1_i3 m.105534;TR136894_c0 | | | | | | |
| g1_i1 m.103924 | phenylalanine ammonia-lyase | 8.13 | 26.02 | 29.05 | 3.02 | secondary metabolism |
| TR27580_c8_g1_i1 m.6412;TR172918_c12_g1_i1 m.224904;TR189856_c0_g1_i1 m.2 | | | | | | |
| 27964;TR158410_c0_g1_i1 m.222664;TR53365_c0_g2_i1 m.11814;TR16132_c0_g2_i1 | | | | | | |
| m.3718 | Cytochrome P450 71D10 | 7.05 | 21.52 | 24.33 | 2.82 | secondary metabolism |
| TR129226_c0_g1_i2 m.73257;TR134229_c0_g1_i2 m.91710;TR129226_c0_g1_i1 m.7 | | | | | | |
| 3256 | | | | | | |
| TR129113_c1_g1_i1 m.72913;TR128964_c2_g1_i1 m.72326;TR128964_c2_g1_i2 m.7 | | | | | | |
| 2327 | | | | | | |
| TR182656_c0_g1_i1 m.226782;TR32489_c0_g1_i1 m.7203 | | | | | | |

| | | | | | | |
|---|---|-------|-------|-------|------|----------------------|
| TR678_c0_g1_i1 m.168;TR678_c0_g2_i1 m.172;TR188048_c0_g1_i1 m.227420;TR42218_c0_g1_i1 m.9004;TR188048_c0_g2_i1 m.227422 | isoflavone reductase-like protein | 7.10 | 21.71 | 24.54 | 2.83 | secondary metabolism |
| TR88550_c0_g1_i1 m.23841;TR81613_c0_g1_i1 m.21838 | phenylalanine ammonia-lyase | 6.31 | 21.83 | 24.48 | 2.66 | secondary metabolism |
| TR144022_c5_g1_i3 m.153120;TR144022_c5_g1_i1 m.153119 | Leucoanthocyanidin dioxygenase | 9.17 | 21.08 | 24.28 | 3.20 | secondary metabolism |
| TR73121_c2_g1_i1 m.18683;TR80104_c0_g1_i1 m.21413;TR80104_c0_g2_i1 m.21414 | | | | | | |
| 4 | phenylalanine ammonia-lyase | 9.54 | 22.72 | 25.97 | 3.25 | secondary metabolism |
| TR63112_c0_g2_i1 m.14893;TR187887_c0_g1_i1 m.227298;TR63112_c0_g1_i1 m.14892 | chalcone isomerase | 8.90 | 23.38 | 26.54 | 3.15 | secondary metabolism |
| TR136614_c0_g2_i1 m.102505;TR135008_c0_g1_i1 m.95058 | omega-hydroxypalmitate o-fenuloyl transferase | 7.54 | 23.84 | 26.76 | 2.91 | secondary metabolism |
| TR117126_c0_g1_i1 m.48486;TR113467_c1_g1_i1 m.43796 | chalcone isomerase | 6.87 | 24.51 | 27.29 | 2.78 | secondary metabolism |
| TR152767_c0_g1_i1 m.221837;TR48719_c0_g1_i1 m.10139 | Costunolide synthase | 9.05 | 21.73 | 24.91 | 3.18 | secondary metabolism |
| TR137449_c3_g1_i1 m.106949;TR139963_c1_g2_i1 m.122248 | anthocyanidin reductase | 16.35 | 22.87 | 26.90 | 4.03 | secondary metabolism |
| TR136343_c0_g3_i1 m.101198;TR95235_c0_g1_i1 m.7648;TR95235_c0_g1_i2 m.7651 | premnaspirodiene oxygenase-like | 11.68 | 20.94 | 24.49 | 3.55 | secondary metabolism |
| TR128175_c2_g1_i1 m.70049;TR127415_c0_g1_i1 m.68120 | 4-coumarate-- ligase 2-like | 18.20 | 21.47 | 25.66 | 4.19 | secondary metabolism |
| TR97650_c7_g1_i1 m.29836;TR91773_c4_g2_i1 m.25785 | flavanone 3-hydroxylase | 14.97 | 22.28 | 26.19 | 3.90 | secondary metabolism |
| TR172987_c0_g1_i1 m.224962;TR159528_c0_g1_i1 m.222981 | phenylalanine ammonia- partial | 21.94 | 22.14 | 26.59 | 4.46 | secondary metabolism |
| TR97650_c7_g1_i1 m.29835;TR91773_c4_g2_i1 m.25784 | flavanone 3-hydroxylase | 28.69 | 24.65 | 29.49 | 4.84 | secondary metabolism |
| TR117084_c1_g1_i1 m.48447;TR108583_c2_g1_i1 m.39201 | flavonoid 3--hydroxylase | 33.46 | 21.22 | 26.29 | 5.06 | secondary metabolism |
| TR128947_c6_g1_i1 m.72236 | flavonoid 3--hydroxylase 2-like | 38.29 | 22.28 | 27.54 | 5.26 | secondary metabolism |
| TR148362_c2_g1_i1 m.147658;TR130640_c11_g1_i1 m.77780 | anthocyanidin -o-glucosyltransferase-like | 37.20 | 21.21 | 26.43 | 5.22 | secondary metabolism |
| TR124549_c2_g1_i1 m.61440;TR122350_c3_g1_i1 m.56759 | dihydroflavonol 4-reductase | 79.00 | 21.16 | 27.46 | 6.30 | secondary metabolism |
| TR116020_c0_g1_i1 m.47158;TR108051_c1_g1_i1 m.38609 | chalcone synthase | 52.03 | 21.13 | 26.83 | 5.70 | secondary metabolism |
| TR141645_c6_g1_i2 m.134170;TR111988_c3_g1_i1 m.41779 | Glycine-rich RNA-binding protein 2 | 8.03 | 22.70 | 25.70 | 3.01 | stress response |
| TR135901_c1_g1_i1 m.98937;TR137506_c1_g1_i1 m.107362;TR137506_c1_g1_i2 m.107363;TR137506_c1_g1_i3 m.107364;TR137506_c1_g1_i4 m.107365 | Probable glutathione peroxidase 8 | 7.18 | 20.59 | 23.43 | 2.84 | stress response |
| TR140002_c9_g1_i1 m.122475;TR139701_c10_g2_i4 m.120777 | heat shock cognate 70 kda protein 2-like | 13.06 | 21.78 | 25.49 | 3.71 | stress response |
| TR149613_c2_g2_i1 m.213806 | Endoplasmic homolog | 9.68 | 20.76 | 24.04 | 3.28 | stress response |
| TR59163_c0_g1_i1 m.131889;TR22274_c0_g1_i1 m.5278;TR59163_c0_g2_i1 m.13192;TR22274_c0_g2_i1 m.5281 | Polyadenylate-binding protein RBP47 | 6.23 | 21.69 | 24.33 | 2.64 | stress response |
| TR137662_c0_g1_i3 m.108128;TR125470_c0_g2_i2 m.63368;TR125470_c0_g2_i1 m.63367 | NO ID | 7.88 | 21.22 | 24.20 | 2.98 | undear |
| TR144022_c5_g1_i6 m.153122 | NO ID | 21.14 | 21.53 | 25.93 | 4.40 | undear |
| TR144022_c5_g1_i7 m.153123;TR143552_c3_g1_i3 m.149131 | NO ID | 39.67 | 22.20 | 27.51 | 5.31 | undear |
| TR137662_c0_g1_i2 m.108127;TR137662_c0_g1_i1 m.108126;TR125470_c0_g2_i4 m.63370;TR125470_c0_g2_i3 m.63369 | NO ID | 31.84 | 21.29 | 26.28 | 4.99 | undear |

| Proteins that decrease in the abscission zone relative to the distal region on Day 6 | | | | | | |
|--|---|-------------|--------------------------------|----------------------------|---|------------------------------|
| name sequence | protein name | fold change | log2(mean intensity Distal D6) | log2(mean intensity AZ D6) | relative abundance [log2(cond.1/control)] | function or category |
| TR61688_c1_g1_i1 1m.14155;TR39707_c0_g1_i1 1m.8548 | metalloendoproteinase 1-like | 0.06 | 25.02 | 20.98 | -4.05 | cell wall transformation |
| TR13970_c0_g2_i1 1m.3254;TR107733_c0_g2_i1 1m.38138;TR13970_c0_g1_i1 1m.3252;TR107733_c0_g1_i1 1m.38136;TR13970_c0_g1_i1 1m.3253;TR107733_c0_g1_i1 1m.38137;TR143597_c1_g4_i1 1m.149550;TR339_c0_g1_i1 1m.109;TR44235_c0_g1_i1 1m.9389;TR18809_c0_g1_i1 1m.22772;TR159193_c0_g1_i1 1m.222905;TR63425_c0_g1_i1 1m.15035 | | | | | | |
| TR54029_c0_g1_i1 1m.11947;TR8658_c0_g1_i1 1m.23229;TR8588_c0_g1_i1 1m.23052 | beta-galactosidase 1-like | 0.08 | 25.22 | 21.51 | -3.71 | cell wall transformation |
| TR145111_c1_g1_i1 1m.163378;TR145227_c2_g2_i2 1m.164615;TR145227_c2_g2_i1 1m.164613 | | | | | | |
| TR126856_c2_g1_i1 1m.66536;TR127424_c1_g1_i1 1m.68140 | polylacturonase-inhibiting protein | 0.11 | 24.54 | 21.37 | -3.17 | cell wall transformation |
| TR135914_c0_g1_i1 1m.98986;TR136740_c0_g1_i1 1m.103077 | beta-d-xylosidase family protein | 0.11 | 29.58 | 26.38 | -3.20 | cell wall transformation |
| TR131555_c1_g2_i9 1m.80987;TR131555_c1_g2_i2 1m.80979;TR131555_c1_g2_i11 1m.80991;TR121532_c0_g1_i8 1m.55138;TR121532_c0_g1_i7 1m.55136;TR131555_c1_g2_i7 1m.80986;TR121532_c0_g1_i9 1m.55140;TR121532_c0_g1_i3 1m.55130;TR121532_c0_g1_i10 1m.55141;TR131555_c1_g2_i6 1m.80984;TR131555_c1_g2_i13 1m.80995;TR131555_c1_g2_i10 1m.80989;TR121532_c0_g1_i6 1m.55134;TR121532_c0_g1_i2 1m.55128;TR121532_c0_g1_i11 1m.55126;TR131555_c1_g2_i12 1m.80994;TR121532_c0_g1_i4 1m.55132 | beta-galactosidase-like isoform x2 | 0.10 | 27.06 | 23.76 | -3.30 | cell wall transformation |
| TR115324_c0_g1_i1 1m.46252;TR117927_c0_g1_i1 1m.49532 | bifunctional udp-glucose 4-epimerase and bark storage protein a | 0.12 | 27.16 | 24.12 | -3.04 | cell wall transformation |
| TR15226_c0_g1_i1 1m.3496;TR151159_c0_g1_i1 1m.221490 | allene oxide synthase | 0.07 | 27.52 | 21.26 | -3.86 | defence |
| TR3514_c0_g2_i1 1m.603;TR27572_c0_g1_i1 1m.6408;TR3514_c0_g1_i1 1m.602;TR27572_c0_g2_i1 1m.6411;TR3514_c0_g1_i1 1m.601;TR27572_c0_g2_i1 1m.6410 | endochitinase p4-like | 0.11 | 32.74 | 29.60 | -3.15 | defence |
| TR91265_c0_g1_i1 1m.25469;TR82987_c0_g1_i1 1m.22205 | pathogenesis-related protein 1-like | 0.05 | 26.18 | 21.98 | -4.21 | defence |
| TR144639_c4_g3_i2 1m.158820 | Pathogen-related protein | 0.13 | 28.37 | 25.48 | -2.89 | defence |
| TR142833_c2_g1_i6 1m.143367;TR142833_c2_g1_i5 1m.143366;TR142833_c2_g1_i4 1m.143365;TR142833_c2_g1_i3 1m.143364;TR141980_c0_g1_i4 1m.136462;TR141980_c0_g1_i2 1m.136460;TR142833_c2_g1_i2 1m.143363;TR142833_c2_g1_i1 1m.143362;TR141980_c0_g1_i5 1m.136463;TR141980_c0_g1_i3 1m.136461;TR141980_c0_g1_i1 1m.136459 | probable protein phosphatase 2c59 | 0.16 | 23.99 | 21.37 | -2.63 | defence |
| TR76022_c0_g1_i1 1m.19813;TR70661_c0_g1_i1 1m.17634 | allene oxide synthase | 0.16 | 27.31 | 24.64 | -2.67 | defence |
| TR103023_c3_g2_i1 1m.34604;TR120086_c1_g1_i1 1m.52113;TR120086_c1_g2_i1 1m.52116;TR160518_c0_g1_i1 1m.223156 | protein yj59-like | 0.09 | 26.09 | 22.59 | -3.51 | defence, signal transduction |
| TR131160_c0_g1_i2 1m.79649;TR130844_c0_g1_i2 1m.78554;TR131160_c0_g1_i1 1m.79648 | 1-aminocyclopropane-1-carboxylate oxidase homolog 4-like | 0.07 | 25.03 | 21.15 | -3.88 | other |
| TR117476_c0_g1_i1 1m.48934 | kynurenine formamidase-like | 0.06 | 25.74 | 21.59 | -4.16 | other |
| TR134506_c0_g1_i2 1m.92943;TR128377_c0_g1_i4 1m.70513;TR134506_c0_g1_i1 1m.92942;TR128377_c0_g1_i3 1m.70512;TR128377_c0_g1_i2 1m.70510;TR134506_c0_g1_i3 1m.92945;TR134506_c0_g1_i5 1m.92949;TR128377_c0_g1_i1 1m.70509;TR128377_c0_g1_i1 1m.70508 | scaffold attachment factor b2 | 0.11 | 23.93 | 20.76 | -3.17 | other |
| TR141555_c0_g1_i1 1m.133458;TR141269_c0_g1_i1 1m.131460 | protein nrt1 ptr family | 0.13 | 23.55 | 20.57 | -2.99 | other |

| | | | | | | |
|--|--|------|-------|-------|-------|----------------------|
| TR92560_c0_g1_i1 m. 26190; TR125671_c1_g2_i1 m. 63875; TR125671_c1_g1_i1 m. 6387 | copper transporter | 0.10 | 25.28 | 22.00 | -3.28 | other |
| 4 | | | | | | |
| TR146214_c8_g2_i6 m. 174083; TR146214_c8_g2_i7 m. 174092; TR141441_c1_g2_i3 m. 132637; TR146214_c8_g2_i9 m. 174095; TR146214_c8_g2_i10 m. 174089; TR141441_c1_g2_i2 m. 132635; TR146214_c8_g2_i8 m. 174086 | photosystem i p700 apoprotein a2 | 0.10 | 24.42 | 21.03 | -3.39 | other |
| TR116456_c5_g1_i1 m. 47758; TR158091_c5_g1_i1 m. 222523 | Histone H1.2 | 0.14 | 24.06 | 21.21 | -2.86 | other |
| TR180671_c0_g1_i1 m. 226195; TR165198_c0_g1_i1 m. 223587; TR171185_c0_g1_i1 m. 2 | polyphenol oxidase | 0.04 | 27.47 | 22.77 | -4.70 | other |
| 24685; TR129953_c0_g1_i1 m. 6850; TR6842_c0_g1_i1 m. 992 | scaffold attachment factor b2 | 0.10 | 25.07 | 21.79 | -3.29 | other |
| TR93977_c1_g1_i1 m. 27086; TR88297_c0_g1_i1 m. 23720; TR26764_c0_g1_i1 m. 6235 | Probable aquaporin PIP2-2 | 0.10 | 25.37 | 22.06 | -3.31 | other |
| TR187948_c0_g1_i1 m. 227349 | | | | | | |
| TR126787_c4_g1_i2 m. 66269; TR128774_c4_g1_i3 m. 71662; TR128774_c4_g1_i1 m. 716 | | | | | | |
| 56; TR128774_c4_g1_i4 m. 71665; TR128774_c4_g1_i2 m. 71659; TR126787_c4_g1_i1 m. 66266; TR126787_c4_g1_i1 m. 66268; TR128774_c4_g1_i4 m. 71666; TR128774_c4_g1_i2 | | | | | | |
| 1 m. 71660 | malate glyoxysomal | 0.02 | 26.81 | 20.90 | -5.91 | primary metabolism |
| TR61875_c0_g1_i1 m. 14238; TR51702_c0_g1_i1 m. 10888 | alpha amylase family protein | 0.10 | 28.98 | 25.60 | -3.38 | primary metabolism |
| TR8481_c0_g1_i1 m. 1442; TR53298_c0_g1_i1 m. 11784 | cell wall vacuolar inhibitor of fructosidase 1 | 0.08 | 25.43 | 21.77 | -3.66 | primary metabolism |
| TR93334_c0_g1_i2 m. 11804; TR53334_c0_g1_i1 m. 11803; TR39690_c0_g1_i1 m. 8541 | cytidine deaminase 1-like | 0.10 | 25.73 | 22.46 | -3.26 | primary metabolism |
| TR146831_c2_g1_i5 m. 180543; TR149708_c27_g2_i2 m. 215290; TR146831_c2_g1_i4 m. 180542; TR146831_c2_g1_i3 m. 180539; TR146831_c2_g1_i1 m. 180535; TR146831_c2_g1_i2 m. 180537; TR149708_c27_g2_i1 m. 215289; TR146831_c2_g1_i2 m. 180538; TR146831_c2_g1_i1 m. 180536 | | | | | | |
| TR135458_c0_g1_i2 m. 96691; TR134458_c8_g1_i1 m. 92689; TR135458_c0_g1_i1 m. 966 | alpha-aminoadipic semialdehyde synthase | 0.08 | 25.52 | 21.87 | -3.65 | primary metabolism |
| 89; TR134458_c8_g1_i2 m. 92691; TR134458_c8_g2_i1 m. 92693 | ketose-bisphosphate aldolase class-II family | | | | | |
| TR140950_c0_g1_i3 m. 129169; TR140950_c0_g1_i1 m. 129167; TR140384_c0_g1_i1 m. 1 | protein isoform 1 | 0.14 | 25.78 | 22.98 | -2.80 | primary metabolism |
| 24969; TR140950_c0_g1_i4 m. 129170; TR140950_c0_g1_i2 m. 129168; TR140384_c0_g1_i2 m. 124970; TR101342_c0_g1_i1 m. 33209; TR103652_c0_g1_i1 m. 35129 | inosine-5-monophosphate dehydrogenase 2-like | 0.11 | 26.41 | 23.18 | -3.23 | primary metabolism |
| TR145321_c9_g1_i3 m. 165455 | Granule-bound starch synthase 1, | | | | | |
| TR134932_c0_g1_i1 m. 94738; TR134791_c0_g1_i2 m. 94185; TR134791_c0_g1_i1 m. 941 | chloroplastic/amyloplastic | 0.13 | 24.53 | 21.64 | -2.89 | primary metabolism |
| 83; TR134932_c0_g1_i2 m. 94740 | senescence-specific cysteine protease sag12- | | | | | |
| TR140093_c4_g1_i6 m. 123191; TR140093_c4_g1_i5 m. 123190 | protein | 0.02 | 27.94 | 22.13 | -5.82 | proteolysis |
| TR145664_c6_g1_i1 m. 168541; TR138653_c2_g1_i2 m. 114143; TR145664_c6_g1_i3 m. 1 | protein aspartic protease in guard cell 2-like | 0.10 | 24.34 | 21.04 | -3.30 | proteolysis |
| 68542; TR138653_c2_g1_i1 m. 114142; TR138653_c2_g1_i3 m. 114144 | probable glutamate carboxypeptidase 2 | 0.10 | 23.97 | 20.65 | -3.32 | proteolysis |
| TR112869_c0_g1_i1 m. 42979; TR106770_c0_g2_i1 m. 36850 | Flavone 3-O-methyltransferase 1 | 0.09 | 25.31 | 21.78 | -3.53 | secondary metabolism |
| TR149628_c0_g1_i1 m. 214063; TR149658_c1_g1_i1 m. 214492; TR149628_c0_g1_i4 m. 2 | | | | | | |
| 140668; TR149628_c0_g1_i2 m. 214064 | anthocyanidin 3-O-glucosyltransferase 2-like | 0.11 | 24.00 | 20.87 | -3.13 | secondary metabolism |
| TR128074_c0_g1_i3 m. 69837; TR147117_c0_g2_i7 m. 183637; TR147117_c0_g2_i3 m. 18 | | | | | | |
| 3629; TR128074_c0_g1_i2 m. 69836; TR147117_c0_g1_i1 m. 183626; TR128074_c0_g1_i1 | peroxidase 73-like | 0.01 | 28.18 | 20.81 | -7.37 | stress response |
| 1 m. 69834; TR147117_c0_g2_i5 m. 183632 | aldehyde dehydrogenase family 7 member | | | | | |
| TR148251_c11_g1_i6 m. 196911; TR147882_c11_g1_i3 m. 192489; TR147882_c11_g1_i2 | b4 | 0.08 | 24.23 | 20.49 | -3.73 | stress response |
| m. 192488 | | | | | | |
| TR95252_c6_g2_i2 m. 28000; TR95252_c6_g2_i1 m. 27998; TR92851_c4_g2_i2 m. 26331; | dna binding | 0.08 | 25.98 | 22.33 | -3.65 | unclear |
| TR92851_c4_g2_i1 m. 26329 | | | | | | |

| | | | | | | |
|---|-------|------|-------|-------|-------|---------|
| TR143830_c0_g1_i1 1m.151655;TR144453_c0_g1_i1 1m.157134 | NO ID | 0.09 | 26.10 | 22.59 | -3.51 | unclear |
| TR143332_c0_g1_i1 1m.147553;TR143097_c1_g1_i2 1m.145459;TR143097_c1_g1_i3 1m.145460;TR143097_c1_g1_i1 1m.145458 | NO ID | 0.11 | 29.90 | 26.66 | -3.24 | unclear |
| TR144453_c0_g1_i1 1m.157133;TR143830_c0_g1_i1 1m.151654 | NO ID | 0.14 | 24.91 | 22.09 | -2.82 | unclear |
| TR130858_c0_g1_i1 1m.78585;TR129320_c0_g1_i1 1m.73493 | NO ID | 0.13 | 24.57 | 21.63 | -2.94 | unclear |

| Proteins that increase in the abscission zone relative to the proximal region on Day 6 | | | | | | |
|---|---|-------------|----------------------------------|----------------------------|---|--------------------------|
| name sequence | protein name | fold change | log2(mean intensity Proximal D6) | log2(mean intensity AZ D6) | relative abundance [log2(cond.1/control)] | function or category |
| TR20048_c0_g1_i1 1m.4705;TR13295_c0_g1_i1 1m.2877;TR20048_c0_g2_i1 1m.4768;TR13295_c0_g2_i1 1m.2880;TR143143_c0_g1_i1 1m.145944;TR131993_c1_g4_i1 1m.82499;TR139918_c0_g1_i1 1m.122016;TR100061_c0_g1_i1 1m.32328;TR20048_c0_g2_i1 1m.4769;TR13295_c0_g2_i1 1m.2881;TR139918_c1_g1_i1 1m.122018;TR116878_c0_g1_i1 1m.48233;TR133370_c0_g1_i1 1m.87689;TR139918_c2_g1_i1 1m.122019 | abc transporter g family member 6-like | 5.63 | 20.74 | 23.24 | 2.49 | cell wall transformation |
| TR8672_c0_g1_i1 1m.1587;TR23332_c0_g2_i1 1m.5682;TR8672_c0_g2_i1 1m.1588;TR23332_c0_g1_i1 1m.5681 | polygalacturonase | 14.58 | 21.26 | 25.13 | 3.87 | cell wall transformation |
| TR96655_c0_g2_i3 1m.29098;TR94490_c0_g1_i1 1m.27421;TR96655_c0_g2_i1 1m.29088 | extensin 2 like, extensin 2 partial | 13.27 | 20.84 | 24.57 | 3.73 | cell wall transformation |
| TR53009_c0_g1_i1 1m.11532;TR39616_c0_g1_i1 1m.8492 | endo beta glucanase | 17.02 | 21.37 | 25.46 | 4.09 | cell wall transformation |
| TR125351_c0_g1_i1 1m.63099;TR127805_c1_g1_i3 1m.69008;TR127805_c1_g1_i1 1m.69006 | expansin like b1 | 27.25 | 20.59 | 25.35 | 4.77 | cell wall transformation |
| TR187879_c1_g1_i1 1m.227292;TR12871_c0_g1_i1 1m.224876 | Probable polygalacturonase | 15.64 | 21.57 | 25.54 | 3.97 | cell wall transformation |
| TR107318_c0_g1_i2 1m.37550;TR101095_c0_g1_i1 1m.33072;TR107318_c0_g1_i1 1m.37549 | Xyloglucan endo transglucosylase hydrolase protein 2 like | 30.40 | 21.02 | 25.95 | 4.93 | cell wall transformation |
| TR126856_c2_g1_i1 1m.66536;TR127424_c1_g1_i1 1m.68140 | beta d xylosidase family protein | 38.37 | 21.12 | 26.38 | 5.26 | cell wall transformation |
| TR111814_c0_g1_i2 1m.41572;TR111814_c0_g1_i1 1m.41570 | alpha - - glucan- protein synthase | 22.73 | 21.20 | 25.71 | 4.51 | cell wall transformation |
| TR115801_c0_g1_i1 1m.46809;TR106356_c0_g1_i1 1m.36457;TR115801_c0_g1_i2 1m.46810 | polygalacturonase qrt2 like | 55.41 | 20.71 | 26.50 | 5.79 | cell wall transformation |
| TR102949_c0_g1_i1 1m.34528 | wound-induced protein win1 | 10.53 | 26.30 | 29.70 | 3.40 | defence |
| TR144639_c4_g3_i2 1m.158820 | Pathogen-related protein | 10.59 | 22.08 | 25.48 | 3.40 | defence |
| TR15226_c0_g1_i1 1m.3496;TR151159_c0_g1_i1 1m.221490 | allene oxide synthase | 11.54 | 20.68 | 24.21 | 3.53 | defence |
| TR76022_c0_g1_i1 1m.19813;TR70661_c0_g1_i1 1m.17634 | allene oxide synthase | 8.92 | 21.49 | 24.64 | 3.16 | defence |
| TR145404_c0_g1_i5 1m.166221;TR145829_c0_g1_i1 1m.170198;TR145404_c0_g1_i3 1m.166219;TR145404_c0_g1_i8 1m.166224;TR168371_c0_g1_i1 1m.224444;TR11120_c0_g1_i1 1m.2288 | Subtilisin-like protease SBT1.9 | | | | | |
| TR130237_c0_g1_i2 1m.76489;TR128267_c0_g1_i1 1m.70254;TR130237_c0_g1_i1 1m.76488 | | 14.88 | 23.62 | 27.52 | 3.90 | defence |
| TR128267_c0_g1_i2 1m.70255 | | | | | | |
| TR3514_c0_g2_i1 1m.603;TR27572_c0_g1_i1 1m.6408;TR3514_c0_g1_i1 1m.602;TR27572_c0_g2_i1 1m.6411;TR3514_c0_g1_i1 1m.601;TR27572_c0_g2_i1 1m.6410 | disease resistance response protein 206 like | 18.10 | 21.41 | 25.58 | 4.18 | defence |
| | endochitinase pr 4 like | 62.91 | 23.62 | 29.60 | 5.98 | defence |

| | | | | | | |
|--|--|--------|-------|-------|------|--------------------|
| TR112327_c2_g1_i1 m.42387;TR112867_c4_g2_i1 m.42978 | thaumatin-like protein 1b | 55.09 | 24.65 | 30.43 | 5.78 | defence |
| TR135242_c0_g1_i3 m.95883;TR135242_c0_g1_i1 m.95881;TR134338_c0_g1_i4 m.92074 | alpha amylase subtilisin inhibitor like | 55.23 | 22.23 | 28.02 | 5.79 | defence |
| ;TR134338_c0_g1_i1 m.92071 | major allergen Pru | 112.35 | 23.09 | 29.90 | 6.81 | defence |
| TR99175_c2_g1_i1 m.31406 | | | | | | |
| TR137442_c0_g1_i2 m.106922;TR136156_c0_g1_i1 m.100274;TR137442_c0_g1_i1 m.106921 | dihydropyrimidine dehydrogenase | 12.70 | 21.46 | 25.13 | 3.67 | other |
| TR126156_c0_g1_i1 m.64934;TR125426_c0_g1_i2 m.63270;TR126156_c0_g1_i2 m.64935 | 1 amino cyclopropane 1 carboxylate oxidase 5 | 13.84 | 20.95 | 24.75 | 3.79 | other |
| ;TR125426_c0_g1_i1 m.63269 | carbonic chloroplastic like | 23.68 | 21.65 | 26.21 | 4.57 | other |
| TR124048_c0_g1_i1 m.60067;TR122051_c0_g1_i1 m.56333 | carlinate racemase like protein | 5.33 | 21.79 | 24.20 | 2.41 | other |
| TR127444_c0_g1_i1 m.68211;TR124734_c0_g1_i1 m.61779;TR29500_c0_g2_i1 m.6784;TR29500_c0_g1_i1 m.6783;TR53435_c0_g2_i1 m.11830 | 2-oxoglutarate and fe-dependent oxygenase superfamily protein | 9.94 | 22.73 | 26.04 | 3.31 | others |
| TR67962_c1_g1_i1 m.16582;TR67267_c1_g1_i1 m.16285 | 5-methyltetrahydropteroyltryglutamate-- | 8.46 | 23.50 | 26.58 | 3.08 | primary metabolism |
| TR144685_c17_g1_i1 m.159304;TR157892_c2_g1_i1 m.222369;TR145901_c2_g1_i1 m.170892;TR150433_c0_g1_i1 m.221140 | homocysteine methyltransferase | | | | | |
| TR139671_c4_g1_i2 m.120577;TR139671_c4_g1_i1 m.120575;TR139082_c5_g1_i1 m.116837;TR139082_c5_g1_i2 m.116839;TR139082_c5_g1_i3 m.116841;TR139671_c4_g1_i3 m.120579 | s-adenosylmethionine synthase 1 | 8.87 | 23.28 | 26.43 | 3.15 | primary metabolism |
| TR117223_c0_g1_i2 m.48583;TR113032_c0_g1_i1 m.43207;TR117223_c0_g1_i1 m.48582 | chorismate mutase chloroplastic | 6.40 | 21.20 | 23.88 | 2.68 | primary metabolism |
| ;TR113032_c0_g1_i2 m.43209;TR117223_c0_g1_i1 m.48581;TR113032_c0_g1_i2 m.43208 | Transaldolase (Fragments) | 6.81 | 20.92 | 23.68 | 2.77 | primary metabolism |
| TR114082_c0_g1_i8 m.44633;TR140881_c5_g1_i3 m.128590 | | | | | | |
| TR140418_c15_g1_i2 m.125190;TR140615_c8_g6_i1 m.126802;TR140615_c8_g9_i1 m.126805;TR140615_c8_g9_i2 m.126806;TR140615_c8_g11_i1 m.126810;TR136425_c0_g1_i1 m.101592;TR128660_c3_g1_i3 m.71392;TR129554_c1_g1_i3 m.74286;TR56256_c0_g1_i1 m.12377;TR55880_c0_g1_i1 m.12319 | acylcoenzyme a oxidase peroxisomal like | 6.98 | 21.01 | 23.82 | 2.80 | primary metabolism |
| TR137225_c0_g1_i1 m.105818;TR135545_c0_g1_i1 m.97142 | phospho-2-dehydro-3-deoxyheptonate aldolase chloroplasticlike | 14.48 | 23.60 | 27.45 | 3.86 | primary metabolism |
| TR123516_c0_g1_i2 m.58654;TR120955_c0_g1_i1 m.53886;TR123516_c0_g1_i1 m.58653 | | | | | | |
| ;TR60578_c0_g2_i1 m.13554;TR18688_c0_g2_i1 m.4556;TR142194_c2_g2_i1 m.138247;TR144873_c1_g1_i5 m.161192;TR144873_c1_g1_i1 m.161185;TR144873_c1_g1_i2 m.161188;TR144873_c1_g1_i7 m.161196;TR142194_c2_g2_i6 m.138252 | Non-specific phospholipase C3 | 12.32 | 21.00 | 24.63 | 3.62 | primary metabolism |
| TR144022_c5_g1_i7 m.153123;TR143552_c3_g1_i3 m.149131 | probable acylactivating enzyme peroxisomal isoform x1 | 25.78 | 22.82 | 27.51 | 4.69 | primary metabolism |
| TR145012_c0_g1_i6 m.162617;TR144462_c0_g1_i5 m.157210;TR144462_c0_g1_i2 m.157206;TR145012_c0_g1_i8 m.162618 | Bifunctional 3-dehydroquinate dehydratase/shikimate dehydrogenase, chloroplastic | 17.08 | 21.31 | 25.41 | 4.09 | primary metabolism |
| TR99429_c1_g1_i1 m.31681;TR99081_c2_g1_i1 m.31313 | 3-hydroxyisobutyryl hydrolase-like protein 5 | 23.57 | 23.15 | 27.71 | 4.56 | primary metabolism |
| TR61875_c0_g1_i1 m.14238;TR51702_c0_g1_i1 m.10888 | alpha amylase family protein | 26.72 | 20.86 | 25.60 | 4.74 | primary metabolism |
| TR94519_c0_g1_i3 m.31095;TR94519_c0_g1_i1 m.31091;TR94519_c0_g1_i2 m.27479;TR98866_c0_g1_i3 m.27480;TR98866_c0_g1_i1 m.27478;TR98866_c0_g1_i2 m.27477;TR98866_c0_g1_i4 m.27483;TR94519_c0_g1_i1 m.31093;TR94519_c0_g1_i2 m.27477;TR94519_c0_g1_i3 m.31095;TR94519_c0_g1_i4 m.27483;TR94519_c0_g1_i5 m.27484;TR94519_c0_g1_i6 m.27485;TR94519_c0_g1_i7 m.27486;TR94519_c0_g1_i8 m.27487;TR94519_c0_g1_i9 m.27488;TR94519_c0_g1_i10 m.27489;TR94519_c0_g1_i11 m.27490;TR94519_c0_g1_i12 m.27491;TR94519_c0_g1_i13 m.27492;TR94519_c0_g1_i14 m.27493;TR94519_c0_g1_i15 m.27494;TR94519_c0_g1_i16 m.27495;TR94519_c0_g1_i17 m.27496;TR94519_c0_g1_i18 m.27497;TR94519_c0_g1_i19 m.27498;TR94519_c0_g1_i20 m.27499;TR94519_c0_g1_i21 m.27500;TR94519_c0_g1_i22 m.27501;TR94519_c0_g1_i23 m.27502;TR94519_c0_g1_i24 m.27503;TR94519_c0_g1_i25 m.27504;TR94519_c0_g1_i26 m.27505;TR94519_c0_g1_i27 m.27506;TR94519_c0_g1_i28 m.27507;TR94519_c0_g1_i29 m.27508;TR94519_c0_g1_i30 m.27509;TR94519_c0_g1_i31 m.27510;TR94519_c0_g1_i32 m.27511;TR94519_c0_g1_i33 m.27512;TR94519_c0_g1_i34 m.27513;TR94519_c0_g1_i35 m.27514;TR94519_c0_g1_i36 m.27515;TR94519_c0_g1_i37 m.27516;TR94519_c0_g1_i38 m.27517;TR94519_c0_g1_i39 m.27518;TR94519_c0_g1_i40 m.27519;TR94519_c0_g1_i41 m.27520;TR94519_c0_g1_i42 m.27521;TR94519_c0_g1_i43 m.27522;TR94519_c0_g1_i44 m.27523;TR94519_c0_g1_i45 m.27524;TR94519_c0_g1_i46 m.27525;TR94519_c0_g1_i47 m.27526;TR94519_c0_g1_i48 m.27527;TR94519_c0_g1_i49 m.27528;TR94519_c0_g1_i50 m.27529;TR94519_c0_g1_i51 m.27530;TR94519_c0_g1_i52 m.27531;TR94519_c0_g1_i53 m.27532;TR94519_c0_g1_i54 m.27533;TR94519_c0_g1_i55 m.27534;TR94519_c0_g1_i56 m.27535;TR94519_c0_g1_i57 m.27536;TR94519_c0_g1_i58 m.27537;TR94519_c0_g1_i59 m.27538;TR94519_c0_g1_i60 m.27539;TR94519_c0_g1_i61 m.27540;TR94519_c0_g1_i62 m.27541;TR94519_c0_g1_i63 m.27542;TR94519_c0_g1_i64 m.27543;TR94519_c0_g1_i65 m.27544;TR94519_c0_g1_i66 m.27545;TR94519_c0_g1_i67 m.27546;TR94519_c0_g1_i68 m.27547;TR94519_c0_g1_i69 m.27548;TR94519_c0_g1_i70 m.27549;TR94519_c0_g1_i71 m.27550;TR94519_c0_g1_i72 m.27551;TR94519_c0_g1_i73 m.27552;TR94519_c0_g1_i74 m.27553;TR94519_c0_g1_i75 m.27554;TR94519_c0_g1_i76 m.27555;TR94519_c0_g1_i77 m.27556;TR94519_c0_g1_i78 m.27557;TR94519_c0_g1_i79 m.27558;TR94519_c0_g1_i80 m.27559;TR94519_c0_g1_i81 m.27560;TR94519_c0_g1_i82 m.27561;TR94519_c0_g1_i83 m.27562;TR94519_c0_g1_i84 m.27563;TR94519_c0_g1_i85 m.27564;TR94519_c0_g1_i86 m.27565;TR94519_c0_g1_i87 m.27566;TR94519_c0_g1_i88 m.27567;TR94519_c0_g1_i89 m.27568;TR94519_c0_g1_i90 m.27569;TR94519_c0_g1_i91 m.27570;TR94519_c0_g1_i92 m.27571;TR94519_c0_g1_i93 m.27572;TR94519_c0_g1_i94 m.27573;TR94519_c0_g1_i95 m.27574;TR94519_c0_g1_i96 m.27575;TR94519_c0_g1_i97 m.27576;TR94519_c0_g1_i98 m.27577;TR94519_c0_g1_i99 m.27578;TR94519_c0_g1_i100 m.27579;TR94519_c0_g1_i101 m.27580;TR94519_c0_g1_i102 m.27581;TR94519_c0_g1_i103 m.27582;TR94519_c0_g1_i104 m.27583;TR94519_c0_g1_i105 m.27584;TR94519_c0_g1_i106 m.27585;TR94519_c0_g1_i107 m.27586;TR94519_c0_g1_i108 m.27587;TR94519_c0_g1_i109 m.27588;TR94519_c0_g1_i110 m.27589;TR94519_c0_g1_i111 m.27590;TR94519_c0_g1_i112 m.27591;TR94519_c0_g1_i113 m.27592;TR94519_c0_g1_i114 m.27593;TR94519_c0_g1_i115 m.27594;TR94519_c0_g1_i116 m.27595;TR94519_c0_g1_i117 m.27596;TR94519_c0_g1_i118 m.27597;TR94519_c0_g1_i119 m.27598;TR94519_c0_g1_i120 m.27599;TR94519_c0_g1_i121 m.27600;TR94519_c0_g1_i122 m.27601;TR94519_c0_g1_i123 m.27602;TR94519_c0_g1_i124 m.27603;TR94519_c0_g1_i125 m.27604;TR94519_c0_g1_i126 m.27605;TR94519_c0_g1_i127 m.27606;TR94519_c0_g1_i128 m.27607;TR94519_c0_g1_i129 m.27608;TR94519_c0_g1_i130 m.27609;TR94519_c0_g1_i131 m.27610;TR94519_c0_g1_i132 m.27611;TR94519_c0_g1_i133 m.27612;TR94519_c0_g1_i134 m.27613;TR94519_c0_g1_i135 m.27614;TR94519_c0_g1_i136 m.27615;TR94519_c0_g1_i137 m.27616;TR94519_c0_g1_i138 m.27617;TR94519_c0_g1_i139 m.27618;TR94519_c0_g1_i140 m.27619;TR94519_c0_g1_i141 m.27620;TR94519_c0_g1_i142 m.27621;TR94519_c0_g1_i143 m.27622;TR94519_c0_g1_i144 m.27623;TR94519_c0_g1_i145 m.27624;TR94519_c0_g1_i146 m.27625;TR94519_c0_g1_i147 m.27626;TR94519_c0_g1_i148 m.27627;TR94519_c0_g1_i149 m.27628;TR94519_c0_g1_i150 m.27629;TR94519_c0_g1_i151 m.27630;TR94519_c0_g1_i152 m.27631;TR94519_c0_g1_i153 m.27632;TR94519_c0_g1_i154 m.27633;TR94519_c0_g1_i155 m.27634;TR94519_c0_g1_i156 m.27635;TR94519_c0_g1_i157 m.27636;TR94519_c0_g1_i158 m.27637;TR94519_c0_g1_i159 m.27638;TR94519_c0_g1_i160 m.27639;TR94519_c0_g1_i161 m.27640;TR94519_c0_g1_i162 m.27641;TR94519_c0_g1_i163 m.27642;TR94519_c0_g1_i164 m.27643;TR94519_c0_g1_i165 m.27644;TR94519_c0_g1_i166 m.27645;TR94519_c0_g1_i167 m.27646;TR94519_c0_g1_i168 m.27647;TR94519_c0_g1_i169 m.27648;TR94519_c0_g1_i170 m.27649;TR94519_c0_g1_i171 m.27650;TR94519_c0_g1_i172 m.27651;TR94519_c0_g1_i173 m.27652;TR94519_c0_g1_i174 m.27653;TR94519_c0_g1_i175 m.27654;TR94519_c0_g1_i176 m.27655;TR94519_c0_g1_i177 m.27656;TR94519_c0_g1_i178 m.27657;TR94519_c0_g1_i179 m.27658;TR94519_c0_g1_i180 m.27659;TR94519_c0_g1_i181 m.27660;TR94519_c0_g1_i182 m.27661;TR94519_c0_g1_i183 m.27662;TR94519_c0_g1_i184 m.27663;TR94519_c0_g1_i185 m.27664;TR94519_c0_g1_i186 m.27665;TR94519_c0_g1_i187 m.27666;TR94519_c0_g1_i188 m.27667;TR94519_c0_g1_i189 m.27668;TR94519_c0_g1_i190 m.27669;TR94519_c0_g1_i191 m.27670;TR94519_c0_g1_i192 m.27671;TR94519_c0_g1_i193 m.27672;TR94519_c0_g1_i194 m.27673;TR94519_c0_g1_i195 m.27674;TR94519_c0_g1_i196 m.27675;TR94519_c0_g1_i197 m.27676;TR94519_c0_g1_i198 m.27677;TR94519_c0_g1_i199 m.27678;TR94519_c0_g1_i200 m.27679;TR94519_c0_g1_i201 m.27680;TR94519_c0_g1_i202 m.27681;TR94519_c0_g1_i203 m.27682;TR94519_c0_g1_i204 m.27683;TR94519_c0_g1_i205 m.27684;TR94519_c0_g1_i206 m.27685;TR94519_c0_g1_i207 m.27686;TR94519_c0_g1_i208 m.27687;TR94519_c0_g1_i209 m.27688;TR94519_c0_g1_i210 m.27689;TR94519_c0_g1_i211 m.27690;TR94519_c0_g1_i212 m.27691;TR94519_c0_g1_i213 m.27692;TR94519_c0_g1_i214 m.27693;TR94519_c0_g1_i215 m.27694;TR94519_c0_g1_i216 m.27695;TR94519_c0_g1_i217 m.27696;TR94519_c0_g1_i218 m.27697;TR94519_c0_g1_i219 m.27698;TR94519_c0_g1_i220 m.27699;TR94519_c0_g1_i221 m.27700;TR94519_c0_g1_i222 m.27701;TR94519_c0_g1_i223 m.27702;TR94519_c0_g1_i224 m.27703;TR94519_c0_g1_i225 m.27704;TR94519_c0_g1_i226 m.27705;TR94519_c0_g1_i227 m.27706;TR94519_c0_g1_i228 m.27707;TR94519_c0_g1_i229 m.27708;TR94519_c0_g1_i230 m.27709;TR94519_c0_g1_i231 m.27710;TR94519_c0_g1_i232 m.27711;TR94519_c0_g1_i233 m.27712;TR94519_c0_g1_i234 m.27713;TR94519_c0_g1_i235 m.27714;TR94519_c0_g1_i236 m.27715;TR94519_c0_g1_i237 m.27716;TR94519_c0_g1_i238 m.27717;TR94519_c0_g1_i239 m.27718;TR94519_c0_g1_i240 m.27719;TR94519_c0_g1_i241 m.27720;TR94519_c0_g1_i242 m.27721;TR94519_c0_g1_i243 m.27722;TR94519_c0_g1_i244 m.27723;TR94519_c0_g1_i245 m.27724;TR94519_c0_g1_i246 m.27725;TR94519_c0_g1_i247 m.27726;TR94519_c0_g1_i248 m.27727;TR94519_c0_g1_i249 m.27728;TR94519_c0_g1_i250 m.27729;TR94519_c0_g1_i251 m.27730;TR94519_c0_g1_i252 m.27731;TR94519_c0_g1_i253 m.27732;TR94519_c0_g1_i254 m.27733;TR94519_c0_g1_i255 m.27734;TR94519_c0_g1_i256 m.27735;TR94519_c0_g1_i257 m.27736;TR94519_c0_g1_i258 m.27737;TR94519_c0_g1_i259 m.27738;TR94519_c0_g1_i260 m.27739;TR94519_c0_g1_i261 m.27740;TR94519_c0_g1_i262 m.27741;TR94519_c0_g1_i263 m.27742;TR94519_c0_g1_i264 m.27743;TR94519_c0_g1_i265 m.27744;TR94519_c0_g1_i266 m.27745;TR94519_c0_g1_i267 m.27746;TR94519_c0_g1_i268 m.27747;TR94519_c0_g1_i269 m.27748;TR94519_c0_g1_i270 m.27749;TR94519_c0_g1_i271 m.27750;TR94519_c0_g1_i272 m.27751;TR94519_c0_g1_i273 m.27752;TR94519_c0_g1_i274 m.27753;TR94519_c0_g1_i275 m.27754;TR94519_c0_g1_i276 m.27755;TR94519_c0_g1_i277 m.27756;TR94519_c0_g1_i278 m.27757;TR94519_c0_g1_i279 m.27758;TR94519_c0_g1_i280 m.27759;TR94519_c0_g1_i281 m.27760;TR94519_c0_g1_i282 m.27761;TR94519_c0_g1_i283 m.27762;TR94519_c0_g1_i284 m.27763;TR94519_c0_g1_i285 m.27764;TR94519_c0_g1_i286 m.27765;TR94519_c0_g1_i287 m.27766;TR94519_c0_g1_i288 m.27767;TR94519_c0_g1_i289 m.27768;TR94519_c0_g1_i290 m.27769;TR94519_c0_g1_i291 m.27770;TR94519_c0_g1_i292 m.27771;TR94519_c0_g1_i293 m.27772;TR94519_c0_g1_i294 m.27773;TR94519_c0_g1_i295 m.27774;TR94519_c0_g1_i296 m.27775;TR94519_c0_g1_i297 m.27776;TR94519_c0_g1_i298 m.27777;TR94519_c0_g1_i299 m.27778;TR94519_c0_g1_i300 m.27779;TR94519_c0_g1_i301 m.27780;TR94519_c0_g1_i302 m.27781;TR94519_c0_g1_i303 m.27782;TR94519_c0_g1_i304 m.27783;TR94519_c0_g1_i305 m.27784;TR94519_c0_g1_i306 m.27785;TR94519_c0_g1_i307 m.27786;TR94519_c0_g1_i308 m.27787;TR94519_c0_g1_i309 m.27788;TR94519_c0_g1_i310 m.27789;TR94519_c0_g1_i311 m.27790;TR94519_c0_g1_i312 m.27791;TR94519_c0_g1_i313 m.27792;TR94519_c0_g1_i314 m.27793;TR94519_c0_g1_i315 m.27794;TR94519_c0_g1_i316 m.27795;TR94519_c0_g1_i317 m.27796;TR94519_c0_g1_i318 m.27797;TR94519_c0_g1_i319 m.27798;TR94519_c0_g1_i320 m.27799;TR94519_c0_g1_i321 m.27800;TR94519_c0_g1_i322 m.27801;TR94519_c0_g1_i323 m.27802;TR94519_c0_g1_i324 m.27803;TR94519_c0_g1_i325 m.27804;TR94519_c0_g1_i326 m.27805;TR94519_c0_g1_i327 m.27806;TR94519_c0_g1_i328 m.27807;TR94519_c0_g1_i329 m.27808;TR94519_c0_g1_i330 m.27809;TR94519_c0_g1_i331 m.27810;TR94519_c0_g1_i332 m.27811;TR94519_c0_g1_i333 m.27812;TR94519_c0_g1_i334 m.27813;TR94519_c0_g1_i335 m.27814;TR94519_c0_g1_i336 m.27815;TR94519_c0_g1_i337 m.27816;TR94519_c0_g1_i338 m.27817;TR94519_c0_g1_i339 m.27818;TR94519_c0_g1_i340 m.27819;TR94519_c0_g1_i341 m.27820;TR94519_c0_g1_i342 m.27821;TR94519_c0_g1_i343 m.27822;TR94519_c0_g1_i344 m.27823;TR94519_c0_g1_i345 m.27824;TR94519_c0_g1_i346 m.27825;TR94519_c0_g1_i347 m.27826;TR94519_c0_g1_i348 m.27827;TR94519_c0_g1_i349 m.27828;TR94519_c0_g1_i350 m.27829;TR94519_c0_g1_i351 m.27830;TR94519_c0_g1_i352 m.27831;TR94519_c0_g1_i353 m.27832;TR94519_c0_g1_i354 m.27833;TR94519_c0_g1_i355 m.27834;TR94519_c0_g1_i356 m.27835;TR94519_c0_g1_i357 m.27836;TR94519_c0_g1_i358 m.27837;TR94519_c0_g1_i359 m.27838;TR94519_c0_g1_i360 m.27839;TR94519_c0_g1_i361 m.27840;TR94519_c0_g1_i362 m.27841;TR94519_c0_g1_i363 m.27842;TR94519_c0_g1_i364 m.27843;TR94519_c0_g1_i365 m.27844;TR94519_c0_g1_i366 m.27845;TR94519_c0_g1_i367 m.27846;TR94519_c0_g1_i368 m.27847;TR94519_c0_g1_i369 m.27848;TR94519_c0_g1_i370 m.27849;TR94519_c0_g1_i371 m.27850;TR94519_c0_g1_i372 m.27851;TR94519_c0_g1_i373 m.27852;TR94519_c0_g1_i374 m.27853;TR94519_c0_g1_i375 m.27854;TR94519_c0_g1_i376 m.27855;TR94519_c0_g1_i377 m.27856;TR94519_c0_g1_i378 m.27857;TR94519_c0_g1_i379 m.27858;TR94519_c0_g1_i380 m.27859;TR94519_c0_g1_i381 m.27860;TR94519_c0_g1_i382 m.27861;TR94519_c0_g1_i383 m.27862;TR94519_c0_g1_i384 m.27863;TR94519_c0_g1_i385 m.27864;TR94519_c0_g1_i386 m.27865;TR94519_c0_g1_i387 m.27866;TR94519_c0_g1_i388 m.27867;TR94519_c0_g1_i389 m.27868;TR94519_c0_g1_i390 m.27869;TR94519_c0_g1_i391 m.27870;TR94519_c0_g1_i392 m.27871;TR94519_c0_g1_i393 m.27872;TR94519_c0_g1_i394 m.27873;TR94519_c0_g1_i395 m.27874;TR94519_c0_g1_i396 m.27875;TR94519_c0_g1_i397 m.27876;TR94519_c0_g1_i398 m.27877; | | | | | | |

| | | | | | | |
|--|--|-------|-------|-------|------|----------------------|
| TR126974_c0_g2_i1 m.66819;TR136166_c0_g1_i2 m.100349;TR136166_c0_g1_i1 m.100347 | Beta-fructofuranosidase | 42.59 | 20.91 | 26.33 | 5.41 | primary metabolism |
| TR347_c0_g1_i1 m.111;TR16490_c0_g1_i1 m.3897 | cytochrome b5 | 40.48 | 20.65 | 25.98 | 5.34 | primary metabolism |
| TR136792_c1_i1_g1_i1 m.103397;TR132472_c1_g1_i2 m.84585;TR136792_c1_i1_g1_i3 m.103398;TR132472_c1_g1_i1 m.84584 | gds1 motif lipase hydrolase family protein | 94.78 | 20.81 | 27.37 | 6.57 | primary metabolism |
| TR144462_c0_g1_i4 m.157209;TR145012_c0_g1_i5 m.162614;TR145012_c0_g1_i1 m.162608;TR144462_c0_g1_i3 m.157207;TR145012_c0_g1_i9 m.162621;TR145012_c0_g1_i2 m.162609;TR145012_c0_g1_i8 m.162619;TR145012_c0_g1_i3 m.162610 | bifunctional 3-dehydroquinate dehydratase shikimate chloroplastic-like | 5.91 | 21.13 | 23.69 | 2.56 | primary metabolism |
| TR130652_c2_g1_i2 m.77821;TR130652_c2_g1_i1 m.77820;TR127276_c7_g1_i1 m.67682 | cysteine proteinase | 33.74 | 21.00 | 26.07 | 5.08 | proteolysis |
| TR103610_c0_g1_i1 m.35097;TR102661_c0_g1_i1 m.34224 | caplike protein 1d1 | 7.86 | 20.70 | 23.68 | 2.98 | proteolysis |
| TR140093_c4_g1_i2 m.123186;TR140093_c4_g1_i1 m.123185;TR130529_c2_g1_i2 m.77464;TR130529_c2_g1_i1 m.77462 | protein aspartic protease In guard cell 2like | 12.22 | 21.23 | 24.84 | 3.61 | proteolysis |
| TR180432_c0_g2_i1 m.226038;TR180914_c0_g1_i1 m.226309;TR180432_c0_g1_i1 m.226037 | Aspartyl protease family protein 1 | 11.28 | 20.95 | 24.45 | 3.50 | proteolysis |
| TR135800_c5_g1_i1 m.98495;TR132526_c2_g1_i2 m.84803;TR132526_c2_g1_i1 m.84800 | cysteine proteinase rd2like | 16.43 | 24.06 | 25.10 | 4.04 | proteolysis |
| TR144716_c0_g1_i1 m.159583 | u6 snrna-associated sm-like protein lsm2 | 13.22 | 21.52 | 25.24 | 3.72 | RNA regulation |
| TR117126_c0_g1_i1 m.48486;TR113467_c1_g1_i1 m.43796 | chalcone isomerase | 1.97 | 23.38 | 24.36 | 0.98 | secondary metabolism |
| TR97650_c7_g1_i1 m.29836;TR91773_c4_g2_i1 m.25785 | flavanone 3-hydroxylase | 14.12 | 22.37 | 26.19 | 3.82 | secondary metabolism |
| TR152767_c0_g1_i1 m.221837;TR48719_c0_g1_i1 m.10139 | Costunolide synthase | 13.20 | 21.19 | 24.91 | 3.72 | secondary metabolism |
| TR98850_c0_g1_i1 m.31055;TR102633_c2_g1_i1 m.34191 | cytochrome p450 cyp82d47-like | 47.18 | 21.74 | 27.30 | 5.56 | secondary metabolism |
| TR132461_c1_g1_i1 m.84509;TR137664_c0_g1_i1 m.108154 | reticuline oxidase-like protein | 44.08 | 20.71 | 26.17 | 5.46 | secondary metabolism |
| TR145678_c4_g3_i2 m.168685;TR145678_c4_g3_i1 m.168684;TR145784_c1_g1_i1 m.169 | reticuline oxidase-like protein | 9.01 | 23.35 | 26.52 | 3.17 | secondary metabolism |
| 772;TR145784_c1_g1_i2 m.169773;TR145678_c4_g3_i3 m.168686 | | | | | | |
| TR91205_c2_g1_i2 m.25396;TR91205_c2_g1_i1 m.25395;TR98968_c7_g1_i2 m.31199;TR98968_c7_g1_i1 m.31197 | caffeoyl- o-methyltransferase 1-like | 5.05 | 24.72 | 27.05 | 2.34 | secondary metabolism |
| TR137449_c3_g1_i1 m.106949;TR139963_c1_g2_i1 m.122248 | anthocyanidin reductase | 7.92 | 23.92 | 26.90 | 2.99 | secondary metabolism |
| TR129361_c0_g1_i1 m.73706;TR112680_c1_g1_i1 m.42842;TR11638_c0_g1_i1 m.2451;TR16272_c0_g2_i1 m.3781;TR16272_c0_g1_i1 m.3780;TR42239_c0_g2_i1 m.9011;TR42239_c0_g1_i1 m.9010;TR142769_c6_g2_i2 m.142765;TR118749_c0_g1_i1 m.50759;TR142769_c6_g2_i1 m.142764;TR118749_c0_g1_i4 m.50760 | secoisolaricresinol dehydrogenase-like | 6.72 | 21.13 | 23.88 | 2.75 | secondary metabolism |
| TR144022_c5_g1_i3 m.153120;TR144022_c5_g1_i1 m.153119 | Leucoanthocyanidin dioxygenase | 9.95 | 20.96 | 24.28 | 3.31 | secondary metabolism |
| TR67190_c0_g1_i1 m.16241;TR78556_c0_g1_i1 m.20841;TR78556_c0_g1_i1 m.20840 | 2-hydroxyisoflavanone dehydratase | 7.65 | 20.78 | 23.72 | 2.94 | secondary metabolism |
| TR88650_c0_g1_i3 m.23841;TR81613_c0_g1_i1 m.21838 | phenylalanine aminolylase | 9.15 | 21.29 | 24.48 | 3.19 | secondary metabolism |
| TR182656_c0_g1_i1 m.226782;TR32489_c0_g1_i1 m.7203 | Cytochrome P450 7D10 | 9.67 | 21.06 | 24.33 | 3.27 | secondary metabolism |
| TR678_c0_g1_i1 m.168;TR678_c0_g2_i1 m.172;TR188048_c0_g1_i1 m.227420;TR42218_c0_g1_i1 m.9004;TR188048_c0_g2_i1 m.227422 | isoflavone reductase like protein | 10.13 | 21.20 | 24.54 | 3.34 | secondary metabolism |
| TR97650_c7_g1_i1 m.29835;TR91773_c4_g2_i1 m.25784 | flavanone 3 hydroxylase | 11.42 | 25.98 | 29.49 | 3.51 | secondary metabolism |
| TR143362_c2_g1_i1 m.147658;TR130640_c11_g1_i1 m.77780 | anthocyanidin o-glucosyltransferase-like | 16.43 | 22.39 | 26.43 | 4.04 | secondary metabolism |
| TR136343_c0_g3_i1 m.101198;TR35235_c0_g1_i1 m.7648;TR35235_c0_g1_i2 m.7651 | premaspirodiene oxygenase-like | 12.89 | 20.67 | 24.49 | 3.69 | secondary metabolism |
| TR120361_c0_g1_i1 m.73705;TR112680_c1_g1_i1 m.42841 | secoisolaricresinol dehydrogenase-like | 10.46 | 20.67 | 24.06 | 3.39 | secondary metabolism |
| TR124549_c0_g1_i1 m.61440;TR122350_c3_g1_i1 m.56759 | dihydroflavonol 4 reductase | 20.92 | 23.08 | 27.46 | 4.39 | secondary metabolism |
| TR165246_c2_g1_i1 m.223627;TR157924_c4_g1_i1 m.222400;TR172984_c0_g1_i1 m.224959;TR150363_c0_g1_i1 m.221098 | transcinnamate-dihydroxylase | 25.44 | 23.49 | 28.16 | 4.67 | secondary metabolism |

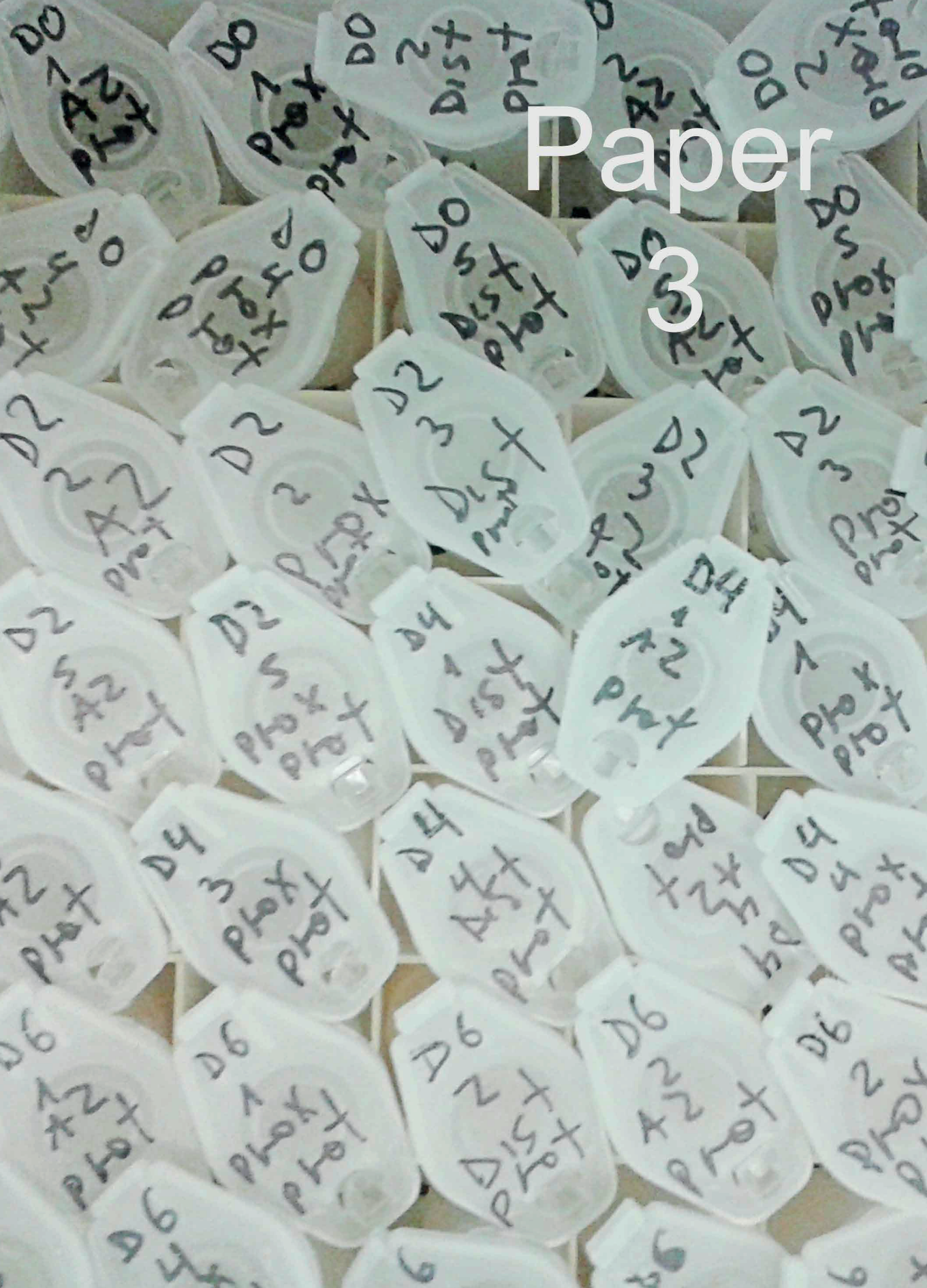
| | | | | | | |
|--|---|--------|-------|-------|------|----------------------|
| TR128947_c6_g1_i1 m. 72236 | Flavonoid 3-hydroxylase 2like | 24.15 | 22.95 | 27.54 | 4.59 | secondary metabolism |
| TR129226_c0_g1_i2 m. 73257; TR134229_c0_g1_i2 m. 91710; TR129226_c0_g1_i1 m. 73256 | secosolaricresinol dehydrogenase like | 13.91 | 21.13 | 24.93 | 3.80 | secondary metabolism |
| TR117084_c1_g1_i1 m. 48447; TR108593_c2_g2_i1 m. 39201 | Flavonoid 3-hydroxylase | 21.34 | 21.87 | 26.29 | 4.42 | secondary metabolism |
| TR27580_c8_g1_i1 m. 6412; TR172918_c12_g1_i1 m. 224904; TR189856_c0_g1_i1 m. 22796 | chalcone synthase, chalcone partial | 21.29 | 26.74 | 31.15 | 4.41 | secondary metabolism |
| TR158410_c0_g1_i1 m. 222664; TR53365_c0_g2_i1 m. 118168; TR68388_c0_g1_i1 m. 16820; | laccase- 14-like isoform x2 | 34.08 | 21.66 | 26.75 | 5.09 | secondary metabolism |
| TR9990_c0_g1_i1 m. 32235; TR199304_c5_g1_i2 m. 118168; TR68388_c0_g1_i1 m. 16820; | phenylalanine ammonia lyase | 25.09 | 21.32 | 25.97 | 4.65 | secondary metabolism |
| TR162830_c0_g1_i1 m. 223395; TR9794_c0_g1_i1 m. 2053 | 4-coumarate ligase 2-like | 28.71 | 20.82 | 25.66 | 4.84 | secondary metabolism |
| TR73121_c2_g1_i1 m. 38683; TR80104_c0_g1_i1 m. 24413; TR80104_c0_g2_i1 m. 2414 | isoflavone reductase like protein | 32.04 | 21.19 | 26.19 | 5.00 | secondary metabolism |
| TR128175_c2_g1_i1 m. 70049; TR127415_c0_g1_i1 m. 68120 | chalcone isomerase | 32.85 | 21.50 | 26.54 | 5.04 | secondary metabolism |
| TR148083_c1_g1_i4 m. 194779; TR147672_c0_g1_i2 m. 188952; TR147672_c0_g1_i1 m. 189 | caffeoyl omethyltransferase | 44.58 | 22.15 | 27.62 | 5.48 | secondary metabolism |
| 951; TR148083_c1_g1_i4 m. 194782; TR148083_c1_g1_i3 m. 194781; TR148083_c1_g1_i2 m | chalcone synthase | 38.00 | 21.58 | 26.83 | 5.25 | secondary metabolism |
| .194780; TR147672_c0_g1_i3 m. 188953 | 4-coumarate--CoA ligase 1 or 2 | 42.88 | 21.11 | 26.53 | 5.42 | secondary metabolism |
| TR63112_c0_g1_i1 m. 34893; TR187887_c0_g1_i1 m. 227298; TR63112_c0_g1_i1 m. 14892 | phenylalanine ammonia partial | 61.27 | 20.66 | 26.59 | 5.94 | secondary metabolism |
| TR137041_c1_g1_i1 m. 104791; TR98968_c1_g1_i1 m. 31196; TR137041_c1_g2_i1 m. 10479 | hydroxycinnamoyl-shikimate quinase | 72.84 | 21.53 | 27.72 | 6.19 | secondary metabolism |
| 2; TR180417_c1_g1_i1 m. 226027; TR137041_c1_g2_i1 m. 104793 | hydroxycinnamoyl transferase isoform 1 | 62.89 | 20.78 | 26.76 | 5.97 | secondary metabolism |
| TR116020_c0_g1_i1 m. 47158; TR108051_c1_g1_i1 m. 38609 | omega hydroxy palmitate o feruloyl transferase | 103.36 | 21.31 | 28.00 | 6.69 | secondary metabolism |
| TR150273_c0_g1_i1 m. 220983; TR158395_c0_g1_i1 m. 222657 | laccase-7 like | 156.28 | 21.76 | 29.05 | 7.29 | secondary metabolism |
| TR172987_c0_g1_i1 m. 224962; TR159528_c0_g1_i1 m. 222981 | Peroxidase 12 | 13.41 | 22.70 | 26.45 | 3.74 | stress response |
| TR172840_c1_g1_i1 m. 224863; TR150098_c0_g1_i1 m. 220735 | peroxidase 12-like | 5.35 | 26.07 | 28.49 | 2.42 | stress response |
| TR136614_c0_g2_i1 m. 102505; TR135008_c0_g1_i1 m. 95058 | peroxidase 12 | 15.15 | 20.76 | 24.68 | 3.92 | stress response |
| TR138438_c0_g1_i1 m. 112914; TR138161_c0_g1_i1 m. 111124; TR138161_c0_g1_i1 m. 111 | probable glutathione s-transferase parc | 11.31 | 21.53 | 25.03 | 3.50 | stress response |
| 125 | blue copper | 13.39 | 21.09 | 24.83 | 3.74 | stress response |
| TR129113_c1_g1_i1 m. 72913; TR128964_c2_g1_i1 m. 72326; TR128964_c2_g1_i2 m. 72327 | desiccation related protein pcc1362 like | 17.74 | 21.10 | 25.25 | 4.15 | stress response |
| TR64432_c0_g1_i3 m. 15265; TR64432_c0_g1_i2 m. 15264 | peroxidase p7-like | 35.18 | 23.72 | 28.85 | 5.14 | stress response |
| TR118345_c1_g1_i1 m. 50178; TR118179_c0_g1_i1 m. 49918; TR47901_c0_g1_i1 m. 9999; T | cationic peroxidase 1like | 172.90 | 22.81 | 30.24 | 7.43 | stress response |
| R82268_c0_g1_i1 m. 22049 | PREDICTED: uncharacterized protein At5g01610-like | 5.89 | 21.45 | 24.01 | 2.56 | unclear |
| TR52958_c0_g2_i1 m. 11481; TR175232_c0_g1_i1 m. 225562; TR52958_c0_g1_i1 m. 11480 | NO ID | 6.77 | 21.44 | 24.20 | 2.76 | unclear |
| TR122998_c1_g1_i1 m. 57844; TR115981_c1_g1_i1 m. 47096; TR122998_c1_g1_i2 m. 57845 | isoform 1 | 8.90 | 21.23 | 24.38 | 3.15 | unclear |
| TR115981_c1_g1_i2 m. 47097 | | | | | | |
| TR102426_c0_g1_i1 m. 33892; TR101045_c0_g2_i1 m. 33051; TR102426_c0_g1_i2 m. 33896 | | | | | | |
| 7 | | | | | | |
| TR101045_c0_g2_i2 m. 33053; TR102426_c0_g2_i1 m. 33894; TR101045_c0_g2_i4 m. 3305 | | | | | | |
| 7 | | | | | | |
| TR99656_c0_g2_i2 m. 31907; TR96813_c0_g2_i2 m. 29240 | | | | | | |
| TR187924_c0_g1_i1 m. 227328; TR130764_c16_g1_i1 m. 78272 | | | | | | |
| TR142141_c2_g1_i1 m. 137795; TR118663_c1_g1_i1 m. 50668; TR112703_c3_g1_i1 m. 4285 | | | | | | |
| 3; TR92489_c0_g1_i1 m. 26172 | | | | | | |
| TR76428_c0_g1_i2 m. 19979; TR76428_c0_g1_i1 m. 19978; TR70091_c0_g1_i2 m. 17372; TR | | | | | | |
| 70091_c0_g1_i1 m. 17371 | | | | | | |
| TR137662_c0_g1_i3 m. 108128; TR125470_c0_g2_i2 m. 63368; TR125470_c0_g2_i1 m. 6336 | | | | | | |
| 7 | | | | | | |
| TR172690_c0_g3_i1 m. 224754; TR172690_c0_g2_i1 m. 224752; TR172690_c0_g1_i1 m. 224 | | | | | | |
| 750; TR157855_c0_g1_i1 m. 222339 | | | | | | |

| | | | | | | |
|---|-----------|--------|-------|-------|------|--------|
| TR143014_c0_g1_i2 m.144805;TR143014_c0_g1_i1 m.144803;TR142866_c0_g1_i2 m.143640;TR142866_c0_g1_i1 m.143638;TR143014_c0_g1_i4 m.144808;TR143014_c0_g1_i3 m.144807 | NO ID | 23.64 | 21.96 | 26.52 | 4.56 | undear |
| TR146872_c7_g11_i3 m.180918;TR145883_c10_g2_i3 m.170696;TR145883_c10_g2_i2 m.170694 | NO ID | 30.25 | 22.81 | 27.73 | 4.92 | undear |
| TR143332_c0_g1_i1 m.147353;TR143097_c1_g1_i2 m.145459;TR143097_c1_g1_i3 m.145460;TR143097_c1_g1_i1 m.145458 | NO ID | 32.26 | 21.65 | 26.66 | 5.01 | undear |
| TR144022_c5_g1_i6 m.153122 | NO ID | 23.97 | 21.35 | 25.93 | 4.58 | undear |
| TR129191_c1_g1_i1 m.73168;TR125696_c1_g1_i1 m.63964 | endo beta | 201.73 | 20.65 | 28.31 | 7.66 | undear |

| Proteins that decrease in the abscission zone relative to the proximal region on Day 6 | | | | | | |
|--|---|-------------|----------------------------------|----------------------------|---|----------------------|
| name sequence | protein name | fold change | log2(mean intensity Proximal D6) | log2(mean intensity AZ D6) | relative abundance [log2(cond.1/control)] | function or category |
| TR180510_c4_g1_i1 m.226089 | ribosome-inactivating protein | 0.03 | 26.08 | 21.13 | -4.95 | defence |
| TR127147_c0_g1_i1 m.67231;TR120094_c2_g1_i1 m.52138 | cucurmosin-like GDSL esterase/lipase 1 | 0.08 | 24.45 | 20.79 | -3.65 | defence |
| TR142902_c0_g1_i3 m.143929;TR143101_c0_g1_i1 m.145477 | Gamma aminobutyrate transaminase 1, mitochondrial | 0.07 | 25.49 | 21.60 | -3.89 | other |
| TR117236_c0_g1_i1 m.48601;TR114109_c0_g1_i1 m.44670;TR142246_c0_g1_i1 m.138596;TR118971_c0_g1_i1 m.50979;TR123763_c0_g1_i1 m.59307;TR142246_c0_g1_i2 m.138598;TR140221_c0_g1_i3 m.123967;TR140221_c0_g1_i2 m.123965;TR140221_c0_g1_i1 m.123963 | FT-interacting protein 1 | 0.11 | 23.51 | 20.30 | -3.21 | other |
| TR118090_c0_g1_i1 m.49765;TR115594_c0_g1_i1 m.46534;TR115594_c0_g1_i2 m.46536;TR118090_c0_g1_i2 m.49766 | acid phosphatase 1 | 0.07 | 25.16 | 21.32 | -3.84 | other |
| TR117712_c0_g1_i2 m.49269;TR117712_c0_g1_i1 m.49268;TR112650_c0_g1_i2 m.42815;TR112650_c0_g1_i1 m.42814 | lachrymatory-factor synthase-like | 0.11 | 24.01 | 20.86 | -3.15 | other |
| TR14332_c0_g2_i1 m.3335;TR103148_c0_g2_i1 m.34711;TR14332_c0_g1_i1 m.3333;TR103148_c0_g1_i1 m.34709;TR14332_c0_g1_i1 m.3334;TR103148_c0_g1_i1 m.34710 | ricin-agglutinin family protein | 0.10 | 29.16 | 25.90 | -3.26 | other |

| | | | | | | |
|---|--|--------------|----------------|----------------|----------------|--|
| TR146428_c1_g1_i3 m.176160;TR146428_c1_g1_i2 m.176158;TR146428_c1_g1_i1 m.176156;TR144929_c2_g1_i3 m.161741;TR146428_c1_g1_i6 m.176166;TR146428_c1_g1_i5 m.176164;TR144929_c2_g1_i4 m.161743;TR144929_c2_g1_i2 m.161739;TR146428_c1_g1_i4 m.176163;TR143344_c0_g1_i9 m.147482;TR143344_c0_g1_i6 m.147478;TR143344_c0_g1_i4 m.147475;TR141914_c0_g1_i9 m.135954;TR141914_c0_g1_i8 m.135952;TR141914_c0_g1_i6 m.135949;TR141914_c0_g1_i5 m.135948;TR141914_c0_g1_i4 m.135947;TR141914_c0_g1_i2 m.135945;TR141914_c0_g1_i10 m.135955;TR144929_c2_g1_i1 m.161738;TR143344_c0_g1_i3 m.147474;TR143344_c0_g1_i2 m.147473;TR141914_c0_g1_i3 m.135946;TR141914_c0_g1_i11 m.135957;TR143344_c0_g1_i7 m.147480;TR143344_c0_g1_i5 m.147477;TR143344_c0_g1_i8 m.147481;TR143344_c0_g1_i1 m.147472;TR141914_c0_g1_i7 m.135951;TR141914_c0_g1_i1 m.135944 | na+ h+ antiporter family protein aquaporin tip4-1 | 0.16 0.13 | 23.42 24.53 | 20.79 21.63 | -2.63 -2.90 | other other |
| TR122629_c0_g1_i1 m.57344;TR120442_c0_g1_i1 m.52864 TR147229_c11_g1_i5 m.184921;TR147229_c11_g1_i2 m.184901;TR147229_c11_g1_i1 m.184891;TR147229_c11_g1_i4 m.184918;TR147229_c11_g1_i3 m.184911 | chorophyll binding Serine hydroxymethyltransferase, mitochondrial | 0.08 | 25.33 | 21.61 | -3.72 | other |
| TR41833_c0_g1_i1 m.8942;TR89600_c1_g1_i2 m.24184 TR144202_c0_g1_i3 m.154540 TR147444_c0_g1_i3 m.187498 | Serine hydroxymethyltransferase 1 Citrate synthase | 0.09 0.07 | 25.83 26.14 | 22.27 22.36 | -3.55 -3.78 | primary metabolism primary metabolism |
| TR116037_c0_g1_i1 m.47178;TR113336_c0_g1_i1 m.43608 TR140691_c1_g1_i1 m.127264;TR140557_c3_g1_i1 m.126284;TR140557_c3_g1_i3 m.126286 | aspartic proteinase nepenthesin-1 terpene synthase 10-like | 0.08 0.05 | 25.32 25.19 | 21.51 21.61 | -3.81 -3.58 | primary metabolism proteolysis |
| TR115421_c0_g1_i2 m.46344;TR114132_c0_g1_i1 m.44700;TR115421_c0_g1_i1 m.46343;TR114132_c0_g1_i2 m.44701 | probable caffeine synthase 4 | 0.07 | 24.77 | 20.92 | -3.85 | secondary metabolism |
| TR143872_c0_g2_i3 m.151939;TR139301_c0_g1_i1 m.118130;TR143872_c0_g2_i4 m.151941;TR143872_c0_g2_i2 m.151938 | NO ID | 0.06 | 24.71 | 20.75 | -3.96 | undear |
| TR129152_c0_g1_i1 m.73048;TR124474_c1_g1_i1 m.61223;TR140446_c4_g5_i1 m.125393 | uncharacterized acetyltransferase at3g50280-like | 0.17 | 26.45 | 23.92 | -2.53 | undear |
| TR143234_c2_g1_i1 m.146722;TR143464_c2_g1_i1 m.148513 | NO ID | 0.11 | 24.74 | 21.56 | -3.18 | undear |

Paper 3



De novo transcriptomic analysis in poinsettia flower during abscission

Luz G. Muñoz-Sanhueza, Mallikarjuna Rao Kovi, YeonKyeong Lee and Anne Kathrine Hvoslef-Eide*

Department of Plant Sciences (IPV), Faculty of Biosciences, Norwegian University of Life Sciences, Norway, Campus Ås, Universitetsstunet 3, 1430 Ås, Norge

*Correspondence: Anne Kathrine Hvoslef-Eide: trine.hvoslef-eide@nmbu.no

luz.munoz@nmbu.no

mallikarjuna.rao.kovi@nmbu.no

yeonkyeong.lee@nmbu.no

Keywords: Abscission, poinsettia, *Euphorbia pulcherrima*, *de novo* transcriptome, cell wall transformation, auxin-related genes, abscission-signaling cascade.

Abstract

The capacity of abscise organs has been an important trait of selection from the very beginning of the plant domestication. Abscission is a process that involves cell separation and a programmed sequenced of events. In nature, abscission can affects the different parts of a plant like, fruits, seeds, steams, floral parts and even roots. Ultimately, the detachment of an organ is the efficient response that the plant gives to an always-changing environment. Environmental conditions, pathogens and the developmental stage of the plant itself can trigger a signaling cascade leading to the abscission of an organ. Nevertheless, in despite of all the research efforts, the mechanism underlying the abscission process, remain elusive. In order to understand the gene mechanisms globally during the abscission process, we have performed a detailed transcriptomic study in poinsettia (*Euphorbia pulcherrima*). Four time points were selected in order to follow up the progression of the abscission process, Day 0, Day 2, Day 4 and Day 6 after decapitation; and three regions of the flower bud were chosen, distal, abscission zone and proximal. Spatial and temporal comparisons of the differentially expressed genes were used to study the expression levels occurring at every place and time in the abscission process. Auxin-related genes such as, transcription factors and transporters, were massively down-regulated by D2, suggesting that the decapitation causes disrupting the auxin flux, leading to auxin-depletion in the flower bud. Cell wall transformation genes changed in expression both over time (temporal) and between the abscission zone and adjacent tissue (spatial), where pectin, cellulose and hemicellulose seem to be the main targets of the remodeling. Important orthologue of cell wall related gene *MYST6*, auxin efflux carrier *PIN1* and abscission-signaling cascade *IDA* were detected for the first time in poinsettia, suggesting an active role in the process.

1. Introduction

Abscission is the detachment of an entire organ from a plant. This action might be the response to a change in the environment or a developmental stimulus. Shrubs trees, for example, shed their leaves seasonally. Another example of abscission is the dispersal of seeds and the shedding of excess flowers to prevent over abundant fruit setting (Addicott, 1982). For crops plants, abscission is highly correlated to yield loss. Abscission of flowers is not only important in fruit trees, but also in flowering ornamental plants, since senescence and premature shed of floral parts, as petals and flower pedicels reduces their ornamental value (Ferrante et al., 2015). Therefore, it is crucial to understand the mechanisms to control abscission in order to prevent yield losses in crops plants and increase decorative value in ornamentals. We have chosen *Euphorbia pulcherrima* (poinsettia), a highly decorative plant during the Christmas time, as our reference plant to study abscission because of its biological characteristics, such the presence of an inflorescence with six developmentally identical flowers and the possibility to induce abscission in a controlled fashion. The flowers of poinsettia abscise in approximately 7 days, depending on environmental conditions, after decapitating the floral organs at a specific point, and the abscission zone (AZ) becomes distinguishable approximately 4 days after the decapitation (Figure 1) (Munster, 2006). Our previous studies have shown that the inducible system to study flower abscission in poinsettia, makes it a valuable model for abscission in general (Lee et al., 2008; Hvorslev-Eide et al., 2016).

The abscission normally takes place in a discrete layer of cells placed in the base of the organ to be detached called abscission zone (AZ). These cells undergo a series of events that eventually will lead to the detachment of the organ. As a start, there is a differentiation of the AZ, then the AZ have to acquire the capabilities to respond to the abscission cues, following on is the activation of the abscission that involves the cell separation between the part of the plant to be detached and the body of the plant, and finally the formation of a protective layer, preparing for exposure to drying out or attacks by microorganisms (Estornell et al., 2013). All these steps require the participation of many genes controlling each stage, and even though numerous genes have been described, the exact mechanisms of how abscission is controlled remain somewhat elusive. The genes *qSH1* and *ATH1*, both coding BEL-type transcription factors (TFs), in the rice grain and the stamen of *Arabidopsis*, respectively, have been proposed to have a role in the differentiation of the AZ after close examination of the phenotypes in their mutants, which had no AZ (Konishi et al., 2006; Gómez-Mena and Sablowski, 2008). Several genes have been found to participate in the activation of abscission in *Arabidopsis*. An important one is the *INFLORESCENCE DEFICIENT IN ABSCISSION (IDA)* (Butenko et al., 2003). *IDA* encodes a peptide that act as a ligand for the receptors-like kinases HAESA and HAESA-like 2 triggering the signaling cascade that involve phosphorylation of an unknown MAPKKK, which in turn phosphorylates the MAPKK4/5 that eventually activates MPK3/6 (Jinn et al., 2000; Cho et al., 2008). MPK3/6 suppresses the TF KNAT1, probably permitting the TFs KNAT2 and KNAT6 to induce the expression of genes related to cell separation (Shi et al., 2011; Butenko et al., 2012). The activation of the abscission process ultimately will promote the dissolution of the middle lamella and its pectic components (Ridley et al., 2001), as well as the cellulosic and hemi-cellulosic components of the cell wall, together with the degradation of the pectin polysaccharides, allowing its disassembly. These are characteristic features of abscission and have been the focus of intense investigation over decades (Abeles, 1969; Gonzalez-Carranza et al., 2007). The action of numerous cell wall transformation proteins

in a temporal and spatial is necessary for the disassembly of the cell wall (Lee et al., 2008; Merelo et al., 2017). The participation of endo-1,4- β -glucanases or cellulases and polygalacturonases (PGs), have also been extensively studied (Abeles, 1969; Riov, 1974), while some others, such as pectate lyases (PLs) and xyloglucan endotransglucosylases hydrolases (XETs) have more recently been shown to be involved in abscission, thus adding more complexity to the cell wall transformation during the abscission process (Tucker et al., 2007; Cai and Lashbrook, 2008).

Abscission has also been studied regarding the regulatory effects of certain hormones, such as auxin. Ellis *et al.* (2005) found that the *Arabidopsis* mutants in the auxin response factors 1 and 2, *arf1* and *arf2*, displayed phenotypes with delayed abscission, suggesting a possible auxin genetic control of the process. Additionally, experimental data suggested the auxin delays abscission when applied to the distal region of cotton petioles (Louie and Addicott, 1970). Moreover, auxin applied to the proximal region of leaf stalks in beans explants accelerate the process (Addicott and Lynch, 1951). These results suggest that during abscission, both the AZ as well as the neighboring areas (distal and proximal) respond to the signals controlling abscission.

Advancement in next generation sequencing technologies, like transcriptome sequencing (RNA-Seq) paved the way for understanding the complex plant responses (Martin et al., 2013). Overall, the aim of the transcriptomic analysis is to detect genes, which are differentially expressed among different conditions, leading to a precise knowledge of the genes or pathways associated with the conditions. In addition, the global transcriptome studies could be performed, even in non-model species, which lacks a genome sequence, and array based assays are commonly used to study gene expression in the model species, such as *Arabidopsis* and tomato (Cai and Lashbrook, 2008; Meir et al., 2010). In abscission, several transcriptome studies have successfully detected novel genes and pathways interactions in many species such as apple (Botton et al., 2011), olive (Parra et al., 2013), melon (Corbacho et al., 2013) and citrus (Merelo et al., 2017).

In this transcriptomic study, we assessed the changes in the transcriptome of the AZ, distal and proximal regions of the poinsettia flower buds after the induction of abscission by decapitation, in a period of 6 days. We describe the effect of the decapitation on the expression of auxin-related genes and cell wall transformation genes after the induction. Additionally, we evaluated the expression of genes from the abscission-signaling cascade.

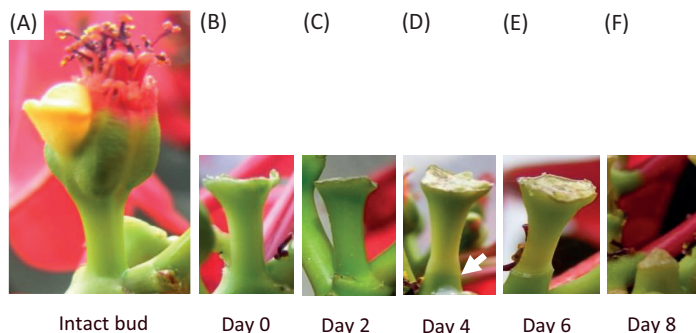


Figure 1. Progression of the process leading to the abscission of the poinsettia flowers after decapitation. A) Intact flower bud. B) Flower bud immediately after decapitation. C) Flower bud two days after the decapitation. D) Flower bud four days after the decapitation and, the AZ is visible (white arrow). E) Flower bud six days after decapitation with the AZ clearly visible. (F) Proximal region with a characteristic cone shape after floral detachment.

2 Materials and methods

2.1 Plant material

Cuttings with two small leaves were taken from *Euphorbia pulcherrima* Willd ex Klotzsch. (Poinsettia) ‘Lilo Red’ (Ecke Ranch, California, USA) mother plants grown under long day conditions (LD) (16 h light from High Pressure Sodium (HPS) lamps) at $150 \mu\text{molm}^{-2}\text{s}^{-1}$, 22°C day/ 20°C night, 70% Relative Humidity (RH)). The cuttings were rooted for two weeks in 7 cm pots in a medium of approximately one third volume coarse perlite and the rest peat-based soil (Gartnerjord, Tjerbo Torvfabrikk, Rakkestad, Norway) under the same conditions of light and RH. The rooted cuttings were then potted into 12 cm pots in the same soil and kept under LD for another 3 weeks, then moved to short day (SD) with 10 h HPS light at $150 \mu\text{molm}^{-2}\text{s}^{-1}$ and 20°C for 24h with 74% RH, to induce flowering.

2.2 Induction of abscission and tissue harvesting

The induction of abscission in the six developmentally identical third order flowers was performed according to our previous work (Munster, 2006; Lee et al., 2008; Hvoslef-Eide et al., 2016) by decapitating with a razor blade just below the floral organs, leaving the floral bottom intact (no visible red remnants of anthers). Under winter conditions in Norway, the abscission zone normally becomes visible four days after the decapitation and the upper portion of the bud abscise after seven or eight days. For this reason, the decapitated flower buds were harvested every 48 h starting from the Day 0 (D0) until Day 6 (D6) after decapitation, frozen in liquid nitrogen and stored at -80°C until the further pre-treatment (cryosectioning, freeze-drying and laser microdissection) before the RNA isolation.

2.3 Cryosectioning and subsequent freeze drying process

The decapitated flower buds were treated according to Muñoz-Sanhueza *et al.* (2018) (manuscript 1 in this thesis). In short: The decapitated flower buds were longitudinally cryosectioned using the Cryostat Microtome HM560 (Microm, Germany). Section thickness was $200 \mu\text{m}$ and the temperature of the knife and the specimen were set up at -16°C and -15°C respectively. Approximately 4-5 cryosections were collected in frame slides polyethylene terephthalate (PET) membrane Leica ($1.4 \mu\text{m}$, ref n° 11505190, Leica Microsystems, Germany) nuclease free. After the collection, the PET membrane

slides were freeze-dried for 24 h at - 45 °C to - 50 °C *in vacuo* (Heto Holten A/S, Allerød, Denmark). A custom-made thermal block was used (4 mm thickness) that had been made to the same size as that of the slides. This was pre-cooled and placed underneath the slide with the samples in order to maintain the whole system cool while sampling.

2.4 Laser Microdissection

The freeze-dried material on the slide PET membranes were placed on the laser microdissection microscope (Leica model 6000, Microsystems, Germany), the objective 6,3X was used to localize the three different tissues to be dissected for further RNA isolation: distal, abscission zone (AZ) and proximal. The software Laser microdissection software V6.7.2.4295 (Leica Microsystems, Germany), was used to control the microscope and select the average conditions of the laser such as the aperture 45, laser power 60 and speed 20. However, some adjustments were made when needed to obtain good samples. The average of areas of the dissected material was $1,4 * 10^7 \mu\text{m}^2$ and the thickness was 200 μm . The mass of the tissues was calculated using the volume obtained. The microdissected tissues were collected inside the cap of a 0,6 ml RNase free microcentrifuge tube, where they fell in by gravity.

2.5 RNA isolation

The RNA isolation from the microdissected tissues was performed using the Ambion RNAqueous®- Micro kit (Ambion Inc., Austin, TX, USA) following supplier instructions with small modifications, such as the use of a micropipette tip to crash the material inside the tube in presence of the lysis buffer. The protocol of isolation was followed by a 20 minutes DNase treatment according to supplier instructions. The RNA was resuspended in 20 μl of nucleases free water, purified by LiCl–EtOH precipitation and stored at -80°C. The concentration and quality of the RNA was analysed using an Agilent 2100 Bioanalyzer (Agilent Technologies, CA, USA) and a RNA 6000 Pico Kit chip (Agilent Technologies, CA, USA), following manufacturer's instructions.

2.6 cDNA library preparation and Illumina sequencing

The RNA isolated was sent to the BGI-Shenzhen, (China) in order to make the libraries and the pair-end sequencing. The libraries were prepared according to the TruSeq RNA Sample Prep Kit v2 (Illumina, San Diego, CA, USA) and DNA initial amount was 200 ng. The pair-end sequencing was carried out in a HiSeq 2000 System (Illumina, CA, USA) using the TruSeq SBS KIT-HS V3 (Illumina, CA, USA).

2.7 De novo transcriptome analysis and assembly validation

After trimming adapter sequences and filtering low quality reads using the sickle program (<https://github.com/najoshi/sickle/blob/master/README.md>), the *de novo* assembly was performed for the clean reads as mentioned by Kovi *et al.* (2016, 2017). Briefly, the clean reads derived from the three tissues; abscission zone (AZ), distal (Dist) and proximal (Prox) at four time points; Day 0 (D0), Day 2 (D2), Day 4 (D4) and Day 6 (D6), with three replicates each, were used to construct the *de novo* assembly using the Trinity assembler (version 2.0.2) (Haas *et al.* 2013).

To evaluate the quality of poinsettia transcriptome assembly, we used the CEGMA software (version 2.4) (Parra *et al.*, 2007). The software ran with default parameters to detect the presence of 248 extremely conserved core eukaryotic genes (CEGs) and their coverage in transcriptome assembly, to evaluate the completeness of the assembly.

2.8 Estimating transcript abundance

Once the assembly quality was assessed, the *de novo* assembled transcripts, was used as a reference to map back the paired end reads from each of the tissue per time point per replicate by bowtie program, with a maximum of one mismatch (–bowtie-n 1). Further, transcript abundance was estimated using RSEM version 1.1.11 (Li and Dewey, 2011) to generate the read count data for the assembled transcripts, separately for each tissue at each time point, with a total of 12 conditions (AZD0, AZD2, AZD4, AZD6, DistD0, DistD2, DisD4, DistD6, ProxD0, ProxD2, ProxD4 and ProxD6).

2.9 Identifying differentially expressed genes

Gene expression levels in the RNA-Seq analysis was measured as expected number of fragments per kilobase of transcript sequence per millions base pairs sequenced (FPKM) (Trapnell et al., 2010). The edgeR program (Robinson et al., 2010) was used to process the transcript matrix files derived from the RNA-Seq by Expectation Maximization (RSEM) program for detecting differentially expressed genes (DEGs), determined with a false Discovery Rate (FDR) of 0.001. Briefly, pairwise comparisons were carried out between all the selected time points and the tissues with a generalized linear model (GLM) estimating a negative binomial distribution to the calculated mean values of the three biologically independent samples. For each gene, fold changes and P values (pval) as well as P values adjusted (padj) for multiple testing with the Benjamini-Hochberg procedure (Benjamini and Hochberg, 1995), were used to control FDR. The sequence with padj of less than 0.001 was deemed to be significantly DEGs. The DEGs obtained from the edgeR program was used as input for clustering, and for constructing multidimensional scaling plots using the R program. The transcripts showing differential expression at any time point in particular tissue type were clustered using a K-means clustering algorithm. Both temporal and spatial comparisons were performed to detect the up / down regulated DEGs.

2.10 BLAST, functional annotation and gene ontology (GO) analysis

BLASTx was performed on the DEGs, followed by annotation using Blast2GO program (Conesa et al., 2005; Conesa and Gotz, 2008) to know the function of the gene sequences. An E-value threshold of 10^{-6} was used for the BLASTx search, and 10^{-10} for the annotation, with a cut-off value of 55 and a GO weight Hsp-hit value of 20. The GO enrichment analysis for the differential GO term distribution was performed with a p-value significance cut-off value of 0.01. GO classifications of DEGs in the AZ, distal and proximal areas were generated using web histogram tool WEGO (Ye et al., 2006). Further, enrichment analysis by Fisher's exact test was performed to understand the in depth role of over-or under represented GO terms across D2, D4 and D6 time points in the AZ using Blast2GO and also the REVIGO (Supek et al., 2011) tools.

2.11 Comparison of significant DEGs to the abscission related genes identified in previous study

To compare the DEGs with the abscission related genes described by Hvoslef-Eide et al. (2016), we collected the sequences from the gene bank accession numbers of these genes. The collected nucleotide sequences were blasted against our transcriptome assembly using BLASTn program. The highly significant hits above 80% coverage were retained to identify the homologous genes related to abscission in our transcriptome data.

2.12 Identification of *MYST6* (a putative rhamnogalacturonan lyase) and *Solanum lycopersicum* and *PIN-FORMED1 (SIPIN1)* in poinsettia

Two important abscission-related genes, *MYST6* and *SIPIN1* sequences were identified in poinsettia in this study. The two gene sequences were collected from NCBI, and a blast performed against our poinsettia transcriptome assembly using BLASTn

program. The two transcripts encoded for these two genes *MYST6* and *SIPIN1*, were further explored to monitor the gene expression at distal, AZ and proximal regions at four time points D0, D2, D4 and D6. In addition, we also performed an RNA *in situ* hybridization to study localization of *MYST6* gene expression.

2.13 RNA *in situ* hybridization of cell wall gene *MYST6* (Rhamnogalacturonan lyase) in the AZ

Flower buds of poinsettia ‘Lilo Red’ induced for abscission and control plants were cut into small pieces (2-3 mm-thick), vacuum infiltrated with fixative (4 % paraformaldehyde in sodium phosphate buffer, pH 7.0 and 0.1 % (v/v) Tween 20) for 1 h, and left overnight at 4°C. Samples were washed in 0.85 % saline, dehydrated through a graded EtOH series (10%, 30%, and 50% all with 0.85% saline) from then into a Tissue-Tek VIP Jr (Sakura, Japan) automatic embedding machine and embedded in paraplast (Sakura, Japan). 10 µm-thick sections were collected on poly-L-lysine coated slides.

The selected sequence for hybridization was labelled through PCR with sense and antisense probes labeled with digoxigenin (DIG). dUTP were prepared using T3 and T7 RNA polymerases (Roche, Germany), respectively, using a single stranded oligo for clone 477 from a cell wall screen in *Zinnia elegans* (gift from Dr. Daniel Fulton, John Innes Centre, Norwich, UK). This was chosen because it was a putative cell wall related gene orthologous to our transcript detected in this study (TR141664_c0_g1_i1), which is encoded for *MYST6* (Rhamnogalacturonan lyase) (Dan Fulton, pers. comm.). The rest of the *in situ* procedure used the protocol is described in Hvoslef-Eide *et al*, (2016). Sections were monitored and recorded under a microscope using bright field optics (Nikon E800, Japan).

3 Results

3.1 *De novo* transcriptome assembly

A total sum of 393,119,567 reads with an average length of 100 bp was generated from the Illumina sequencing. The *de novo* assembly produced 473,308 contigs with N50 (50% of the assembly containing contigs having equal or larger length than this value) of 1,347 bp. The maximum contig length was 14,822 bp (Table 1). CEGMA (Core Eukaryotic Genes Mapping Approach) analysis confirmed the quality and the extensiveness of the transcriptome assembly with presence of 97% of complete core of CEGs (Core Eukaryotic Genes) and 99.19% of at least partially represented CEGs. The average number of orthologues per CEG was 4.33 and the percentage of detected CEGs with more than one orthologue was 99.59 % (Table 2). This indicates that the RNA-Seq was successful and picks up the most of the genes in poinsettia.

Table 1. Characteristics of the *de novo* transcriptome assembly in poinsettia flower bud during abscission.

| Parameter | Number |
|-------------------------|-------------|
| Min. contig length (bp) | 224 |
| N50 (bp) | 1,347 |
| Max. contig length (bp) | 14,822 |
| Total no. of contigs | 473,308 |
| Sum of the reads | 393,119,567 |

Table 2. Results of CEGMA analysis for validation of the *de-novo* assembly in poinsettia.

| Out of 248 CEGs | Poinsettia |
|--|------------|
| % of fully represented | 97.18 |
| % of at least partially represented | 99.19 |
| Average number of orthologs per CEG | 4.33 |
| % of detected CEGs with more than 1 ortholog | 99.59 |

3.2 Detection of DEGs among the three regions of the flower bud at different stages of the abscission process

The *de novo* assembly was used to perform pairwise comparisons between the samples with a fold change ≥ 2 and a FDR ≤ 0.001 to detect highly significant DEGs. The spatial and temporal comparisons discovered 22,101 highly differentially expressed transcripts. To determine the relationships among all the samples, the 22,101 DEGs were clustered according level of expression and showed in heat maps for the spatial and the temporal comparisons (Figure 2). In the heat maps for the spatial comparisons (A-C), the AZ grouped together with the distal region at the D2 and D4, while at the D6, the AZ grouped together with the proximal region. In the temporal comparisons (D-F), the three regions at the D4 were always grouped with the D6 and then with the D2, while the D0 showed different pattern of expression compared to the other time points.

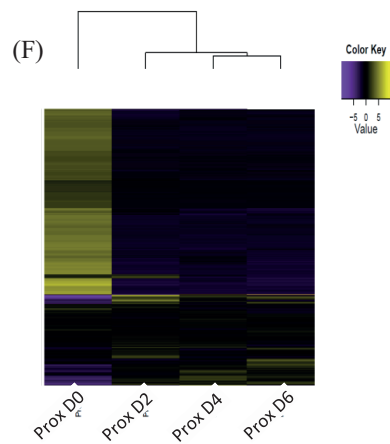
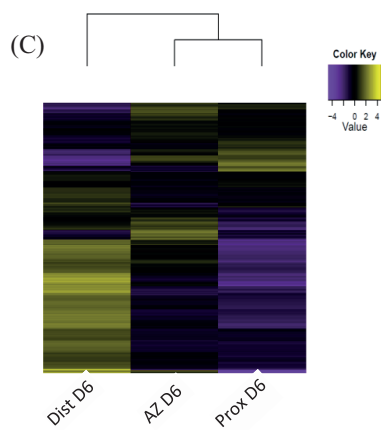
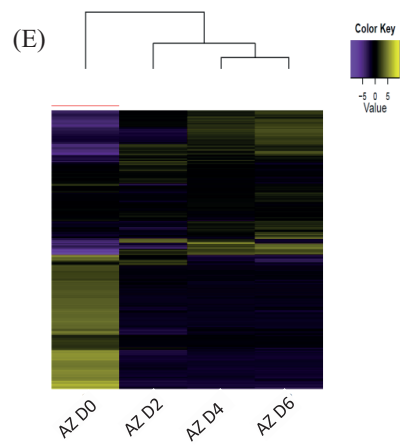
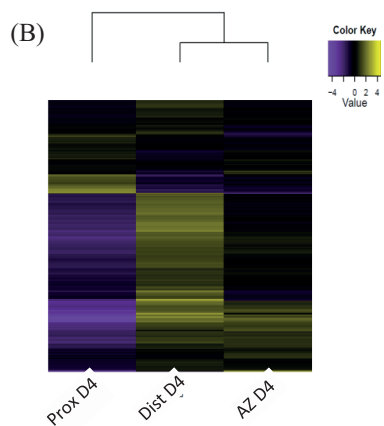
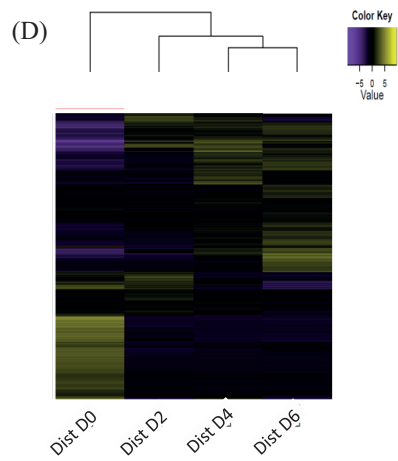
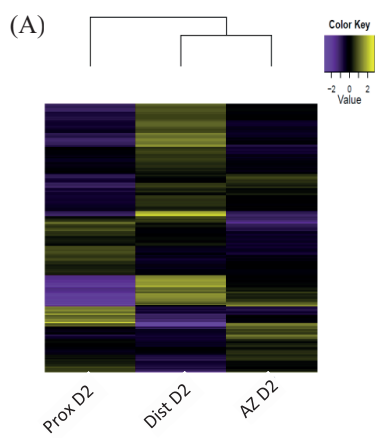


Figure 2. Heat maps showing the relationship among the samples of spatial and temporal comparisons during abscission in poinsettia flowers. A-C) Spatial comparison, A) Day 2, B) Day 4 and C) Day 6 after decapitation to induce flower abscission. D-F) Temporal comparison, D) Distal region (Dist), E) abscission zone (AZ) and F) Proximal region (Prox).

The spatial comparison on D2 showed higher number of DEGs between the distal and the proximal regions of the flower bud with 41 genes up-regulated and 111 genes down-regulated relative to the other comparisons distal region and AZ and proximal region and AZ (Figure 3). The distal region compared to the AZ showed 17 and 20 genes up- and down-regulated, respectively. The AZ compared to the proximal region exhibited that 28 and 18 genes were up- and down-regulated, respectively. A similar trend was observed on D4 with more numbers of genes changing expression compared to D2. The highest number of DEGs were found in the comparison between the distal and the proximal regions where 157 and 729 genes were up- and down-regulated, respectively at D4. The comparison between the distal region and the AZ on D4 showed 19 and 22 up- and down-regulated genes, respectively. In the comparison between the AZ and proximal region, 44 and 37 genes were up- and down-regulated, respectively. On D6, the number of genes differentially expressed in the comparison between the distal and proximal regions increased dramatically reaching 532 and 2,035 up- and down-regulated genes, respectively. The comparison between the distal region and the AZ showed that 187 and 131 genes were up- and down-regulated. When exploring the comparison between the AZ and the proximal region, a lower number of DEGs were discovered with 37 up-regulated genes and 80 down-regulated genes (Figure 3).

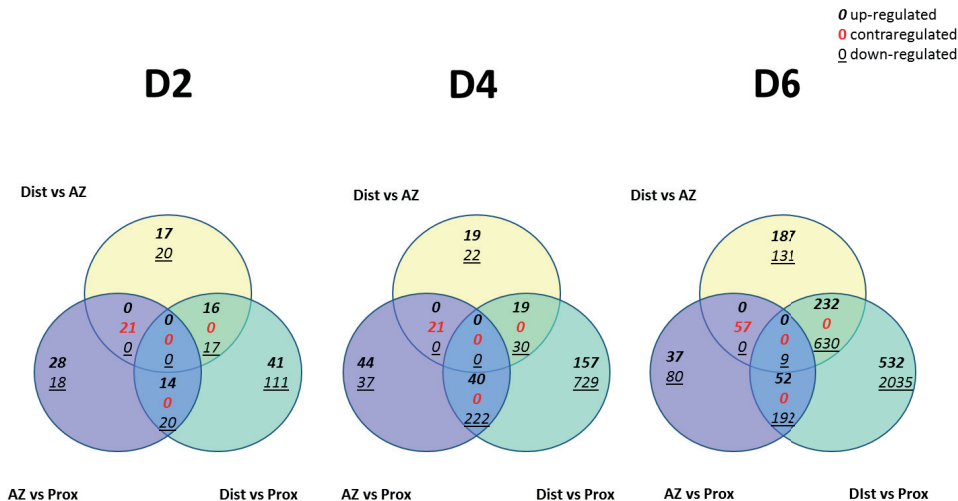


Figure 3. Venn diagrams show the number of differentially expressed genes during abscission in poinsettia flowers for spatial comparisons. Bold numbers indicate up-regulated genes, underlined numbers indicate down-regulated genes and red numbers indicate contra-regulated genes; which are up-regulated under one condition and down-regulated under the

other condition. Yellow circles illustrate Distal vs Abscission zone (AZ), purple circles illustrate AZ vs Proximal and green circles illustrate Distal vs Proximal.

We investigated the identity of the cell wall transformation-related genes up-regulated in the AZ at D2, D4 and D6 related to the other two adjacent regions. One cell wall transformation gene was up-regulated in the AZ during D2 (extension-2-partial) and one transcript on D4 (endoglucanase 9-like), however on D6, more diversity of genes were up-regulated in the AZ, 23 transcripts belonging to extensins, endoglucanases, expansins, endo- β -glucanases (cellulases), glucomannan 4- β -mannosyltransferases, PLs, udp-arabinopyranose mutase and PGs were up-regulated in the AZ on D6 Table 3. The values of Log2FC of the cell wall transformation genes up-regulated in the AZ compared to the other two regions are listed in the Supplementary Table 1.

Table 3. Up-regulated cell wall transformation-related transcripts in the abscission zone of poinsettia flower bud related to the distal or proximal regions on Day 2 Day4 and Day 6.

| Day 2 up-regulated in the AZ compared to proximal | |
|--|--------------------------|
| Gene product | No of transcripts |
| extensin-2- partial | 1 |
| | |
| Day 4 up-regulated in the AZ compared to proximal | |
| Gene product | No of transcripts |
| endoglucanase 9-like | 1 |
| | |
| Day 6 up-regulated in AZ compared to distal | |
| Gene product | No of transcripts |
| endoglucanase 9-like | 1 |
| expansin-b3-like | 3 |
| endoglucanase 9 | 1 |
| endo- β -glucanase | 3 |
| glucomannan 4- β -mannosyltransferase 9 | 2 |
| glucomannan 4- β -mannosyltransferase 2-like | 1 |
| probable pectate lyase 8 | 2 |
| endoglucanase 11-like | 1 |
| | |
| Day 6 up-regulated in AZ compared to proximal | |
| Gene product | No of transcripts |
| extensin-2-like | 1 |
| extensin-2- partial | 1 |
| α -expansin 4 | 1 |
| endo- β -glucanase | 2 |
| udp-arabinopyranose mutase 1 | 1 |
| expansin-a4 | 1 |
| polygalacturonase-like | 1 |
| polygalacturonase precursor family protein | 1 |

The temporal comparisons were carried out to identify DEGs during the abscission process by comparing each stage with the previous stage. Starting from the D0 with 48 h intervals until D6 after the decapitation, we used each region of the decapitated flower for the comparisons (Figure 4). The number of DEGs varied substantially among the three time points and the three regions of bud. The largest number of DEGs were expressed two days after decapitation (D2), less DEGs were expressed at D4 and D6. In the AZ, 1,382 and 4,353 up- and down-regulated genes were identified at D2. The distal region showed 1,544 and 3,806 up- and down-regulated genes. In the proximal region, 924 and 4,525 up- and down-regulated genes were found, respectively.

For the comparison D4 vs D2, the total number of DEGs in the distal region was higher than in the other two regions of the bud with 223 and 89 up- and down-regulated genes. The same comparison for the AZ revealed 109 genes up-regulated and 62 genes down-regulated. Only 25 genes were up-regulated and 56 genes were down-regulated in the proximal region in the comparison between D4 and D2.

The last pairwise comparison, in the transition from D4 to D6, a higher number of DEGs in the distal region was found, compared to the other two regions; 224 and 83 genes were up- and down-regulated. In the AZ, 23 and 26 genes were up- and down-regulated, respectively. In the proximal region, the same number of genes (43 genes) were up- and down-regulated (Figure 4).

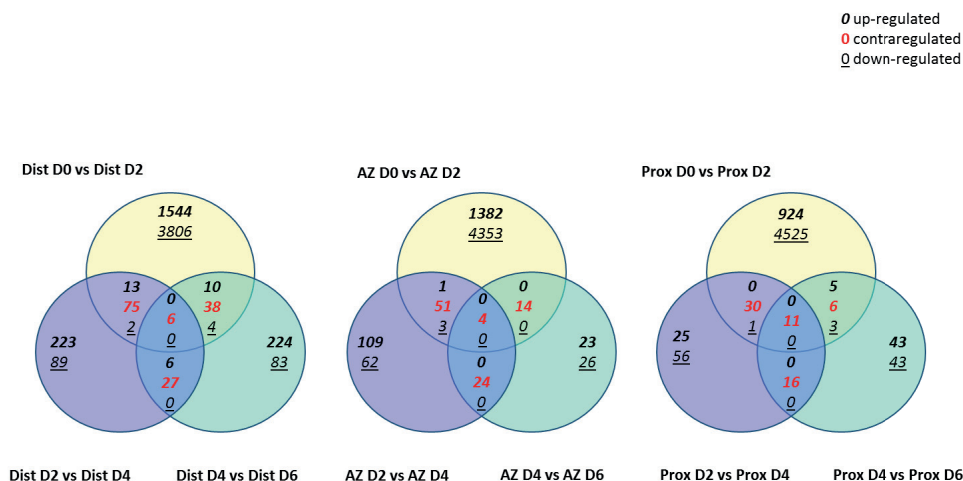


Figure 4. Venn diagrams show the number of differentially expressed genes during abscission in poinsettia flowers for temporal comparisons. Bold numbers indicate up-regulated genes, underlined numbers indicate down-regulated genes and red numbers indicate contra-regulated genes; which are up-regulated under one condition and down-regulated under the other condition. Yellow circles illustrate Day 2 (D2) vs Day 0 (D0), purple circles illustrate Day 4 (D4) vs (D2) and green circles illustrate Day 6 (D6) vs (D4).

3.3 Blast and Gene annotation of differentially expressed transcripts.

BLASTx was performed for the 22,101 differentially expressed transcripts in all the conditions using BLAST2GO program (Conesa et al., 2005) and InterProScan (Jones et al., 2014) databases in order to annotate the transcripts. Out of 22,101 transcripts, 14,172

transcripts were successfully annotated (Supplementary Figure 1A). Top-hit species distribution for blast annotation of the DEGs in the poinsettia flowers during abscission are illustrated in Supplementary Figure 1B. Physic nut (*Jatropha curcas*) had the highest hit with more than orthologous 7,000 genes, castor bean (*Ricinus communis*) was the second one with almost 5,500 orthologous genes. Both these species belong to the same family as poinsettia, the *Euphorbiaceae* family. Putative descriptions and functions for these transcripts were mainly assigned based on the annotations from these two species.

GO classification of DEGs identified in the three regions of the flower bud abscission (distal, AZ and proximal regions) were derived by WEGO GO (Web Gene Ontology Annotation Plotting) (Figure 5) (Ye et al., 2006). The results are classified into the three categories of the GO which are cellular component (CC), molecular function (MF) and biological process (BP). Only significant p-values ($p\text{-value} \leq 0.01$) were considered for being included in the histogram. The CC GO terms “chromosome” and the “cytoskeleton”, “intracellular non-membrane-bounded organelle” were higher in the AZs than in the other two regions of the bud. Several BP GO terms related with cell cycle such as “cell cycle”, “cell division”, “chromosome organization”, “DNA metabolic process” and the “M phase of mitotic cell cycle” were found in the AZs, additionally to “organelle organization” and “cellular component organization”. The number of genes with MF GO terms such as lyase activity and with BP GO terms such as autophagy and cellular catabolic process was higher in the distal region (Figure 5). In the proximal regions, the number of genes with BP GO terms like “cellular biosynthetic process”, “intracellular transport”, “nuclear transport”, “signal transduction”, “macromolecule biosynthetic process” and “gene expression” was higher than in the other two regions of the flower bud (Figure 5).

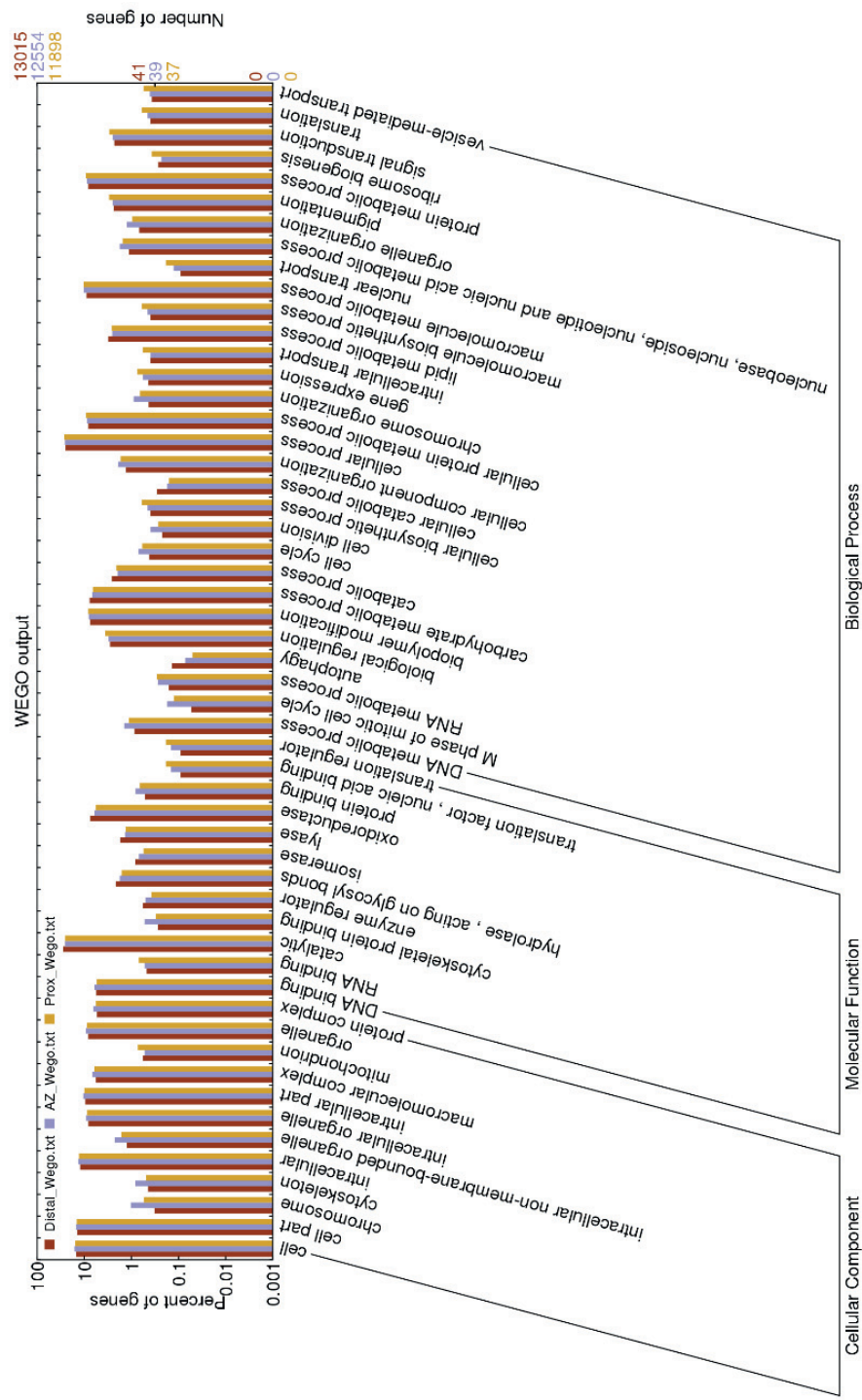
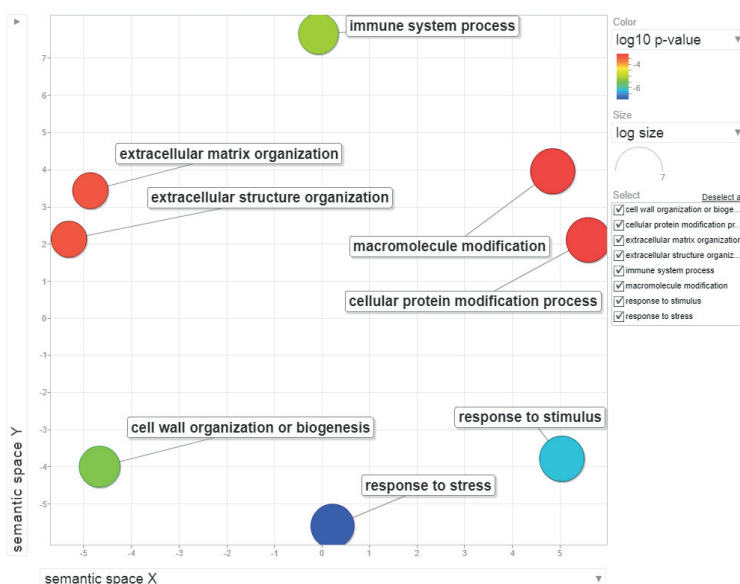


Figure 5. Gene Ontology classification of the differentially expressed genes during abscission in the three regions of the poinsettia flower bud into the three categories including cellular component, molecular function and biological process.

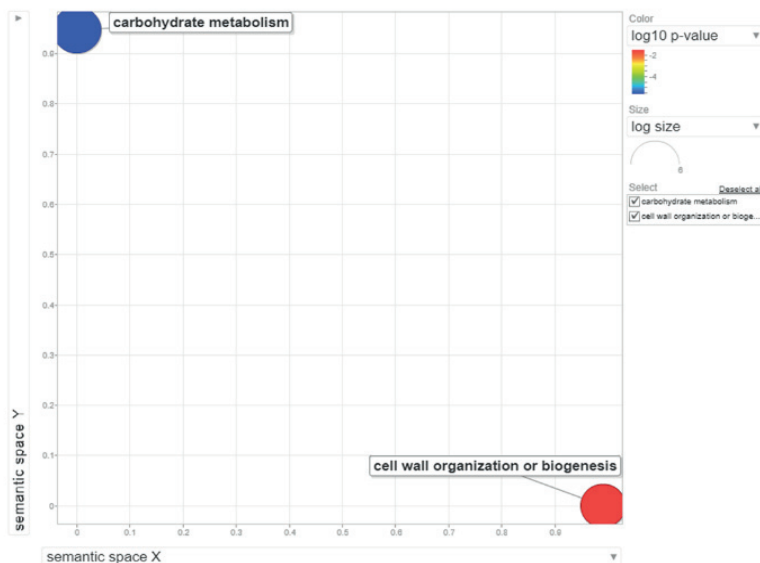
3.4 Enrichment analysis in the abscission zone at different time points

To get a better overview of the processes taking place in the AZ during abscission, an enrichment analysis by Fisher's exact test (p-value of 0.01) was performed. The background used to determine those GO terms under- or over-represented in the AZs was the 22,101 DEGs among the tissues and time points. The tool REVIGO helps to visualize the long lists of GO terms generated by reducing their complexity (removing the redundant ones) and plotting the remaining GO terms according to semantic similarity. In the BP, eight GO terms were enriched in the AZ at D2 including 'response to stress', 'response to stimulus', 'immune system process', 'cell wall organization or biogenesis', 'extracellular matrix organization', 'extracellular structure organization', 'macromolecule modification' and 'cellular protein modification process' (Figure 6A). The BP GO term 'cell wall organization or biogenesis' was also enriched in the AZ at D4 after the decapitation together with the 'carbohydrate metabolic process' (Figure 6B). On the D6, GO terms in BP related to biosynthesis were identified in the AZ, such as 'macromolecule biosynthesis' and 'organic substance biosynthesis', in addition to 'nitrogen compound metabolic process' and 'gene expression' and 'translation'. (Figure 6C).

(A)



(B)



(C)

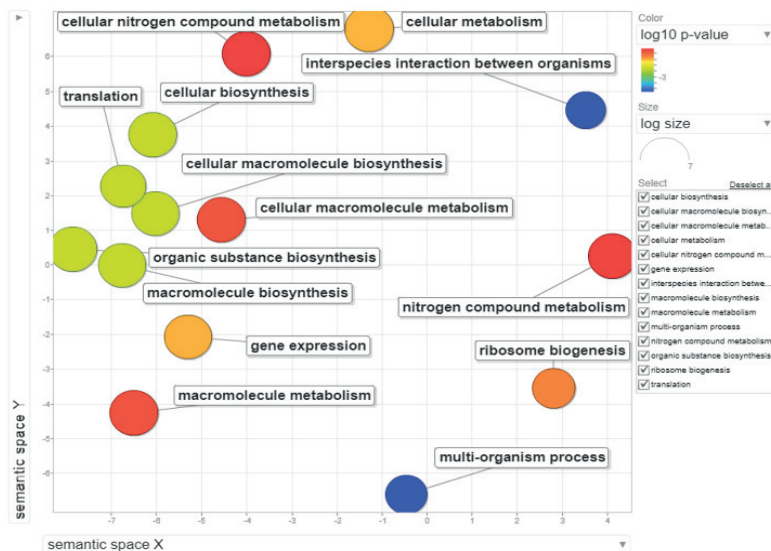


Figure 6. Visualization of the enrichment analysis on the category of ‘biological process’ performed in the abscission zone (AZ) of the poinsettia flowers during the abscission process. (A) AZ at Day 2. (B) AZ at Day 4 and (C) AZ at Day 6. Blue color indicates Gene Ontology categories with higher p-values, while red shows lower p-values.

3.5 Auxin-related transcripts

Based on the hypothesis that the decapitation of the flower bud interrupts the supply of auxin from the apical part (source) to the rest of the flower bud (sink), we selected auxin-related transcripts like transcriptional factors, auxin carriers, auxin-response genes and genes involved in regulating the auxin homeostasis for further analysis (Table 4). Only three transcripts related to auxin were up-regulated from D0 to D2; the auxin-responsive protein *iaa26*-like and two auxin-responsive family proteins (Supplementary Table 2A), while 232 transcripts were down-regulated (Supplementary Table 2B), of which 86 were down-regulated in the AZ. Table 4 lists the down-regulated auxin-transcripts in the AZ on D2 sorted by type of gene product. 22 transcripts were involved in auxin homeostasis, conjugation and hydrolysis of conjugates. One transcript was related to auxin biosynthesis (probable indole-3-pyruvate monooxygenase *yucca10*). In addition, 45 transcription factors were down-regulated already after 48h. Twelve transcripts were involved in auxin transport, including the important auxin efflux carrier component 1 family protein (*PIN1*), auxin efflux carrier component 8 (*PIN8*) and the protein kinase pinoid, (*PID*) which activates *PIN1*. We have chosen to focus on a recent publication in tomato and found the orthologue of *Solanum PIN1* (*SIPIN1*) was identified in poinsettia; the transcript (TR139620_c0_g2_i1) detected has 77% identity to the *SIPIN1*. The expression of this transcript in our studies showed similar expression as *SIPIN1* in tomato abscission by Shi *et al.* (2017) (Figure 7). Higher expression was seen in distal, while very low expression in AZ and proximal on D0, almost no expression observed later in D2, D4 and D6.



Figure 7. The gene expression of *SIPIN1* observed in D0, D2, D4 and D6 across distal, AZ and proximal zones. *SIPIN1* gene expression observed only at D0, with highest expression at distal and thereafter gradual decrease of expression from AZ to proximal.

Table 4. Down-regulated auxin-related transcripts in poinsettia flower bud abscission zones (AZ) on Day2 compared to the AZ on Day 0.

| Gene product | No of transcripts |
|---|-------------------|
| Auxin conjugation, homeostasis and biosynthesis | |
| probable indole-3-acetic acid-amido synthetase | 13 |
| iaa-amino acid hydrolase ilr1-like 4 | 6 |
| indole-3-acetic acid-amido synthetase | 2 |
| probable indole-3-pyruvate monooxygenase yucca10 | 1 |
| Auxin-induced proteins (repressors TFs) | |
| auxin-induced protein aux22 | 4 |
| auxin-induced protein 15a-like | 7 |
| protein topless-like | 1 |
| auxin-induced protein 22d | 1 |
| auxin-induced protein aux28-like | 3 |
| auxin-induced protein 6b | 1 |
| auxin-induced protein 6b-like | 1 |
| auxin-induced protein | 1 |
| Auxin-responsive proteins (repressors TFs) | |
| auxin-responsive protein iaa4-like | 1 |
| auxin-responsive protein iaa4 | 2 |
| auxin-responsive protein iaa1 | 6 |
| auxin-responsive protein iaa14-like | 3 |
| auxin-responsive protein iaa27 | 1 |
| auxin-responsive protein iaa8-like | 1 |
| auxin-responsive protein iaa27-like | 2 |
| auxin-responsive protein | 2 |
| Auxin carrier and transport | |
| auxin efflux carrier component 1 family protein (<i>PIN1</i>) | 5 |
| auxin efflux carrier component 8 (<i>PIN8</i>) | 4 |
| probable auxin efflux carrier component 1c | 1 |
| protein kinase pinoid (<i>PID</i>) | 1 |
| serine threonine-protein phosphatase pp2a-3 catalytic subunit | 1 |
| Auxin response factors | |
| auxin response factor 4 | 4 |
| auxin response factor | 2 |
| auxin response factor 19 | 1 |
| auxin response factor 18 isoform x1 | 1 |
| Auxin response genes | |
| saur-like auxin-responsive protein | 2 |
| auxin-responsive protein saur61-like | 4 |
| indole-3-acetic acid-induced protein arg2-like | 1 |

3.6 Cell wall transformation-related transcripts

In order for an organ to be detached from a plant, the middle lamella and general cell wall degradation is a prerequisite. Therefore, we studied transcripts with cell wall transformation functions with a different expression pattern on D2 compared to D0. We identified 58 transcripts up-regulated in the AZ only (Table 5) and 96 down-regulated only in the AZ (Supplementary Table 3B). Among the up-regulated genes in the AZ on D2, three transcripts codify for extensins, 16 for glucosidases, 18 pectinesterases, 5 β -xylosidases, 4 β -galactosidases, 2 PGs and 10 other different types of cell wall transformation genes. We also discovered that approximately 100 more transcripts down-regulated than up-regulated in the three regions of the flower bud (Supplementary Table 3A and 3B).

Table 5. Up-regulated cell wall transformation-related transcripts in poinsettia flower bud abscission zones (AZ) on Day 2 compared to the AZ on Day 0.

| Gene product | No of transcripts |
|---|-------------------|
| Extensins | |
| extensin-2- partial | 2 |
| extensin-2-like | 1 |
| β-glucosidases | |
| β -glucosidase 41 isoform x1 | 3 |
| β -glucosidase 41 | 7 |
| β -glucosidase 11-like isoform x1 | 1 |
| β -glucosidase 16-like isoform x2 | 2 |
| β -glucosidase 12-like | 1 |
| glucan endo- β -glucosidase-like | 2 |
| Pectinesterases | |
| pectinacylesterase family protein | 11 |
| pectin acylesterase 8 isoform x1 | 1 |
| probable pectinesterase 68 | 3 |
| pectinesterase | 1 |
| probable pectinesterase 53 | 2 |
| β-xylosidases | |
| β -xylosidase α -l-arabinofuranosidase 2-like | 2 |
| β -d-xylosidase family protein | 2 |
| β -xylosidase α -l-arabinofuranosidase 2 | 1 |
| β-galactosidases | |
| β -galactosidase-like isoform x2 | 2 |
| β -galactosidase protein 1 | 2 |
| Polygalacturonases | |
| probable polygalacturonase | 2 |
| Others | |
| bifunctional udp-glucose 4-epimerase and udp-xylose 4-epimerase 1 | 4 |
| protein trichome birefringence-like 43 | 1 |
| protein notum homolog | 3 |

3.7 Expression of *MYST6* (Rhamnogalacturonan lyase) gene in poinsettia

We have chosen to use a putative *MYST6*, found in differential display (DD) in *Zinnia* (Dan Fulton, personal comm), as one of the genes involved in the separation zone. The RNA *in situ* hybridization of poinsettia flowers with a probe from this *Zinnia* DD, which has sequence homology to *Arabidopsis* At2g22620 and *MYST6*. *MYST6* belongs to a Rhamnogalacturonan lyase family. The RNA *in situ* hybridization was performed in poinsettia flowers. The expression of this gene follows the AZ through the pedicel on D6 (Figure 8A) and the break of the AZ is seen on D7 (Figure 8B), while still expressing *MYST6*. The expression of transcript (TR141664_c0_g1_i1), identified as *MYST6* in poinsettia transcriptome also correlated with the *in situ* hybridization results. The gene expression of *MYST6* in temporal comparisons of AZ, not observed in D0 and D2, while gradually increased from D4 with highest expression observed at D6 in AZ (Figure 8C). Where as in spatial comparisons at D6, expression levels increased from distal to AZ, while no expression observed in proximal (Figure 8D).

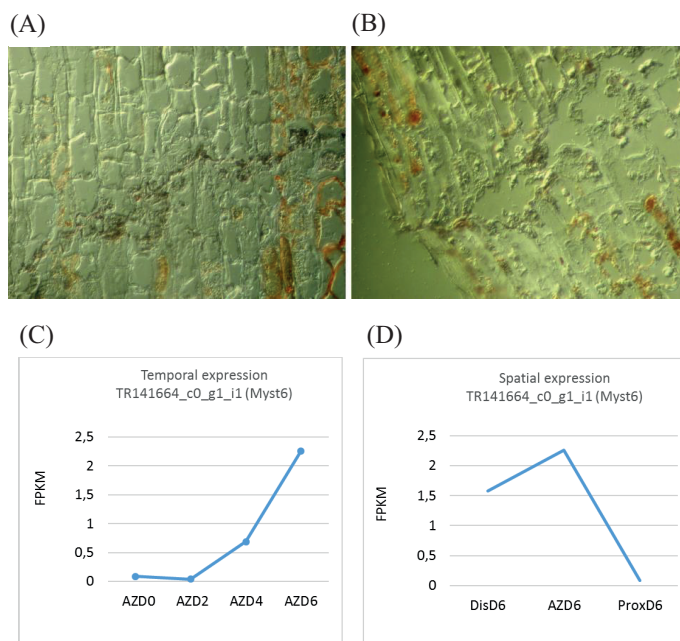


Figure 8. RNA *in situ* hybridization in poinsettia on D6 (A) and D7 (B) with the antisense probe of *MYST6*, this particular probe was made from a homolog in *Zinnia elegans* (gift from Dan Fulton, John Innes Centre, Norwich). Image taken with 25x magnification. The gene expression of *MYST6* observed in temporal comparisons (C) in AZ and spatial comparisons (D) in D6. *MYST6* not expressed in D0 and D2, while gradually increased from D4 to D6 in AZ. While in spatial comparisons at D6, higher expression levels observed at AZ.

3.8 Identification of genes previously found as regulating abscission in poinsettia

Previous studies in our group identified 29 genes differentially expressed in the AZ of poinsettia flower bud over the period from induction to abscission (Hvoslef-Eide *et al.*, 2016). To test their expression behavior in the present transcriptomic study, we used the sequences of these genes to look for their presence in the temporal comparison, between D0 and D2 in AZ. The results showed 11 sequences up-regulated in the AZ on D2 and five down-regulated in the AZ on D2 (Table 6A and Table 6B). The 11 gene products include members of the cytochrome family, caspases-like, glucosidases, histone deacetylase, bidirectional sugar transporter as well as a RNA-binding protein, a eukaryotic translation factor, a DNA RNA polymerase, a NADH dehydrogenase and a histone demethylase. Regarding the five genes product down-regulated, members of the glycine-rich protein family, DNA-directed RNA polymerase, fk506-binding protein, eukaryotic translation initiation factor and β -glucosidase were identified.

Table 6A. Up-regulated genes identified in the AZ of poinsettia flowers for the temporal comparison D0 vs D2 during abscission, also found in Hvoslef-Eide *et al.* 2016.

| Gene product | No of transcripts |
|---|-------------------|
| cytochrome family subfamily polypeptide | 1 |
| eukaryotic translation initiation factor 3 subunit j-like | 1 |
| casp-like protein 1d1 | 2 |
| casp-like protein aralydraft_485429 | 1 |
| rna-binding protein cabeza-like | 1 |
| β -glucosidase 41 | 6 |
| β -glucosidase 41 isoform x1 | 1 |
| β -glucosidase 12-like | 1 |
| histone deacetylase 18-like protein | 2 |
| glucan endo- β -glucosidase-like | 1 |
| nadh dehydrogenase subunit 4 | 1 |
| lysine-specific histone demethylase 1 homolog 3 | 1 |
| bidirectional sugar transporter n3-like | 2 |
| dna rna polymerases superfamily protein | 1 |

Table 6B. Down-regulated genes identified in the AZ of poinsettia flowers for the temporal comparison D0 vs D2 during abscission, also found in Hvoslef-Eide *et al.* 2016.

| Gene | No of transcripts |
|---|-------------------|
| glycine-rich protein a3 | 2 |
| dna-directed rna polymerase chloroplastic | 1 |
| fk506-binding protein 4-like | 1 |
| eukaryotic translation initiation factor 1a | 2 |
| β -glucosidase 17 | 1 |

3.9 Identification of genes in the abscission-signaling cascade

In this transcriptomic study, three members of the abscission-signaling cascade were found differentially expressed in different time points and regions of the flower bud: *IDA*, which it was up-regulated in the distal region on D4 compared to D2 in the temporal comparison (Table 7A). The other genes involved in the abscission-signaling cascade are the receptor HAESA (receptor-like protein kinase 5), that was down-regulated in all the three regions of the flower bud on D2 relative to D0 in the temporal comparisons. And, the *MPK3* (mitogen-activated protein kinase 3) that was also down-regulated on D2 in the AZ and in the proximal region in the temporal comparison (Table 7B).

Table 7. Genes involved in the abscission-signaling cascade, differentially expressed in the spatial or temporal comparisons in poinsettia flower bud. (A) Log2FC of *IDA* (protein ida) during temporal comparisons Distal Day 4 vs Distal Day 2. (B) Log2FC of HAESA (protein kinase 5 and *MPK3* (mitogen activated kinase 3) during temporal comparisons Day 2 vs Day 0.

| A. Temporal comparisons – up-regulated | | | | |
|---|------------------------------------|-------------------------------|---------------------------|-------------------------------|
| Transcript ID | Gene product | $Log2(\frac{DistD4}{DistD2})$ | | |
| TR13705_c0_g2_i1 | protein ida | 5,304 | | |
| TR10921_c0_g1_i1 | protein ida | 5,774 | | |
| B. Temporal comparisons –down-regulated | | | | |
| Transcript ID | Gene product | $Log2(\frac{DistD2}{DistD0})$ | $Log2(\frac{AZD2}{AZD0})$ | $Log2(\frac{ProxD2}{ProxD0})$ |
| TR98629_c0_g1_i1 | receptor-like protein kinase 5 | -5,696 | -6,597 | -6,698 |
| TR115682_c0_g1_i3 | receptor-like protein kinase 5 | -10,143 | -8,127 | -7,726 |
| TR180721_c0_g1_i1 | mitogen-activated protein kinase 3 | N.A. | -3.156 | -3.222 |
| TR180490_c0_g1_i1 | mitogen-activated protein kinase 3 | N.A. | -3.250 | -3.162 |

4 Discussion

4.1 The spatial and temporal comparisons shows different perspectives of the changes in gene expression during abscission

In this study, the changes in the transcriptome of the poinsettia flowers over the time course of abscission has been assessed. Three regions of the flower bud (AZ, distal and proximal) were used to determine the changes in expression during a six days period (D0 to D6), one day prior to expected abscission on D7. A total of 22,101 transcripts were found differentially expressed among all the flower regions and time points. The spatial comparisons showed the D2 as the time point with least changes in gene expression among the three regions (Figure 3). On contrary, the temporal comparisons showed the biggest changes in genes expression in the transition from D0 to D2, (Figure 4).

The study of the changes in gene expression during abscission unraveled how space and time are prominent actors in the development of the program underlying the organ detachment. The results of the WEGO analysis offered an overview of the processes in each region of the flower bud. The GO terms “lyases”, “autophagy” and “cellular catabolic process” (Figure5). tell us that the distal region undergoes a massive disassembly of cellular components for nutrients salvaging, this phenomenon is observed in senescence (Yamada et al., 2009). The distal region prepares for dying as an active process, and this process involves recycling of cellular components after a macromolecule degradation program.

Interestingly, while the distal region undergoes a catabolic disassembly, WEGO analysis (Figure 5) shows that GO terms as “biosynthesis”, “intracellular transport”, “macromolecular biosynthetic process” and “signal transduction” are the ones with more genes in the proximal region, suggesting that this part of the bud deals with the cellular materials coming from the distal part and reuses molecules for biosynthesis.

The AZ also has a specific profile of genes changing. The GO terms “chromosome”, “cytoskeleton”, “cell cycle”, “DNA metabolic process” and “cell division” (Figure 5), all give us a clue about one of the requirements for abscission in poinsettia, the cell division of the AZ cells. Cell division within the AZ has been reported by Lee *et al.* 2008 on D5 and by other authors (Webster, 1968; Sexton et al., 1977). These results illustrate the importance of abscission studies from a spatiotemporal perspective, and including the adjacent regions to the AZ, distal and proximal. This rearrangement of the cell structure in the AZ is most likely a prerequisite also in other species with a secondary AZ development (Hvoslef-Eide et al, 2016).

4.2 The effect of decapitation on gene expression of auxin-related genes

4.2.1 Auxin transporters and auxin homeostasis are down-regulated at D2

Addicott *et al.* (1955) hypothesized that there is a close correlation between auxin gradients and abscission. Auxin synthesis occurs in the shoot apex, flowers and leaves; thus, auxins needs to be transported from the synthesis sites to the rest of the plant by auxin transporters. The most important for our studies are the efflux transporters, like PIN proteins. The PIN proteins are responsible for the polarized transport of auxin from cell to cell because of their asymmetrical localization in the cells (Křeček et al., 2009) . In this study, the *PIN1* and *PIN8* were both down-regulated, suggesting that the auxin flux has been disrupted. It has been observed that auxin regulates the expression of some PIN genes (Schrader et al., 2003; Vieten et al., 2005).

A recent study on tomato demonstrates that SIPIN1 regulates the auxin efflux during abscission (Shi et al., 2017). These authors have compared the expression levels of *PIN1* in

proximal, AZ and distal regions, in a very similar manner to our experimental set up. Our studies shows the expression of our poinsettia orthologue of TR139620_c0_g2_i1 (*SIPIN1*) with the highest expression in the distal part. The gene expression gradually decreased in AZ and proximal areas at D0, while there was almost no expression observed for the rest of the abscission process (Figure 7) in accordance with the findings of Shi *et al.* (2017). Thus, we have demonstrated that the decapitation of the bud, i.e. removing auxin-producing tissue, contributed to the down-regulation of these transporters as a result of the disruption of the auxin flux (Table 4).

Additionally, the protein kinase pinoid (*PID*) which is a protein kinase that activates PIN1, that enables the directional intercellular flux of auxin (Li *et al.*, 2011), was also down-regulated. Not only auxin transporters were down-regulated, but also auxin-homeostasis genes seem to be affected in the AZ on D2. Several transcripts (13) of the probable indole-3-acetic acid-amido synthetase (*GH3*) are down-regulated. GH3 conjugates auxin with several amino acids to cope to excess of auxin (Staswick *et al.*, 2005), indicating that this gene is no longer needed because of the reduced auxin levels.

4.2.2 Auxin- related transcription factors are also down-regulated on D2

There are two classes of TFs that control the expression of auxin response genes (Guilfoyle and Hagen, 2007). The first class is the auxin-responsive factors (ARFs), these TFs bind to the auxin response elements (AuxREs) onto the promoters of auxin response genes. ARFs might activate or repress AuxRE, depending on a domain on the ARF proteins. The second class of TFs are the auxin-induced proteins (Aux/IAA), which are repressors of the auxin response (Guilfoyle and Hagen, 2007). The Aux/IAA family members are expressed in response to the auxin levels (Abel *et al.*, 1995), thus it makes sense that in the absence or reduced levels of auxin, these TFs would be down-regulated, as is the case in our DEGs on D2.

Zuo *et al.* (2012) studied the expression profiles of the auxin-responsive genes *Aux/IAA* during tomato pedicel abscission induced by ethylene. The authors studied this phenomenon by Real Time PCR probes and found that not all the *Aux/IAAs* responded in the same way; some decreased their expression levels (*IAA1*, 3, 5, 8, 9, 10, 16, 17 and 27), others increased (*IAA2*, 4, 6, 7, 11, 12, 13, 26 and 29) when measured 0.5 h after excision. In the poinsettia transcriptome, significant changes in gene expression of auxin-related genes were observed only on D2, but not in the later harvest times. In addition, the number of auxin-related genes that were down-regulated was significantly higher than the up-regulated (Supplementary Table 2A), as a result of the removal of the auxin source (floral organs). Zuo *et al.* (2012) reported that some of the *Aux/IAA* genes increased their expression levels in the beginning (0.5 h) and then, decreased them later on. We were not able to pick up on such subtle changes, as the *Aux/IAA* genes in our case were down-regulated at D2 in poinsettia, we observed no changes in expression levels thereafter. A possible explanation for this difference in behavior of the *Aux/IAA* genes from Zuo *et al.* (2012) study is the timing of harvesting the samples. Abscission response is faster in tomato flower pedicel, within hours, compared to poinsettia flower, which normally takes seven days. In addition, our samples were harvested every second day, the first 48 h after decapitation. We might have missed capturing the slight changes in gene expression right before or after the D2 harvest.

In this transcriptomic study, the disruption of the auxin flux might have provoked the down-regulation of several TFs, such as *ARFs* and *AUX/IAA*, which in turn might have turned off several genes regulated by auxin, for example, small auxin up-regulated RNAs (*SAURs*) and other *AUX/IAA* (Nagpal *et al.*, 2005; Okushima *et al.*, 2005). This cascade of down-

regulation might have amplified the down-regulation effect, contributing to the high number of transcripts down-regulated on D2. The down-regulation of all these auxin-related genes suggest that there is a depletion of auxin by D2. We believe that the auxin production in the floral organs might prevent abscission from taking place, to ensure that the flower can produce a seed for reproduction of the plant. This is in accordance with a lot of evidence that auxin is involved in abscission (Addicott and Lynch, 1951; Addicott et al., 1955; Basu et al., 2013). By decapitating the floral organs, the remaining flower becomes auxin-depleted contributing to the down-regulation of the auxin-response genes.

4.3 Changes in cell wall transformation-related genes, spatial and temporal overview

Abscission involves the dissolution of the middle lamella and the primary cell wall in the AZ, to enable organ detachment. Several studies confirm that the dissolution of the middle lamella and the cell wall is the product of the combined action of several cell wall transformation enzymes in a highly orchestrated manner (Sexton, 1979; Roberts et al., 2002; Wu and Burns, 2004; Cai and Lashbrook, 2008; Merelo et al., 2017).

The enrichment analysis performed in the AZs at each time point, showed the GO term BF category “cell wall transformation or biogenesis” to be overrepresented in both D2 and D4, confirming the relevance of these processes involving changes in the cell wall. Based on previous work in our group, it was expected to find over-representation of cell wall transformation genes starting from D2, since the biggest changes happened during the first 48 h in the AFLP-DD in poinsettia (Hvoslef-Eide et al., 2016). The present study using a RNA-Seq represents a much higher resolution of up- and down-regulated genes, giving us a higher number of DEGs overall. The changes in the cell wall composition on D4, making the AZ visible, is the consequence of earlier processes that starts before. Lee *et al.* (2008) also detected a pre-abscission cell wall transformation, using monoclonal antibodies to cell wall epitopes, at D2 in the distal region of the flower bud, even though the AZ was not visibly before D4-5.

The spatial comparisons showed that the AZ exhibit a low number of up-regulated cell wall transformation genes until D4. However, towards the end of the process by D6, the AZ showed several cell wall transformation genes being up-regulated related to distal and proximal areas in the bud (Table 3). Considering all the spatial comparisons, the classes of genes found were: endoglucanases (cellulases), expansins, extensins, PLs, glucomannan 4- β -mannosyltransferase, and udp-arabinopyranose mutase 1. These enzymes are related to pectin, cellulose and hemicellulose degradation and in the case of expansin with the relaxation of the cell wall during growth and development (Cosgrove et al., 2002). This is in total accordance with previous findings in poinsettia using monoclonal antibodies and Fourier transform infrared microspectroscopy (FT-IR) analysis to determine the changes in cell wall (Lee et al, 2008). We have also previously seen genes associated with endoreduplication, which would fit with expansins being active to increase cell size towards the time of detachment of the flowers (Hvoslef-Eide et al., 2016).

The temporal comparisons showed that genes from cell wall transformations are both down- and up-regulated already after 24 h (Supplementary Table 3A and 3B). Regarding the types of genes up-regulated over the time course of abscission (temporally), it was possible to deduct that pectin, cellulose and hemicellulose are the targets of these genes. The temporal comparisons showed that cell wall transformation-related transcripts that were up-regulated on D2 in the AZ included: extensins, glucosidases, PEs, β -xylosidases, galactosidases and PGs among others, (Table 5). We therefore hypothesize that the first pre-abscission event in the AZ

encompasses cellulose, pectin and hemicellulose degradation. It is likely that the middle lamella starts its degradation already by D2, although, the visible signs of the cell wall remodeling is only clear from D4 or D5, as seen as a ring of AZ around the pedicel, with a clear distinction in color between the distal and proximal part of the bud (Figure 1D).

Even though in both spatial and temporal comparisons, the macromolecules target of transformation were the same, pectin, cellulose and hemicellulose, a different profile of genes was found in both temporal as well as in the spatial comparisons. We interpret this finding as the confirmation that the disassembly of the cell wall during abscission follows a highly controlled series of events, and that the different enzymes participating in the task contributed with their hydrolytic specificities to the organ detachment, and confirms the occurrence of DEGs in the three regions analyzed in a highly orchestrated manner.

4.3.1 Spatiotemporal changes in polygalacturonases (PGs)

PGs cleave the α -galacturonic acid residues from the polygalacturonic acid polymers, such as homogalacturonan (HG) from pectin. The middle lamella is rich in pectic substances (Ridley et al., 2001), and has been appointed as the first target to be degraded during abscission (Bornman, 1967). Increased PG activity was detected in citrus leaf explants already by Riov (1974). Meir *et al.* (2010) described a sequential pattern of expression for three PG genes in tomato flower abscission PG1, PG2 and PG4; the first two were up-regulated 8 h after the induction of abscission by removal of the flower in tomato, while PG4 was up-regulated much earlier 2 h. We found two probable PG genes up-regulated in the AZ on D2 (Table 5) and three in the distal region (Supplementary Table 3A). Since a substantial number of cell wall transformation genes were differentially expressed by D2, we expected to find more PGs, however we speculate that since pectin is a highly complex polysaccharide, presenting different level of modification and substitutions, other enzymes may be needed first to clear the way for the PGs to exert their catalytic activity. Additionally, because PGs were up-regulated in the AZD6 related to proximal, we deduce that this gene is necessary all the way until the organ detachment is completed.

4.3.2 Spatiotemporal changes in extensins

Merkouropoulos and Shirsat (2003) evaluated the expression of the fusion gene *atExt1::gus* under different stresses, they described expression of the fusion gene in damaged stems and leaves. Additionally the authors described the expression of the fusion gene in the AZ of sepals, petals and stamen of *Arabidopsis*. Another work where extensins were up-regulated was in the transcriptomic of the stamen abscission in *Arabidopsis* (Cai and Lashbrook, 2008). In the present transcriptomic study, extensins were up-regulated in the three regions of the flower bud on D2 during the temporal comparisons (Supplementary Table 3A). and in the spatial comparisons in the AZ D2 and D6 compared to the proximal regions. Extensins are hydroxyproline-rich glycoproteins, with amphipathic properties that self-assemble in a network that interact with pectin (Cannon et al., 2008). Considering the self-assembly properties of extensin, we hypothesize that the extensin-pectin network might strengthen the cell wall, making a suitable physical barrier for pathogens, a characteristic especially useful after the organ detachment in order to protect the exposed surface.

4.3.3 Spatial changes in expansins

Expansins cause relaxation of the cell wall by disrupting non-covalent hydrogen bonds in the cellulose fibers in the cell wall (McQueen-Mason and Cosgrove, 1994). Expansins play

an important role in fruit softening as well as in cell growth processes (Brummell et al., 1999; Baluska et al., 2000), all processes where cell wall remodeling is necessary. Evidence of participation of expansins in abscission was given by Tsuchiya *et al.* (2015), who discovered increased polyclonal antibody labelling of expansins in the AZs of flower in tomato. Moreover, when Cho and Cosgrove (2000) manipulated the expression of expansins using sense and antisense sequences in *Arabidopsis*, the authors reported that abscission was boosted in the sense lines, while in the antisense lines, was reduced. The up-regulation of expansins during the spatial comparisons in the AZ D6 compared to distal and proximal suggest that relaxation of the cell wall is one of the mechanism by which the cell wall is remodeled during abscission, a probable consequence of it is allowing to other enzymes to hydrolyze the complex polysaccharides that constitute the cell wall, but also, as previously mentioned, in order to allow cell enlargement after endoreduplication, possibly to actively push the organ off.

4.3.4 Spatial changes in pectate lyases

PLs belong to the enzymes with pectinase activity; this enzyme attacks the homogalacturonan bone in pectin, hydrolyzing the (1→4)- α -D- galacturonic acid linkages. Sun and Van Nocker (2010) used a reporter gene approach to evaluate the expression of several PL-like promoters in *Arabidopsis* in different cell separation processes, they found that PL-like genes were expressed in the AZ of petals, sepals and stamens two days before anthesis until the shedding of the perianth organs. We found PL genes up-regulated in the AZ on D6, suggesting that this enzyme might be acting in later stages in the abscission process in poinsettia. A similar conclusion was achieved by Cheng *et al.* (2015), who studied citrus fruit calix abscission induced by ethylene, they discovered that PL was a late induced gene in the 24h ethylene treatment compared to other cell wall transformation genes that were up-regulated already after 4 h treatment.

4.3.5 Spatial changes in endoglucanases or cellulases

Endo β -glucanase or cellulase was one of the first enzymes described as participating in the cell wall loosening in abscission (Abeles, 1969). This enzyme catalyze the hydrolysis of (1→4)- β -D-glucosidic linkages in cellulose. In this study, endoglucanases were up-regulated in the AZ by D4 compared to proximal and there was an increase of this gene in the AZ by D6 related to both adjacent regions (Table 3). This result, suggest that the cellulose degradation on D6 might be carried on mainly by this enzyme, whereas on D2, the temporal comparisons showed that glucosidases might be undertaking the cellulose degradation task. We believe that both enzymes contribute to lower the levels of cellulose in the AZ D7 reported by Lee *et al.* (2008).

4.3.6 Spatial changes in glucomannan 4- β -mannosyltransferase 9

Glucomannan 4- β -mannosyltransferase 9 belong to the glycosyltransferases and participates in the synthesis of the backbone of one of the polysaccharides that compose hemicellulose (galactomannan). The promoter of glucomannan 4- β -mannosyltransferase 9 (CSLA9) linked to GUS gave expression in the abscission zone of the peduncle in *Arabidopsis* Zhu *et al* (2003). This suggests that this enzyme also has a role in the AZ. Three glucomannan 4- β -mannosyltransferase transcripts were up-regulated in the AZ D6 compared to distal in this transcriptomic study. They were the only transcripts that codified for enzymes related to hemicellulose synthesis in the whole experiment, suggesting that hemicellulose is not only

being degraded by β -xylosidases and β -galactosidases (up-regulated on D2 in the temporal comparisons), but also synthesized during D6. We interpret this finding as an indication that the cell wall is remodeling during abscission, involves hydrolysis and synthesis of cell wall components.

4.3.7 Temporal changes in pectinesterases

Pectinesterases is the largest group of cell wall transformation genes that increased their expression in the AZ on D2; 12 pectinacylesterases (PAE) and six pectinesterases (PE) or pectin methylesterases (PME). Pectin consists mainly of three polysaccharides rich in galacturonic acid: homogalacturonan (HG), rhamnogalacturonan I (RG-I) and rhamnogalacturonan II (RG-II). HG can display modifications and substitutions, such as methyl esterification and acetylation, respectively (Willats et al., 2001). PAEs hydrolyze acetyl esters in the HG that form the pectin and PEs or PMEs catalyze the de-esterification of pectin into methanol and pectate. Both the de-acetylation, as well as the de-esterification of the pectin polymers, might facilitate the action of other pectin-degrading enzymes such as PGs (Willats et al., 2001; Gille and Pauly, 2012). Thus, it is likely that PAE and PE are the first enzymes acting on pectin in order to disassemble the pectin network that constitutes the middle lamella and the primary cell wall. Lee *et al.* (2008) reported a pattern of occurrence of HG epitopes in the AZ and the distal region of poinsettia flower at D7 compatible with de-esterification of HG. It is likely that de-esterification phenomenon reported by Lee *et al.* (2008) towards the end of the abscission process (D7) might have started on D2, based on the evidence in this paper. Previous evidence of the participation of PEs during the abscission process was given by Wang *et al.* (2005). The authors described a slight increase of PE activity in the AZ of the tomato pedicel explant. The up-regulation of PAEs and PEs, support the hypothesis that the middle lamella is the first target in the dissolution of the cell wall. The middle lamella is made up of pectin, and there are several early reports suggesting its dissolution as a first step in the organ abscission (Lee, 1911; Bornman, 1967).

4.3.8 Temporal changes in β -glucosidases

Glucosidases degrade cellulose polymers, and cellulose is part of the primary cell wall together with hemicellulose and pectin. Corbacho *et al.* (2013) reported up-regulation of one β -glucosidases during the early induction of mature fruit abscission in melon. Lower levels of cellulose have been reported by FT-IR in the cells of the AZ compared to proximal region in poinsettia flower bud on D7 (Lee et al., 2008). Our transcriptomic study yielded 16 β -glucosidases genes up-regulated in the AZ of the poinsettia flower by D2. We think that it is plausible that the action of these up-regulated genes on D2 combined with the up-regulation of endo β -glucanase or cellulose in the AZ D6, resulted on the quantifiable loss of cellulose observed on D7 by Lee *et al.* (2008).

4.3.9 Temporal changes in galactosidases

β -galactosidases catalyze the hydrolysis of terminal non-reducing β -D-galactose residues in β -D-galactosides. Evidence of the significant contribution of β -galactosidase to the hemicellulose and pectin degradation in papaya fruit softening, has been provided by Lazan *et al.* (1995). Cell wall softening occurs both in ripening, as well as during abscission. Up-regulation of β -galactosidases in mature orange abscission has been documented (Wu and Burns, 2004) as well as in the early stages of the induction of melon fruit abscission (Corbacho

et al., 2013). In our study, four β -galactosidases were up-regulated in the AZ on D2 (Table 5), but was not exclusive to the AZ (Supplementary Table 3A), since it was up-regulated also in the distal and proximal regions. We speculate that D-galactose residues from the side chains of hemicellulose or pectin (RG-I) are being released during the first two days after the induction of abscission in poinsettia flowers.

4.3.10 Temporal changes in β -xylosidases

Xylan is one of the polysaccharides that compose the hemicellulose. Xylan is made up of xyloses residues that are hydrolyzed by β -xylosidases from the main chain. β -xylosidases have been described in fruitlet abscission zone in peach (Ruperti et al., 2002). In this transcriptomic study, 5 transcripts of β -xylosidases were up-regulated in the AZ by D2 (Table 5), three of them code for bifunctional enzymes with a secondary catalytic activity that hydrolyze the terminal non-reducing α -L-arabinofuranoside residues in α -L-arabinosides, suggesting that these two types of β -xylosidases collaborate together in the hydrolysis of the xylan and its substituents.

4.4 *In situ* hybridization of *MYST6*

Our RNA *in situ* hybridization of *MYST6* (Rhamnogalacturonan lyase), shown in Figure 8A and 8B, reveal the very precise gene expression restricted to the AZ only, on D6 and D7. The expression levels in the transcriptome (Figure 8C and 8D) confirms this; the putative *MYST6* gene is expressed at a higher level in the AZ on D6, than in the other regions and other time points. We conclude that this gene is likely involved during the final breakdown of the cell wall prior to abscission. There is very little published on *MYST6*, (PhD thesis from Purdue in 2010 (Zhou), which has not yet been published elsewhere). Personal communication with Maureen McCann (2018) have confirmed that they have been able to express an orthologue of *MYST6*, the *Arabidopsis* gene encoding RG-I lyase (AtRGIL6) in poplar and it does have RG lyase activity, and enhanced cell separation. The theory of *MYST6* action in the xylem cells of *Zinnia* is to dissolve the cell walls in the bottom of the cells, as the xylem tubes grow to enable the xylem to be hollow as each cell grow on top of each other (Keith Roberts, pers. Comm). This would fit very well with the dissolving action seen from D6 to D7 for *MYST6* in Figure 8A and 8B.

4.5 Identification of genes in the abscission-signaling cascade

Using temporal comparisons, we confirm the presence of previously described important abscission-related genes, such as the *IDA* (Butenko et al., 2003), *HAESA* receptor (Jinn et al., 2000) and *MPK3* (Cho et al., 2008). The signaling cascade leading to the activation of abscission was elucidated in *Arabidopsis* (Jinn et al., 2000; Butenko et al., 2003; Cho et al., 2008) and some of these have also been found in citrus (Estornell et al., 2015), all strongly suggesting that this activation pathway is highly conserved among plant species. Because *IDA* was up-regulated on D4, we conclude that *IDA* is also playing a role in the activation of abscission in poinsettia flower buds. *HAESA* receptor and *MPK3* were rather surprisingly down-regulated on D2, suggesting that it might not be involved in the activation of the abscission-signaling cascade together with *IDA*. MAPKs participate in a plethora of responses in the cell, thus we hypothesize that the differential expression of *MPK3* might be related with other processes taking place within the cell on D2, for example defensive and abiotic stress responses (Kovtun et al., 2000; Asai et al., 2002).

It has been postulated that IDA and the HAESA receptor trigger the expression of cell wall transformation genes contributing to the cell separation process. Niederhuth *et al.* (2013) reported the decrease in expression of enzymes that breakdown pectin, such as PGs, PEs and pectin lyases in the abscission mutant *hae hsl2*. Additionally, Stenvik *et al.* (2006) reported that IDA induced the expression of an arabinogalactan protein 24. Even though the major changes in expression of cell wall transformation genes took place in the transition from D0 to D2, the AZ only becomes visible on D4 in poinsettia flower bud. This is an indication that the cell wall remodeling is a complex process that takes time to reach a level of visibility and that is not exclusive of one specific harvest time. On the contrary, it seems to be a summative process that starts early (by D2) and end with the detachment of the organ. Considering the pattern of expression of IDA in poinsettia flower bud, we speculate that IDA might be involved in the up-regulation of cell wall transformation genes by D4 onwards.

4.6 Validation of the genes previously found as regulating abscission in poinsettia

Our group has previously identified genes related with the abscission of poinsettia flower bud by conducting an AFLP-DD experiment, where 29 transcripts with putative role in abscission were cloned and blasted out of the 225 bands differentially expressed over the period of abscission to take place, from decapitation to detachment (Munster, 2006; Hvosllef-Eide *et al.*, 2016). In order to compare with these results, we looked for these 29 sequences in this transcriptomic study, concentrating on the results up to D4. We found 16 of these 29 transcripts differentially expressed during the D2, confirming that the changes in gene expression taking place in this time point, were decisive to the progression of the abscission process. Among the most important genes, we highlight several transcripts of cell wall transformation, like β -glucosidases and glucan endo- β -glucosidases, these findings corroborate the results of the enrichment analysis in the AZ on D2 and D4 (Figure 6A and 6B) and the cell wall transformation genes reported as up-regulated during D2 in poinsettia flower bud (temporal comparisons). Thus showing the potential of this poinsettia transcriptome in identifying the previously detected abscission related genes.

5 References

- Abel, S., Nguyen, M.D., and Theologis, A. (1995). ThePS-IAA4/5-like Family of Early Auxin-inducible mRNAs in *Arabidopsis thaliana*. *Journal of Molecular Biology* 251(4), 533-549.
- Abeles, F.B. (1969). Abscission: Role of Cellulase. *Plant Physiology* 44(3), 447-452.
- Addicott, F.T. (1982). *Abscission*. London, England: Univeristy of California Press, LTD. .
- Addicott, F.T., and Lynch, R.S. (1951). Acceleration and Retardation of Abscission by Indoleacetic Acid. *Science* 114 (2974), 688-689. doi: [doi: 10.1126/science.114.2974.688].
- Addicott, F.T., Lynch, R.S., and Carns, H.R. (1955). Auxin Gradient Theory of Abscission Regulation. *Science* 121(3148), 644-645. doi: 10.1126/science.121.3148.644.
- Asai, T., Tena, G., Plotnikova, J., Willmann, M.R., Chiu, W.L., Gomez-Gomez, L., *et al.* (2002). MAP kinase signalling cascade in *Arabidopsis* innate immunity. *Nature* 415(6875), 977-983. doi: 10.1038/415977a.
- Baluska, F., Salaj, J., Mathur, J., Braun, M., Jasper, F., Samaj, J., *et al.* (2000). Root hair formation: F-actin-dependent tip growth is initiated by local assembly of profilin-supported F-actin meshworks accumulated within expansin-enriched bulges. *Developmental Biology* 227(2), 618-632. doi: 10.1006/dbio.2000.9908.
- Basu, M.M., Gonzalez-Carranza, Z.H., Azam-Ali, S., Tang, S., Shahid, A.A., and Roberts, J.A. (2013). The manipulation of auxin in the abscission zone cells of *Arabidopsis* flowers reveals that

- indoleacetic acid signaling is a prerequisite for organ shedding. *Plant Physiology* 162(1), 96-106. doi: 10.1104/pp.113.216234.
- Benjamini, Y., and Hochberg, Y. (1995). Controlling the False Discovery Rate - a Practical and Powerful Approach to Multiple Testing. *J Roy Stat Soc B Met* 57(1), 289 - 300.
- Bornman, C. (1967). Some ultrastructural aspects of abscission in *Coleus* and *Gossypium*. *South African Journal of Science* 63, 325-331.
- Botton, A., Eccher, G., Forcato, C., Ferrarini, A., Begheldo, M., Zermiani, M., et al. (2011). Signaling pathways mediating the induction of apple fruitlet abscission. *Plant Physiology* 155(1), 185 - 208.
- Brummell, D.A., Harpster, M.H., Civello, P.M., Palys, J.M., Bennett, A.B., and Dunsmuir, P. (1999). Modification of Expansin Protein Abundance in Tomato Fruit Alters Softening and Cell Wall Polymer Metabolism during Ripening. *The Plant Cell* 11(11), 2203.
- Butenko, M.A., Patterson, S.E., Grini, P.E., Stenvik, G.E., Amundsen, S.S., Mandal, A., et al. (2003). Inflorescence deficient in abscission controls floral organ abscission in *Arabidopsis* and identifies a novel family of putative ligands in plants. *The Plant Cell* 15(10), 2296-2307.
- Butenko, M.A., Shi, C.L., and Aalen, R.B. (2012). KNAT1, KNAT2 and KNAT6 act downstream in the IDA-HAE/HSL2 signaling pathway to regulate floral organ abscission. *Plant Signaling & Behavior* 7(1), 135-138. doi: 10.4161/psb.7.1.18379.
- Cai, S., and Lashbrook, C.C. (2008). Stamen abscission zone transcriptome profiling reveals new candidates for abscission control: enhanced retention of floral organs in transgenic plants overexpressing *Arabidopsis* ZINC FINGER PROTEIN2. *Plant Physiology* 146(3), 1305-1321. doi: 10.1104/pp.107.110908.
- Cannon, M.C., Terneus, K., Hall, Q., Tan, L., Wang, Y., Wegenhart, B.L., et al. (2008). Self-assembly of the plant cell wall requires an extensin scaffold. *Proceedings of the National Academy of Sciences* 105(6), 2226.
- Cheng, C., Zhang, L., Yang, X., and Zhong, G. (2015). Profiling gene expression in citrus fruit calyx abscission zone (AZ-C) treated with ethylene. *Molecular Genetics and Genomics* 290(5), 1991-2006. doi: 10.1007/s00438-015-1054-2.
- Cho, H.T., and Cosgrove, D.J. (2000). Altered expression of expansin modulates leaf growth and pedicel abscission in *Arabidopsis thaliana*. *Proceedings of the National Academy of Sciences* 97(17), 9783-9788. doi: 10.1073/pnas.160276997.
- Cho, S.K., Larue, C.T., Chevalier, D., Wang, H., Jinn, T.-L., Zhang, S., et al. (2008). Regulation of floral organ abscission in *Arabidopsis thaliana*. *Proceedings of the National Academy of Sciences* 105(40), 15629-15634. doi: 10.1073/pnas.0805539105.
- Conesa, A., and Gotz, S. (2008). Blast2GO: A comprehensive suite for functional analysis in plant genomics. *Int J Plant Genomics* 2008, 619832. doi: 10.1155/2008/619832.
- Conesa, A., Gotz, S., Garcia-Gomez, J.M., Terol, J., Talon, M., and Robles, M. (2005). Blast2GO: a universal tool for annotation, visualization and analysis in functional genomics research. *Bioinformatics* 21(18), 3674-3676. doi: 10.1093/bioinformatics/bti610.
- Corbacho, J., Romojaro, F., Pech, J.-C., Latché, A., and Gomez-Jimenez, M.C. (2013). Transcriptomic Events Involved in Melon Mature-Fruit Abscission Comprise the Sequential Induction of Cell-Wall Degrading Genes Coupled to a Stimulation of Endo and Exocytosis. *PLoS ONE* 8(3), e58363. doi: 10.1371/journal.pone.0058363.
- Cosgrove, D.J., Li, L.C., Cho, H.T., Hoffmann-Benning, S., Moore, R.C., and Blecker, D. (2002). The growing world of expansins. *Plant and Cell Physiology* 43(12), 1436-1444.
- Ellis, C.M., Nagpal, P., Young, J.C., Hagen, G., Guilfoyle, T.J., and Reed, J.W. (2005). AUXIN RESPONSE FACTOR1 and AUXIN RESPONSE FACTOR2 regulate senescence and floral organ abscission in *Arabidopsis thaliana*. *Development* 132(20), 4563-4574.
- Estornell, L.H., Agustí, J., Merelo, P., Talón, M., and Tadeo, F.R. (2013). Elucidating mechanisms underlying organ abscission. *Plant Science* 199-200(0), 48-60.

- Estornell, L.H., Wildhagen, M., Pérez-Amador, M.A., Talón, M., Tadeo, F.R., and Butenko, M.A. (2015). The IDA peptide controls abscission in Arabidopsis and Citrus. *Frontiers in Plant Science* 6. doi: 10.3389/fpls.2015.01003.
- Ferrante, A., Trivellini, A., Scuderi, D., Romano, D., and Vernieri, P. (2015). Post-production physiology and handling of ornamental potted plants. *Postharvest Biology and Technology* 100(0), 99-108.
- Gille, S., and Pauly, M. (2012). O-acetylation of plant cell wall polysaccharides. *Front Plant Science* 3, 12. doi: 10.3389/fpls.2012.00012.
- Gómez-Mena, C., and Sablowski, R. (2008). ARABIDOPSIS THALIANA HOMEBOX GENE1 Establishes the Basal Boundaries of Shoot Organs and Controls Stem Growth. *The Plant Cell* 20(8), 2059-2072. doi: 10.1105/tpc.108.059188.
- Gonzalez-Carranza, Z.H., Elliott, K.A., and Roberts, J.A. (2007). Expression of polygalacturonases and evidence to support their role during cell separation processes in Arabidopsis thaliana. *Journal of Experimental Botany*, erm222. doi: 10.1093/jxb/erm222.
- Guilfoyle, T.J., and Hagen, G. (2007). Auxin response factors. *Current Opinion in Plant Biology* 10(5), 453-460. doi: 10.1016/j.pbi.2007.08.014.
- Hvoslef-Eide, A.K., Munster, C.M., Mathiesen, C.A., Ayeh, K.O., Melby, T.I., Rasolomanana, P., et al. (2016). Primary and Secondary Abscission in Pisum sativum and Euphorbia pulcherrima—How Do They Compare and How Do They Differ? *Frontiers in Plant Science* 6(1204). doi: 10.3389/fpls.2015.01204.
- Jinn, T.L., Stone, J.M., and Walker, J.C. (2000). HAESA, an Arabidopsis leucine-rich repeat receptor kinase, controls floral organ abscission. *Genes & Development* 14(1), 108-117.
- Jones, P., Binns, D., Chang, H.Y., Fraser, M., Li, W., McAnulla, C., et al. (2014). InterProScan 5: genome-scale protein function classification. *Bioinformatics* 30(9), 1236-1240. doi: 10.1093/bioinformatics/btu031.
- Konishi, S., Izawa, T., Lin, S.Y., Ebana, K., Fukuta, Y., Sasaki, T., et al. (2006). An SNP Caused Loss of Seed Shattering During Rice Domestication. *Science* 312(5778), 1392-1396. doi: 10.1126/science.1126410.
- Kovi, M.R., Abdelhalim, M., Kunapareddy, A., Ergon, Å., Tronsmo, A.M., Brurberg, M.B., et al. (2016). Global transcriptome changes in perennial ryegrass during early infection by pink snow mould. *Scientific Reports* 6, 28702. doi: 10.1038/srep28702.
- Kovi, M.R., Amdahl, H., Alsheikh, M., and Rognli, O.A. (2017). De novo and reference transcriptome assembly of transcripts expressed during flowering provide insight into seed setting in tetraploid red clover. *Scientific Reports* 7, 44383. doi: 10.1038/srep44383.
- Kovtun, Y., Chiu, W.-L., Tena, G., and Sheen, J. (2000). Functional analysis of oxidative stress-activated mitogen-activated protein kinase cascade in plants. *Proceedings of the National Academy of Sciences* 97(6), 2940-2945. doi: 10.1073/pnas.97.6.2940.
- Křeček, P., Skůpa, P., Libus, J., Naramoto, S., Tejos, R., Friml, J., et al. (2009). The PIN-FORMED (PIN) protein family of auxin transporters. *Genome Biology* 10(12), 249-249. doi: 10.1186/gb-2009-10-12-249.
- Lazan, H., Selamat, M.K., and Ali, Z.M. (1995). β -Galactosidase, polygalacturonase and pectinesterase in differential softening and cell wall modification during papaya fruit ripening. *Physiologia Plantarum* 95(1), 106-112. doi: 10.1111/j.1399-3054.1995.tb00815.x.
- Lee, E. (1911). The Morphology of Leaf-fall. *Annals of Botany* 25(97), 51-106.
- Lee, Y., Derbyshire, P., Knox, J.P., and Hvoslef-Eide, A.K. (2008). Sequential cell wall transformations in response to the induction of a pedicel abscission event in Euphorbia pulcherrima (poinsettia). *The Plant Journal* 54(6), 993-1003. doi: 10.1111/j.1365-3113.2008.03456.x.
- Li, B., and Dewey, C.N. (2011). RSEM: accurate transcript quantification from RNA-Seq data with or without a reference genome. *BMC Bioinformatics* 12, 323. doi: 10.1186/1471-2105-12-323.
- Li, H., Lin, D., Dhonukshe, P., Nagawa, S., Chen, D., Friml, J., et al. (2011). Phosphorylation switch modulates the interdigitated pattern of PIN1 localization and cell expansion in Arabidopsis leaf epidermis. *Cell Research* 21(6), 970-978. doi: 10.1038/cr.2011.49.

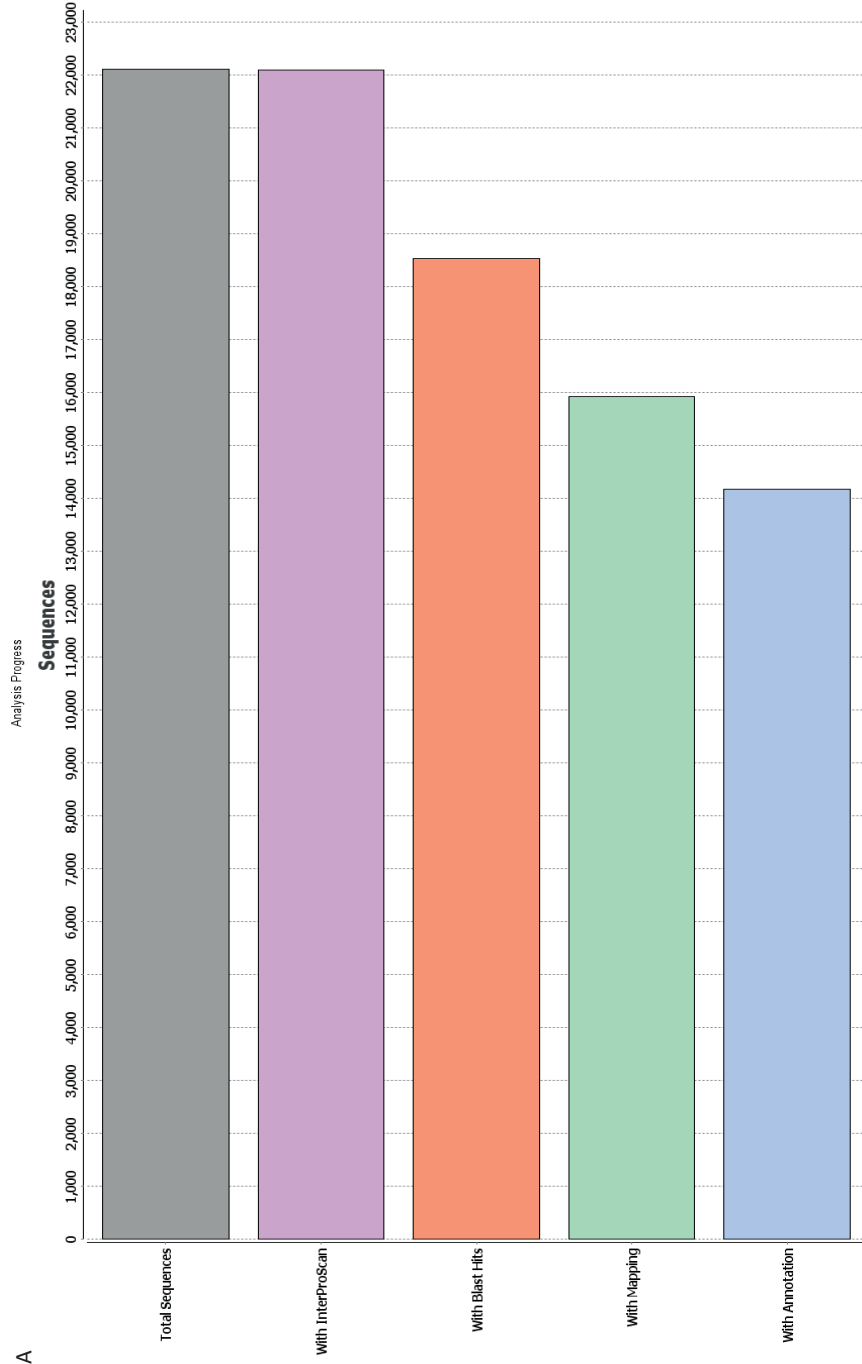
- Louie, D.S., Jr., and Addicott, F.T. (1970). Applied Auxin Gradients and Abscission in Explants. *Plant Physiology* 45(6), 654-657.
- Martin, L.B., Fei, Z., Giovannoni, J.J., and Rose, J.K. (2013). Catalyzing plant science research with RNA-seq. *Front Plant Sci* 4(66), 66. doi: 10.3389/fpls.2013.00066.
- McQueen-Mason, S., and Cosgrove, D.J. (1994). Disruption of hydrogen bonding between plant cell wall polymers by proteins that induce wall extension. *Proceedings of the National Academy of Sciences* 91(14), 6574-6578.
- Meir, S., Philosoph-Hadas, S., Sundaresan, S., Selvaraj, K.S., Burd, S., Ophir, R., et al. (2010). Microarray analysis of the abscission-related transcriptome in the tomato flower abscission zone in response to auxin depletion. *Plant Physiology* 154(4), 1929-1956. doi: 10.1104/pp.110.160697.
- Merelo, P., Agusti, J., Arbona, V., Costa, M.L., Estornell, L.H., Gómez-Cadenas, A., et al. (2017). Cell Wall Remodeling in Abscission Zone Cells during Ethylene-Promoted Fruit Abscission in Citrus. *Frontiers in Plant Science* 8(126). doi: 10.3389/fpls.2017.00126.
- Merkouroupoulos, G., and Shirsat, A. (2003). The unusual Arabidopsis extensin gene atExt1 is expressed throughout plant development and is induced by a variety of biotic and abiotic stresses. *Planta* 217(3), 356-366.
- Muñoz-Sanhueza, L.G., Lee, Y., Tillmann, M., Cohen, J.D., and Hvostlef-Eide, A.K. (2018). Auxin analysis using laser microdissected plant tissues sections. *BMC Plant Biology* 18(1), 133. doi: 10.1186/s12870-018-1352-z.
- Munster, C. (2006). *On the flower abscission of poinsettia (Euphorbia pulcherrima Willd. Ex Klotzsch) - A molecular and plant hormonal study*. Norwegian University of Life Sciences.
- Nagpal, P., Ellis, C.M., Weber, H., Ploense, S.E., Barkawi, L.S., Guilfoyle, T.J., et al. (2005). Auxin response factors ARF6 and ARF8 promote jasmonic acid production and flower maturation. *Development* 132(18), 4107-4118. doi: 10.1242/dev.01955.
- Niederhuth, C.E., Patharkar, O.R., and Walker, J.C. (2013). Transcriptional profiling of the Arabidopsis abscission mutant hae hsl2 by RNA-Seq. *BMC Genomics* 14(37), 37. doi: 10.1186/1471-2164-14-37.
- Okushima, Y., Overvoorde, P.J., Arima, K., Alonso, J.M., Chan, A., Chang, C., et al. (2005). Functional genomic analysis of the AUXIN RESPONSE FACTOR gene family members in Arabidopsis thaliana: unique and overlapping functions of ARF7 and ARF19. *The Plant Cell* 17(2), 444-463. doi: 10.1105/tpc.104.028316.
- Parra, G., Bradnam, K., and Korf, I. (2007). CEGMA: a pipeline to accurately annotate core genes in eukaryotic genomes. *Bioinformatics* 23(9), 1061-1067. doi: 10.1093/bioinformatics/btm071.
- Parra, R., Paredes, M., Sanchez-Calle, I., and Gomez-Jimenez, M. (2013). Comparative transcriptional profiling analysis of olive ripe-fruit pericarp and abscission zone tissues shows expression differences and distinct patterns of transcriptional regulation. *BMC Genomics* 14(1), 866.
- Ridley, B.L., O'Neill, M.A., and Mohnen, D. (2001). Pectins: structure, biosynthesis, and oligogalacturonide-related signaling. *Phytochemistry* 57(6), 929-967.
- Riov, J. (1974). A polygalacturonase from citrus leaf explants: role in abscission. *Plant Physiology* 53(2), 312-316.
- Roberts, J.A., Elliott, K.A., and Gonzalez-Carranza, Z.H. (2002). Abscission, Dehiscence, and other Cell Separation Processes. *Annual Review of Plant Biology* 53(1), 131-158. doi: 10.1146/annurev.arplant.53.092701.180236.
- Robinson, M., McCarthy, D., and Smyth, G. (2010). edgeR: a bioconductor package for differential expression analysis of digital gene expression data. *Bioinformatics* 26(1), 139 - 140.
- Ruperti, B., Cattivelli, L., Pagni, S., and Ramina, A. (2002). Ethylene-responsive genes are differentially regulated during abscission, organ senescence and wounding in peach (*Prunus persica*) *Journal of Experimental Botany* 53 (368), 429-437.
- Schrader, J., Baba, K., May, S.T., Palme, K., Bennett, M., Bhalerao, R.P., et al. (2003). Polar auxin transport in the wood-forming tissues of hybrid aspen is under simultaneous control of

- developmental and environmental signals. *Proceedings of the National Academy of Sciences* 100(17), 10096.
- Sexton, R. (1979). Spatial and temporal aspects of cell separation in the foliar abscission zones of *Impatiens sultani* Hook. *Protoplasma* 99(1), 53-66. doi: 10.1007/BF01274069.
- Sexton, R., Jamieson, G.G.C., and Allan, M.H.I.L. (1977). An ultrastructural study of abscission zone cells with special reference to the mechanism of enzyme secretion. *Protoplasma* 91(4), 369-387. doi: 10.1007/BF01291927.
- Shi, C.-L., Stenvik, G.-E., Vie, A.K., Bones, A.M., Pautot, V., Proveniers, M., et al. (2011). Arabidopsis Class I KNOTTED-Like Homeobox Proteins Act Downstream in the IDA-HAE/HSL2 Floral Abscission Signaling Pathway. *The Plant Cell* 23(7), 2553-2567. doi: 10.1105/tpc.111.084608.
- Shi, Z., Jiang, Y., Han, X., Liu, X., Cao, R., Qi, M., et al. (2017). SIPIN1 regulates auxin efflux to affect flower abscission process. *Scientific Reports* 7(1), 14919. doi: 10.1038/s41598-017-15072-7.
- Staswick, P.E., Serban, B., Rowe, M., Tiryaki, I., Maldonado, M.T., Maldonado, M.C., et al. (2005). Characterization of an Arabidopsis Enzyme Family That Conjugates Amino Acids to Indole-3-Acetic Acid. *The Plant Cell* 17(2), 616.
- Stenvik, G.E., Butenko, M.A., Urbanowicz, B.R., Rose, J.K., and Aalen, R.B. (2006). Overexpression of INFLORESCENCE DEFICIENT IN ABCISSION activates cell separation in vestigial abscission zones in Arabidopsis. *The Plant Cell* 18(6), 1467-1476.
- Sun, L., and van Nocker, S. (2010). Analysis of promoter activity of members of the PECTATE LYASE-LIKE (PLL) gene family in cell separation in Arabidopsis. *BMC Plant Biology* 10(1), 152. doi: 10.1186/1471-2229-10-152.
- Supek, F., Bošnjak, M., Škunca, N., and Šmuc, T. (2011). REVIGO Summarizes and Visualizes Long Lists of Gene Ontology Terms. *PLOS ONE* 6(7), e21800. doi: 10.1371/journal.pone.0021800.
- Trapnell, C., Williams, B.A., Pertea, G., Mortazavi, A., Kwan, G., van Baren, M.J., et al. (2010). Transcript assembly and quantification by RNA-Seq reveals unannotated transcripts and isoform switching during cell differentiation. *Nature Biotechnology* 28(5), 511-515. doi: 10.1038/nbt.1621.
- Tsuchiya, M., Satoh, S., and Iwai, H. (2015). Distribution of XTH, Expansin, and Secondary-wall-related CesA in Floral and Fruit Abscission Zones during Fruit Development in Tomato (*Solanum lycopersicum*). *Frontiers in Plant Science* 6. doi: 10.3389/fpls.2015.00323.
- Tucker, M.L., Burke, A., Murphy, C.A., Thai, V.K., and Ehrenfried, M.L. (2007). Gene expression profiles for cell wall-modifying proteins associated with soybean cyst nematode infection, petiole abscission, root tips, flowers, apical buds, and leaves. *Journal of Experimental Botany* 58(12), 3395-3406. doi: 10.1093/jxb/erm188.
- Vieten, A., Vanneste, S., Wiśniewska, J., Benková, E., Benjamins, R., Beeckman, T., et al. (2005). Functional redundancy of PIN proteins is accompanied by auxin-dependent cross-regulation of PIN expression. *Development* 132(20), 4521.
- Wang, Y.C., Li, T.L., Meng, H.Y., and Sun, X.Y. (2005). Optimal and spatial analysis of hormones, degrading enzymes and isozyme profiles in tomato pedicel explants during ethylene-induced abscission. *Plant Growth Regulation* 46, 97-107.
- Webster, B.D. (1968). Anatomical Aspects of Abscission. *Plant Physiology* 43(9), 1512-1544.
- Willats, W.G.T., McCartney, L., Mackie, W., and Knox, J.P. (2001). Pectin: cell biology and prospects for functional analysis. *Plant Molecular Biology* 47(1), 9-27. doi: 10.1023/a:1010662911148.
- Wu, Z.C., and Burns, J.K. (2004). A β -galactosidase gene is expressed during mature fruit abscission of 'Valencia' orange (*Citrus sinensis*). *Journal of Experimental Botany* 55(402), 1483-1490.
- Yamada, T., Ichimura, K., Kanekatsu, M., and van Doorn, W.G. (2009). Homologs of Genes Associated with Programmed Cell Death in Animal Cells are Differentially Expressed During Senescence of *Ipomoea nil* Petals. *Plant and Cell Physiology* 50(3), 610-625. doi: 10.1093/pcp/pcp019.
- Ye, J., Fang, L., Zheng, H., Zhang, Y., Chen, J., Zhang, Z., et al. (2006). WEGO: a web tool for plotting GO annotations. *Nucleic Acids Research* 34(Web Server issue), W293-297. doi: 10.1093/nar/gkl031.

- Zhu, Y., Nam, J., Carpita, N.C., Matthysse, A.G., and Gelvin, S.B. (2003). Agrobacterium-Mediated Root Transformation Is Inhibited by Mutation of an Arabidopsis Cellulose Synthase-Like Gene. *Plant Physiology* 133(3), 1000.
- Zuo, X., Xu, T., Qi, M., Lv, S., Li, J., Gao, S., et al. (2012). Expression patterns of auxin-responsive genes during tomato flower pedicel abscission and potential effects of calcium. *Australian Journal of Botany* 60(1), 68-78.

Supplementary Figures

A



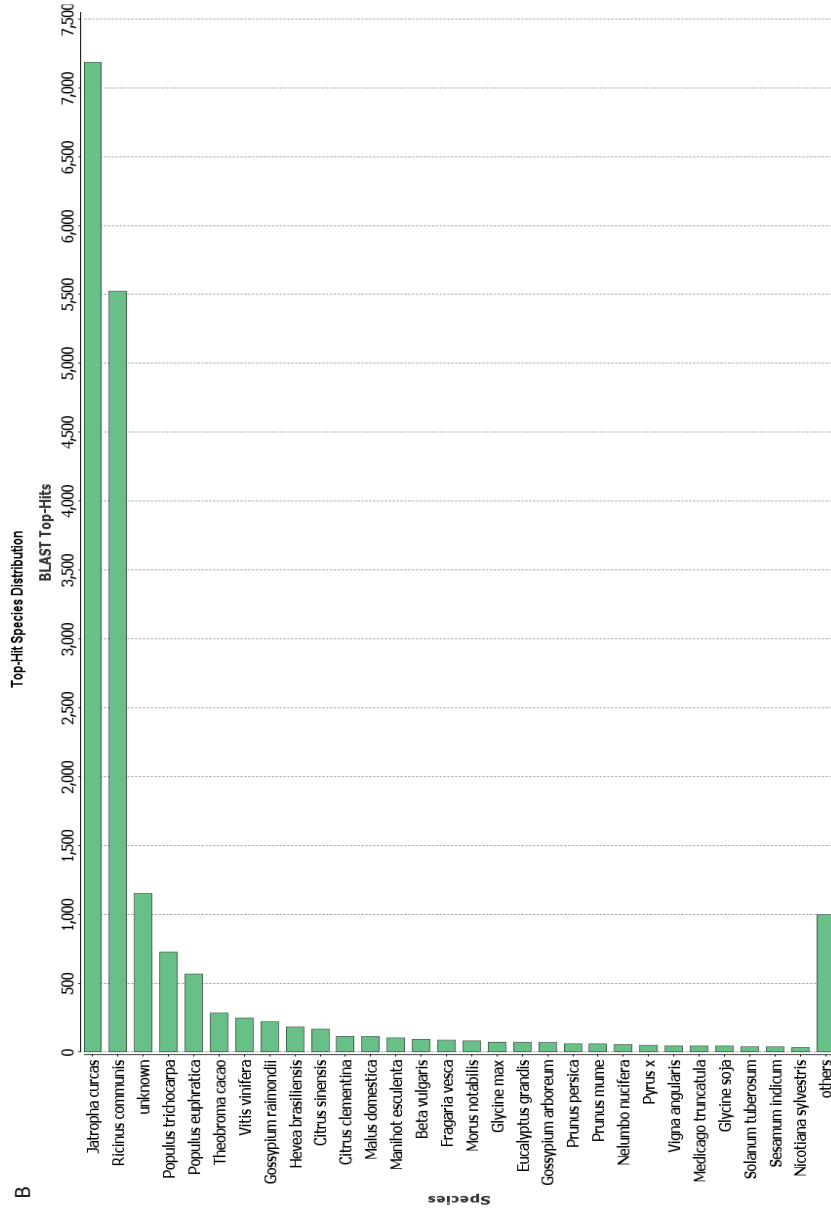


Figure 1. (A) Distribution of number of sequences resulting after each one of the scanning with different databases using the program Blast2GO. (B) Top-hit species distribution for blast annotation of the differentially expressed genes in the poinsettia flower bud during abscission.

Supplementary Table 1

Up-regulated cell wall transformation genes in the AZ in the spatial comparisons on D2, D4 and D6

| Day 2 up-regulated in the AZ compared to proximal | | |
|---|---------------------|--------|
| Transcript ID | Gene product | Log2FC |
| TR96655_c0_g2_i1 | extensin-2- partial | 4,05 |

| Day 4 up-regulated in the AZ compared to proximal | | |
|---|----------------------|--------|
| Transcript ID | Gene product | Log2FC |
| TR58493_c0_g2_i1 | endoglucanase 9-like | 5,31 |

| Day 6 up-regulated in AZ compared to distal | | |
|---|---|--------|
| Transcript ID | Gene product | Log2FC |
| TR58493_c0_g2_i1 | endoglucanase 9-like | 6,92 |
| TR43022_c0_g1_i1 | expansin-b3-like | 4,47 |
| TR29530_c0_g2_i1 | expansin-b3-like | 4,3 |
| TR29530_c0_g1_i1 | expansin-b3-like | 8,7 |
| TR23055_c0_g2_i1 | endoglucanase 9 | 4,21 |
| TR145769_c1_g1_i1 | endo- -beta-glucanase | 3,51 |
| TR144553_c0_g1_i2 | endo- -beta-glucanase | 3,43 |
| TR144553_c0_g1_i1 | endo- -beta-glucanase | 4,33 |
| TR140924_c0_g1_i1 | glucomannan 4-beta-mannosyltransferase 9 | 3,92 |
| TR140278_c0_g1_i1 | glucomannan 4-beta-mannosyltransferase 10 | 4,44 |
| TR127289_c0_g1_i5 | glucomannan 4-beta-mannosyltransferase 2-like | 4,06 |
| TR123878_c1_g1_i1 | probable pectate lyase 8 | 3,69 |
| TR123636_c0_g1_i2 | probable pectate lyase 8 | 3,85 |
| TR111515_c0_g1_i1 | endoglucanase 11-like | 4,26 |

| Day 6 up-regulated in AZ compared to proximal | | |
|---|--|--------|
| Transcript ID | Gene product | Log2FC |
| TR96655_c0_g2_i3 | extensin-2-like | 4,18 |
| TR94490_c0_g1_i1 | extensin-2- partial | 3,46 |
| TR61526_c0_g1_i1 | alpha-expansin 4 | 3,85 |
| TR53009_c0_g1_i1 | endo- -beta-glucanase | 4,07 |
| TR39616_c0_g1_i1 | endo- -beta-glucanase | 4,29 |
| TR140555_c4_g1_i11 | udp-arabinopyranose mutase 1 | 3,75 |
| TR130139_c2_g1_i2 | expansin-a4 | 3,65 |
| TR120809_c0_g1_i1 | polygalacturonase-like | 4,28 |
| TR111506_c0_g2_i1 | polygalacturonase precursor family protein | 4,2 |

Supplementary Table 2A

Up-regulated genes related to auxin in the temporal comparison D0 vs D2

| Transcript ID | Gene product | Tissue | Log2FC |
|-------------------|-------------------------------------|----------|--------|
| TR139817_c1_g1_i7 | auxin-responsive protein iaa26-like | proximal | 8,18 |
| TR79223_c0_g1_i1 | auxin-responsive family protein | AZ | 4,18 |
| TR79223_c0_g1_i1 | auxin-responsive family protein | distal | 4,03 |

Supplementary Table 2B

Down-regulated genes related to auxin in the temporal comparison D0 vs D2

| Transcript ID | Gene product | Tissue | Log2FC |
|--------------------|--|----------|--------|
| TR142028_c0_g1_i1 | probable indole-3-acetic acid-amido synthetase | AZ | -11,82 |
| TR142756_c0_g1_i2 | probable indole-3-acetic acid-amido synthetase | AZ | -11,81 |
| TR138808_c5_g2_i3 | iaa-amino acid hydrolase ilr1-like 4 | proximal | -11,38 |
| TR65713_c0_g2_i1 | auxin-induced protein aux22 | distal | -11,30 |
| TR76917_c0_g1_i1 | auxin-induced protein aux22 | distal | -11,24 |
| TR138808_c5_g2_i6 | iaa-amino acid hydrolase ilr1-like 4 | proximal | -10,78 |
| TR138697_c7_g2_i5 | probable indole-3-acetic acid-amido synthetase | distal | -10,52 |
| TR76917_c0_g2_i2 | auxin-induced protein aux22 | distal | -9,96 |
| TR65713_c0_g1_i1 | auxin-induced protein aux22 | distal | -9,92 |
| TR139620_c0_g2_i2 | auxin efflux carrier component 1 family protein | distal | -9,88 |
| TR76917_c0_g1_i1 | auxin-induced protein aux22 | AZ | -9,86 |
| TR65713_c0_g2_i1 | auxin-induced protein aux22 | AZ | -9,79 |
| TR139620_c0_g2_i2 | auxin efflux carrier component 1 family protein | AZ | -9,78 |
| TR71658_c0_g1_i1 | auxin efflux carrier component 8 | distal | -9,75 |
| TR135673_c1_g1_i6 | auxin response factor 4 | AZ | -9,62 |
| TR133182_c3_g1_i5 | auxin response factor 4 | AZ | -9,59 |
| TR142756_c0_g1_i1 | probable indole-3-acetic acid-amido synthetase | AZ | -9,54 |
| TR123854_c0_g2_i2 | auxin-induced protein 15a-like | distal | -9,33 |
| TR129676_c0_g1_i2 | probable indole-3-pyruvate monooxygenase yucca10 | proximal | -9,32 |
| TR142028_c0_g1_i2 | probable indole-3-acetic acid-amido synthetase | AZ | -9,30 |
| TR135673_c1_g1_i13 | auxin response factor 4 | distal | -9,29 |
| TR76917_c0_g2_i2 | auxin-induced protein aux22 | AZ | -9,26 |
| TR8517_c0_g2_i1 | auxin efflux carrier component 8 | proximal | -9,26 |
| TR138697_c7_g2_i4 | probable indole-3-acetic acid-amido synthetase | AZ | -9,18 |
| TR123854_c0_g2_i2 | auxin-induced protein 15a-like | AZ | -9,12 |
| TR142028_c0_g1_i2 | probable indole-3-acetic acid-amido synthetase | distal | -9,11 |
| TR148572_c5_g1_i9 | protein topless-like | AZ | -9,05 |
| TR139482_c4_g2_i5 | probable indole-3-acetic acid-amido synthetase | AZ | -9,03 |
| TR65713_c0_g1_i1 | auxin-induced protein aux22 | AZ | -8,98 |
| TR125726_c2_g1_i2 | auxin-responsive protein saur61-like | proximal | -8,94 |
| TR71658_c0_g1_i1 | auxin efflux carrier component 8 | AZ | -8,90 |

| | | | |
|--------------------|---|----------|-------|
| TR135673_c1_g1_i11 | auxin response factor 4 | distal | -8,83 |
| TR19113_c0_g2_i1 | auxin-responsive protein iaa1 | distal | -8,70 |
| TR76230_c0_g2_i1 | auxin response factor | AZ | -8,68 |
| TR130962_c1_g1_i1 | auxin-induced protein 15a-like | AZ | -8,62 |
| TR111423_c0_g2_i1 | auxin-responsive protein iaa4-like | AZ | -8,62 |
| TR104930_c0_g2_i1 | auxin-induced protein 22d | AZ | -8,49 |
| TR148572_c5_g1_i9 | protein topless-like | distal | -8,49 |
| TR125870_c0_g1_i1 | indole-3-acetic acid-amido synthetase | proximal | -8,46 |
| TR125726_c2_g1_i1 | auxin-responsive protein saur61-like | distal | -8,45 |
| TR177973_c0_g1_i1 | saur-like auxin-responsive protein | AZ | -8,45 |
| TR135673_c1_g1_i12 | auxin response factor 4 | AZ | -8,44 |
| TR147728_c0_g2_i1 | probable auxin efflux carrier component 1c | distal | -8,42 |
| TR125726_c2_g1_i2 | auxin-responsive protein saur61-like | AZ | -8,42 |
| TR122385_c0_g4_i1 | auxin-responsive protein saur61-like | proximal | -8,39 |
| TR73178_c0_g1_i1 | auxin-responsive protein iaa4 | distal | -8,35 |
| TR140732_c1_g1_i1 | saur-like auxin-responsive protein | distal | -8,35 |
| TR66190_c0_g1_i1 | auxin-responsive protein iaa4 | AZ | -8,34 |
| TR94922_c0_g1_i1 | auxin-binding protein abp19a | distal | -8,31 |
| TR104930_c0_g2_i1 | auxin-induced protein 22d | distal | -8,31 |
| TR123795_c0_g1_i1 | auxin-responsive protein iaa14-like | distal | -8,31 |
| TR125726_c2_g1_i1 | auxin-responsive protein saur61-like | proximal | -8,30 |
| TR123564_c0_g1_i1 | indole-3-acetic acid-amido synthetase | proximal | -8,30 |
| TR122510_c0_g2_i1 | auxin-responsive protein iaa14-like | distal | -8,28 |
| TR116886_c0_g2_i1 | auxin-responsive protein iaa1 | AZ | -8,18 |
| TR122385_c0_g4_i1 | auxin-responsive protein saur61-like | AZ | -8,18 |
| TR142756_c0_g1_i2 | probable indole-3-acetic acid-amido synthetase | proximal | -8,17 |
| TR142756_c0_g1_i3 | probable indole-3-acetic acid-amido synthetase | distal | -8,16 |
| TR142756_c0_g1_i3 | probable indole-3-acetic acid-amido synthetase | AZ | -8,14 |
| TR139482_c4_g2_i3 | indole-3-acetic acid-amido synthetase | proximal | -8,12 |
| TR125726_c2_g1_i1 | auxin-responsive protein saur61-like | AZ | -8,10 |
| TR170515_c0_g1_i1 | saur-like auxin-responsive protein | AZ | -8,10 |
| TR147666_c5_g1_i1 | auxin response factor 19 | AZ | -7,96 |
| TR76230_c0_g2_i1 | auxin response factor | distal | -7,85 |
| TR138697_c7_g2_i1 | probable indole-3-acetic acid-amido synthetase | AZ | -7,79 |
| TR133182_c3_g1_i3 | auxin response factor 4 | proximal | -7,78 |
| TR139482_c4_g2_i1 | probable indole-3-acetic acid-amido synthetase | AZ | -7,71 |
| TR138697_c7_g2_i2 | probable indole-3-acetic acid-amido synthetase | AZ | -7,58 |
| TR138808_c5_g2_i6 | iaa-amino acid hydrolase ilr1-like 4 | AZ | -7,51 |
| TR139482_c4_g2_i2 | probable indole-3-acetic acid-amido synthetase | AZ | -7,41 |
| TR147728_c0_g1_i3 | auxin efflux carrier component 1 family protein | AZ | -7,28 |
| TR79164_c0_g2_i1 | auxin response factor | distal | -7,24 |
| TR142756_c0_g1_i1 | probable indole-3-acetic acid-amido synthetase | proximal | -7,15 |
| TR139482_c4_g2_i5 | probable indole-3-acetic acid-amido synthetase | proximal | -7,09 |
| TR57659_c0_g2_i1 | auxin-induced protein 15a-like | distal | -6,95 |
| TR142028_c0_g1_i1 | probable indole-3-acetic acid-amido synthetase | distal | -6,86 |

| | | | |
|--------------------|---|----------|-------|
| TR138808_c5_g2_i6 | iaa-amino acid hydrolase ilr1-like 4 | distal | -6,78 |
| TR79164_c0_g2_i1 | auxin response factor | AZ | -6,74 |
| TR135060_c4_g1_i1 | iaa-amino acid hydrolase ilr1-like 4 | proximal | -6,72 |
| TR139620_c0_g2_i1 | probable auxin efflux carrier component 1c | AZ | -6,70 |
| TR142756_c0_g1_i2 | probable indole-3-acetic acid-amido synthetase | distal | -6,63 |
| TR123769_c0_g1_i1 | auxin efflux carrier component 1 family protein | AZ | -6,57 |
| TR116886_c0_g1_i1 | auxin-responsive protein iaa1 | distal | -6,48 |
| TR139482_c4_g2_i4 | probable indole-3-acetic acid-amido synthetase | distal | -6,44 |
| TR146654_c11_g1_i1 | auxin-responsive protein iaa1 | AZ | -6,43 |
| TR108763_c0_g1_i1 | auxin-induced protein 15a-like | distal | -6,42 |
| TR135673_c1_g1_i6 | auxin response factor 4 | distal | -6,40 |
| TR135673_c1_g1_i12 | auxin response factor 4 | distal | -6,30 |
| TR122385_c0_g4_i2 | auxin-responsive protein saur61-like | proximal | -6,25 |
| TR146654_c11_g1_i1 | auxin-responsive protein iaa1 | distal | -6,25 |
| TR123564_c0_g1_i1 | indole-3-acetic acid-amido synthetase | distal | -6,24 |
| TR19113_c0_g1_i1 | auxin-responsive protein iaa1 | proximal | -6,24 |
| TR135673_c1_g1_i12 | auxin response factor 4 | proximal | -6,19 |
| TR142756_c0_g1_i1 | probable indole-3-acetic acid-amido synthetase | distal | -6,17 |
| TR139482_c4_g2_i2 | probable indole-3-acetic acid-amido synthetase | distal | -6,16 |
| TR123564_c0_g1_i1 | indole-3-acetic acid-amido synthetase | AZ | -6,11 |
| TR138697_c7_g2_i1 | probable indole-3-acetic acid-amido synthetase | distal | -6,11 |
| TR138808_c5_g2_i3 | iaa-amino acid hydrolase ilr1-like 4 | AZ | -6,05 |
| TR139482_c4_g2_i4 | probable indole-3-acetic acid-amido synthetase | AZ | -6,04 |
| TR8517_c0_g1_i1 | auxin efflux carrier component 8 | AZ | -6,03 |
| TR125870_c0_g1_i1 | indole-3-acetic acid-amido synthetase | AZ | -6,02 |
| TR125870_c0_g1_i1 | indole-3-acetic acid-amido synthetase | distal | -6,01 |
| TR141309_c0_g1_i1 | auxin-responsive protein iaa1 | proximal | -5,98 |
| TR138808_c5_g2_i2 | iaa-amino acid hydrolase ilr1-like 4 | proximal | -5,88 |
| TR108763_c0_g1_i1 | auxin-induced protein 15a-like | AZ | -5,85 |
| TR177973_c0_g1_i1 | saur-like auxin-responsive protein | distal | -5,78 |
| TR126027_c0_g1_i3 | protein kinase pinoid | AZ | -5,78 |
| TR147728_c0_g1_i1 | auxin efflux carrier component 1 family protein | AZ | -5,78 |
| TR138808_c5_g2_i3 | iaa-amino acid hydrolase ilr1-like 4 | distal | -5,76 |
| TR181138_c0_g1_i1 | auxin-induced protein aux28-like | proximal | -5,75 |
| TR181138_c0_g1_i1 | auxin-induced protein aux28-like | AZ | -5,71 |
| TR122385_c0_g4_i2 | auxin-responsive protein saur61-like | AZ | -5,70 |
| TR123795_c0_g1_i1 | auxin-responsive protein iaa14-like | proximal | -5,70 |
| TR122385_c0_g4_i2 | auxin-responsive protein saur61-like | distal | -5,68 |
| TR76230_c0_g2_i1 | auxin response factor | proximal | -5,68 |
| TR79164_c0_g2_i1 | auxin response factor | proximal | -5,67 |
| TR122368_c0_g1_i1 | auxin-induced protein 15a-like | AZ | -5,66 |
| TR138697_c7_g2_i1 | probable indole-3-acetic acid-amido synthetase | proximal | -5,65 |
| TR19113_c0_g1_i1 | auxin-responsive protein iaa1 | AZ | -5,60 |
| TR133182_c3_g1_i3 | auxin response factor 4 | distal | -5,60 |
| TR135060_c4_g1_i1 | iaa-amino acid hydrolase ilr1-like 4 | distal | -5,58 |

| | | | |
|--------------------|---|----------|-------|
| TR123769_c0_g1_i2 | auxin efflux carrier component 1 family protein | AZ | -5,53 |
| TR19113_c0_g2_i1 | auxin-responsive protein iaa1 | AZ | -5,53 |
| TR123769_c0_g1_i1 | auxin efflux carrier component 1 family protein | distal | -5,52 |
| TR147728_c0_g1_i1 | auxin efflux carrier component 1 family protein | proximal | -5,51 |
| TR139620_c0_g2_i1 | probable auxin efflux carrier component 1c | distal | -5,50 |
| TR104930_c0_g2_i1 | auxin-induced protein 22d | proximal | -5,49 |
| TR122368_c0_g1_i1 | auxin-induced protein 15a-like | distal | -5,44 |
| TR158230_c0_g1_i1 | auxin-induced protein aux28-like | proximal | -5,41 |
| TR123795_c0_g1_i2 | auxin-responsive protein iaa14-like | AZ | -5,41 |
| TR147728_c0_g1_i1 | auxin efflux carrier component 1 family protein | distal | -5,40 |
| TR126027_c0_g1_i3 | protein kinase pinoid | distal | -5,40 |
| TR73178_c0_g1_i1 | auxin-responsive protein iaa4 | AZ | -5,39 |
| TR138863_c0_g1_i2 | probable indole-3-acetic acid-amido synthetase | proximal | -5,37 |
| TR111423_c0_g2_i1 | auxin-responsive protein iaa4-like | distal | -5,37 |
| TR122385_c0_g4_i1 | auxin-responsive protein saur61-like | distal | -5,37 |
| TR133182_c3_g1_i3 | auxin response factor 4 | AZ | -5,36 |
| TR181138_c0_g1_i1 | auxin-induced protein aux28-like | distal | -5,33 |
| TR19113_c0_g1_i1 | auxin-responsive protein iaa1 | distal | -5,33 |
| TR147728_c0_g1_i3 | auxin efflux carrier component 1 family protein | distal | -5,31 |
| TR71658_c0_g2_i1 | auxin efflux carrier component 8 | AZ | -5,30 |
| TR8517_c0_g2_i1 | auxin efflux carrier component 8 | AZ | -5,30 |
| TR142028_c0_g1_i2 | probable indole-3-acetic acid-amido synthetase | proximal | -5,30 |
| TR116886_c0_g1_i1 | auxin-responsive protein iaa1 | proximal | -5,25 |
| TR135060_c4_g1_i3 | iaa-amino acid hydrolase ilr1-like 4 | proximal | -5,25 |
| TR138697_c7_g2_i2 | probable indole-3-acetic acid-amido synthetase | distal | -5,25 |
| TR139482_c4_g2_i1 | probable indole-3-acetic acid-amido synthetase | distal | -5,24 |
| TR90681_c0_g2_i1 | auxin-induced protein 15a-like | distal | -5,20 |
| TR66190_c0_g1_i1 | auxin-responsive protein iaa4 | distal | -5,20 |
| TR125726_c2_g1_i2 | auxin-responsive protein saur61-like | distal | -5,20 |
| TR138697_c7_g2_i5 | probable indole-3-acetic acid-amido synthetase | AZ | -5,16 |
| TR138697_c7_g2_i4 | probable indole-3-acetic acid-amido synthetase | proximal | -5,15 |
| TR122510_c0_g1_i1 | auxin-responsive protein iaa14-like | AZ | -5,14 |
| TR141309_c0_g1_i1 | auxin-responsive protein iaa1 | distal | -5,12 |
| TR130962_c1_g1_i2 | auxin-induced protein 15a-like | distal | -5,11 |
| TR123795_c0_g1_i2 | auxin-responsive protein iaa14-like | distal | -5,10 |
| TR8517_c0_g1_i1 | auxin efflux carrier component 8 | distal | -5,10 |
| TR122510_c0_g1_i1 | auxin-responsive protein iaa14-like | distal | -5,05 |
| TR130962_c1_g1_i1 | auxin-induced protein 15a-like | distal | -5,03 |
| TR123795_c0_g1_i1 | auxin-responsive protein iaa14-like | AZ | -4,99 |
| TR57659_c0_g2_i1 | auxin-induced protein 15a-like | AZ | -4,99 |
| TR138808_c5_g2_i1 | iaa-amino acid hydrolase ilr1-like 4 | distal | -4,99 |
| TR146654_c11_g1_i1 | auxin-responsive protein iaa1 | proximal | -4,97 |
| TR158230_c0_g1_i1 | auxin-induced protein aux28-like | AZ | -4,95 |
| TR138697_c7_g2_i2 | probable indole-3-acetic acid-amido synthetase | proximal | -4,94 |
| TR141309_c0_g1_i1 | auxin-responsive protein iaa1 | AZ | -4,93 |

| | | | |
|-------------------|--|----------|-------|
| TR135060_c4_g1_i1 | iaa-amino acid hydrolase ilr1-like 4 | AZ | -4,91 |
| TR123769_c0_g1_i2 | auxin efflux carrier component 1 family protein | distal | -4,91 |
| TR142756_c0_g1_i3 | probable indole-3-acetic acid-amido synthetase | proximal | -4,91 |
| TR116382_c0_g1_i2 | indole-3-acetic acid-induced protein arg2-like | proximal | -4,91 |
| TR147728_c0_g1_i3 | auxin efflux carrier component 1 family protein | proximal | -4,82 |
| TR116886_c0_g1_i1 | auxin-responsive protein iaa1 | AZ | -4,81 |
| TR111423_c0_g2_i1 | auxin-responsive protein iaa4-like | proximal | -4,79 |
| TR127301_c0_g1_i2 | auxin-induced protein aux28-like | proximal | -4,77 |
| TR130962_c1_g1_i2 | auxin-induced protein 15a-like | proximal | -4,76 |
| TR85220_c0_g1_i1 | auxin-induced protein 6b | proximal | -4,69 |
| TR138808_c5_g2_i2 | iaa-amino acid hydrolase ilr1-like 4 | distal | -4,67 |
| TR132207_c0_g1_i1 | probable indole-3-pyruvate monooxygenase yucca10 | AZ | -4,62 |
| TR139482_c4_g2_i2 | probable indole-3-acetic acid-amido synthetase | proximal | -4,59 |
| TR123854_c0_g2_i2 | auxin-induced protein 15a-like | proximal | -4,59 |
| TR177973_c0_g1_i1 | saur-like auxin-responsive protein | proximal | -4,59 |
| TR138808_c5_g2_i1 | iaa-amino acid hydrolase ilr1-like 4 | AZ | -4,58 |
| TR85220_c0_g1_i1 | auxin-induced protein 6b | AZ | -4,53 |
| TR139482_c4_g2_i4 | probable indole-3-acetic acid-amido synthetase | proximal | -4,50 |
| TR132207_c0_g1_i3 | probable indole-3-pyruvate monooxygenase yucca10 | proximal | -4,45 |
| TR71658_c0_g2_i1 | auxin efflux carrier component 8 | distal | -4,38 |
| TR138808_c5_g2_i2 | iaa-amino acid hydrolase ilr1-like 4 | AZ | -4,38 |
| TR123795_c0_g1_i2 | auxin-responsive protein iaa14-like | proximal | -4,37 |
| TR71658_c0_g2_i1 | auxin efflux carrier component 8 | proximal | -4,34 |
| TR170515_c0_g1_i1 | saur-like auxin-responsive protein | distal | -4,33 |
| TR158230_c0_g1_i1 | auxin-induced protein aux28-like | distal | -4,33 |
| TR135060_c4_g1_i3 | iaa-amino acid hydrolase ilr1-like 4 | AZ | -4,32 |
| TR98952_c0_g1_i1 | auxin-induced protein 6b-like | distal | -4,31 |
| TR8517_c0_g1_i1 | auxin efflux carrier component 8 | proximal | -4,28 |
| TR139620_c0_g2_i2 | auxin efflux carrier component 1 family protein | proximal | -4,23 |
| TR145728_c0_g1_i3 | auxin response factor 18 isoform x1 | AZ | -4,22 |
| TR123769_c0_g1_i1 | auxin efflux carrier component 1 family protein | proximal | -4,20 |
| TR133182_c3_g1_i5 | auxin response factor 4 | distal | -4,19 |
| TR138808_c5_g2_i1 | iaa-amino acid hydrolase ilr1-like 4 | proximal | -4,18 |
| TR135060_c4_g1_i3 | iaa-amino acid hydrolase ilr1-like 4 | distal | -4,11 |
| TR122510_c0_g1_i1 | auxin-responsive protein iaa14-like | proximal | -4,10 |
| TR13346_c0_g1_i1 | auxin-responsive protein iaa8-like | distal | -4,08 |
| TR188104_c2_g1_i1 | indole-3-acetic acid-induced protein arg2-like | proximal | -3,94 |
| TR187931_c2_g1_i1 | indole-3-acetic acid-induced protein arg2-like | proximal | -3,92 |
| TR139482_c4_g2_i1 | probable indole-3-acetic acid-amido synthetase | proximal | -3,90 |
| TR116382_c0_g1_i2 | indole-3-acetic acid-induced protein arg2-like | distal | -3,89 |
| TR98952_c0_g1_i1 | auxin-induced protein 6b-like | AZ | -3,89 |
| TR132207_c0_g1_i1 | probable indole-3-pyruvate monooxygenase yucca10 | proximal | -3,83 |
| TR126731_c0_g1_i2 | auxin-responsive protein iaa27 | AZ | -3,74 |
| TR130048_c2_g1_i1 | indole-3-acetic acid-induced protein arg2-like | proximal | -3,73 |
| TR16082_c0_g2_i1 | auxin-induced protein 15a-like | AZ | -3,72 |

| | | | |
|-------------------|---|----------|-------|
| TR13346_c0_g1_i1 | auxin-responsive protein iaa8-like | AZ | -3,72 |
| TR116382_c0_g1_i1 | indole-3-acetic acid-induced protein arg2-like | proximal | -3,68 |
| TR146387_c1_g1_i5 | auxin-induced protein | AZ | -3,65 |
| TR16082_c0_g2_i1 | auxin-induced protein 15a-like | distal | -3,64 |
| TR141505_c0_g2_i8 | serine threonine-protein phosphatase pp2a-3 catalytic subunit | AZ | -3,62 |
| TR53289_c0_g3_i1 | auxin-induced protein 15a-like | AZ | -3,55 |
| TR116382_c0_g1_i2 | indole-3-acetic acid-induced protein arg2-like | AZ | -3,51 |
| TR116086_c0_g1_i1 | auxin-responsive protein | distal | -3,49 |
| TR188104_c2_g1_i1 | indole-3-acetic acid-induced protein arg2-like | distal | -3,46 |
| TR150258_c0_g1_i1 | auxin-responsive protein iaa27-like | AZ | -3,46 |
| TR187931_c2_g1_i1 | indole-3-acetic acid-induced protein arg2-like | distal | -3,44 |
| TR120593_c0_g1_i1 | auxin-responsive protein | AZ | -3,42 |
| TR138697_c7_g2_i5 | probable indole-3-acetic acid-amido synthetase | proximal | -3,39 |
| TR53289_c0_g3_i1 | auxin-induced protein 15a-like | distal | -3,38 |
| TR126717_c0_g1_i1 | auxin-induced protein aux28-like | proximal | -3,38 |
| TR180757_c0_g1_i1 | auxin-responsive protein iaa27-like | AZ | -3,38 |
| TR126717_c0_g1_i1 | auxin-induced protein aux28-like | distal | -3,38 |
| TR57659_c0_g2_i1 | auxin-induced protein 15a-like | proximal | -3,37 |
| TR127301_c0_g1_i1 | auxin-induced protein aux28-like | proximal | -3,36 |
| TR116086_c0_g1_i1 | auxin-responsive protein | AZ | -3,30 |
| TR127301_c0_g1_i1 | auxin-induced protein aux28-like | distal | -3,24 |
| TR150258_c0_g1_i1 | auxin-responsive protein iaa27-like | proximal | -3,20 |
| TR126717_c0_g1_i1 | auxin-induced protein aux28-like | AZ | -3,09 |

Supplementary Table 3A

Up-regulated genes related to cell wall transformation in the temporal comparison D0 vs D2

| Transcript ID | Gene product | Tissue | Log2FC |
|--------------------|-------------------------------------|----------|--------|
| TR139185_c5_g1_i5 | pectinacetylesterase family protein | distal | 13,86 |
| TR119630_c0_g1_i1 | beta-galactosidase protein 1 | distal | 13,82 |
| TR96655_c0_g2_i1 | extensin-2- partial | AZ | 13,33 |
| TR147978_c4_g2_i1 | beta-glucosidase 41 isoform x1 | distal | 12,23 |
| TR133797_c4_g1_i3 | beta-glucosidase 11-like isoform x1 | proximal | 11,20 |
| TR147978_c4_g2_i12 | beta-glucosidase 41 | distal | 11,14 |
| TR147978_c4_g2_i5 | beta-glucosidase 41 isoform x1 | distal | 11,09 |
| TR136740_c0_g1_i1 | beta-galactosidase-like isoform x2 | distal | 11,00 |
| TR135914_c0_g1_i1 | beta-galactosidase-like isoform x2 | distal | 10,99 |
| TR147431_c0_g1_i6 | beta-glucosidase 41 | distal | 10,99 |
| TR147978_c4_g2_i18 | beta-glucosidase 41 | distal | 10,98 |
| TR127424_c1_g1_i1 | beta-d-xylosidase family protein | distal | 10,93 |
| TR84738_c0_g1_i1 | beta-glucosidase 16-like isoform x2 | distal | 10,86 |

| | | | |
|--------------------|---|----------|-------|
| TR147978_c4_g2_i1 | beta-glucosidase 41 isoform x1 | AZ | 10,86 |
| TR96655_c0_g2_i3 | extensin-2-like | AZ | 10,86 |
| TR147431_c0_g1_i2 | beta-glucosidase 41 | AZ | 10,85 |
| TR71087_c0_g1_i2 | beta-glucosidase 16-like isoform x2 | distal | 10,84 |
| TR94490_c0_g1_i1 | extensin-2- partial | AZ | 10,66 |
| TR147978_c4_g2_i12 | beta-glucosidase 41 | AZ | 10,56 |
| TR142408_c2_g1_i4 | pectinacylesterase family protein | AZ | 10,51 |
| TR133797_c4_g1_i3 | beta-glucosidase 11-like isoform x1 | AZ | 10,46 |
| TR147978_c4_g2_i18 | beta-glucosidase 41 | AZ | 10,26 |
| TR147978_c4_g2_i5 | beta-glucosidase 41 isoform x1 | AZ | 10,16 |
| TR126856_c2_g1_i1 | beta-d-xylosidase family protein | distal | 10,05 |
| TR147978_c4_g2_i2 | beta-glucosidase 41 isoform x1 | distal | 10,04 |
| TR142161_c0_g1_i2 | beta-xylosidase alpha-l-arabinofuranosidase 2-like | AZ | 9,95 |
| TR148537_c0_g1_i8 | glucan endo- -beta-glucosidase | proximal | 9,88 |
| TR147978_c4_g2_i2 | beta-glucosidase 41 isoform x1 | AZ | 9,85 |
| TR141731_c0_g1_i1 | beta-xylosidase alpha-l-arabinofuranosidase 2-like | AZ | 9,68 |
| TR138729_c0_g1_i3 | pectinacylesterase family protein | distal | 9,65 |
| TR142408_c2_g1_i7 | pectinacylesterase family protein | distal | 9,65 |
| TR147431_c0_g1_i6 | beta-glucosidase 41 | AZ | 9,63 |
| TR147431_c0_g1_i3 | beta-glucosidase 41 | proximal | 9,59 |
| TR147978_c4_g2_i1 | beta-glucosidase 41 isoform x1 | proximal | 9,56 |
| TR147978_c4_g2_i15 | beta-glucosidase 41 | AZ | 9,47 |
| TR96655_c0_g2_i1 | extensin-2- partial | proximal | 9,40 |
| TR96655_c0_g2_i3 | extensin-2-like | distal | 9,27 |
| TR160034_c0_g1_i1 | protein trichome birefringence-like 43 | distal | 9,23 |
| TR127424_c1_g1_i1 | beta-d-xylosidase family protein | AZ | 9,21 |
| TR142408_c2_g1_i7 | pectinacylesterase family protein | AZ | 9,18 |
| TR71087_c0_g1_i2 | beta-glucosidase 16-like isoform x2 | AZ | 9,11 |
| TR136740_c0_g1_i1 | beta-galactosidase-like isoform x2 | AZ | 9,10 |
| TR94490_c0_g1_i1 | extensin-2- partial | distal | 9,07 |
| TR71087_c0_g1_i1 | beta-glucosidase 12-like | AZ | 9,03 |
| TR147978_c4_g2_i15 | beta-glucosidase 41 | distal | 8,86 |
| TR131555_c1_g2_i10 | bifunctional udp-glucose 4-epimerase and udp-xylose 4-epimerase 1 | distal | 8,74 |
| TR126856_c2_g1_i1 | beta-d-xylosidase family protein | AZ | 8,67 |
| TR142161_c0_g1_i2 | beta-xylosidase alpha-l-arabinofuranosidase 2-like | distal | 8,60 |
| TR131555_c1_g2_i11 | bifunctional udp-glucose 4-epimerase and udp-xylose 4-epimerase 1 | AZ | 8,50 |
| TR141731_c0_g1_i2 | beta-xylosidase alpha-l-arabinofuranosidase 2 | distal | 8,47 |
| TR142408_c2_g1_i6 | pectin acylesterase 8 isoform x1 | distal | 8,44 |
| TR121532_c0_g1_i10 | bifunctional udp-glucose 4-epimerase and udp-xylose 4-epimerase 1 | distal | 8,41 |
| TR147978_c4_g2_i5 | beta-glucosidase 41 isoform x1 | proximal | 8,31 |
| TR142408_c2_g1_i6 | pectin acylesterase 8 isoform x1 | AZ | 8,24 |
| TR123936_c0_g1_i2 | probable pectinesterase 68 | AZ | 8,20 |

| | | | |
|--------------------|---|----------|------|
| TR147497_c2_g1_i6 | pectinesterase | proximal | 8,18 |
| TR147431_c0_g1_i5 | beta-glucosidase 41 | AZ | 8,09 |
| TR135914_c0_g1_i1 | beta-galactosidase-like isoform x2 | AZ | 8,09 |
| TR121532_c0_g1_i2 | bifunctional udp-glucose 4-epimerase and udp-xylose 4-epimerase 1 | AZ | 8,01 |
| TR160034_c0_g1_i1 | protein trichome birefringence-like 43 | AZ | 8,01 |
| TR8672_c0_g1_i1 | polygalacturonase | distal | 7,98 |
| TR119630_c0_g1_i2 | beta-galactosidase protein 1 | distal | 7,80 |
| TR96655_c0_g2_i1 | extensin-2- partial | distal | 7,67 |
| TR94490_c0_g1_i1 | extensin-2- partial | proximal | 7,09 |
| TR127424_c1_g1_i1 | beta-d-xylosidase family protein | proximal | 6,98 |
| TR142408_c2_g1_i4 | pectinacetylerase family protein | distal | 6,75 |
| TR126856_c2_g1_i1 | beta-d-xylosidase family protein | proximal | 6,70 |
| TR119630_c0_g1_i1 | beta-galactosidase protein 1 | AZ | 6,55 |
| TR142408_c2_g1_i5 | pectinacetylerase family protein | distal | 6,54 |
| TR147431_c0_g1_i5 | beta-glucosidase 41 | distal | 6,42 |
| TR136740_c0_g1_i1 | beta-galactosidase-like isoform x2 | proximal | 6,37 |
| TR138729_c0_g1_i5 | pectinacetylerase family protein | distal | 6,28 |
| TR113211_c2_g1_i1 | glucan endo- -beta-glucosidase-like | distal | 6,27 |
| TR136245_c2_g1_i1 | protein notum homolog | distal | 6,14 |
| TR63804_c0_g1_i1 | protein trichome birefringence-like 43 | distal | 6,07 |
| TR138857_c1_g1_i1 | protein notum homolog | distal | 5,98 |
| TR147978_c4_g2_i10 | beta-glucosidase 41 | distal | 5,96 |
| TR123936_c0_g1_i1 | probable pectinesterase 68 | AZ | 5,94 |
| TR138729_c0_g1_i5 | pectinacetylerase family protein | AZ | 5,93 |
| TR138729_c0_g1_i8 | pectinacetylerase family protein | distal | 5,90 |
| TR117243_c3_g1_i1 | glucan endo- -beta-glucosidase-like | distal | 5,90 |
| TR136245_c2_g1_i1 | protein notum homolog | AZ | 5,86 |
| TR138729_c0_g1_i6 | pectinacetylerase family protein | distal | 5,78 |
| TR138729_c0_g1_i8 | pectinacetylerase family protein | AZ | 5,76 |
| TR84738_c0_g1_i1 | beta-glucosidase 16-like isoform x2 | AZ | 5,75 |
| TR141731_c0_g1_i2 | beta-xylosidase alpha-l-arabinofuranosidase 2 | AZ | 5,73 |
| TR138729_c0_g1_i6 | pectinacetylerase family protein | AZ | 5,69 |
| TR138857_c1_g1_i1 | protein notum homolog | AZ | 5,69 |
| TR130700_c0_g1_i1 | probable pectinesterase 68 | AZ | 5,54 |
| TR135914_c0_g1_i1 | beta-galactosidase-like isoform x2 | proximal | 5,50 |
| TR119630_c0_g1_i2 | beta-galactosidase protein 1 | AZ | 5,47 |
| TR142408_c2_g1_i1 | pectinacetylerase family protein | distal | 5,41 |
| TR130700_c0_g1_i1 | probable pectinesterase 68 | distal | 5,21 |
| TR142408_c2_g1_i2 | pectinacetylerase family protein | AZ | 5,11 |
| TR119630_c0_g1_i1 | beta-galactosidase protein 1 | proximal | 5,01 |
| TR147589_c6_g1_i1 | pectinesterase | AZ | 4,93 |
| TR131555_c1_g2_i9 | bifunctional udp-glucose 4-epimerase and udp-xylose 4-epimerase 1 | distal | 4,86 |
| TR130700_c0_g1_i1 | probable pectinesterase 68 | proximal | 4,85 |

| | | | |
|--------------------|---|----------|------|
| TR123936_c0_g1_i1 | probable pectinesterase 68 | distal | 4,84 |
| TR142408_c2_g1_i2 | pectinacetylerase family protein | distal | 4,81 |
| TR138729_c0_g1_i10 | pectinacetylerase family protein | distal | 4,79 |
| TR121532_c0_g1_i8 | bifunctional udp-glucose 4-epimerase and udp-xylose 4-epimerase 1 | distal | 4,78 |
| TR147589_c6_g1_i1 | pectinesterase | distal | 4,75 |
| TR139185_c5_g1_i5 | pectinacetylerase family protein | AZ | 4,70 |
| TR138729_c0_g1_i7 | pectinacetylerase family protein | distal | 4,69 |
| TR123935_c0_g1_i4 | protein notum homolog | AZ | 4,67 |
| TR113211_c2_g1_i1 | glucan endo- -beta-glucosidase-like | AZ | 4,65 |
| TR138729_c0_g1_i1 | pectinacetylerase family protein | distal | 4,60 |
| TR138729_c0_g1_i3 | pectinacetylerase family protein | AZ | 4,54 |
| TR131616_c1_g1_i1 | probable polygalacturonase | distal | 4,53 |
| TR123936_c0_g1_i1 | probable pectinesterase 68 | proximal | 4,51 |
| TR141584_c9_g1_i3 | probable beta-d-xylosidase 7 | distal | 4,51 |
| TR121532_c0_g1_i8 | bifunctional udp-glucose 4-epimerase and udp-xylose 4-epimerase 1 | AZ | 4,50 |
| TR130499_c1_g1_i1 | probable polygalacturonase | distal | 4,47 |
| TR117243_c3_g1_i1 | glucan endo- -beta-glucosidase-like | AZ | 4,45 |
| TR96655_c0_g2_i2 | extensin-2-like | distal | 4,36 |
| TR142408_c2_g1_i2 | pectinacetylerase family protein | proximal | 4,24 |
| TR142408_c2_g1_i1 | pectinacetylerase family protein | AZ | 4,21 |
| TR138857_c1_g1_i1 | protein notum homolog | proximal | 3,97 |
| TR136245_c2_g1_i1 | protein notum homolog | proximal | 3,95 |
| TR121532_c0_g1_i2 | bifunctional udp-glucose 4-epimerase and udp-xylose 4-epimerase 1 | distal | 3,91 |
| TR147978_c4_g2_i10 | beta-glucosidase 41 | AZ | 3,86 |
| TR73905_c0_g1_i1 | glucan endo- -beta-glucosidase 7 | distal | 3,84 |
| TR142408_c2_g1_i5 | pectinacetylerase family protein | AZ | 3,81 |
| TR147431_c0_g1_i3 | beta-glucosidase 41 | distal | 3,80 |
| TR138729_c0_g1_i1 | pectinacetylerase family protein | AZ | 3,79 |
| TR142408_c2_g1_i5 | pectinacetylerase family protein | proximal | 3,77 |
| TR117952_c0_g1_i1 | protein trichome birefringence-like 38 | distal | 3,71 |
| TR149481_c6_g1_i1 | glucan endo- -beta-glucosidase 7 | distal | 3,70 |
| TR53056_c0_g1_i2 | glucan endo- -beta-glucosidase 7 | distal | 3,67 |
| TR93444_c0_g1_i1 | probable xyloglucan endotransglucosylase hydrolase protein 31 | distal | 3,64 |
| TR112710_c4_g1_i1 | probable xyloglucan endotransglucosylase hydrolase protein 30 | AZ | 3,64 |
| TR113211_c2_g1_i1 | glucan endo- -beta-glucosidase-like | proximal | 3,60 |
| TR106786_c1_g1_i1 | probable xyloglucan endotransglucosylase hydrolase protein 30 | AZ | 3,58 |
| TR106757_c1_g1_i6 | probable pectinesterase 53 | AZ | 3,53 |
| TR133797_c4_g1_i3 | beta-glucosidase 11-like isoform x1 | distal | 3,51 |
| TR131555_c1_g2_i9 | bifunctional udp-glucose 4-epimerase and udp-xylose 4-epimerase 1 | AZ | 3,50 |

| | | | |
|-------------------|---|----------|------|
| TR131555_c1_g2_i2 | bifunctional udp-glucose 4-epimerase and udp-xylose 4-epimerase 1 | distal | 3,49 |
| TR51632_c0_g1_i1 | glucan endo- -beta-glucosidase 7 | distal | 3,48 |
| TR41098_c0_g2_i1 | probable xyloglucan endotransglucosylase hydrolase protein 31 | distal | 3,43 |
| TR117243_c3_g1_i1 | glucan endo- -beta-glucosidase-like | proximal | 3,34 |
| TR106786_c1_g1_i1 | probable xyloglucan endotransglucosylase hydrolase protein 30 | distal | 3,31 |
| TR112710_c4_g1_i1 | probable xyloglucan endotransglucosylase hydrolase protein 30 | distal | 3,28 |
| TR99506_c2_g1_i5 | probable pectinesterase 53 | AZ | 3,23 |
| TR147431_c0_g1_i4 | beta-glucosidase 41 | distal | 3,23 |
| TR147431_c0_g1_i2 | beta-glucosidase 41 | distal | 3,23 |
| TR150803_c0_g1_i1 | protein trichome birefringence-like 39 | distal | 3,19 |
| TR53056_c0_g1_i1 | glucan endo- -beta-glucosidase 7 | distal | 3,17 |
| TR51632_c0_g1_i2 | glucan endo- -beta-glucosidase 7 | distal | 3,14 |
| TR131616_c1_g1_i1 | probable polygalacturonase | AZ | 3,09 |
| TR130499_c1_g1_i1 | probable polygalacturonase | AZ | 3,08 |

Supplementary Table 3B

Down-regulated genes related to cell wall transformation in the temporal comparison D0 vs D2

| Transcript ID | Gene product | Tissue | Log2FC |
|--------------------|---|----------|--------|
| TR130582_c0_g1_i2 | xyloglucan endotransglycosylase 6 | AZ | -12,21 |
| TR113089_c0_g1_i1 | expansin s1 precursor family protein | distal | -11,35 |
| TR115645_c0_g1_i1 | expansin s1 precursor family protein | distal | -11,34 |
| TR145915_c0_g1_i5 | probable xyloglucan glycosyltransferase 12 | proximal | -11,28 |
| TR129143_c0_g1_i1 | probable pectinesterase pectinesterase inhibitor 51 | AZ | -10,79 |
| TR135109_c1_g1_i3 | glucan endo- -beta-glucosidase | proximal | -10,77 |
| TR144913_c1_g1_i2 | probable pectinesterase pectinesterase inhibitor 51 | AZ | -10,65 |
| TR93063_c0_g1_i2 | probable xyloglucan endotransglucosylase hydrolase protein 23 | AZ | -10,41 |
| TR132324_c2_g1_i3 | xyloglucan endotransglucosylase hydrolase family protein | AZ | -10,32 |
| TR139850_c0_g4_i1 | polygalacturonase at1g48100-like | distal | -10,24 |
| TR113089_c0_g1_i1 | expansin s1 precursor family protein | AZ | -10,23 |
| TR144913_c1_g1_i2 | probable pectinesterase pectinesterase inhibitor 51 | distal | -10,22 |
| TR148164_c5_g1_i15 | beta-glucosidase 17-like | distal | -10,17 |
| TR103072_c0_g1_i1 | probable xyloglucan glycosyltransferase 12 | proximal | -10,08 |
| TR129143_c0_g1_i1 | probable pectinesterase pectinesterase inhibitor 51 | distal | -9,99 |

| | | | |
|--------------------|---|----------|-------|
| TR78545_c0_g2_i1 | polygalacturonase at1g48100-like | distal | -9,82 |
| TR148164_c5_g1_i15 | beta-glucosidase 17-like | proximal | -9,61 |
| TR111871_c0_g1_i1 | xyloglucan endotransglucosylase hydrolase protein 22 | proximal | -9,38 |
| TR78545_c0_g1_i1 | polygalacturonase at1g48100-like | distal | -9,35 |
| TR130582_c0_g1_i2 | xyloglucan endotransglycosylase 6 | proximal | -9,35 |
| TR142028_c0_g1_i1 | probable indole-3-acetic acid-amido synthetase | proximal | -9,34 |
| TR138155_c4_g1_i6 | callose synthase 8 | proximal | -9,14 |
| TR8194_c0_g1_i1 | probable xyloglucan glycosyltransferase 12 | proximal | -9,12 |
| TR78545_c0_g2_i2 | polygalacturonase at1g48100-like | distal | -9,09 |
| TR90861_c0_g1_i1 | beta-glucosidase 40 | AZ | -8,98 |
| TR78545_c0_g2_i1 | polygalacturonase at1g48100-like | AZ | -8,98 |
| TR150454_c0_g1_i1 | expansin a10 | AZ | -8,90 |
| TR139045_c3_g2_i10 | beta-glucosidase 17-like | distal | -8,88 |
| TR692_c0_g1_i1 | probable xyloglucan glycosyltransferase 12 | distal | -8,75 |
| TR139045_c3_g2_i14 | beta-glucosidase 17-like | AZ | -8,74 |
| TR78545_c0_g2_i1 | polygalacturonase at1g48100-like | proximal | -8,71 |
| TR78545_c0_g1_i1 | polygalacturonase at1g48100-like | AZ | -8,45 |
| TR165341_c0_g1_i1 | expansin a10 | distal | -8,42 |
| TR46212_c0_g1_i1 | expansin a10 | distal | -8,42 |
| TR8194_c0_g2_i1 | probable xyloglucan glycosyltransferase 12 | AZ | -8,31 |
| TR145997_c1_g1_i15 | polygalacturonase at1g48100-like | AZ | -8,27 |
| TR165341_c0_g1_i1 | expansin a10 | AZ | -8,14 |
| TR78545_c0_g2_i2 | polygalacturonase at1g48100-like | AZ | -8,10 |
| TR130582_c0_g1_i3 | xyloglucan endotransglucosylase hydrolase family protein | proximal | -8,08 |
| TR133667_c0_g1_i1 | callose synthase 5 | distal | -8,07 |
| TR78513_c0_g1_i1 | expansin a10 | distal | -8,07 |
| TR150454_c0_g1_i1 | expansin a10 | distal | -8,04 |
| TR139045_c3_g2_i9 | beta-glucosidase 17-like | proximal | -8,02 |
| TR8194_c0_g2_i1 | probable xyloglucan glycosyltransferase 12 | proximal | -8,02 |
| TR148674_c8_g1_i1 | probable xyloglucan endotransglucosylase hydrolase protein 23 | AZ | -7,99 |
| TR148674_c8_g1_i4 | xyloglucan endotransglucosylase hydrolase family protein | proximal | -7,89 |
| TR181282_c0_g1_i1 | probable beta-d-xylosidase 5 isoform x2 | proximal | -7,66 |
| TR132324_c1_g1_i3 | xyloglucan endotransglucosylase hydrolase family protein | proximal | -7,52 |
| TR148674_c8_g1_i1 | probable xyloglucan endotransglucosylase hydrolase protein 23 | proximal | -7,42 |
| TR115645_c0_g1_i1 | expansin s1 precursor family protein | AZ | -7,31 |
| TR165291_c0_g1_i1 | probable beta-d-xylosidase 5 isoform x2 | proximal | -7,29 |
| TR58640_c0_g2_i1 | xyloglucan endotransglycosylase hydrolase | proximal | -7,28 |
| TR134208_c0_g1_i3 | expansin alpha | AZ | -7,25 |
| TR148674_c8_g1_i4 | xyloglucan endotransglucosylase hydrolase family protein | AZ | -7,23 |

| | | | |
|--------------------|---|----------|-------|
| TR95781_c0_g1_i1 | probable xyloglucan endotransglucosylase hydrolase protein 23 | AZ | -7,22 |
| TR91766_c0_g1_i2 | probable xyloglucan endotransglucosylase hydrolase protein 23 | AZ | -7,21 |
| TR132324_c1_g1_i1 | xyloglucan endotransglucosylase hydrolase family protein | AZ | -7,04 |
| TR145187_c5_g1_i1 | probable pectinesterase pectinesterase inhibitor 7 | proximal | -6,98 |
| TR137044_c0_g1_i2 | expansin alpha | distal | -6,97 |
| TR130582_c0_g1_i3 | xyloglucan endotransglucosylase hydrolase family protein | AZ | -6,97 |
| TR58640_c0_g2_i1 | xyloglucan endotransglycosylase hydrolase | AZ | -6,95 |
| TR137044_c0_g1_i1 | expansin alpha | distal | -6,93 |
| TR49790_c0_g3_i1 | xyloglucan endotransglycosylase hydrolase | proximal | -6,85 |
| TR134208_c0_g1_i8 | expansin alpha | AZ | -6,82 |
| TR145915_c0_g1_i2 | probable xyloglucan glycosyltransferase 12 | AZ | -6,80 |
| TR91766_c0_g1_i3 | probable xyloglucan endotransglucosylase hydrolase protein 23 | proximal | -6,78 |
| TR132496_c0_g1_i4 | glucan endo- -beta-glucosidase | AZ | -6,77 |
| TR92321_c0_g1_i1 | xyloglucan endotransglucosylase hydrolase protein 22 | proximal | -6,54 |
| TR132496_c0_g1_i4 | glucan endo- -beta-glucosidase | proximal | -6,50 |
| TR134208_c0_g1_i3 | expansin alpha | distal | -6,47 |
| TR49790_c0_g1_i1 | xyloglucan endotransglycosylase hydrolase | proximal | -6,45 |
| TR144913_c1_g1_i2 | probable pectinesterase pectinesterase inhibitor 51 | proximal | -6,36 |
| TR93063_c0_g1_i2 | probable xyloglucan endotransglucosylase hydrolase protein 23 | proximal | -6,33 |
| TR132324_c1_g1_i3 | xyloglucan endotransglucosylase hydrolase family protein | AZ | -6,32 |
| TR134208_c0_g1_i2 | expansin alpha | AZ | -6,31 |
| TR130582_c0_g1_i2 | xyloglucan endotransglycosylase 6 | distal | -6,30 |
| TR134208_c0_g1_i2 | expansin alpha | distal | -6,29 |
| TR130582_c0_g1_i1 | probable xyloglucan endotransglucosylase hydrolase protein 23 | AZ | -6,29 |
| TR44861_c0_g1_i1 | probable xyloglucan glycosyltransferase 12 | AZ | -6,28 |
| TR132324_c1_g1_i1 | xyloglucan endotransglucosylase hydrolase family protein | proximal | -6,28 |
| TR103072_c0_g1_i1 | probable xyloglucan glycosyltransferase 12 | AZ | -6,24 |
| TR129143_c0_g1_i1 | probable pectinesterase pectinesterase inhibitor 51 | proximal | -6,24 |
| TR93063_c0_g1_i1 | probable xyloglucan endotransglucosylase hydrolase protein 23 | AZ | -6,19 |
| TR148164_c5_g1_i15 | beta-glucosidase 17-like | AZ | -6,18 |
| TR49790_c0_g1_i1 | xyloglucan endotransglycosylase hydrolase | AZ | -6,18 |
| TR181282_c0_g1_i1 | probable beta-d-xylosidase 5 isoform x2 | AZ | -6,17 |
| TR95781_c0_g1_i1 | probable xyloglucan endotransglucosylase hydrolase protein 23 | proximal | -6,14 |

| | | | |
|-------------------|---|----------|-------|
| TR58640_c0_g2_i1 | xyloglucan endotransglycosylase hydrolase | distal | -6,13 |
| TR8194_c0_g1_i1 | probable xyloglucan glycosyltransferase 12 | AZ | -6,13 |
| TR91766_c0_g1_i2 | probable xyloglucan endotransglucosylase hydrolase protein 23 | proximal | -6,12 |
| TR91766_c0_g1_i3 | probable xyloglucan endotransglucosylase hydrolase protein 23 | AZ | -6,12 |
| TR145187_c5_g1_i1 | probable pectinesterase pectinesterase inhibitor 7 | AZ | -6,11 |
| TR49790_c0_g3_i1 | xyloglucan endotransglycosylase hydrolase | AZ | -6,11 |
| TR132324_c1_g1_i2 | xyloglucan endotransglucosylase hydrolase family protein | AZ | -6,11 |
| TR91766_c0_g1_i1 | probable xyloglucan endotransglucosylase hydrolase protein 23 | AZ | -6,11 |
| TR137044_c0_g1_i1 | expansin alpha | AZ | -6,08 |
| TR115645_c0_g1_i1 | expansin s1 precursor family protein | proximal | -6,06 |
| TR149101_c5_g1_i6 | probable polygalacturonase at1g80170 | proximal | -6,04 |
| TR135903_c2_g3_i1 | expansin alpha | AZ | -6,00 |
| TR91766_c0_g1_i1 | probable xyloglucan endotransglucosylase hydrolase protein 23 | proximal | -5,99 |
| TR692_c0_g1_i1 | probable xyloglucan glycosyltransferase 12 | AZ | -5,98 |
| TR165291_c0_g1_i1 | probable beta-d-xylosidase 5 isoform x2 | AZ | -5,94 |
| TR14891_c0_g1_i1 | probable xyloglucan glycosyltransferase 12 | proximal | -5,93 |
| TR130582_c0_g1_i1 | probable xyloglucan endotransglucosylase hydrolase protein 23 | distal | -5,92 |
| TR58468_c0_g2_i1 | probable xyloglucan glycosyltransferase 12 | AZ | -5,91 |
| TR14891_c0_g1_i1 | probable xyloglucan glycosyltransferase 12 | AZ | -5,88 |
| TR130582_c0_g1_i1 | probable xyloglucan endotransglucosylase hydrolase protein 23 | proximal | -5,87 |
| TR144530_c2_g1_i3 | probable xyloglucan glycosyltransferase 12 | AZ | -5,87 |
| TR134208_c0_g1_i1 | expansin alpha | AZ | -5,86 |
| TR140866_c1_g1_i1 | glucan endo- -beta-glucosidase 12 | AZ | -5,86 |
| TR141963_c0_g1_i1 | pectinesterase 2-like | proximal | -5,85 |
| TR140514_c0_g1_i1 | pectinesterase 2-like | proximal | -5,82 |
| TR58640_c0_g3_i1 | xyloglucan endotransglycosylase hydrolase | distal | -5,79 |
| TR135109_c1_g1_i3 | glucan endo- -beta-glucosidase | AZ | -5,76 |
| TR93063_c0_g1_i1 | probable xyloglucan endotransglucosylase hydrolase protein 23 | proximal | -5,72 |
| TR49790_c0_g1_i1 | xyloglucan endotransglycosylase hydrolase | distal | -5,70 |
| TR148674_c8_g1_i2 | probable xyloglucan endotransglucosylase hydrolase protein 23 | proximal | -5,63 |
| TR91766_c0_g1_i3 | probable xyloglucan endotransglucosylase hydrolase protein 23 | distal | -5,61 |
| TR134208_c0_g1_i5 | expansin alpha | distal | -5,61 |
| TR140298_c1_g1_i2 | glucan endo- -beta-glucosidase 12 | AZ | -5,59 |
| TR58640_c0_g3_i1 | xyloglucan endotransglycosylase hydrolase | proximal | -5,56 |
| TR8194_c0_g1_i1 | probable xyloglucan glycosyltransferase 12 | distal | -5,55 |

| | | | |
|--------------------|---|----------|-------|
| TR148674_c8_g1_i1 | probable xyloglucan endotransglucosylase hydrolase protein 23 | distal | -5,54 |
| TR103072_c0_g1_i2 | probable xyloglucan glycosyltransferase 12 | proximal | -5,53 |
| TR49790_c0_g3_i1 | xyloglucan endotransglycosylase hydrolase | distal | -5,47 |
| TR148674_c8_g1_i2 | probable xyloglucan endotransglucosylase hydrolase protein 23 | AZ | -5,46 |
| TR137044_c0_g1_i4 | expansin alpha | distal | -5,40 |
| TR93063_c0_g1_i2 | probable xyloglucan endotransglucosylase hydrolase protein 23 | distal | -5,38 |
| TR95781_c0_g1_i1 | probable xyloglucan endotransglucosylase hydrolase protein 23 | distal | -5,36 |
| TR103072_c0_g1_i2 | probable xyloglucan glycosyltransferase 12 | AZ | -5,35 |
| TR145915_c0_g1_i2 | probable xyloglucan glycosyltransferase 12 | proximal | -5,35 |
| TR132324_c1_g1_i3 | xyloglucan endotransglucosylase hydrolase family protein | distal | -5,32 |
| TR137044_c0_g1_i2 | expansin alpha | AZ | -5,30 |
| TR52886_c0_g1_i1 | probable xyloglucan glycosyltransferase 12 | distal | -5,29 |
| TR132324_c1_g1_i2 | xyloglucan endotransglucosylase hydrolase family protein | proximal | -5,28 |
| TR52886_c0_g1_i1 | probable xyloglucan glycosyltransferase 12 | AZ | -5,24 |
| TR132496_c0_g1_i1 | glucan endo- -beta-glucosidase | proximal | -5,22 |
| TR91766_c0_g1_i1 | probable xyloglucan endotransglucosylase hydrolase protein 23 | distal | -5,17 |
| TR692_c0_g1_i1 | probable xyloglucan glycosyltransferase 12 | proximal | -5,16 |
| TR113089_c0_g1_i1 | expansin s1 precursor family protein | proximal | -5,11 |
| TR145915_c0_g1_i5 | probable xyloglucan glycosyltransferase 12 | AZ | -5,10 |
| TR132324_c1_g1_i1 | xyloglucan endotransglucosylase hydrolase family protein | distal | -5,03 |
| TR58640_c0_g3_i1 | xyloglucan endotransglycosylase hydrolase | AZ | -5,03 |
| TR93063_c0_g1_i1 | probable xyloglucan endotransglucosylase hydrolase protein 23 | distal | -5,02 |
| TR144530_c2_g1_i3 | probable xyloglucan glycosyltransferase 12 | proximal | -5,01 |
| TR52886_c0_g1_i1 | probable xyloglucan glycosyltransferase 12 | proximal | -5,00 |
| TR145187_c5_g1_i1 | probable pectinesterase pectinesterase inhibitor 7 | distal | -4,98 |
| TR130582_c0_g1_i3 | xyloglucan endotransglucosylase hydrolase family protein | distal | -4,97 |
| TR134208_c0_g1_i8 | expansin alpha | distal | -4,97 |
| TR132324_c2_g1_i3 | xyloglucan endotransglucosylase hydrolase family protein | proximal | -4,94 |
| TR148674_c8_g1_i4 | xyloglucan endotransglucosylase hydrolase family protein | distal | -4,93 |
| TR132324_c2_g1_i1 | xyloglucan endotransglucosylase hydrolase family protein | proximal | -4,93 |
| TR92321_c0_g1_i1 | xyloglucan endotransglucosylase hydrolase protein 22 | AZ | -4,92 |
| TR44861_c0_g1_i1 | probable xyloglucan glycosyltransferase 12 | proximal | -4,87 |
| TR148164_c5_g1_i16 | beta-glucosidase 17-like | AZ | -4,84 |

| | | | |
|--------------------|---|----------|-------|
| TR58468_c0_g2_i1 | probable xyloglucan glycosyltransferase 12 | proximal | -4,82 |
| TR140298_c1_g1_i1 | glucan endo- -beta-glucosidase 12 | AZ | -4,79 |
| TR140866_c1_g1_i1 | glucan endo- -beta-glucosidase 12 | distal | -4,79 |
| TR44861_c0_g1_i1 | probable xyloglucan glycosyltransferase 12 | distal | -4,78 |
| TR103072_c0_g1_i2 | probable xyloglucan glycosyltransferase 12 | distal | -4,77 |
| TR52386_c0_g1_i1 | beta-galactosidase 5 | distal | -4,76 |
| TR147223_c0_g1_i3 | probable xyloglucan glycosyltransferase 5 | distal | -4,74 |
| TR120237_c0_g1_i1 | probable pectate lyase 5 | distal | -4,74 |
| TR134208_c0_g1_i6 | expansin alpha | distal | -4,74 |
| TR144530_c2_g1_i3 | probable xyloglucan glycosyltransferase 12 | distal | -4,74 |
| TR144530_c2_g1_i1 | probable xyloglucan glycosyltransferase 12 | AZ | -4,73 |
| TR133667_c0_g1_i1 | callose synthase 5 | proximal | -4,69 |
| TR103072_c0_g1_i1 | probable xyloglucan glycosyltransferase 12 | distal | -4,69 |
| TR129143_c0_g1_i3 | probable pectinesterase pectinesterase inhibitor 51 | proximal | -4,68 |
| TR145915_c0_g1_i1 | probable xyloglucan glycosyltransferase 12 | proximal | -4,67 |
| TR145915_c0_g1_i2 | probable xyloglucan glycosyltransferase 12 | distal | -4,60 |
| TR124781_c1_g1_i1 | probable pectate lyase 5 | distal | -4,58 |
| TR129143_c0_g1_i2 | probable pectinesterase pectinesterase inhibitor 51 | AZ | -4,55 |
| TR145997_c1_g1_i10 | polygalacturonase at1g48100-like | distal | -4,54 |
| TR83309_c0_g1_i2 | glucan endo- -beta-glucosidase 11-like | distal | -4,53 |
| TR114154_c0_g1_i2 | probable pectinesterase pectinesterase inhibitor 7 | proximal | -4,52 |
| TR144530_c2_g1_i1 | probable xyloglucan glycosyltransferase 12 | proximal | -4,48 |
| TR132324_c2_g1_i3 | xyloglucan endotransglucosylase hydrolase family protein | distal | -4,44 |
| TR141963_c0_g1_i1 | pectinesterase 2-like | AZ | -4,44 |
| TR91766_c0_g1_i2 | probable xyloglucan endotransglucosylase hydrolase protein 23 | distal | -4,43 |
| TR132324_c1_g1_i2 | xyloglucan endotransglucosylase hydrolase family protein | distal | -4,43 |
| TR145915_c0_g1_i1 | probable xyloglucan glycosyltransferase 12 | distal | -4,42 |
| TR139045_c3_g2_i1 | beta-glucosidase 17-like | distal | -4,41 |
| TR145769_c1_g1_i1 | endo- -beta-glucanase | distal | -4,41 |
| TR144913_c1_g1_i3 | probable pectinesterase pectinesterase inhibitor 51 | proximal | -4,39 |
| TR144530_c1_g1_i2 | probable xyloglucan glycosyltransferase 12 | proximal | -4,37 |
| TR144913_c1_g1_i1 | probable pectinesterase pectinesterase inhibitor 51 | proximal | -4,36 |
| TR144913_c1_g1_i3 | probable pectinesterase pectinesterase inhibitor 51 | AZ | -4,35 |
| TR144913_c1_g1_i3 | probable pectinesterase pectinesterase inhibitor 51 | distal | -4,33 |
| TR111871_c0_g1_i1 | xyloglucan endotransglucosylase hydrolase protein 22 | AZ | -4,28 |

| | | | |
|--------------------|---|----------|-------|
| TR129143_c0_g1_i2 | probable pectinesterase pectinesterase inhibitor 51 | proximal | -4,27 |
| TR59229_c0_g1_i1 | beta-galactosidase 5 | distal | -4,19 |
| TR134208_c0_g1_i5 | expansin alpha | AZ | -4,19 |
| TR129143_c0_g1_i3 | probable pectinesterase pectinesterase inhibitor 51 | AZ | -4,15 |
| TR139850_c0_g4_i1 | polygalacturonase at1g48100-like | AZ | -4,15 |
| TR144913_c1_g1_i1 | probable pectinesterase pectinesterase inhibitor 51 | distal | -4,12 |
| TR182657_c0_g1_i1 | callose synthase 5 | distal | -4,09 |
| TR140298_c1_g1_i1 | glucan endo- -beta-glucosidase 12 | distal | -4,06 |
| TR148674_c4_g1_i1 | xyloglucan endotransglucosylase hydrolase family protein | proximal | -4,06 |
| TR132324_c2_g1_i2 | xyloglucan endotransglucosylase hydrolase family protein | proximal | -4,05 |
| TR124233_c0_g1_i1 | probable pectinesterase pectinesterase inhibitor 7 | proximal | -4,05 |
| TR144530_c1_g1_i2 | probable xyloglucan glycosyltransferase 12 | AZ | -4,04 |
| TR129143_c0_g1_i2 | probable pectinesterase pectinesterase inhibitor 51 | distal | -4,03 |
| TR129143_c0_g1_i3 | probable pectinesterase pectinesterase inhibitor 51 | distal | -4,02 |
| TR145997_c1_g1_i10 | polygalacturonase at1g48100-like | AZ | -4,00 |
| TR129741_c0_g1_i1 | probable xyloglucan endotransglucosylase hydrolase protein 32 | AZ | -3,99 |
| TR141646_c0_g1_i1 | glucan endo- -beta-glucosidase 12-like | distal | -3,98 |
| TR150454_c0_g1_i1 | expansin a10 | proximal | -3,97 |
| TR134208_c0_g1_i6 | expansin alpha | proximal | -3,96 |
| TR108277_c0_g1_i2 | pectate lyase | distal | -3,95 |
| TR144553_c0_g1_i2 | endo- -beta-glucanase | distal | -3,95 |
| TR129741_c0_g1_i1 | probable xyloglucan endotransglucosylase hydrolase protein 32 | distal | -3,94 |
| TR165341_c0_g1_i1 | expansin a10 | proximal | -3,94 |
| TR144913_c1_g1_i1 | probable pectinesterase pectinesterase inhibitor 51 | AZ | -3,93 |
| TR145615_c0_g1_i2 | xyloglucan glycosyltransferase 4 | proximal | -3,92 |
| TR141646_c0_g1_i1 | glucan endo- -beta-glucosidase 12-like | AZ | -3,91 |
| TR131857_c0_g1_i1 | probable xyloglucan endotransglucosylase hydrolase protein 32 | AZ | -3,91 |
| TR15243_c0_g2_i1 | expansin-like a2 | AZ | -3,91 |
| TR145615_c0_g1_i2 | xyloglucan glycosyltransferase 4 | AZ | -3,88 |
| TR137044_c0_g1_i4 | expansin alpha | AZ | -3,85 |
| TR145915_c0_g1_i5 | probable xyloglucan glycosyltransferase 12 | distal | -3,84 |
| TR140298_c1_g1_i2 | glucan endo- -beta-glucosidase 12 | distal | -3,83 |
| TR79862_c0_g1_i2 | expansin-like a1 | AZ | -3,81 |
| TR144530_c2_g1_i4 | probable xyloglucan glycosyltransferase 12 | proximal | -3,77 |
| TR117749_c0_g1_i2 | pectate lyase | distal | -3,76 |

| | | | |
|-------------------|---|----------|-------|
| TR139045_c3_g2_i1 | beta-glucosidase 17-like | AZ | -3,65 |
| TR145769_c1_g1_i1 | endo- -beta-glucanase | AZ | -3,63 |
| TR15243_c0_g2_i1 | expansin-like a2 | proximal | -3,63 |
| TR145915_c0_g1_i1 | probable xyloglucan glycosyltransferase 12 | AZ | -3,62 |
| TR59229_c0_g1_i2 | beta-galactosidase 5 | AZ | -3,62 |
| TR79862_c0_g1_i2 | expansin-like a1 | proximal | -3,60 |
| TR131857_c0_g1_i1 | probable xyloglucan endotransglucosylase hydrolase protein 32 | distal | -3,58 |
| TR114154_c0_g1_i2 | probable pectinesterase pectinesterase inhibitor 7 | AZ | -3,54 |
| TR140866_c1_g1_i1 | glucan endo- -beta-glucosidase 12 | proximal | -3,49 |
| TR52386_c0_g1_i2 | beta-galactosidase 3 | distal | -3,47 |
| TR114154_c0_g1_i1 | probable pectinesterase pectinesterase inhibitor 7 | AZ | -3,47 |
| TR144530_c2_g1_i2 | probable xyloglucan glycosyltransferase 12 | proximal | -3,45 |
| TR144530_c2_g1_i4 | probable xyloglucan glycosyltransferase 12 | AZ | -3,44 |
| TR130139_c2_g2_i1 | expansin | distal | -3,44 |
| TR135903_c2_g3_i2 | expansin alpha | AZ | -3,41 |
| TR145915_c0_g1_i3 | probable xyloglucan glycosyltransferase 12 | proximal | -3,40 |
| TR124233_c0_g1_i1 | probable pectinesterase pectinesterase inhibitor 7 | AZ | -3,40 |
| TR140298_c1_g1_i1 | glucan endo- -beta-glucosidase 12 | proximal | -3,38 |
| TR135903_c2_g3_i2 | expansin alpha | distal | -3,36 |
| TR144553_c0_g1_i2 | endo- -beta-glucanase | AZ | -3,36 |
| TR144530_c2_g1_i1 | probable xyloglucan glycosyltransferase 12 | distal | -3,35 |
| TR98404_c0_g1_i1 | glucan endo- -beta-glucosidase 2 | AZ | -3,29 |
| TR130139_c2_g2_i1 | expansin | AZ | -3,28 |
| TR142813_c0_g1_i4 | beta-galactosidase 5 | distal | -3,26 |
| TR145915_c0_g1_i3 | probable xyloglucan glycosyltransferase 12 | AZ | -3,18 |
| TR129741_c0_g1_i1 | probable xyloglucan endotransglucosylase hydrolase protein 32 | proximal | -3,16 |
| TR130139_c2_g2_i2 | expansin | distal | -3,15 |
| TR135903_c2_g2_i1 | expansin | distal | -3,14 |
| TR123636_c0_g1_i2 | probable pectate lyase 8 | distal | -3,11 |
| TR144530_c2_g1_i2 | probable xyloglucan glycosyltransferase 12 | AZ | -3,07 |
| TR132324_c2_g1_i2 | xyloglucan endotransglucosylase hydrolase family protein | AZ | -3,06 |
| TR135903_c2_g2_i1 | expansin | AZ | -3,06 |
| TR148674_c4_g1_i1 | xyloglucan endotransglucosylase hydrolase family protein | AZ | -3,04 |

ISBN: 978-82-575-1511-9

ISSN: 1894-6402



Norwegian University
of Life Sciences

Postboks 5003
NO-1432 Ås, Norway
+47 67 23 00 00
www.nmbu.no